Complex hyperbolic lattices and moduli spaces of flat surfaces

Irene Pasquinelli

A Thesis presented for the degree of
Doctor of Philosophy

Geometry Research Group
Department of Mathematical Sciences
University of Durham
England

September 2018

Thesis

Irene Pasquinelli

Submitted for the degree of Doctor of Philosophy

September 2018

Abstract

This work studies the Deligne-Mostow lattices in $PU(2,1)$. These were introduced by Deligne and Mostow in several works (see [Mos80], [DM86], [Mos86], [Mos88]), using monodromy of hypergeometric functions. The same lattices were rediscovered by Thurston (see [Thu98]) using a geometric construction, which consists of studying possible configurations of cone points on a sphere of area 1 when the cone angles are prescribed. This space has a complex hyperbolic structure and certain automorphisms of the sphere which swap pairs of cone points, generate a lattice for some choice of initial cone angles (more precisely, the Deligne-Mostow lattices). Among these, we will consider the ones in $PU(2,1)$. We use Thurston's approach to study the metric completion of this space, which is obtained by making pairs of cone points coalesce. Following the works of Parker [Par06] and Boadi-Parker [BP15], we build a polyhedron. Using the Poincaré polyhedron theorem, we prove that the polyhedron we find is indeed a fundamental domain. Moreover, we give presentations for all Deligne-Mostow lattices in $PU(2,1)$, calculate their volumes and show that they are coherent with the known commensurability theorems.

Declaration

The work in this thesis is based on research carried out in the Geometry Research Group at the Department of Mathematical Sciences, England. No part of this thesis has been submitted elsewhere for any other degree or qualification and it is all my own work unless referenced to the contrary in the text. Chapters 4-5-6 of this thesis contain research which has been previously submitted to research journals for publication (see [Pas16] and [Pas17]).

Statement of Copyright

Acknowledgements

The greatest *thank you* goes to my supervisor, for his constant support in work and in life, for his patience, for everything I have learnt from him, for helping me build my self-confidence and for being an inspiration at every stage of my PhD.

I want to thank Professor Kojima and his research group at Tokyo Institute of Technology, for the interesting conversations and the encouraging environment during my visit. I am grateful to EPSRC and Durham University for having funded my PhD and to JSPS for supporting my research fellowship in Japan. I would also like to thank hosts, colleagues and friends met in schools, conferences and research visits, as well as the funding institutes for my trips, as I find collaborative learning much more insightful than working on my own.

I also wish to thank my mathematical mentors across the years: Corinna Ulcigrai, Andrea Sambusetti, Luigia Spina, for teaching me to see the beauty of mathematics and for encouraging me to make it my job.

A special *thank you* goes to Zuzanna, Smita, Sam, Galane, Stephan, Gabriel, my officemates, all the friends and colleagues in the department and in college, to my friends from dance classes and to the friends in Japan, because, to do good work, trips, coffee breaks and nights out are just as important as the time sitting at your desk. To Maria, Rossella and Deborah, for holding onto me throughout the years and keeping in touch despite the distance. To Alice, for being the only friend who really understands how our family works.

In conclusione, un *grazie* speciale a mia madre Paola e mio padre Mario, per la sicurezza che qualsiasi cosa accada e qualsiasi decisione prenda, posso sempre contare sul loro supporto. E alla nonna e a tutta la famiglia, per l'affetto, l'educazione, il supporto e l'esempio che mi hanno dato nel corso degli anni.

Contents

Chapter 1

Introduction

One of the main goals in complex hyperbolic geometry is to study lattices in $PU(n,1)$. In fact, there are relatively few methods to construct them and they are rarely explicit. Moreover, many of these constructions use number theory to find arithmetic lattices, which makes it more interesting to study non arithmetic lattices arising by geometric constructions. The relation between arithmetic groups and lattices in symmetric spaces is interesting on its own. Complex hyperbolic space is the only rank one symmetric space of non-compact type where the relation is not completely settled. While we know that all arithmetic groups are lattices, examples of non arithmetic lattices are only known in low dimension (≤ 3). More details about arithmeticity can be found in Section 2.5. An account of the known constructions (not including some recent developments) can be found in the survey from Parker [Par09].

For a long time the Deligne-Mostow lattices were the only known (commensurability classes of) non arithmetic complex hyperbolic lattices and even now there are very few known. Other than the Deligne-Mostow lattices, we only have two other constructions that give non-arithmetic lattices. One is in the recent works from Deraux-Parker-Paupert [DPP16] and [DPP], where 22 commensurability classes of lattices in $PU(2,1)$ are constructed. The other is a group constructed by Couwenberg-Heckman-Looijenga, recently identified by Deraux (see [Der17]) as the only known non-arithmetic lattice in $PU(3,1)$, other than the Deligne-Mostow ones.

Deligne-Mostow lattices first appeared in [Mos80], [DM86], [Mos86] and in [Mos88]. They arise as monodromy of hypergeometric functions, a construction that dates back to Picard, Lauricella and others. More precisely, they start with a *ball N-tuple* $\mu = (\mu_1, \dots \mu_N)$, i.e. a set of N real numbers between 0 and 1 such that $\sum \mu_i = 2$, from which they construct some lattices in $PU(N-3,1)$. Then, in [Mos86], Mostow deduced a sufficient condition on μ for the monodromy group to be discrete, called condition ΣINT. This improved the sufficient condition called INT and introduced by Picard, who worked on the case of $PU(2,1)$. Only finitely many ball N-tuples satisfy condition ΣINT, giving a finite list of lattices in dimensions between 2 and 9 (i.e. $5 \leq N \leq 12$). Mostow in [Mos88] proved that for $N \geq 7$ condition ΣINT exactly characterises discreteness, while for $N = 6$ there is exactly one ball 6-tuple which does not satisfy the condition but still gives discrete monodromy. For $N = 5$, Mostow found nine ball 5-tuples which do not satisfy ΣINT but for which he could not prove that the monodromy groups were not discrete. Sauter in [Sau90] proved that all nine give monodromy groups that are commensurable to one arising from a ball 5-tuple that satisfies the condition ΣINT and hence they are also discrete. Combining the works of Deligne, Mostow and Sauter, one gets a finite and exhaustive list of ball N-tuples μ that give rise to a lattice using this construction (see also the book of Deligne and Mostow [DM93], which extends Sauter's work about commensurability classes). Any other value gives non-discrete monodromy. The construction from Deligne and Mostow is summarised in Section 3.1.

An alternative interpretation of these lattices was given by Thurston [Thu98] in terms of cone metrics on a sphere. Thurston's construction is the one at the origin of our work. His construction consists of considering a sphere with N cone singularities v_i for $i = 1, \dots, N$, of cone angle θ_i at v_i between 0 and 2π. They must then satisfy the discrete Gauss-Bonnet formula (i.e. $\sum \alpha_i = 4\pi$, where $\alpha_i = 2\pi - \theta_i$ are the curvatures at the cone points). He proves that the moduli space of such cone metrics with prescribed cone angles and area 1 has a complex hyperbolic structure of dimension $N-3$. He considers the group of automorphisms of the sphere swapping cone points with same cone angles and their squares when the cone angles are different. These are half or full Dehn

twists along a curve passing through the two cone points. He then gives an explicit, sufficient condition on the cone angles for this group to be a lattice. This condition is called the orbifold condition and is equivalent to Mostow's ΣINT condition. More details about Thurston's construction can be found in Section 3.2.

In [Koj01], Kojima proved that the two constructions from Deligne-Mostow and from Thurston are equivalent and can be seen as putting the same complex hyperbolic structure on the same space $\mathcal{Q}$. This is summarised in Section 3.3.

This work deals with the Deligne-Mostow lattices in $PU(2,1)$, which arise from ball 5-tuples. Our goal is to build fundamental domains and give explicit presentations for all of them. This answers Problem 6.5 and Problem 6.4 of [Par09].

All of the Deligne-Mostow lattices in $PU(2,1)$ have some symmetries, coming from the fact that some of the μ_i's having the same value. In Thurston's approach, this means that some of the cone points on the sphere have the same cone angle. In particular, the lattices will have (at least) either a 2-fold or 3-fold symmetry (i.e. they will have two or three cone points with the same cone angle respectively). They may have more symmetries, which reflect in symmetries of the fundamental polyhedra.

For some of the lattices with 3-fold symmetry, a fundamental domain has already been constructed, since the higher symmetry makes them a little easier to work on. These lattices can be parametrised using two values (p,k) (or (p,t) in Mostow's notation, see (3.4.2)) and can be divided in four broad types according to the values of these parameters, which determine the type (i.e. the dynamical behaviour, see Section 2.2) of some special maps. The types are defined at the end of Section 3.4.1. In particular, Deraux, Falbel and Paupert in [DFP05] gave a construction for some of the Deligne-Mostow groups, which we say are of second type. Later, Parker in [Par06] constructed a fundamental polyhedron for the Livné lattices (or lattices of third type) using a different method. Later on, Boadi and Parker in [BP15] used the same method to obtain a fundamental domain for Mostow groups of the first type. The part of this work about lattices with 3-fold symmetry (Chapter 5) fills in the final gap in the sense that it provides

a construction for a fundamental domain for lattices of the fourth type as well. Moreover, the construction described contains all the previous constructions in the following sense. One can build a single polyhedron and see all the polyhedra found in the previous cases as a deformation of the one constructed here, which is obtained by making triplets of points collapse to a single one. Section 5.7 is dedicated to the study of the relation between the work presented here and the fundamental domains previously built. The contents of Chapter 5 has been published in [Pas16].

The method to build the fundamental domain for the 3-fold symmetry lattices can also be adapted to construct building blocks for the fundamental domain for lattices with 2-fold symmetry in the following sense. One could forget about the symmetries and give a completely general construction, which is valid whatever the initial cone points are. Considering a generic cone metric on the sphere (without any symmetry), we can parametrise it by cutting along a curve passing through the cone points and develop the metric on a plane in a polygonal form, getting an octagon Π with pairs of sides of same length identified. One can recover the cone metrics by gluing the associated sides of the polygon back together. Such polygon can be described by three complex parameters which are related to the sides of the polygon, and we use them to give a set of projective coordinates. One can then use these coordinates to show that Thurston's theorem holds: by expressing the area in terms of the parameters one can see that it is a Hermitian form H of signature (1,2) on $\mathbb{C}^3$; since the area must be positive and we consider metrics of area one (hence configurations up to rescaling), we get a complex hyperbolic 2-space as the moduli space.

One can then introduce the *moves* on the cone structures, which are maps on the sphere corresponding to swapping two cone points, i.e. applying a half Dehn twist along a curve containing two cone points or applying a full Dehn twist. These are automorphisms of the sphere (and hence isometries of $\mathbf{H}^2_{\mathbb{C}}$) when the cone points which are swapped have the same cone angle. Before specialising to the case with symmetries, we also consider maps that swap cone points with different cone angles. This means that we land on a new cone metric after applying the move. We will hence apply the move twice in order to come back to the same

cone metric and have an automorphism of the sphere. While swapping cone points with same cone angle in the symmetric case is natural, the moves corresponding to full Dehn twists (i.e. swapping twice cone points with different cone angles) were first introduced by Thurston (and called butterfly moves) and generalised here to our case.

Moreover, we show how one can build a polyhedron associated to the ordered set of cone angles. Following Thurston's idea, we consider what happens when pairs of cone singularities approach each other until they coalesce, becoming a single point. These configurations are the vertices of the polyhedron. We want to remark that this is completely general and a cone manifold can be built even if the cone angles we started from do not give a lattice. This is described in Chapter 4, where the structure of these polyhedra is studied. Each side of the polyhedron (i.e. maximal dimension facet) is contained in a bisector. Bisectors are among the best understood subspaces of the complex hyperbolic plane and have some useful properties. In fact, one of the main difficulties in building fundamental domains in complex hyperbolic space is that there are no totally geodesic real hypersurfaces. Some possible substitutes, successful in some cases, are bisectors. Bisectors are foliated in two ways by totally geodesic subspaces and their intersection is well understood. More details about the structure of bisectors and bisector intersections can be found in Section 2.3. By intersecting the sides and calculating the dimension of these intersections we then find also 2-dimensional and 1-dimensional facets of the polyhedron. These are referred to as the ridges and the edges respectively.

For suitable initial cone points (in the lists in Sections 3.4.1 and 3.4.2), some of the moves will be automorphisms of the sphere with cone singularities (i.e. swap cone points with same cone angle or swap cone points twice), and we will consider the group Γ generated by the moves (or their compositions). Then, in the 3-fold symmetry case the polyhedron is actually a fundamental domain for the lattice Γ, provided we start from the right set of cone singularities (i.e. from cone angles in the list in Section 3.4.1) and up to collapsing triplets of points. In the 2-fold symmetry case this polyhedron is a building block for the fundamental domain of Γ, which will consist of the union of three copies of this polyhedron,

each for a different ordering of the cone points. Chapter 6 describes how to take the three copies and how they are glued. The content of Chapters 4 and 6 have been submitted for publication in [Pas17].

To prove that the polyhedra we have built are effectively fundamental domains, we use the Poincaré polyhedron theorem. Section 2.4 explains the version we will use in detail. To use the Poincaré theorem, the polyhedron needs to satisfy a few conditions. In particular, the generators have to pair the sides, sending one in the other, in a way that satisfies certain properties. Because of this they are called side pairing maps. Moreover, we also have some conditions on the ridges, the most difficult of which is to prove that the polyhedron and its images under the side pairing maps tessellate a neighbourhood of the interior of each ridge (local tessellation property).

The power of the Poincaré polyhedron theorem lies not only in the fact that it proves that the group is discrete and the polyhedron is indeed a fundamental domain for the group, but also in the fact that it gives a presentation for the group. The conditions on sides and ridges consist, in fact, also of some relations on the maps, called reflection relations and cycle relations respectively. Using the side pairing maps as generators and such relations, we obtain a full presentation for the group.

In the presentation, the relations are given only by cycle transformations which are either regular elliptic or complex reflections with certain parameters related to the lattice as their order. When an order is positive, we have a complex reflection with respect to a complex line. When the associated parameter is negative, the transformation is a complex reflection in a point so it is not a cycle transformation and it does not appear in the presentation. When it is ∞ we have a parabolic element, a fixed point on the boundary and again no relation in the presentation. The last two cases are related to the modifications of the polyhedron that we mentioned. In fact, when one of the parameters is negative or infinite, a triangular ridge collapses to a single point, which is on the boundary when the parameter is infinite. Although a presentation for the lattices was already given in the work of Deligne and Mostow, it is a bit technical to write, because it relies heavily on their notation.

The description of the polyhedra is also very explicit, due to the use of two or three suitable sets of coordinates (for the 3- and 2-fold symmetry cases respectively), which enormously simplify the calculations. This allows us to calculate the orbifold Euler characteristic of the polyhedron, as the sum (with alternating signs with the dimension of the facets) of the order of the stabiliser of one element for each orbit of facets. Then we can calculate the volume of the quotient $\Gamma \backslash \mathbf{H}^2_{\mathbb{C}}$, with a universal proportionality constant of the orbifold Euler characteristic. The calculations of the volumes and the coherence check with the commensurability theorems known for these lattices (see 3.5) can be found in Chapter 7.

The main method used in this work is a generalisation of the construction that Parker used in [Par06] to build fundamental domains.

This work is organised as follows. Chapter 2 contains all the background about complex hyperbolic geometry needed for the main results. It starts with the basic definition of complex hyperbolic space, then describes its space of isometries and how to classify them according to their dynamical behaviour. It continues with a detailed description of the structure of bisectors, which contain the sides of our fundamental polyhedra. We will then give the version of the Poincaré polyhedron theorem which we will use to prove that the polyhedra constructed are indeed fundamental domains. Chapter 2 ends with a brief account of the relation between arithmeticity and lattices in our setting.

Chapter 3 talks about the history of the lattices that are the main topic of this work. It summarises the works of Deligne and Mostow which constructs the lattices as monodromy of hypergeometric functions. Moreover, it briefly gives an account of Thurston's reinterpretation of the same lattices, using cone metric on a sphere of area 1 and it explains why they are different interpretations of the same lattices, following the work of Kojima. It also gives a complete list of the Deligne-Mostow lattices in dimension 2, split in those with 3- and 2-fold symmetry and explains how to parametrise them. Finally, it summarises the known commensurability theorems which relate the lattices we are considering.

Chapter 4 explains how to equip any cone metric on a sphere (independently on the symmetry on the cone angles) with a complex hyperbolic structure and how to associate certain maps and a polyhedron to it. Then it studies in detail the

structure of the polyhedron, proving that the sides are all contained in bisectors and studying their intersections.

Chapters 5 and 6 explain how to build the polyhedron in the two specific cases of lattices with 3- and 2-fold symmetry, specify which of the moves previously introduced we want to consider to generate the lattice and use the Poincaré polyhedron theorem to prove that the polyhedron is a fundamental domain. These chapters include the main theorems 5.4.1 and 6.3.1 and their proofs. They also include explicit presentations for each of the groups and an explanation of how to degenerate the polyhedron to cover all cases.

Chapter 7 is devoted to the calculations related to the volumes of the quotients of $\mathbf{H}^2_{\mathbb{C}}$ by the lattices. The tables with the orbits of the facets, the stabilisers and their orders are presented here, considering each possible deformation of the polyhedra. Moreover, the chapter ends with an explanation of how the volumes we calculated are coherent with the known commensurability theorems (see Section 3.5).

Chapter 8 is an account of the future directions this research can take. On the one hand, one could try and generalise this construction to Deligne-Mostow lattices in dimension 3, using the complex 2-dimensional polyhedra found here as facets of the new polyhedra. On the other, it is also known that a similar analysis as Thurston's can be done for a torus with certain cone singularities (see Veech [Vee93] and Ghazouani-Pirio [GP17]). One could then parametrise the cone metrics and hope to use a similar procedure as done here to find lattices, potentially new (non-arithmetic) ones. The chapter mentions some of the preliminary work we did in these two new directions.

Chapter 2

Complex hyperbolic geometry

In this chapter we will first define the complex hyperbolic space, give some of its main properties and describe some of its subspaces. Then we will talk about its group of isometries and how to classify them. Finally we will present a version of the Poincaré polyhedron theorem, which is a very useful tool to prove that a polyhedron is a fundamental domain for a certain discrete subgroup and discuss arithmeticity of lattices. Most of the information presented here can be found in the book of Goldman [Gol99].

The complex hyperbolic space arises naturally as a complex analogue of the real hyperbolic space $\mathbf{H}^n_{\mathbb{R}}$. The real hyperbolic plane is, in fact, an example of complex hyperbolic space of dimension 1. Generalising this construction to a complex vector space we get complex hyperbolic space.

2.1 The complex hyperbolic space

Let us take a complex vector space $\mathbb{C}^{n,1}$ of dimension $n+1$, equipped with a Hermitian form of signature $(n,1)$. We consider the Hermitian form in matrix form, given by a Hermitian matrix H (i.e. $H = H^*$), which is non singular, with n positive eigenvalues and one negative. Here A^* will always be defined by $A^* = \overline{A^T}$ and the same notation will be used for vectors.

Such a matrix gives a Hermitian inner product on $\mathbb{C}^{n,1}$, which we denote

$$\langle \mathbf{z}, \mathbf{w} \rangle = \mathbf{w}^* H \mathbf{z}.$$

For any $\mathbf{z} \in \mathbb{C}^{n,1}$, its norm under the product just defined, $\langle \mathbf{z}, \mathbf{z} \rangle = \mathbf{z}^* H \mathbf{z}$, is real, but can be positive, negative or zero. We hence decompose the space $\mathbb{C}^{n,1} \setminus \{0\}$ into subspaces V_+, V_0, V_- made of vectors where $\langle \mathbf{z}, \mathbf{z} \rangle$ is positive, zero or negative, respectively.

We now projectivise $\mathbb{C}^{n,1} \setminus \{0\}$ by identifying all non-zero complex multiples of a given vector. In other words, we are considering the projection $\mathbb{P}$ of $\mathbb{C}^{n,1} \setminus \{0\}$ onto $\mathbb{CP}^n$. The projection $\mathbb{P}$ is well defined on V_+, V_0 and V_-, because for $\lambda \in \mathbb{C} \setminus \{0\}$, we have

$$\langle \lambda \mathbf{z}, \lambda \mathbf{z} \rangle = (\lambda \mathbf{z})^* H (\lambda \mathbf{z}) = |\lambda|^2 \mathbf{z}^* H \mathbf{z} = |\lambda|^2 \langle \mathbf{z}, \mathbf{z} \rangle$$

and hence $\langle \lambda \mathbf{z}, \lambda \mathbf{z} \rangle$ and $\langle \mathbf{z}, \mathbf{z} \rangle$ have the same sign. In other words $\mathbf{z}$ and $\lambda \mathbf{z}$ must be in the same subspace.

We are now ready to define the complex hyperbolic space.

Definition 2.1.1. The n-dimensional complex hyperbolic space for a Hermitian form H is $\mathbf{H}^n_{\mathbb{C}} = \mathbb{P}V_-$, i.e. the space of vectors of negative norm, up to multiplication by complex numbers.

Its boundary is $\partial \mathbf{H}^n_{\mathbb{C}} = \mathbb{P}V_0$ and we will denote $\overline{\mathbf{H}}^n_{\mathbb{C}} = \mathbf{H}^n_{\mathbb{C}} \cup \partial \mathbf{H}^n_{\mathbb{C}}$ for the compactification of complex hyperbolic space.

On this space we consider the Bergman metric, given by the area element

$$ds^2 = \frac{-4}{\langle \mathbf{z}, \mathbf{z} \rangle^2} \det \begin{pmatrix} \langle \mathbf{z}, \mathbf{z} \rangle & \langle d\mathbf{z}, \mathbf{z} \rangle \\ \langle \mathbf{z}, d\mathbf{z} \rangle & \langle d\mathbf{z}, d\mathbf{z} \rangle \end{pmatrix}.$$

For two points $\mathbf{z}$ and $\mathbf{w}$, their distance $\varrho(\mathbf{z}, \mathbf{w})$ is given by

$$\cosh^2 \left(\frac{\varrho(\mathbf{z}, \mathbf{w})}{2} \right) = \frac{\langle \mathbf{z}, \mathbf{w} \rangle \langle \mathbf{w}, \mathbf{z} \rangle}{\langle \mathbf{z}, \mathbf{z} \rangle \langle \mathbf{w}, \mathbf{w} \rangle}. \tag{2.1.1}$$

The (real) sectional curvature is no longer constant as it was the case for real hyperbolic space, but is pinched between $-1/4$ and -1.

2.2 The group of isometries and its subgroups

The group of holomorphic isometries of $\mathbf{H}^n_{\mathbb{C}}$ is generated by the projectivisation of the group of matrices that are unitary with respect to H. More precisely, let

$U(H)$ be the group of square matrices of dimension $n+1$ such that $A^*HA = H$. We say that such matrices are unitary with respect to H. Naturally, we will have $SU(H)$ the subgroup of such matrices with determinant equal 1.

To get the holomorphic isometries of $\mathbf{H}^n_{\mathbb{C}}$, we need to projectivise this group as we did for the space itself, so the holomorphic isometry group of $\mathbf{H}^n_{\mathbb{C}}$ is

$$PU(H) = {}^{U(H)}\!\diagup\!_{\{e^{i\theta}I\colon \theta \in [0,2\pi)\}}.$$

This group and complex conjugation generate the full isometry group of $\mathbf{H}^n_{\mathbb{C}}$. Sometimes, to stress the dimension of the complex hyperbolic space this group acts on, we will denote it as $PU(n,1)$, since the group only depends on the signature and not on the form chosen. As a symmetric space, we can write $\mathbf{H}^n_{\mathbb{C}}$ as the quotient $\mathbf{H}^n_{\mathbb{C}} = {}^{PU(n,1)}\!\diagup\!_{U(n)}$, since $U(n)$ is the stabiliser of the origin in the ball model of $\mathbf{H}^n_{\mathbb{C}}$.

The elements of $PU(H)$ can be classified in the following way.

As we mentioned before, when $n = 1$ the space $\mathbf{H}^1_{\mathbb{C}}$ coincides with $\mathbf{H}^2_{\mathbb{R}}$ and the group $PU(1,1)$ is the same as $PSL(2,\mathbb{R})$. In this case, the isometries are classified into three types: elliptic, parabolic and hyperbolic. Their class in completely determined by their dynamics, i.e. by the number and position of the fixed points. A similar classification holds for the elements of $PU(n,1)$. An element $\gamma \in PU(n,1)$ can be either

1. *loxodromic* if it fixes exactly two points on $\partial\mathbf{H}^n_{\mathbb{C}}$,
2. *parabolic* if it has a unique fixed point on $\partial\mathbf{H}^n_{\mathbb{C}}$,
3. *elliptic*, if it has one or more fixed points inside $\mathbf{H}^n_{\mathbb{C}}$.

Let us now set $n = 2$ and look more closely at the holomorphic isometries of $\mathbf{H}^2_{\mathbb{C}}$ (i.e. the elements of $PU(2,1)$), which are the ones we will be using in this work. In this case we can also relate the dynamics with the algebraic properties (in particular with their eigenvalues).

1. Let $A \in PU(2,1)$ be loxodromic. Since fixed points on the boundary correspond to null eigenvectors (i.e. eigenvectors $\mathbf{v}$ with $\langle \mathbf{v}, \mathbf{v}\rangle = 0$), A must have two null eigenvectors corresponding to two eigenvalues λ and $\overline{\lambda}^{-1}$ such

that $|\lambda| > 1$ and hence $|\overline{\lambda}^{-1}| < 1$. This means that one of the two directions of the eigenvectors will be expanding and the other will be contracting. The element A preserves the complex line L spanned by the two eigenvectors. Moreover, loxodromic elements are semisimple and hence diagonalisable. Its diagonal form will have diagonal elements $\lambda = re^{i\theta}$, $\overline{\lambda}^{-1} = r^{-1}e^{i\theta}$ and $\overline{\lambda}\lambda^{-1} = e^{-2i\theta}$. When A has all real eigenvalues, we say that A is strictly hyperbolic.

2. Let now $A \in PU(2,1)$ be parabolic. Parabolic isometries are the only ones that are not semisimple (i.e. that are not diagonalisable). In this case A has a repeated eigenvalue of modulus 1, whose corresponding eigenspace is generated by a null vector. Parabolic isometries can be of two types:

   - If there is one eigenvalue with multiplicity 3, then A is *pure parabolic*. This means that is has a unipotent lift in $SU(2,1)$ so these are sometimes also called *unipotent*, as the case where all eigenvalues are 1 belongs to this class. In other words, pure parabolic isometries have all eigenvalues equal the same cube root of unity. These are conjugate to Heisenberg translations, which can be either horizontal or vertical.
   - If A has one eigenvalue with multiplicity 2, then it is said to be *ellipto-parabolic* or *screw-parabolic*. In other words, the eigenvalues are $e^{i\theta}$, $e^{i\theta}$ and $e^{-2i\theta}$. Then A will act as a composition of a rotation around the complex line along which it translates, This produces a spiralling screw-like dynamics (possibly tilted), hence the name.

3. Finally, let $A \in PU(2,1)$ be an elliptic isometry. In this case the group generated by A is a cyclic group that is compact in $PU(2,1)$. Again, the eigenvalues corresponding to A all have norm 1. Elliptic isometries are of two types.

   - When all eigenvalues are distinct, we say that A is *regular elliptic*. Then A fixes a unique point inside $\mathbf{H}^2_{\mathbb{C}}$ corresponding to a negative eigenvector.
   - When there is a repeated eigenvalue, A is a *complex reflection*. It can

either be a complex reflection in a complex line L or on a point $\mathbf{w}$. In the first case the eigenspace associated to the repeated eigenvalue is generated by a positive and a negative vector (generating L). In the second case, it is generated by two positive vectors. Complex reflections in lines are also called *boundary elliptic*, since they also fix points on the boundary. The name of complex reflection comes from the fact that they fix a line (or a point) and rotate $\mathbf{H}^2_{\mathbb{C}}$ around it. This should not lead the reader to think that they have order 2 like Euclidian reflections do. Complex reflection can in fact have higher order.

One can also describe the classes of isometries in terms of traces. Take A to be one of the representatives in the projective equivalence class such that $\det A = 1$, i.e. $A \in SU(2,1)$. Since each matrix in $PU(2,1)$ has three lifts to $SU(2,1)$ which differ by a cube root of unity, A is well defined up to multiplication by a cube root of unity. Let $f(t) = |t|^4 - 8\,\mathrm{Re}(t^3) + 18|t|^2 - 27$ and $\tau(A) = \mathrm{Tr}(A)$ be the trace function. Since the function f is invariant under multiplication by roots of unity, the discussion is independent on the lift, when calculated on the trace of A (see below). Then A is

- loxodromic if and only if $f(\tau(A)) > 0$;
- pure-parabolic if and only if $\tau(A)$ is 3 times a cube root of unity; in particular it will satisfy $f(\tau(A)) = 0$;
- screw-parabolic if and only if the following three conditions are satisfied:
  1. $\tau(A)$ is not 3 times a cube root of unity,
  2. $f(\tau(A)) = 0$,
  3. A is not diagonalisable (i.e. is it parabolic);
- a complex reflection (in either a complex line or a point) if and only if the following three conditions are satisfied:
  1. $\tau(A)$ is not 3 times a cube root of unity,

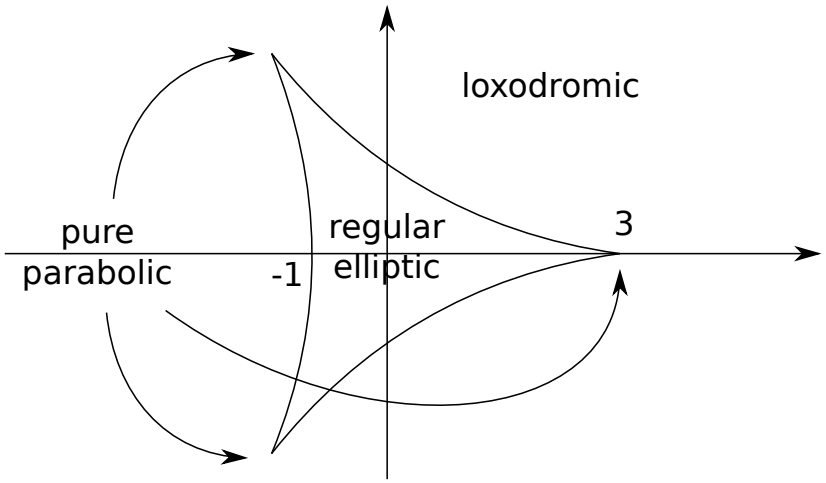

Figure 2.1: The deltoid of zeros of the trace function.

2. $f(\tau(A)) = 0$,

3. A is diagonalisable (i.e. it is elliptic);

- regular elliptic if and only if $f(\tau(A)) < 0$.

One can draw the set of zeros of the trace function in the complex plane representing the possible values of the trace, obtaining a curve called a deltoid (see Figure 2.1). If the trace is a complex number inside the deltoid, then the corresponding isometry is regular elliptic. If it is outside the deltoid, then the isometry is loxodromic. The three possible traces of pure parabolic isometries correspond to the three corners of the deltoid. The smooth points on the deltoid correspond to either screw-parabolic maps or to complex reflections.

Of all the subgroups of this group of holomorphic isometries, in this work we will consider those that are lattices, in the following sense.

Definition 2.2.1. A subgroup $\Gamma < PU(H)$ is a *lattice* when it is discrete and the quotient $\Gamma \backslash \mathbf{H}^n_{\mathbb{C}}$ has finite volume with respect to the Bergman metric.

One way to give a lattice is to build a fundamental domain for it.

Definition 2.2.2. Consider $\Gamma < PU(n,1)$ acting on $\mathbf{H}^n_{\mathbb{C}}$. A *fundamental domain* for the action is an open and connected set $D \subset \mathbf{H}^n_{\mathbb{C}}$ such that

- $D \cap A(D) = \emptyset$, for all $A \in \Gamma$, $A \neq \mathrm{Id}$,
- $\bigcup_{A\in\Gamma} A(\overline{D}) = \mathbf{H}^n_{\mathbb{C}}$, where $\overline{D}$ is the closure of D in $\mathbf{H}^n_{\mathbb{C}}$.

We will be interested in commensurability classes of lattices.

Definition 2.2.3. We say that two subgroups Γ_1 and Γ_2 of $PU(n,1)$ are *commensurable* if there is an element $A \in PU(n,1)$ such that the intersection $\Gamma_1 \cap A\Gamma_2 A^{-1}$ has finite index in both Γ_1 and $A\Gamma_2 A^{-1}$.

2.3 Bisectors

One of the most important classes of submanifolds in complex hyperbolic geometry is that of bisectors. In this section we will give a brief description and describe the main properties we will need. These subspaces have been widely studied and more details can be found in [Gol99].

Bisectors are defined as the locus of points in the complex hyperbolic space which are equidistant from two given points, say $[\mathbf{z}_i]$ and $[\mathbf{z}_j]$, which denote the equivalence classes under the projection $\mathbb{P}$ of points $\mathbf{z}_i$ and $\mathbf{z}_j$ in V_-. By the formula in (2.1.1), we have

$$\frac{\langle \mathbf{z}, \mathbf{z}_j\rangle\langle \mathbf{z}_j, \mathbf{z}\rangle}{\langle \mathbf{z}, \mathbf{z}\rangle\langle \mathbf{z}_j, \mathbf{z}_j\rangle} = \cosh^2\left(\frac{\varrho([\mathbf{z}],[\mathbf{z}_j])}{2}\right) = \cosh^2\left(\frac{\varrho([\mathbf{z}],[\mathbf{z}_i])}{2}\right) = \frac{\langle \mathbf{z}, \mathbf{z}_i\rangle\langle \mathbf{z}_i, \mathbf{z}\rangle}{\langle \mathbf{z}, \mathbf{z}\rangle\langle \mathbf{z}_i, \mathbf{z}_i\rangle}.$$

If the lifts $\mathbf{z}_i$ and $\mathbf{z}_j$ of $[\mathbf{z}_i]$ and $[\mathbf{z}_j]$ are chosen to have the same norm (which is always possible), the definition becomes:

$$B = B([\mathbf{z}_i],[\mathbf{z}_j]) = \{[\mathbf{z}] \in \mathbf{H}^2_{\mathbb{C}} \colon |\langle \mathbf{z}, \mathbf{z}_i\rangle| = |\langle \mathbf{z}, \mathbf{z}_j\rangle|\}.$$

From now on, since everything we do will be independent of the lift chosen, we will omit the square brackets and use the notation $\mathbf{z}$ for both $[\mathbf{z}] \in \mathbf{H}^2_{\mathbb{C}}$ and a lift $\mathbf{z} \in V_-$.

We remark that this holds even for null vectors, i.e. one can define $B([\mathbf{z}_i],[\mathbf{z}_j])$ even if $\langle \mathbf{z}_i, \mathbf{z}_i\rangle = \langle \mathbf{z}_j, \mathbf{z}_j\rangle = 0$. One can also extend this definition to the case when the lifts of $\mathbf{z}_i$ and $\mathbf{z}_j$ are in V_+. The extension of these to $\mathbb{CP}^2$ are called *extors* and more details can be found in [Gol99].

The complex line L spanned by $\mathbf{z}_i$ and $\mathbf{z}_j$ is called the *complex spine* of the bisector. Inside L there is a geodesic γ which is the intersection between the complex spine and the bisector and it is called the *spine* of the bisector.

In the complex hyperbolic space there are no totally geodesic real hypersurfaces, and therefore also the bisectors are obviously not totally geodesic. However, they can be foliated by totally geodesic subspaces in two different ways: with slices or with meridians.

The foliation by slices first appeared in the works of Giraud [Gir21] and Mostow [Mos80]. To define the slices first take the map Π_L, which is the orthogonal projection of the whole space onto the complex spine L. Then B is the preimage under Π_L of the spine γ. We hence define a *slice* to be a fibre of the map Π_L, i.e. the preimage of a point of γ. Slices are complex lines and hence embedded copies of $\mathbf{H}^1_{\mathbb{C}}$ with the Poincaré metric, seen as restriction of the Bergman metric. They realise the curvature bound of -1.

The other foliation is by meridians and can be found in Goldman's book [Gol99]. A *meridian* is a totally geodesic Lagrangian plane containing the spine γ. Lagrangian planes are the images under elements of $PU(2,1)$ of points in $\mathbf{H}^2_{\mathbb{C}}$ with real coordinates in the ball model. They are embedded copies of the real hyperbolic plane equipped with the Klein-Beltrami metric and realise the curvature bound of $-1/4$. The bisector is the union of all its meridian. A meridian is also the set of points fixed by an antiholomorphic involution which swaps $\mathbf{z}_i$ and $\mathbf{z}_j$.

Other important subspaces related to bisectors are Giraud discs, which are motivated by the theorem below, stated by Giraud in Theorem 4 of [Gir21] and can also be found as Theorem 8.3.3 in Goldman's book [Gol99]. Roughly speaking, every time that two bisectors are in a generic position (in the sense specified in the theorem below), one can find a third bisector which also contains their intersection. Giraud discs are discs contained in the intersection of the three bisectors.

Theorem 2.3.1. *Let B_1 and B_2 be two bisectors with complex spines L_1 and L_2 respectively. Assume that*

- *L_1 and L_2 are distinct,*
- *$B_1 \cap L_2 = B_2 \cap L_1 = \emptyset$.*

Then there is at most one other bisector B_3 containing $B_1 \cap B_2$.

If we want to understand bisector intersections, we need to look at the complex spines. If the two complex spines coincide, the bisectors are said to be *cospinal* and this means that the four points are contained in a common complex line (the complex spine). In this case the bisectors intersect if and only if the spines intersect and the bisector intersection is then a complex line (for more details, see Section 2.5 of [DPP16]). This case is ruled out by the first condition in the theorem. Since complex lines that intersect in two or more points necessarily coincide, the only other possible case is when the complex spines intersect in a single point. In this section we will only consider the case when the intersection point is inside complex hyperbolic space (it will not always be the case in our work, but, provided that one is careful in some details, a similar analysis can be done). The second condition in Theorem 2.3.1 ensures that the intersection point does not belong to the spines (since the spines lie in the bisectors). Then the bisectors are called *coequidistant* because there exist three points $\mathbf{z}_i, \mathbf{z}_j$ and $\mathbf{z}_k$ (not all contained in a complex line) such that the two bisectors can be written as $B_1 = B(\mathbf{z}_i, \mathbf{z}_j)$ and $B_2 = B(\mathbf{z}_i, \mathbf{z}_k)$. Now we can reformulate Giraud's theorem following Proposition 2.4 of [DPP16] as

Theorem 2.3.2. *Let z_i, z_j and z_k be three points in $\boldsymbol{H}^2_{\mathbb{C}}$ not contained in a common complex line. Then, when it is non-empty, the intersection of $B_1 = B(z_i, z_j)$ and $B_2 = B(z_i, z_k)$ is a smooth non totally geodesic disc contained in exactly three bisectors $B(z_i, z_j), B(z_i, z_k)$ and $B(z_j, z_k)$.*

We are now ready to define a Giraud disc as follows.

Definition 2.3.3. In the setting of the previous theorem, the intersection of B_1 and B_2 is called a *Giraud disc* and denoted $B(\mathbf{z}_i, \mathbf{z}_j, \mathbf{z}_k)$.

Bisectors are very important because the lack of totally geodesic real hypersurfaces is one of the biggest obstructions to the usual methods for constructing

lattices without relying on arithmetic construction (which always give arithmetic lattices). In fact, the "walls" of fundamental domains in the real hyperbolic case are totally geodesic and one needs a suitable substitute with "nice enough" properties for the complex hyperbolic space. Bisectors have been successful so far because of this special structure they have and they will indeed be the "walls" of the fundamental domains built in this work.

2.4 The Poincaré polyhedron theorem

Once we have built polyhedra whose sides are contained in bisectors, we will use the Poincaré polyhedron theorem to prove that they are indeed fundamental domains for the lattices we want. Here we will present the version of the Poincaré polyhedron theorem that we will use, following the one in [Par06]. Though the theorem can be stated in more generality, here we will always have $X = \mathbf{H}^2_{\mathbb{C}}$.

Definition 2.4.1. A *combinatorial polyhedron* is a cellular space homeomorphic to a compact polytope, with ridges contained in exactly two sides. A *polyhedron* D is the realisation of a combinatorial polyhedron as a cell complex in X. A polyhedron is *smooth* if its cells are smooth. Again, by convention, we will take the polyhedron to be open.

For the Poincaré polyhedron theorem we will need some conditions on the sides and on the ridges of the polyhedron. We will now present such conditions. A smooth polyhedron satisfying all of them is called a *Poincaré polyhedron*.

Let D be a smooth polyhedron in X with sides S_j, side pairing maps $T_j \in \mathrm{Is}(X)$ such that:

(S.1) For each side S_i of D, there is another side S_j of D and a side-pairing map T_i such that $T_i(S_i) = S_j$.

(S.2)[*reflection relation*] If $T_i(S_i) = S_j$, then $T_i = T_j^{-1}$. This implies that if $i = j$, then $T_i^2 = \mathrm{Id}$. The relations $T_i = T_j^{-1}$ are called reflection relations.

(S.3) $T_i^{-1}(D) \cap D = \emptyset$.

(S.4) $T_i^{-1}(\overline{D}) \cap \overline{D} = S_i$.

(S.5) There are only finitely many sides in D and each side contains only finitely many ridges.

(S.6) There exists $\delta > 0$ such that for each pair of disjoint sides, they are at distance at least δ apart.

To list the conditions on the ridges we first need to explain what the cycle transformations are. Let S_1 be a side of D and F be a ridge in the boundary of S_1. Also, let T_1 be the side pairing map associated to S_1 and consider the image under T_1 of the ridge F. Each ridge is contained in the boundary of exactly two sides. $T_1(F)$ will hence be in the boundary of $T_1(S_1)$, but also in the boundary of some other side S_2. We call T_2 the side-pairing map associated to S_2 and we apply it to the ridge $T_1(F)$. Iterating this procedure, we get a sequence of ridges, a sequence of sides S_i and a sequence of maps T_i. Since we assume that the number of sides and the number of ridges are finite(condition (S.5)), these sequences must be periodic. Let k be the smallest integer such that all three sequences (the sequence of ridges, the sequence of sides and the sequence of maps) are periodic with period k. Then $T_k \circ \cdots \circ T_2 \circ T_1(F) = F$ and we call $T_k \circ \cdots \circ T_2 \circ T_1$ the *cycle transformation* at the ridge F. Now, for $T = T_k \circ \cdots \circ T_2 \circ T_1$ and m an integer, we define:

$$\begin{array}{lllll} U_0 = 1, & U_1 = T_1, & .. & U_{k-1} = T_{k-1} \circ .. \circ T_2 \circ T_1, \\ U_k = T, & U_{k+1} = T_1 \circ T, & .. & U_{2k-1} = T_{k-1} \circ .. \circ T_1 \circ T, \\ \vdots & \vdots & \vdots & \end{array}$$

$$U_{(m-1)k} = T^{m-1}, \quad U_{(m-1)k+1} = T_1 \circ T^{m-1}, \quad .. \quad U_{mk-1} = T_{k-1} \circ .. \circ T_1 \circ T^{m-1}.$$

The ridge conditions are then the following.

(F.1) Every ridge is a submanifold of X, homeomorphic to a ball of codimension 2.

(F.2) For each ridge F with cycle transformation T, there exists an integer ℓ such that T^ℓ restricted to F is the identity. This means that a power of T fixes F pointwise.

(F.3)[*cycle relations*] For each ridge F with cycle transformation T, there exists an integer m such that $(T^\ell)^m$ is the identity on the whole space X. Moreover, for the U_i defined previously, the preimages $U_i^{-1}(D)$, for $i = 0, \ldots, m\ell k - 1$ are disjoint and the closures of such polyhedra $U_i^{-1}(\overline{D})$ cover a neighbourhood of the interior of F. In this case we say that D and its images tessellate a neighbourhood of F. The relations $T^{\ell m} = \mathrm{Id}$ are called cycle relations.

The Poincaré polyhedron theorem now states

Theorem 2.4.2. *Let D be a Poincaré polyhedron with side-pairing transformations $T_j \in \Sigma$, satisfying side conditions* (S.1)–(S.6) *and ridge conditions* (F.1)–(F.3). *Then the group Γ generated by the side-pairing transformations is a discrete subgroup of* $\mathrm{Is}(X)$ *and D is a fundamental domain for its action. A presentation for such group is given by*

$$\Gamma = \left\langle \Sigma : \begin{array}{l} \textit{reflection relations} \\ \textit{cycle relations} \end{array} \right\rangle.$$

In Section 5.6 we will use an alternative version of the Poincaré polyhedron theorem, as we will consider fundamental polyhedra for coset decompositions, which can be found in Section 3.2 of [DPP16]. We will here give a brief account of the differences with the version above.

This is used when the polyhedron D is invariant under the action of a non trivial finite group Υ preserving the cells. Moreover, we need Υ to be compatible with the side pairing maps in the following sense.

Definition 2.4.3. For a side S_i with associated side pairing map T_i and a $K \in \Upsilon$, let $S_j = K(S_i)$ with its side pairing T_j. Then we say that the action of Υ on D is *compatible* with the action of the side pairing maps if for each $K \in \Upsilon$ and S_i side, $T_j = KT_iK^{-1}$.

In our case Υ will be a finite cyclic group. Then we will need to consider Γ as the group generated by Υ and the side pairing maps. When considering the cycles described above one needs to consider the orbits under Υ of the ridges. Cycles then will stop as soon as we land in the same orbit under the action of Υ on the initial ridge. The cycle relation will be obtained by applying the element of Υ that sends the new ridge back to the initial one. Changing the initial ridge only corresponds to a cyclic permutation of the components of the cycle transformation T. Hence, we only need to consider the cycle associated to one ridge per orbit of the Υ-action.

2.5 Arithmeticity of lattices

One of the main open problems in complex hyperbolic geometry is the arithmeticity of lattices. Roughly speaking, a subgroup is arithmetic if it is discrete in the initial group "in a similar way" to $\mathbb{Z}$ being discrete in $\mathbb{R}$.

More precisely, we have the following.

Definition 2.5.1. Let $\mathcal{G} \subset GL(m, \mathbb{C})$ be a linear algebraic group (i.e. all the coefficients of elements in $\mathcal{G}$ satisfy polynomial equations with coefficients in $\mathbb{Q}$) and define $\mathcal{G}_{\mathbb{Z}} = \mathcal{G} \cap GL(m, \mathbb{Z})$ and $\mathcal{G}_{\mathbb{R}} = \mathcal{G} \cap GL(m, \mathbb{R})$. For G a semisimple Lie group, let $\varphi \colon \mathcal{G}_{\mathbb{R}} \to G$ be a continuous, surjective homomorphism with compact kernel. We say that $\Gamma < G$ is *arithmetic* if it is commensurable with $\varphi(\mathcal{G}_{\mathbb{Z}})$. We remark that this is a property of Γ, independent on the φ chosen.

As mentioned earlier in this chapter, the complex hyperbolic space is a symmetric space and more specifically it is a rank 1 symmetric space of non-compact type. The other rank 1 symmetric spaces of non-compact type are the real hyperbolic n-space $\mathbf{H}^n_{\mathbb{R}}$, the quaternionic hyperbolic n-space $\mathbf{H}^n_{\mathbb{H}}$ and the octonionic hyperbolic 2-space $\mathbf{H}^2_{\mathbb{O}}$. Among these, the complex hyperbolic space is the only one in which the relation between arithmeticity and lattices has not been settled. In all symmetric spaces of non-compact type, arithmetic groups are lattices, shown in the work of Borel and Harish-Chandra (see [BHC62]). Moreover, in higher rank symmetric spaces of non-compact type, (irreducible) lattices are always arithmetic, thanks to Margulis' superrigidity theorem (see [Mar84]). The converse though is not always true: the works of Corlette [Cor92] and of Gromov and Schoen [GS92] show that non arithmetic lattices are only admissible in $PO(n, 1)$ and $PU(n, 1)$, the (holomorphic) isometry groups of real and complex hyperbolic space. This means that for $\mathbf{H}^2_{\mathbb{O}}$ and $\mathbf{H}^n_{\mathbb{H}}$ when $n \geq 2$ all lattices are arithmetic. In the real hyperbolic space $\mathbf{H}^n_{\mathbb{R}}$ there exist non-arithmetic lattices for all $n \geq 2$, thanks to the work [GPS88] of Gromov and Piatetski-Shapiro.

It is then natural to ask the same question for the complex hyperbolic space, but a general answer is not known. Only some examples of non-arithmetic complex hyperbolic lattices in low dimensions are known. More specifically, Mostow and Deligne-Mostow first (see Chapter 3) built some examples of non-arithmetic

complex hyperbolic lattices in $\mathbf{H}^2_{\mathbb{C}}$. Deraux, Parker and Paupert recently (see [DPP16] and [DPP]) found some more examples. In dimension 3, Deligne and Mostow found the first example of non-arithmetic lattice in $\mathbf{H}^3_{\mathbb{C}}$ and recently Deraux (see [Der17]) identified a group found by Couwenberg-Heckman-Looijenga as the second known example. For $\mathbf{H}^n_{\mathbb{C}}$, $n \geq 4$, it is still an open question whether non-arithmetic lattices exist.

In this work we will study the Deligne-Mostow lattices in $PU(2,1)$, including the non-arithmetic ones.

Chapter 3

Deligne-Mostow lattices

In this section, we will introduce the lattices we will consider all through this work. First, we will summarise the construction by Deligne and Mostow, from which the lattices take their name. Then, we will describe the reinterpretation due to Thurston, which is more relevant to our case, since it is geometric. Later, we will explain how these two constructions are equivalent, following the work of Kojima. Finally, we will list all the lattices that Deligne and Mostow found and we will mention the commensurability theorems that relate some of them. This chapter is just a brief summary of some the main constructions related to the lattices that we will be treating, as explaining these works in more depth is beyond the purpose of this work. For more details and for proofs, one can see the works of Deligne and Mostow [Mos80], [DM86], [Mos86], [Mos88], the work of Thurston [Thu98] and the work of Kojima [Koj01].

The starting point of both constructions is the configuration spaces of points in $\mathbb{CP}^1$. Let us consider N disjoint marked points on $\mathbb{CP}^1$, as shown in Figure 3.1. We will denote the points as $z_1, \cdots z_N$. This means that we are considering the product of N copies of $\mathbb{CP}^1$, each copy determining the position of one of the N points. Since we want the marked points to be pairwise distinct, we exclude the diagonal set, in the sense that we exclude elements in the product where any two components coincide. These points will be included again later when considering the metric completion.

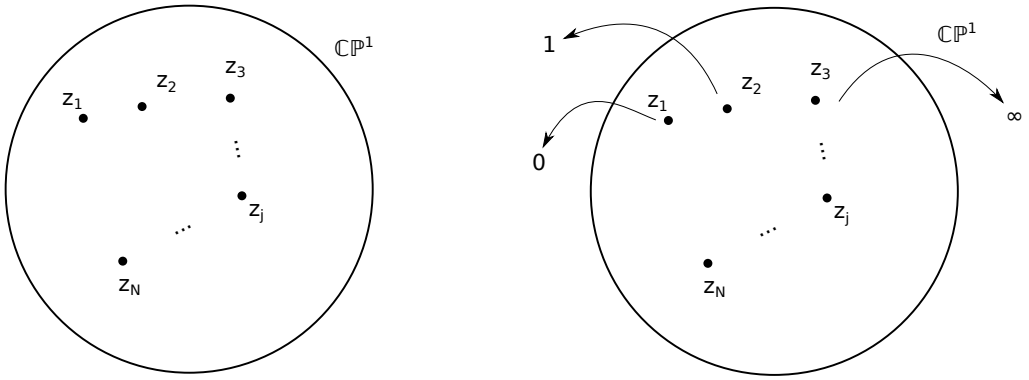

Figure 3.1: The marked points on $\mathbb{CP}^1$ and how to describe a canonical representative in $\mathcal{Q}$.

In other words, we define the *configuration space* $\mathcal{M}$ as

$$\mathcal{M} = \underbrace{\mathbb{CP}^1 \times \cdots \times \mathbb{CP}^1}_{N \text{ times}} \backslash \Delta,$$

where Δ is the diagonal of the product. Now $PSL(2,\mathbb{C})$ acts by Möbius transformations on $\mathcal{M}$ as $g \cdot (z_1, \cdots, z_N) = (g \cdot z_1, \cdots, g \cdot z_N)$, for $g \in PGL(2,\mathbb{C})$ and so we can identify elements in $\mathcal{M}$ up to this action. Hence we define

$$\mathcal{Q} = \mathcal{M} \big/ PGL(2,\mathbb{C}) \cdot$$

We will denote $[z_1, \cdots z_N] \in \mathcal{Q}$ to be the equivalence class of $(z_1, \cdots z_N) \in \mathcal{M}$. We will choose a canonical representative in $\mathcal{Q}$ by sending the first three points z_1, z_2 and z_3 to $0, 1$ and ∞ respectively. The triple transitivity of the action of $PGL(2,\mathbb{C})$ on $\mathbb{CP}^1$ means that we can identify the configuration space $\mathcal{M}$ with the product $\mathcal{Q} \times PGL(2,\mathbb{C})$. This is done by associating to a configuration its canonical representative in $\mathcal{Q}$, as explained and the map in $PGL(2,\mathbb{C})$, i.e. by sending the initial configuration to the representative.

Example 3.0.1. Let us consider the case where $N = 5$ and try to understand the space $\mathcal{Q}$. Since we say that we consider the elements of $\mathcal{Q}$ as the representatives which have the first three marked points in 0, 1 and ∞, $\mathcal{Q}$ is a subset of $\mathbb{CP}^1 \times \mathbb{CP}^1$, as we only need to determine the positions of m_4 and m_5. Now, since we excluded

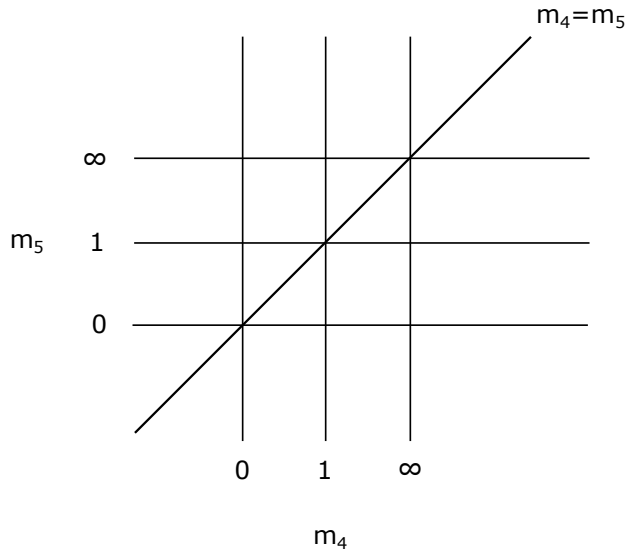

Figure 3.2: Tha space $\mathcal{Q}$ when $n = 5$.

the diagonal in the configuration space, we do not want any of these two to be equal to $0, 1$ or ∞, as the first three marked points are already in these positions. In other words, we are excluding the six lines $m_4 = 0, 1, \infty$ and $m_5 = 0, 1, \infty$. Moreover, the last two points must be disjoint, so we exclude also a seventh line described by $m_4 = m_5$. Therefore $\mathcal{Q}$ can be identified with the complement in $\mathbb{CP}^1 \times \mathbb{CP}^1$ of these seven lines (see Figure 3.2). In three of these points, three lines meet. To symmetrise the construction we can consider the blow up at these three points, hence $\mathcal{Q}$ is the complement of ten lines in $(\mathbb{CP}^1 \times \mathbb{CP}^1)\#3\overline{\mathbb{CP}^2}$, as it includes the seven lines we already had plus three more that "cut" the points with triple intersection.

Starting from this configuration space, two constructions have been studied. The first one, introduced by Deligne and Mostow in [DM86], starts from a ball N-tuple, which consists of N real numbers $\mu = (\mu_1, \cdots \mu_N)$ such that $\sum_j \mu_j = 2$ and $0 < \mu_j < 1$ (see Definition 3.1.1). Then there is a way of constructing a complex hyperbolic structure on $\mathcal{Q}$, described in Section 3.1 and denoted $DM(\mu)$.

Similarly, one can start from a vector $\theta = (\theta_1, \cdots \theta_n)$ such that $\sum_j (2\pi - \theta_j) = 4\pi$ and $0 < \theta_j < 2\pi$. Then one can construct a complex hyperbolic structure on

$\mathcal{Q}$ (or sometimes on a suitable quotient, see Remark 3.1.4) denoted here as $T(\theta)$. This is the one explained in Section 3.2. The following theorem from Kojima (see [Koj01]) says that these two structures are equivalent.

Theorem 3.0.2. *We have $DM(\mu) = T(\theta)$, when $\theta_j = 2\pi(1-\mu_j)$.*

The following sections 3.1, 3.2 and 3.3 will present the two constructions and prove this theorem.

3.1 Monodromy of hypergeometric functions

We will now summarise the construction from Deligne and Mostow that leads to the lattices that we will study in this work, in the form presented in [Koj01]. The lattices arise as monodromy groups of hypergeometric functions. First we will explain how Deligne and Mostow in [DM86] constructed a complex hyperbolic structure on $\mathcal{Q}$. They started with the following.

Definition 3.1.1. A *ball N-tuple* $\mu = (\mu_1, \cdots, \mu_N)$ is a set of N real numbers such that

$$\sum_{i=1}^{N} \mu_i = 2, \qquad 0 < \mu_i < 1, \qquad i = 1, \cdots, N. \tag{3.1.1}$$

Now choose a configuration $m = (m_1, \cdots m_N) \in \mathcal{M}$. We will denote $\mathbf{P}_m = \mathbb{CP}^1 \setminus \{m_1, \ldots, m_N\}$. The elements of the ball N-tuple are the weights associated to the points in m. Then one can consider the 1-form defined by

$$\omega_m = \prod_j (z - m_j)^{-\mu_j} dz. \tag{3.1.2}$$

For two indices $a, b \in \{1, \cdots, N\}$ and choosing a path in $\mathbf{P}_m$ (except for the endpoints), we can define the hypergeometric function

$$F_{ab}(m) = \int_{z_a}^{z_b} \omega_m. \tag{3.1.3}$$

This is a multivalued function since, for example, the value of the integral depends on the path chosen, but it can be lifted to a single valued function on $\widetilde{\mathcal{Q}}$, the universal cover of $\mathcal{Q}$, which we will do later.

We now want to explain how to construct a family of complex hyperbolic structures on $\mathcal{Q}$, indexed by the ball N-tuple μ. Then we will explain how to associate a subgroup Γ_μ of $PU(N-3,1)$ to each μ.

Let us consider a flat complex line bundle L_m on $\mathbf{P}_m$. We choose the one determined by asking that the holonomy along a loop around each of the m_j is the complex multiplication by $e^{2\pi i\mu_j}$. Moreover, we fix a Hermitian structure on L_m. The idea is that the form ω_m is hard to study in $\mathbf{P}_m$, but easier on L_m.

The next step of Deligne and Mostow's work was to prove that the compact cohomology is all we need to study the 1-forms on $\mathbf{P}_m$. In other words,

Proposition 3.1.2. *$H^1_c(\boldsymbol{P}_m, L_m) \cong H^1(\boldsymbol{P}_m, L_m)$.*

Moreover, we claim that the dimension of this complex vector space is $N-2$. In fact, to calculate the dimension, one needs to remember that the Euler characteristic is the alternating sum of the Betti numbers, i.e. of the dimension of the cohomology groups. But since L_m is non trivial, the 0-cohomology vanishes and so does the 2-cohomology by Poincaré duality. The Euler characteristic of $\mathbf{P}_m$ is

$$\chi(\mathbf{P}_m) = \chi(\mathbb{CP}^1) - \chi(\{m_1, \cdots m_N\}) = 2 - N.$$

Now in the sum of the Betti numbers only the dimension of $H^1(\mathbf{P}_m, L_m)$, with negative sign, remains, so the dimension is $-(2-N) = N-2$. Moreover, the Hermitian structure on L_m defines a Hermitian structure on $H^1(\mathbf{P}_m, L_m)$.

Now we have that the Poincaré duality pairing induces the map

$$\begin{array}{rccccc} \psi_0 \colon H^1_c(\mathbf{P}_m, L_m) \times H^1_c(\mathbf{P}_m, \overline{L}_m) & \to & H^2_c(\mathbf{P}_m, \mathbb{C}) & \xrightarrow{\sim} & \mathbb{C} \\ (\omega_1, \omega_2) & \mapsto & \omega_1 \wedge \omega_2 & \mapsto & \displaystyle\int_{\mathbf{P}_m} \omega_1 \wedge \omega_2 \end{array}$$

and we can consider the form on $H^1_c(\mathbf{P}_m, L_m)$ defined as

$$\begin{array}{rcl} \psi \colon H^1_c(\mathbf{P}_m, L_m) \times H^1_c(\mathbf{P}_m, L_m) & \to & \mathbb{C} \\ (\omega, \eta) & \mapsto & \displaystyle -\frac{1}{2\pi i}\psi_0(\omega, \overline{\eta}) = -\frac{1}{2\pi i}\int_{\mathbf{P}_m} \omega \wedge \overline{\eta}. \end{array}$$

Hence

$$\psi_0(\omega_1, \omega_2) = \int_{\mathbf{P}_m} \omega_1 \wedge \omega_2 \qquad \text{and} \qquad \psi(\omega, \eta) = -\frac{1}{2\pi i}\psi_0(\omega, \overline{\eta}). \tag{3.1.4}$$

Using Hodge theory, Deligne and Mostow proved that ψ is a Hermitian form of signature $(1, N-3)$ and that ω_m defined in (3.1.2) is in the positive component of the space with respect to ψ.

Let us now consider U a contractible neighbourhood of m in $\mathcal{M}$. In other words, we are considering small perturbations of the positions of the points in the configuration. The line bundle L_m can be extended uniquely to a flat complex line bundle L_U on $\bigcup_{m\in U} \mathbf{P}_m$. Moreover, taking a covering $\mathcal{M} = \bigcup_j U_j$, one can use the L_{U_j}'s to define flat vector bundles which can be projectified and glued together into a flat projective space bundle on $\mathcal{M} = \mathcal{Q} \times PGL(2,\mathbb{C})$. We call this flat projective space bundle $B(\mu)$. Its fibres are the spaces $\mathbb{P}H^1_c(\mathbf{P}_m, L_m) \cong \mathbb{CP}^{N-3}$, since it is the projectivisation of the fibre of a vector bundle of rank $N-2$ as we mentioned.

Now one can show that the map which associates to each point $m \in \mathcal{M}$ the projective class $[\omega_m]$ of the form ω_m defined in (3.1.2) is a holomorphic section ω_μ of $B(\mu)$

$$\begin{aligned} \omega_\mu \colon \mathcal{M} &\to B(\mu) \\ m &\mapsto [\omega_m] \in \mathbb{P}H^1_c(\mathbf{P}_m, L_m) \cong \mathbb{CP}^{N-3}. \end{aligned}$$

This section is equivariant with respect to the action of $PGL(2,\mathbb{C})$, so it passes to the quotient $\mathcal{Q}$ and we have a section on $\mathcal{Q}$, seen as $\mathcal{Q} \times \{\mathrm{Id}\} \subset \mathcal{M} = \mathcal{Q} \times PGL(2,\mathbb{C})$

$$\omega_\mu|_{\mathcal{Q}} \colon \mathcal{Q} = \mathcal{Q} \times \{\mathrm{Id}\} \to B(\mu)|_{\mathcal{Q}}.$$

Now consider the universal cover $p \colon \widetilde{\mathcal{Q}} \to \mathcal{Q}$. Then we can pull back the projective bundle $B(\mu)|_{\mathcal{Q}}$ by p and get a projective bundle $\widetilde{B(\mu)|_{\mathcal{Q}}}$ on $\widetilde{\mathcal{Q}}$. Moreover, $\widetilde{B(\mu)|_{\mathcal{Q}}}$ admits the product structure $\widetilde{B(\mu)|_{\mathcal{Q}}} = \widetilde{\mathcal{Q}} \times B(\mu)|_0$, where $0 \in \mathcal{Q}$ is a fixed base point configuration in $\mathcal{Q}$, so we can denote the projection of the bundle as p_1, being the projection on the first term of the product space. The map p_2 will be the projection on the second term of the product. We can pull back $\omega_\mu|_{\mathcal{Q}}$ by p and get a section of this new bundle. Now consider the projection on the second factor $p_2 \colon \widetilde{\mathcal{Q}} \times B(\mu)|_0 \to B(\mu)|_0$ and take the composition of the pull back

$p^*\omega_\mu|_{\mathcal{Q}}$ and the projection p_2. We will denote it $\widetilde{\omega_\mu}$.

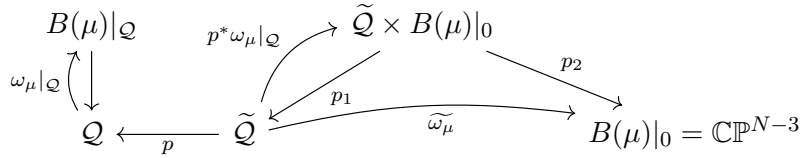

To determine the form ω_μ it is enough to give the value of its integral along paths connecting two points in m. This means that is is enough to determine the values of the functions F_{ab} in (3.1.3). In other words, we are lifting the multi valued function F_{ab} on $\mathcal{Q}$ to a single valued function on $\widetilde{\mathcal{Q}}$.

Deligne and Mostow then prove the following.

Proposition 3.1.3. • $\operatorname{Im}\widetilde{\omega_\mu} \subset \mathbb{B}$, *the unit ball with respect to* ψ *in* $\mathbb{CP}^{N-3}$;

- $\widetilde{\omega_\mu}$ *is locally biholomorphic;*
- $\widetilde{\omega_\mu}$ *is invariant under the action of* $\pi_1(\mathcal{Q})$ *and preserves the Bergmann metric on* $\mathbb{B}$.

Now we can pull back by $\widetilde{\omega_\mu}$ the metric on $\mathbb{B}$ to $\widetilde{\mathcal{Q}}$ and by the last point of the proposition this descends to a complex hyperbolic structure on $\mathcal{Q}$, which we denote $DM(\mu)$.

Since $\widetilde{\omega_\mu}$ is equivariant with respect to $\pi_1(\mathcal{Q})$, it induces a representation

$$\rho_\mu \colon \pi_1(\mathcal{Q}) \to PGL(N-2, \mathbb{C}).$$

We will call this the *monodromy action* and $\Gamma_\mu = \operatorname{Im}\rho_\mu$ is the *monodromy group*. One can prove that the elements of Γ_μ preserve the Hermitian form given by the complex hyperbolic structure on $\mathcal{Q}$ and hence lie in $PU(N-3, 1)$.

Remark 3.1.4. We will mostly consider the groups $\Gamma_{\mu\Sigma}$, related to the Γ_μ in the following way. Let $\mathcal{S}_N$ be the group of permutations on N letters and let Σ be the subgroup of $\mathcal{S}_N$ permuting some of the marked points having same weight, i.e. for all $\sigma \in \Sigma$, we have $\sigma(z_i) = z_j$ only if $\mu_i = \mu_j$. Then we can consider the subset Q' of Q on which Σ acts without fixed points and extend the monodromy map to Q'/Σ. Then $\Gamma_{\mu\Sigma}$ is the image of the monodromy representation of $\pi_1\left(Q'/\Sigma\right)$. Note that Σ doesn't have to be the full group of symmetries of the ball N-tuple.

In [Mos86], Mostow gave a criterion for a ball N-tuple to give a lattice in $PU(N,1)$, which is the following.

Definition 3.1.5. A ball N-tuple μ satisfies the condition ΣINT if, for a pair of indices $i,j \in \{1,\cdots,N\}$ satisfying $\mu_i + \mu_j < 1$, we have one of the following:

- either $1-\mu_i-\mu_j = 1/n_{ij}$ for some $n_{ij} \in \mathbb{Z}$,
- or $\mu_i = \mu_j$ and $1/2 - \mu_i = 1/m_{ij}$ for some $m_{ij} \in \mathbb{Z}$.

Then,

Theorem 3.1.6. *If a ball N-tuple μ satisfies the condition ΣINT, then the associated group Γ_μ is a lattice in $PU(N-3,1)$.*

We remark that in general this is not an if and only if. In [Mos88], Mostow showed that for $N-3 \geq 4$, the condition ΣINT characterises discreteness. On the other hand, for $N-3=3$ there is exactly one discrete group non satisfying ΣINT. For $N-3=2$, which is the case we will consider in this work, Mostow could show that all groups except 9 were either non-discrete or satisfied ΣINT. Later, Sauter (see [Sau90]) proved that the remaining 9 groups are also discrete and that they are commensurable to the lattices found by Deligne and Mostow, but obtained considering different generators. These are the Deligne-Mostow lattices in $PU(2,1)$ that are not treated in this work.

3.2 Cone metrics on the sphere

In [Thu98], Thurston gave a different interpretation of the same lattices in terms of cone metrics on a sphere.

Let us start with the following.

Definition 3.2.1. Let M be a surface. Then a point $p \in M$ is a *cone singularity* if the total angle θ_0 around p is different from 2π. The corresponding angle θ_0 is called a *cone angle*. The angle $\alpha_0 = 2\pi - \theta_0$ is called the *curvature* at the point p. In other words, p is a cone point of cone angle θ_0 if a neighbourhood of p in M is modelled on the cone

$$C_{\theta_0} = \{z = re^{i\theta}, 0 < \theta < \theta_0\}/\sim,$$

where $\sim$ denotes the identification $r \sim re^{i\theta_0}$. We will call a *flat cone metric* on the surface M a metric that is locally modelled on $\mathbb{R}^2$ except for a finite number of points which are cone singularities.

Even though in general cone singularities can have cone angles bigger than 2π, in this work we will always consider cone points with cone angles (and hence curvatures) in $(0, 2\pi)$.

Example 3.2.2.

- If we consider a cube and smooth the edges (i.e. we consider a metric that is smooth neat the interior points of the edges), then we remain with a sphere with eight cone singularities. Around each singularity three squares meet, so the total angle around is $\frac{3\pi}{2}$.
- In general, a Euclidean polyhedron is a cone metric on a sphere given by smoothing the sides and which has cone singularities at the vertices.
- A different example of a cone metric on a sphere is a pillowcase, i.e. two squares glued along the boundary. This is a cone metric with four cone points of cone angles π.

Take now a cone metric on a surface M with N cone singularities of angles $(\theta_1, \cdots, \theta_N)$. Then it must satisfy the discrete version of the Gauss-Bonnet theorem, i.e.

$$\sum(2\pi - \theta_i) = 2\pi(2 - 2g), \tag{3.2.1}$$

where g is the genus of M (see, for example [McM17]).

Remembering that the curvatures are $\alpha_i = 2\pi - \theta_i$, we will consider cone metrics on a sphere with curvatures satisfying

$$\sum_{i=1}^{N} \alpha_j = 4\pi, \qquad 0 < \alpha_i < 2\pi, \qquad \text{for } i = 1, \ldots, N. \tag{3.2.2}$$

Moreover, we will consider some special cone metrics.

Definition 3.2.3. We say that a cone metric with curvatures as in (3.2.2) satisfies the *orbifold condition* if, for any pair α_i, α_j such that $\alpha_i + \alpha_j < 2\pi$, then

- either $2\pi - \alpha_i - \alpha_j$ divides 2π,
- or $\alpha_i = \alpha_j$ and $\pi - \alpha_i$ divides 2π.

Thurston's main result is to consider the moduli space of cone metrics with fixed cone angles on a sphere and to prove that they form a complex hyperbolic cone manifold. Intuitively, cone manifolds have singularities like the ones obtained from n-dimensional polyhedra by glueing together pairs of $(n-1)$-dimensional facets. More precisely, they can be defined by induction as follows.

Definition 3.2.4. Let X be a complete connected Riemannian n-manifold and G a group of isometries of X. The space X will be our model space. We remark that G does not need to be the full isometries of X and that it does not necessarily act transitively (hence this is not necessarily a symmetric space).

An (X, G)-*manifold* is a space equipped with a covering by open sets homeomorphic to (a subset of) X, such that the transition maps on the intersections of the open sets are in G.

Now we will define a cone manifold by induction on the dimension.

- If X has dimension 1, then an (X, G)-*cone manifold* is just an (X, G)-manifold.

- If X has dimension k, then for each $p \in X$ consider G_p the stabiliser of p in G and $X_p \subset T_pX$ the unit tangent sphere in the tangent space at p. Then (X_p, G_p) has dimension $k-1$ and so we know how to define an (X_p, G_p)-cone manifold Y. Now to Y one can associate the cone over Y, denoted as $C(Y)$, in the following way. To a subset of X_p one can associate the cone at p in the tangent space over X_p and project it onto X via the exponential map (up to rescaling the radius to make the exponential map be an embedding). Now Y is modelled on X_p, so we can use the transition maps in G_p to glue these cones together and get the cone $C(Y)$.

  Now an (X, G)-cone manifold is a space M such that for each $x \in M$, a neighbourhood of x in M is isometric to $C(Y)$ for some compact, connected (X_p, G_p)-cone manifold Y.

Thurston proved the following.

Theorem 3.2.5. *Let $\alpha_1, \cdots, \alpha_N$ be N real numbers in $(0, 2\pi)$ whose sum is 4π. Then the set of Euclidean cone metrics on the sphere with cone points of curvatures*

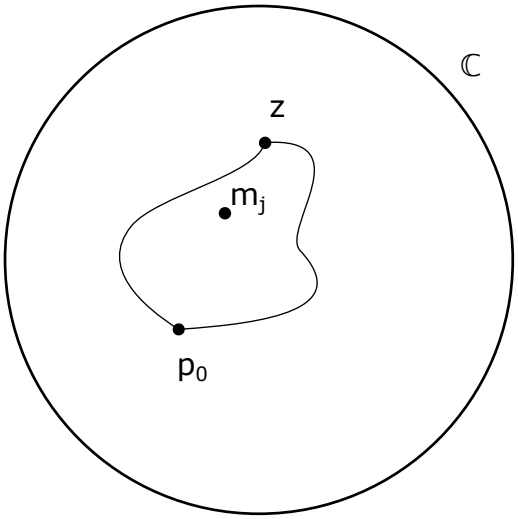

Figure 3.3: Two paths going around a marked point in different ways.

α_i and area 1 form a complex hyperbolic manifold of dimension $N-3$, whose metric completion is a complex hyperbolic cone-manifold of finite volume. This cone manifold is an orbifold if and only if the α_i's satisfy the orbifold condition.

Remark 3.2.6. The lack of completeness comes from the fact that one can build Cauchy sequences of cone metrics where two cone points get closer and closer. The limit cone metric is where the two cone points coalesce and it does not belong to the manifold because the number of cone points is now decreased. To build the metric completion one needs to add configurations obtained by pairs of cone points coalescing.

Note that Thurston's construction is done on the quotient of $\mathcal{Q}$ by relabelling the cone points with same cone angle (see Remark 3.1.4).

The set of cone metrics is related to the space $\mathcal{Q}$ introduced at the beginning of the chapter. As previously remarked, the common root of both constructions is the 1-form in (3.1.2). Now, if we choose a base point p_0 and a path outside of the marked points, we can integrate the form along the path and get

$$h(z) = \int_{p_0}^{z} \omega_m = \int_{p_0}^{z} \prod_j (t - m_j)^{-\mu_j} dt. \tag{3.2.3}$$

This is not a well defined function, but it is multi-valued, since paths going around

the marked points in different ways (see Figure 3.3) give different values of the integral. At the same time, one can see it as a map $h\colon \widetilde{\mathbf{P}}_m \to \mathbb{C}$, from the universal cover of $\mathbf{P}_m = \mathbb{CP}^1 \setminus \{m_1, \dots, m_n\}$.

One can calculate the pre-schwarzian of h, which is h''/h',

$$\begin{aligned}\frac{h''}{h'} &= \frac{\sum_k (-\mu_k)(z-m_k)^{-\mu_k-1}\prod_{j\neq k}(z-m_j)^{-\mu_j}}{\prod_j (z-m_j)^{-\mu_j}} \\ &= \frac{\sum_k (-\mu_k)(z-m_k)^{-\mu_k-1}}{(z-m_k)^{-\mu_k}} = \sum_k \frac{-\mu_k}{z-m_k}\end{aligned}$$

and see that it is a single-valued function. Kojima explains that this implies that one can pass between two images of h obtained using two different paths (i.e. change of analytic continuation around a singular point) using an affine map $z \mapsto az + b$. Moreover, one can see that such a map is Euclidean (i.e. it preserves a Euclidean structure on $\mathbb{C}$), so $|a| = 1$. This allows the map on the universal cover to pass to the quotient. In other words, let us take the Euclidean structure on $\mathbb{C}$ preserved by the affine map. We then pull it back using $h\colon \widetilde{\mathbf{P}}_m \to \mathbb{C}$ and get a Euclidean structure on the universal cover. But the projection of the universal cover on $\mathbf{P}_m$ gives us a Euclidean structure on $\mathbf{P}_m$ itself, since the Euclidean structure on $\mathbb{C}$ is preserved by the changes of image. Its completion gives cone points singularities at the marked points m_j, of angles $2\pi(1-\mu_j)$. We denote such a sphere with cone points by Δ_m.

In this way, we created a map $\mathcal{M} \ni m \mapsto \Delta_m$. This correspondence is not quite 1:1, but it becomes a bijection if we consider it as a map

$$\mathcal{Q} \xrightarrow{1:1} \{\Delta_m\}_{m\in\mathcal{Q}}/\mathbb{C}^*,$$

which means that we are considering $\mathcal{M}$ up to projective equivalence, as explained at the beginning of this chapter, and the cone spheres up to similarity. In other words, we are relating the ball N-tuple as in (3.1.1) and the curvature as in (3.2.2) and saying that for a ball N-tuple $(\mu_1, \dots, \mu_N)$ we can construct a cone metric on the sphere with curvatures α_i and vice versa by imposing

$$\alpha_i = 2\pi - \theta_i = 2\pi\mu_i. \tag{3.2.4}$$

Moreover, we have the following.

Lemma 3.2.7. *Mostow's condition ΣINT for ball N-tuples (see 3.1.5) is equivalent to Thurston's orbifold condition for curvatures at cone points of a sphere (see 3.2.3).*

We will now give local coordinates around $\Delta_{m_0} \in {}^{\{\Delta_m\}_{m\in\mathcal{Q}}}\!/_{\mathbb{C}^*}$, which we will use to show the equivalence in Section 3.3. Thurtson's first step is to prove that triangulations on Δ_m with vertices at the cone points exist. Then we can fix a triangulation $\mathcal{T}$ and define E the set of all oriented edges of $\mathcal{T}$ in $\Delta_m \setminus \{\textit{cone points}\}$, choosing an orientation. For $e \in E$, up to passing to the universal cover, one can consider $i(e)$ and $t(e)$ the initial and terminal points of e respectively and then calculate h on the two endpoints and consider $h(i(e)), h(t(e)) \in \mathbb{C}$. Then for each $e \in E$ we can define $z_m(e)$ as the difference of the two endpoints. This gives the map

$$\begin{aligned} z_m \colon E &\to \mathbb{C} \\ e &\mapsto z_m(e) = h(t(e)) - h(i(e)). \end{aligned}$$

Now the map z_m satisfies the following properties:

1. If e_1, e_2 and e_3 surround a triangle, then $z_m(e_1) + z_m(e_2) + z_m(e_3) = 0$;
2. $z_m(\gamma e) = H(\gamma) z_m(e)$, where γ is an element of $\pi_1(\mathbf{P}_m)$, acting on E and $H(\gamma)$ is the rotational part of the holonomy of γ. In other words, when in the universal cover we change the homotopy class, we still get cocycles, but with twisted coefficients.

Conversely, a neighbourhood of Δ_{m_0} can be described as

$$Z = \{z \colon E \to \mathbb{C} \text{ satisfying properties 1. and 2., } \forall\, \gamma \in \pi_1(\mathbf{P}_m)\},$$

since any cocycle determines triangles that glue up forming the sphere with cone singularities. This is a vector space of dimension $N - 2$.

Now one can also consider the map

$$\begin{aligned} \text{Area} \colon Z &\to \mathbb{C} \\ z_m &\mapsto \text{Area}\, \Delta_m \end{aligned} \tag{3.2.5}$$

and prove that this is a Hermitian form of signature $(1, N-3)$. The area form induces a complex hyperbolic structure on the ball $\mathbb{B} \subset \mathbb{P}Z$, and so by using the local coordinates on the cone spheres up to similarity, it induces a complex hyperbolic structure on $\mathcal{Q}$. We denote its completion by $T(\mu)$.

3.3 Equivalent constructions

We now want to give an idea of how to prove Theorem 3.0.2. This will proceed in two steps. First, we will show that the two local charts we constructed are the same (Lemma 3.3.1). Then we will show that the metrics are the same, hence so are their completions (Lemma 3.3.2).

Lemma 3.3.1. *There is a bijection*

$$\begin{aligned} \mathbb{CP}^{N-3} = B(\mu)|_0 &\xrightarrow{1:1} \mathbb{P}Z \\ \omega_m &\mapsto z_m. \end{aligned}$$

Proof. Since Z is a vector space of dimension $N-2$, z_m is determined by its value on $N-2$ edges $e_1, \cdots e_{N-2}$. Then the correspondence is given by

$$z_m(e_j) = \int_{h(e_j)} dz = \int_{e_j} h^* dz = \int_{e_j} h' dz = \int_{e_j} \omega_m,$$

since these values are enough to determine ω_m. ∎

Lemma 3.3.2. *The correspondence in Lemma 3.3.1 also gives that the area Hermitian form in* (3.2.5) *is equal to* $\pi\psi$.

Proof. Since the area of the whole cone sphere is made up of the sum of the areas of the triangles in the triangulation $\mathcal{T}$, it is enough to verify the equation on a triangle. Now, by definition, the area of a triangle Δ is

$$\begin{aligned} \text{Area}\,\Delta &= -\frac{1}{2i}\int_{h(\Delta)} dz \wedge d\overline{z} = -\frac{1}{2i}\int_{\Delta} h^*(dz \wedge d\overline{z}) = -\frac{1}{2i}\int_{\Delta} |h'(z)|^2 dz \wedge d\overline{z} \\ &= -\frac{1}{2i}\int_{\Delta} h'(z)dz \wedge \overline{h'(z)dz} = -\frac{1}{2i}\int_{\Delta} \omega_m \wedge \overline{\omega}_m \\ &= -\frac{1}{2i}\psi_0|_{\Delta}(\omega_m, \overline{\omega}_m) = \pi\psi|_{\Delta}(\omega_m, \omega_m), \end{aligned}$$

where the second row follows from the fact that we can write $|h'(z)|^2 = h'(z)\overline{h'(z)}$ and the third row follows from the definitions of ψ_0 and ψ in (3.1.4) ∎

3.4 The list of lattices

Putting together Deligne, Mostow and Thurston's work, one gets to a complete list of lattices that can arise using their construction. This list can be found, for example, in the table in the Appendix of Thurston's paper [Thu98]. In this work, we will consider all the 2-dimensional lattices that appear in the list by Deligne and Mostow. This excludes some of the ball 5-tuples that still give lattices, namely those that do not satisfy the condition ΣINT and the cases when $p = \infty$. It was shown later by Sauter in [Sau90] that these also give lattices which are all commensurable to some of the lattices that we treat in this work. The 2-dimensional lattices arise when considering ball 5-tuples or equivalently a sphere with five cone singularities. All of them have some special symmetry, namely they have either 3- or 2-fold symmetry. This means that either two or three of the elements in the ball 5-tuple are the same, or, equivalently, that the cone angles of either two or three of the cone points have the same value. In the rest of this section, we will list the ball 5-tuples that give lattices and introduce the parameters that we will use to study them.

3.4.1 Lattices with 3-fold symmetry

In this section we will list the Deligne-Mostow lattices with 3-fold symmetry. More specifically, we will describe, following [Par09], how to parametrise them and which special quantities are associated to them. We will always assume that the 3-fold symmetry is given by $\mu_2 = \mu_3 = \mu_4$.

Since there are five cone points, three of them have the same cone angle. Now the discrete Gauss-Bonnet formula (see (3.2.1)) guarantees that two parameters are enough to uniquely identify a ball 5-tuple. To each ball 5-tuple, we associate the curvature and the cone angles of the singularities on the sphere, from which we can obtain a lattice in the way we will see in the following chapters. Here, we will use two parameters p and k to identify the lattices associated to a certain ball 5-tuple and we will denote the lattice as (p, k). These parameters are related

to the ball 5-tuple in the following way.

$$\mu_1 = \frac{1}{2} + \frac{1}{p} - \frac{1}{k}, \qquad \mu_2 = \mu_3 = \mu_4 = \frac{1}{2} - \frac{1}{p}, \qquad \mu_5 = \frac{2}{p} + \frac{1}{k}. \tag{3.4.1}$$

In some of the literature on the subject, the lattices are identified by the two parameters p and t instead. The parameter t is a real number used by Mostow to describe the lattices, together with $p = 3, 4, 5$ in [Mos80] and is defined as

$$t = \frac{1}{p} + \frac{2}{k} - \frac{1}{2} = \mu_5 - \mu_1. \tag{3.4.2}$$

It is called the phase shift, because Mostow's phase parameter is φ, defined by $\varphi^3 = e^{\pi i t}$. One particular critical value of this parameter is $\frac{1}{2} - \frac{1}{p}$. We will say, following Mostow, that it is a lattice with *large phase shift* if the condition $|t| > \frac{1}{2} - \frac{1}{p}$ holds. The opposite condition is a *small phase shift*. This value is important because it corresponds to a change of sign in the parameter l defined below. In Section 5.4 we will see why this is relevant for our analysis.

To each lattice we also associate some other quantities that depend on p and k. All these values are important because they will be the order of some special elements of the lattice associated to the ball 5-tuple. These parameters are defined from p and k in the following way:

$$\frac{1}{l} = \frac{1}{2} - \frac{1}{p} - \frac{1}{k}, \qquad \frac{1}{d} = \frac{1}{2} - \frac{3}{p}. \tag{3.4.3}$$

Table 3.1 summarizes all Deligne-Mostow lattices with three fold symmetry. The lattices are divided according to the values of the four parameters in the first four columns, p, k, l and d. The last column is the value of the orbifold Euler characteristic for the lattice associated, calculated in Chapter 7. We remark that we always consider the lattice modulo the symmetry given by the 3-fold symmetry (or the 4-fold symmetry, when present). Other symmetries are ignored.

Lattice (p,k)	p	k	l	d	t	μ_1	$\mu_{2,3,4}$	μ_5	χ
(3,4)	3	4	-12	-2	1/3	7/12	1/6	11/12	1/288
(3,5)	3	5	-30	-2	7/30	19/30	1/6	13/15	2/225
(3,6)	3	6	∞	-2	1/6	2/3	1/6	5/6	1/72

(4,3)	4	3	-12	-4	5/12	5/12	1/4	5/6	1/72
(4,4)	4	4	∞	-4	1/4	1/2	1/4	3/4	1/64
(5,2)	5	2	-5	-10	7/10	1/5	3/10	9/10	1/200
(5,5/2)	5	5/2	-10	-10	1/2	3/10	3/10	4/5	1/200
(5,3)	5	3	-30	-10	11/30	11/30	3/10	11/15	8/225
(6,2)	6	2	-6	∞	2/3	1/6	1/3	5/6	1/72
(6,3)	6	3	∞	∞	1/3	1/3	1/3	2/3	1/18
(3,7)	3	7	42	-2	5/42	29/42	1/6	17/21	61/3528
(3,8)	3	8	24	-2	1/12	17/24	1/6	19/24	11/576
(3,9)	3	9	18	-2	1/18	13/18	1/6	7/9	13/648
(3,10)	3	10	15	-2	1/30	11/15	1/6	23/30	37/1800
(3,12)	3	12	12	-2	0	3/4	1/6	3/4	1/48
(4,5)	4	5	20	-4	3/20	11/20	1/4	7/10	33/800
(4,6)	4	6	12	-4	1/12	7/12	1/4	2/3	13/288
(4,8)	4	8	8	-4	0	5/8	1/4	5/8	3/64
(5,4)	5	4	20	-10	1/5	9/20	3/10	13/20	23/400
(5,5)	5	5	10	-10	1/10	1/2	3/10	3/5	13/200
(6,4)	6	4	12	∞	1/6	5/12	1/3	7/12	11/144
(6,6)	6	6	6	∞	0	1/2	1/3	1/2	1/12
(7,2)	7	2	-7	14	9/14	1/7	5/14	11/14	1/49
(8,2)	8	2	-8	8	5/8	1/8	3/8	3/4	3/128
(9,2)	9	2	-9	6	11/18	1/9	7/18	13/18	2/81
(10,2)	10	2	-10	5	3/5	1/10	2/5	7/10	1/40
(12,2)	12	2	-12	4	7/12	1/12	5/12	2/3	7/288
(18,2)	18	2	-18	3	5/9	1/18	4/9	11/18	13/648
(7,3)	7	3	42	14	13/42	13/42	5/14	13/21	61/882
(8,3)	8	3	24	8	7/24	7/24	3/8	7/12	11/144
(9,3)	9	3	18	6	5/18	5/18	7/18	5/9	13/162
(10,3)	10	3	15	5	4/15	4/15	2/5	8/15	37/450
(12,3)	12	3	12	4	1/4	1/4	5/12	1/2	1/12
(18,3)	18	3	9	3	2/9	2/9	4/9	4/9	13/162

(7,7/2)	7	7/2	14	14	3/14	5/14	5/14	4/7	1/49
(8,4)	8	4	8	8	1/8	3/8	3/8	1/2	3/128
(9,9/2)	9	9/2	6	6	1/18	7/18	7/18	4/9	2/81
(10,5)	10	5	5	5	0	2/5	2/5	2/5	1/40
(12,6)	12	6	4	4	1/12	5/12	5/12	1/3	7/288

Table 3.1: Deligne-Mostow lattices with three fold symmetry.

The first four groups are based on the possible combinations of the signs of the parameters l and d. Sometimes we will refer to these groups as lattices of type one, two, three and four. The fifth group is where $k = \frac{p}{2}$. Together with the lattice where $p = 5$ and $k = \frac{5}{2}$, these are the 4-fold symmetry lattices.

Note also that one can also write k, l and d in terms of the ball 5-tuple as follows.

$$k = (1 - \mu_2 - \mu_1)^{-1}, \qquad l = (1 - \mu_2 - \mu_5)^{-1}, \qquad d = (1 - \mu_1 - \mu_5)^{-1}.$$

Then the integrality condition in 3.1.5 asks for the three values to be integers.

3.4.2 Lattices with 2-fold symmetry

In this section, we will consider the lattices with 2-fold symmetry and list them with some important parameters associated to the lattices. We will assume that the 2-fold symmetry is given by $\mu_2 = \mu_3$. Sometimes the lattices will have an extra symmetry and we will also have $\mu_1 = \mu_4$.

We will identify the lattices using three parameters p, k and p'. We will denote the lattice as (p, k, p'). They are related to the ball 5-tuple in the following way:

$$\mu_1 = \frac{1}{2} + \frac{1}{p'} - \frac{1}{k}, \quad \mu_2 = \mu_3 = \frac{1}{2} - \frac{1}{p'}, \quad \mu_4 = \frac{1}{2} + \frac{1}{p'} - \frac{1}{p}, \quad \mu_5 = \frac{1}{p} + \frac{1}{k}.$$

By similarity with the 3-fold symmetry case, to each lattice we will also associate numbers k', l, l', d, which (together with p, k and p') are the orders of some

maps in the group and are defined as follows.

$$\frac{1}{l} = \frac{1}{2} + \frac{1}{p'} - \frac{1}{p} - \frac{1}{k}, \qquad \frac{1}{k'} = \frac{1}{p} + \frac{1}{k} - \frac{2}{p'},$$
$$\frac{1}{l'} = \frac{1}{2} - \frac{1}{p'} - \frac{1}{k}, \qquad \frac{1}{d} = \frac{1}{2} - \frac{1}{p'} - \frac{1}{p}.$$

In the following table we give the values of the ball 5-tuple associated to the lattice (p, k, p').

Lattice (p, k, p')	μ_1	μ_2	μ_3	μ_4	μ_5
(6,6,3)	2/3	1/6	1/6	2/3	1/3
(10,10,5)	3/5	3/10	3/10	3/5	1/5
(12,12,6)	7/12	1/3	1/3	7/12	1/6
(18,18,9)	5/9	7/18	7/18	5/9	1/9
(4,4,3)	7/12	1/6	1/6	7/12	1/2
(4,4,5)	9/20	3/10	3/10	9/20	1/2
(4,4,6)	5/12	1/3	1/3	5/12	1/2
(3,3,4)	5/12	1/4	1/4	5/12	2/3
(3,3,3)	2/3	1/6	1/6	1/2	1/2
(2,6,6)	1/2	1/3	1/3	1/6	2/3
(2,4,3)	7/12	1/6	1/6	1/3	3/4
(2,3,3)	1/2	1/6	1/6	1/3	5/6
(3,4,4)	1/2	1/4	1/4	5/12	7/12

Table 3.2: The Deligne-Mostow lattices with 2-fold symmetry.

Below are the values of the important parameters we will need, together with the value of the orbifold Euler characteristic χ as calculated in Chapter 7.

Lattice (p, k, p')	p	k	p'	k'	l	l'	d	χ
(6,6,3)	6	6	3	-3	2	∞	∞	1/24
(10,10,5)	10	10	5	-5	2	5	5	3/40
(12,12,6)	12	12	6	-6	2	4	4	7/96
(18,18,9)	18	18	9	-9	2	3	3	13/216

(4,4,3)	4	4	3	-6	3	-12	-12	1/24
(4,4,5)	4	4	5	10	5	20	20	99/800
(4,4,6)	4	4	6	6	6	12	12	13/96
(3,3,4)	3	3	4	6	12	-12	-12	7/48
(3,6,3)	3	6	3	-6	3	∞	-6	1/12
(2,6,6)	2	6	6	3	∞	6	-6	1/8
(2,4,3)	2	4	3	12	12	-12	-3	7/96
(2,3,3)	2	3	3	6	∞	-6	-3	1/24
(3,4,4)	3	4	4	12	6	∞	-12	17/96

Table 3.3: The values of the parameters for the 2-fold symmetry lattices.

We remark that the first class contains the lattices with 2-2-fold symmetry, while the second one the lattices with only 2-fold symmetry. As mentioned, the lattices with 2-2-fold symmetry also have $\mu_1 = \mu_4$, which implies that $p = k$ (and hence we have a lattice of the form (p, p, p')) and that $l' = d$. An exception is the case of $(3, 6, 3)$ where we choose the 2-fold symmetry to be at $\mu_4 = \mu_5$, which swaps the roles of k' and l' and the roles of k and l. This is because for the construction of the fundamental domain we always want p, k, p' and k' to be finite.

3.5 Commensurability theorems

Since commensurable lattices share many of the properties we are interested in (including arithmeticity), it is important to study the lattices up to commensurability.

Sauter in [Sau90] and Deligne and Mostow in [DM93] studied which lattices belong to the same commensurability class. This work originated by the fact that Mostow found some ball 5-tuple that did not satisfy the condition ΣINT (see 3.1.5), but he could not prove that the associated groups were not discrete. Sauter proved that each of these produced a group commensurable to one for

which Mostow had proved discreteness. Later, Deligne and Mostow extended Sauter's work. An account of most of the commensurability theorems that we will use can also be found in [Par09].

The first one we will need is Theorem 10.6 of [DM93], in the form found in Theorem 3.8 of [Par09].

Theorem 3.5.1. *Let a and b be rational numbers in $(0,1)$ with $\frac{1}{2} < a+b < 1$ and consider the ball 5-tuples*

$$\mu^{(1)} = (a, a, b, b, 2-2a-2b),$$
$$\mu^{(2)} = \left(1-b, 1-a, a+b-\frac{1}{2}, a+b-\frac{1}{2}, 1-a-b\right).$$

Consider the groups of symmetries of $\mu^{(1)}$ and $\mu^{(2)}$ (i.e. the subgroup of $\mathcal{S}_5$ permuting elements of the ball 5-tuple with same value), which are $\Sigma_1 = \langle (1,2),(3,4)\rangle \cong \mathbb{Z}_2 \times \mathbb{Z}_2$ and $\Sigma_2 = \langle (3,4)\rangle \cong \mathbb{Z}_2$ respectively. Then the associated groups $\Gamma_{\mu^{(1)}\Sigma_1}$ and $\Gamma_{\mu^{(2)}\Sigma_2}$ are isomorphic.

From this theorem, one can deduce the following corollaries. The first one corresponds to Corollary 3.9 in [Par09], which is a reformulation of Corollary 10.18 of [DM93] and generalises Theorem 6.2 of [Sau90]. The second one corresponds to Corollary 3.10 of [Par09].

Corollary 3.5.2. *Let*

$$\mu^{(1)} = \left(\frac{1}{2}+\frac{1}{p}, \frac{1}{2}+\frac{1}{p}, \frac{1}{2}-\frac{2}{p}, \frac{1}{2}-\frac{2}{p}, \frac{2}{p}\right),$$
$$\mu^{(2)} = \left(\frac{1}{2}-\frac{1}{p}, \frac{1}{2}-\frac{1}{p}, \frac{1}{2}-\frac{1}{p}, \frac{1}{p}, \frac{1}{2}+\frac{2}{p}\right),$$
$$\mu^{(3)} = \left(\frac{1}{2}-\frac{1}{p}, \frac{1}{2}-\frac{1}{p}, \frac{1}{2}-\frac{1}{p}, \frac{1}{2}-\frac{1}{p}, \frac{4}{p}\right).$$

Then the groups $\Gamma_{\mu^{(i)}}$ associated to these ball 5-tuples are commensurable.

Corollary 3.5.3. *Let*

$$\mu^{(1)} = \left(\frac{1}{2}-\frac{1}{k}, \frac{1}{2}-\frac{1}{k}, \frac{1}{4}+\frac{1}{k}, \frac{1}{4}+\frac{1}{k}, \frac{1}{2}\right),$$
$$\mu^{(2)} = \left(\frac{1}{4}, \frac{1}{4}, \frac{1}{4}, \frac{3}{4}-\frac{1}{k}, \frac{1}{2}+\frac{1}{k}\right).$$

Then the groups $\Gamma_{\mu^{(i)}}$ associated to these ball 5-tuples are commensurable.

Moreover, we will use Theorem 6.1 from Sauter [Sau90] (see also Theorem 11.22 in [DM93]), in the formulation of Theorem 3.11 of [Par09].

Theorem 3.5.4. *Let*

$$\mu^{(1)} = \left(\frac{1}{2} - \frac{1}{p}, \frac{1}{2} - \frac{1}{p}, \frac{1}{2} - \frac{1}{p}, \frac{1}{6} + \frac{1}{p}, \frac{1}{3} + \frac{2}{p}, \right),$$
$$\mu^{(2)} = \left(\frac{1}{6}, \frac{1}{6}, \frac{1}{6}, \frac{5}{6} - \frac{1}{p}, \frac{2}{3} + \frac{1}{p}\right).$$

Then the groups $\Gamma_{\mu^{(i)}}$ associated to these ball 5-tuples are commensurable.

Note that we are now referring to the groups associated without considering the symmetries (as we did in the previous theorem). In fact, the new ball 5-tuples, obtained by choosing some values of a and b, have different symmetries from the previous theorem (see also Proposition 4.10 of [Par09]). It is possible to deduce the index of commensurability by considering the old and new symmetry groups. For further details of the indices of commensurability in these theorems, one can see the discussion in Section 7.3, where for each pair of commensurable lattices we calculate the index and verify it on the calculation of the orbifold Euler characteristic.

Finally, Proposition 7.10 of [DPP] (see also Section A.6 in their appendix) shows that

Proposition 3.5.5. *The Thompson group $\mathcal{T}(p, E_2)$, for $p = 4$ is (conjugate to) a subgroup of index 3 in the Deligne-Mostow group $\Gamma_{\mu\Sigma}$ associated to $\mu = (3, 3, 5, 6, 7)/12$, where $\Sigma = \langle(1, 2)\rangle \cong \mathbb{Z}_2$.*

Chapter 4

The cone manifold

In this chapter we will not consider the symmetry in the ball 5-tuples. From Thurtson's work (see Section 3.2), let us consider a cone metric on the sphere with prescribed cone angles and area 1. Then we can change the position of the cone points on the sphere (i.e. consider all the possible configurations of these cone points) and get a complex hyperbolic structure on the moduli space. The Hermitian form is given by the area form. This structure makes the moduli space a complex hyperbolic manifold, which is not complete. If we consider its metric completion, we get a complex hyperbolic cone manifold, which is an orbifold only when we choose the cone angles accurately. We now want to study this cone manifold.

In the first part of this chapter we will see in details how to parametrise cone metrics on the sphere of area 1 with five cone singularities. We will explicitly calculate the area form that gives the complex hyperbolic structure. This is a generic construction and does not depend on whether the cone angles we choose give a lattice or not, nor on whether the cone points have same angles or not. The only restriction on the cone angles in this case is that the Hermitian form we obtain must have the required signature. We will also consider some maps acting on our space of configurations and explain how they change the configuration.

In the second part of this chapter we will show how to build a polyhedron in the moduli space starting from the cone metrics and using the coordinates we introduced. These polyhedra are the building blocks for the cone manifold

describing the moduli space. In some cases (like the 3-fold symmetry case), the polyhedron will exactly describe the cone manifold (or a fundamental domain for the lattice when the cone manifold is an orbifold); in some others we will need multiple copies (with different parameters) and in some others the polyhedron will contain multiple copies of the cone manifold (when one has extra symmetries).

4.1 The space of configurations

Following Thurston, consider a cone metric on the sphere of area 1 with cone points of fixed cone angles $\theta_0, \theta_1, \theta_2, \theta_3$ and θ_4 with $0 < \theta_i < 2\pi$. By the discrete version of Gauss-Bonnet formula (see (3.2.1)), they satisfy $\sum(2\pi - \theta_i) = 4\pi$.

Since we have 5 cone singularities, a priori the configurations are described by 5 parameters. The discrete Gauss-Bonnet formula guarantees that the value of the fifth angle is determined by the previous four. To prescribe the cone angles we will use the parameters

$$\alpha = \frac{\theta_1}{2}, \qquad \beta = \frac{\theta_2}{2}, \qquad \theta = \frac{\theta_2}{2} + \frac{\theta_3}{2} - \pi, \qquad \varphi = \frac{\theta_0}{2} + \frac{\theta_1}{2} - \pi. \tag{4.1.1}$$

They have a geometric meaning which is made clear in Figure 4.1. Then we will denote a cone metric with these cone angles as $(\alpha, \beta, \theta, \varphi)$. By definition of the parameters, we are considering a flat sphere with 5 cone singularities of angles

$$(2(\pi + \varphi - \alpha), 2\alpha, 2\beta, 2(\pi + \theta - \beta), 2(\pi - \theta - \varphi)). \tag{4.1.2}$$

As one can see in the upper-left-hand side of Figure 4.1, the order of the angles is given by starting in the lower left corner and continuing counter-clockwise. Therefore the angle θ_i is the cone angle of the cone point v_i for $i = 0, 1, 2, 3$ and θ_4 is the cone angle of the cone point v_*. Remember that in the case of configurations that give lattices described in Section 3.4, the angles are related to the ball 5-tuples by (3.2.4) (note that the indices are shifted to be coherent with the name of the vertices v_i).

We now fix the cone angles (so fix a configuration $(\alpha, \beta, \theta, \varphi)$). Our goal is to parametrise all possible positions of the cone points on the sphere and to show how one can pass from the cone metric to its coordinates and viceversa.

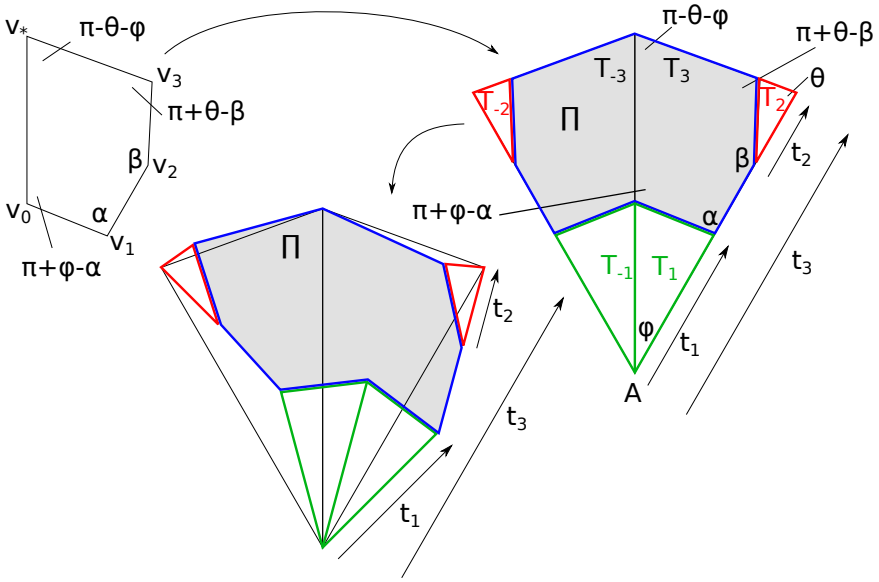

Figure 4.1: The configuration $(\alpha, \beta, \theta, \varphi)$.

Let us first consider the easier case of when the five cone singularities are all along the equator of the sphere, forming a pentagonal pillowcase (i.e. two congruent pentagons glued along their boundary).

Take a path in the sphere that starts from v_0 and passes in order through v_1, v_2, v_3, ending in v_*. We now cut through this path and open up the surface, obtaining an octagon like the one in the upper-right-hand side of Figure 4.1, which we call Π. The condition of all points being on the equator means that we can cut along a geodesic which divides the cone angle in half.

To be able to express the vertices of Π in coordinates, we decide that the vertex v_* coincides with the origin of the complex plane and we place Π such that the coordinate of v_0 is a multiple of i by a negative real number. The vertices with positive real coordinates will be called v_1, v_2, v_3, while the corresponding vertices with negative real coordinates will be v_{-1}, v_{-2}, v_{-3}.

The sides of Π are pairwise identified through a reflection with respect to the imaginary axis and this identification allows us to recover the cone metric on the sphere. More precisely, the vertices v_i are identified to v_{-i} and the side $v_i v_{i+1}$ is identified to the side $v_{-i} v_{-(i+1)}$, for $i = 0, 1, 2, 3, *$. Since only the boundary

points and not the interior are identified, this gives us back the shape of the cone metric as two pentagons glued along the boundary, forming the pentagonal pillowcase from which we started.

We can also describe Π in terms of the three real parameters t_1, t_2 and t_3 as shown in the picture. Let us take three triangles T_1, T_2 and T_3 in the following way. The triangle T_1 is built on the side v_0v_1 and has angles $\pi-\alpha$ at v_1, $\alpha-\varphi$ at v_0 and φ. Then t_1 is the side opposite $\alpha-\varphi$, pointing towards v_1. We denote the third vertex of T_1 as A. The triangle T_2 is built on the side v_2v_3 and has angles $\pi-\beta$ at v_2, $\beta-\theta$ at v_3 and θ. Then t_2 is the side opposite $\beta-\theta$. The triangle T_3 is built on the side v_*A and has angles φ at A, $\pi-\theta-\varphi$ at v_* and θ. Then t_3 is the side opposite $\pi-\theta-\varphi$.

Since in this case all the possible variations in the cone metric are the possible distances of the various points, one just needs a parameter describing the length of the sides of each of the three triangles, in order to have the whole configuration (hence the cone metric) completely determined. Since all the angles are determined by the cone angles, it is enough to parametrise one side of each of the triangles and to do this we will use the parameters t_1, t_2 and t_3.

We just explained how to associate a set of three parameters to each configuration of points on the equator.

Conversely, start from the three real parameters t_1, t_2 and t_3 and take three triangles T_i, with angles as above and one side t_i as above, for $i=1,2,3$. We now construct an octagon Π by first taking a copy of the triangle T_3, with the vertex with angle $\pi-\theta-\varphi$ at 0 and the one with angle φ along the negative imaginary axis. Then remove from T_3 a copy of T_2 by making the two vertices of angle θ coincide and by making t_2 and t_3 be collinear, both vectors pointing towards the common corner of the two triangles T_3 and T_2. Similarly, remove from the figure obtained, a copy of T_1 such that the vertex of angle φ of T_1 coincides with the one of T_3 with the same angle and such that t_1, t_3 are collinear and pointing in the same direction. At this point we reflect the whole construction along the imaginary axis, obtaining three more triangles T_{-3}, T_{-2} and T_{-1}. We consider the quadrilateral made of the two triangles T_3 and T_{-3}, from which we delete triangles T_i, for $i\in\{\pm1,\pm2\}$. The figure obtained is an octagon Π as in Figure

4.1. This is clearly the same figure as we described previously once we label the vertices as before. Gluing the sides of Π as explained above, one can recover the cone metric associated to the parameters.

We now consider a generic metric on the sphere and the same procedure applies, but now we need to allow the three real parameters t_1, t_2 and t_3 to be complex (i.e. not to be aligned), in order to describe all possible mutual positions of the singularities. This encodes the fact that two pieces of the geodesic might not divide the cone angle they share into two equal angles.

We construct an octagon by taking the same three triangles and making the same vertices of the triangles coincide as before, but the three variables will be two dimensional vectors representing the sides of the triangles and they will no longer line up. The configuration will be as the bottom part of Figure 4.1.

As before, we can recover the metric on the sphere by identifying the side $v_i v_{i+1}$ to the side $v_{-i} v_{-(i+1)}$, for $i = 0, 1, 2, 3, *$. We obviously obtain a manifold with cone singularities which is homeomorphic to the sphere and has five cone points of angles equal to those that we had in the beginning.

The vertices of the configuration will have coordinates as follows.

$$
\begin{aligned}
A &= -i\frac{\sin\theta}{\sin(\theta+\varphi)}t_3,\\
v_0 &= -i\frac{\sin\theta}{\sin(\theta+\varphi)}t_3 + i\frac{\sin\alpha}{\sin(\alpha-\varphi)}t_1,\\
v_1 &= -i\frac{\sin\theta}{\sin(\theta+\varphi)}t_3 + ie^{-i\varphi}t_1,\\
v_{-1} &= -i\frac{\sin\theta}{\sin(\theta+\varphi)}t_3 + ie^{i\varphi}t_1,\\
v_2 &= -ie^{-i\varphi}t_2 + ie^{-i(\theta+\varphi)}\frac{\sin\varphi}{\sin(\theta+\varphi)}t_3,\\
v_{-2} &= -ie^{i\varphi}t_2 + ie^{i(\theta+\varphi)}\frac{\sin\varphi}{\sin(\theta+\varphi)}t_3,\\
v_3 &= -ie^{-i(\theta+\varphi)}\frac{\sin\beta}{\sin(\beta-\theta)}t_2 + ie^{-i(\theta+\varphi)}\frac{\sin\varphi}{\sin(\theta+\varphi)}t_3,\\
v_{-3} &= -ie^{i(\theta+\varphi)}\frac{\sin\beta}{\sin(\beta-\theta)}t_2 + ie^{i(\theta+\varphi)}\frac{\sin\varphi}{\sin(\theta+\varphi)}t_3.
\end{aligned}
$$

Note that the frame used for the v_i's and the t_i's are not the same, as the real and imaginary axes are rotated. This is so that the real values of the t_i's are

along the side of T_3 opposite the vertex of angle $\pi - \theta - \varphi$.

Remark also that the denominators only vanish in very degenerate configurations, in which the triangle T_3 degenerates to a line. We will assume that this never happens, since this is the case for the values of the angles that we will consider in the following sections.

Since the Hermitian form of the complex hyperbolic structure described later in this section is given by the area, we will calculate it in terms of our coordinates. In the case of real variables, the area of the right half of the octagon can be obtained taking the area of T_3 and subtracting the area of T_1 and the area of T_2. We then need to double this quantity to get the total area of Π. When allowing the variables to be complex, we can see, using a cut and paste map, that the area is given by the same formula.

Hence the area of the octagon Π is given by

$$\text{Area}\,\Pi = \frac{\sin\theta\sin\varphi}{\sin(\theta+\varphi)}|t_3|^2 - \frac{\sin\theta\sin\beta}{\sin(\beta-\theta)}|t_2|^2 - \frac{\sin\varphi\sin\alpha}{\sin(\alpha-\varphi)}|t_1|^2. \tag{4.1.3}$$

We will see now how the moduli space of cone metrics on the sphere of area 1, seen as the different shapes of polygons Π that we can achieve, has a complex hyperbolic structure.

As we saw in Section 2, the 2-dimensional complex hyperbolic space is by definition the set of points for which a certain Hermitian form is positive, up to projectivisation. First of all, up to now, all three parameters t_1, t_2, t_3 were freely chosen, but for our purpose two configurations such that the parameters are proportionals by the same constant are the same. This is because we are considering the cone metrics to have fixed area, following Thurston (see [Thu98], Theorem 0.2). From now on, we will hence fix $t_3 = 1$. Note that this is one of the possible normalisations, different from asking for the area to be 1 (as in [Thu98]). Recall that the area is given by (4.1.3) in terms of t_1, t_2 and t_3. The coordinates t_1 and t_2 will hence vary while keeping (4.1.3) positive. This is the only restriction we need on the parameters. On the moduli space of cone metrics on the sphere this is equivalent to projectivising the coordinates.

Let us now consider the area as given in equation (4.1.3). If we consider the

Hermitian matrix

$$H = H(\alpha, \beta, \theta, \varphi) = \begin{bmatrix} -\frac{\sin\varphi \sin\alpha}{\sin(\alpha-\varphi)} & 0 & 0 \\ 0 & -\frac{\sin\theta \sin\beta}{\sin(\beta-\theta)} & 0 \\ 0 & 0 & \frac{\sin\varphi \sin\theta}{\sin(\theta+\varphi)} \end{bmatrix}, \tag{4.1.4}$$

such a formula is equivalent to saying

$$\text{Area}(\Pi) = \mathbf{t}^* H \mathbf{t}.$$

In this sense, the area gives a Hermitian form of signature (1,2) on $\mathbb{C}^3$.

Since these parameters only make sense if the area of Π (and so the area of the cone metric) is positive, we define our model of complex hyperbolic space as

$$\mathbf{H}^2_{\mathbb{C}} = \{\mathbf{t} \colon \langle \mathbf{t}, \mathbf{t} \rangle = \mathbf{t}^* H \mathbf{t} > 0\} =$$
$$= \left\{ \begin{bmatrix} t_1 \\ t_2 \\ 1 \end{bmatrix} \colon -\frac{\sin\varphi \sin\alpha}{\sin(\alpha-\varphi)}|t_1|^2 - \frac{\sin\theta \sin\beta}{\sin(\beta-\theta)}|t_2|^2 + \frac{\sin\varphi \sin\theta}{\sin(\theta+\varphi)} > 0 \right\}.$$

We will allow the octagon Π to self intersect and consider the signed area. For the (signed) area to be positive and to have the right signature are the only conditions on a set of three complex numbers to give a cone metric. Meanwhile, two sets of parameters can sometimes give the same cone metric, as we will see later on.

4.2 Moves

In this section we will introduce some maps that will play a key role in the following sections, since they or their compositions will be the generators of the lattices. We will call these special maps the *moves*.

In general, the moves will be swapping cone points. When the two cone points have the same cone angle, then the move will be an automorphism of the sphere, hence preserving the area form, and hence it will be an element of $PU(2,1)$. When they do not have the same cone angle, we will need to apply it twice in order to land on the same configuration of cone points. The moves can be seen as (half) Dehn twists of the sphere along a curve around the two cone points which they

swap. In this section we will not consider any symmetry and just describe how the moves act on the configuration by changing the cone angles and hence the parameters $(\alpha, \beta, \theta, \varphi)$.

The move R_1 exchanges the two cone points v_2 and v_3 with their cone angles, while R_2 exchanges v_1 and v_2. Since the moves change the values of our parameters, we will denote the move R_i as $R_i(\alpha, \beta, \theta, \varphi)$ to say that $R_i \colon (\alpha, \beta, \theta, \varphi) \mapsto (\alpha', \beta', \theta', \varphi')$, unless the angles of the configuration we start from is obvious. This means, for example, that when composing two maps $T(\alpha, \beta, \theta, \varphi)$ and $S(\alpha, \beta, \theta, \varphi)$, we need to consider that the second map is applied to the new angles, so we are doing the composition

$$S(\alpha', \beta', \theta', \varphi') \circ T(\alpha, \beta, \theta, \varphi) \tag{4.2.1}$$

because $(\alpha, \beta, \theta, \varphi) \overset{T}{\mapsto} (\alpha', \beta', \theta', \varphi') \overset{S}{\mapsto} (\alpha'', \beta'', \theta'', \varphi'')$. Similarly, when calculating inverses we have

$$[T(\alpha, \beta, \theta, \varphi)]^{-1} = T^{-1}(\alpha', \beta', \theta', \varphi'), \tag{4.2.2}$$

since $T \colon (\alpha, \beta, \theta, \varphi) \mapsto (\alpha', \beta', \theta', \varphi')$ and $T^{-1} \colon (\alpha', \beta', \theta', \varphi') \mapsto (\alpha, \beta, \theta, \varphi)$.

We now want to express the moves in matrix form. The matrix of $R_1(\alpha, \beta, \theta, \varphi)$ is obtained from the equations $v_0' = v_0$, $v_*' = v_*$, $v_1' = v_1$, $v_3' = v_2$ and $v_{-2}' = v_3$, where the v_i's are the coordinates in the $(\alpha, \beta, \theta, \varphi)$ configuration and the v_i''s in the $(\alpha', \beta', \theta', \varphi')$ configuration. If we call t_1, t_2 the variables in the coordinates of the v_i's and t_1', t_2' the variables in the coordinates of the v_i''s, this gives the equations

$$t_1' = t_1, \qquad t_2' = e^{i\theta} \frac{\sin(\beta' - \theta')}{\sin \beta'} t_2, \qquad t_2' = e^{i\theta} \frac{\sin \beta}{\sin(\beta - \theta)} t_2.$$

These give a unique solution because R_1 exchanges the angles around v_2 and v_3, so it exchanges β with $\beta - \theta$ and hence $\beta' - \theta' = \beta$, $\beta' = \beta - \theta$ and $\theta' = \theta$ (see Figure 4.2). The matrix of R_1 is then

$$R_1(\alpha, \beta, \theta, \varphi) = \begin{bmatrix} 1 & 0 & 0 \\ 0 & e^{i\theta} \frac{\sin \beta}{\sin(\beta - \theta)} & 0 \\ 0 & 0 & 1 \end{bmatrix}. \tag{4.2.3}$$

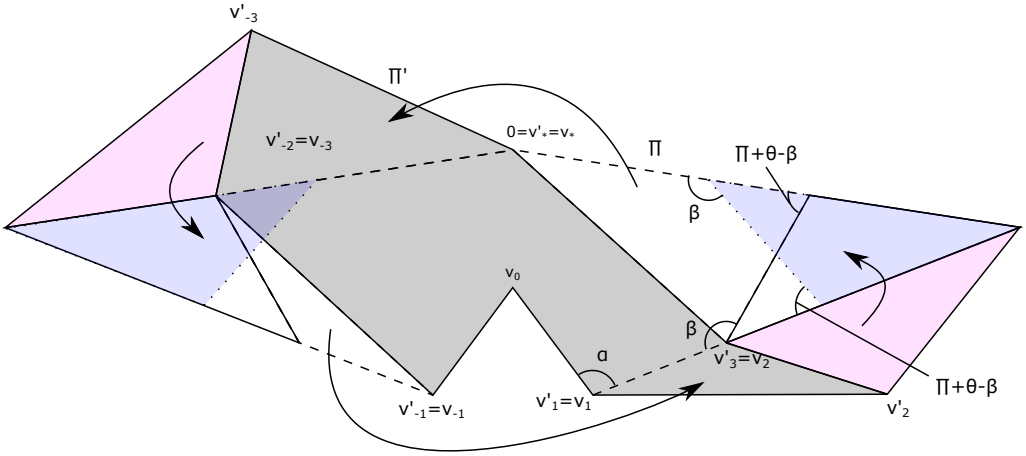

Figure 4.2: The move R_1.

Similarly, one can find the matrix of R_2 by simultaneously solving the equations $v_0' = v_0$, $v_*' = v_*$, $v_2' = v_1$, $v_{-1}' = v_{-2}$ and $v_3' = v_3$. The first thing to do is to find the values of the angles in the image. The values of $\alpha - \varphi$ and $\theta + \varphi$ remain unchanged (i.e. $\alpha' - \varphi' = \alpha - \varphi$ and $\theta' + \varphi' = \theta + \varphi$), because they are related to the two cone angles v_* and v_0 which do not change. Moreover, since the move fixes v_3, also the value of $\pi + \theta - \beta$ remains unchanged, so $\pi + \theta' - \beta' = \pi + \theta - \beta$. Furthermore, since the move exchanges v_1 and v_2, $\alpha' = \beta$ and $\beta' = \alpha$. From these equations one can deduce that $\varphi' = \varphi + \beta - \alpha$ and $\theta' = \theta + \alpha - \beta$. Applying this to the equations we need to solve gives the following matrix.

$$R_2(\alpha, \beta, \theta, \varphi) = \frac{1}{\sin(\theta + \alpha - \beta)\sin(\varphi + \beta - \alpha)} \cdot$$
$$\cdot \begin{bmatrix} \sin\alpha \sin\theta' e^{i(\alpha-\varphi)} & \sin(\alpha-\varphi)\sin\theta' e^{i\alpha} & -\sin(\alpha-\varphi)\sin\theta' e^{i\alpha} \\ \sin(\beta-\theta)\sin\varphi' e^{i\beta} & \sin\varphi' \sin\beta e^{i(\beta-\theta)} & -\sin(\beta-\theta)\sin\varphi' e^{i\beta} \\ \sin(\theta+\varphi)\sin\alpha e^{i\beta} & \sin(\theta+\varphi)\sin\beta e^{i\alpha} & A \end{bmatrix}, \quad (4.2.4)$$

with $\varphi' = \varphi + \beta - \alpha$ and $\theta' = \theta + \alpha - \beta$ and

$$\begin{aligned} A &= \sin\theta\sin\varphi' - \sin(\theta+\varphi)\sin\beta e^{i\alpha} \\ &= \sin\varphi\sin\theta' - \sin(\theta+\varphi)\sin\alpha e^{i\beta} \\ &= \sin\theta\sin\varphi\cos(\alpha-\beta) - \sin\theta\cos\varphi\sin\alpha e^{i\beta} - \cos\theta\sin\varphi\sin\beta e^{i\alpha}. \end{aligned} \quad (4.2.5)$$

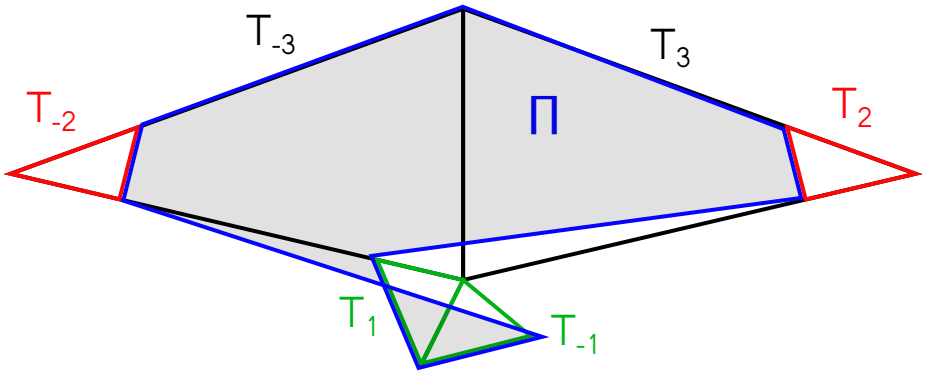

Figure 4.3: The octagon obtained after applying A_1.

The third move A_1 will swap v_0 and v_1 twice. This is because, since these two cone points will usually have different cone angles, we directly apply a full Dehn twist. This move is the generalisation of the "butterfly moves" used by Thurston in [Thu98]. In his case, he was moving one side across a region shaped like a butterfly such that in the end the signed area is the same. Here, we make the triangle T_1 rotate so that the vertices v_*, v_2, v_3 remain fixed, while v_1' coincides with v_{-1}. We obtain an octagon with a point of self intersection and we will consider the signed area to have it preserved after applying the move. The corresponding cone metric on the sphere can still be recovered by gluing together the same sides.

As we can see in Figure 4.3, the triangles T_2 and T_3 remain fixed and hence so are the variables z_2 and z_3. The third triangle is rotated of an angle of 2φ. Moreover, this time the move starts and lands in the same configuration. Its matrix is

$$A_1(\alpha, \beta, \theta, \varphi) = \begin{bmatrix} e^{2i\varphi} & 0 & 0 \\ 0 & 1 & 0 \\ 0 & 0 & 1 \end{bmatrix}. \tag{4.2.6}$$

In the following, we will also need some composition of the moves. We now want to calculate $P = R_1 R_2$ and $J = PA_1$. As we already mentioned, after applying the first transformation the angles have changed. Looking at Figure 4.4,

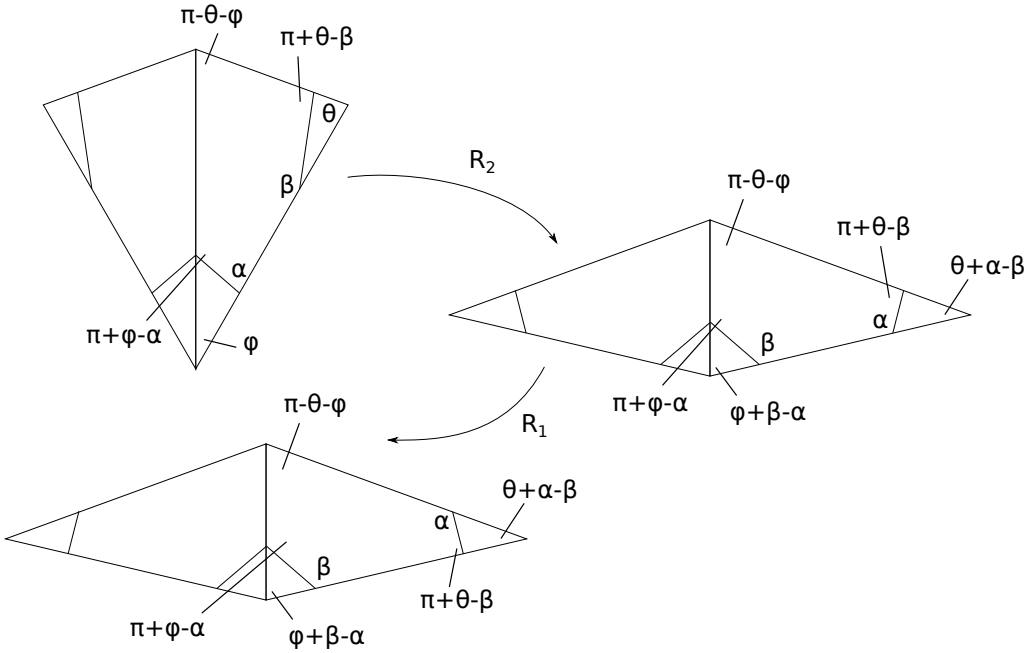

Figure 4.4: The action of P on the angles.

one can deduce that

$$
\begin{aligned}
P(\alpha,\beta,\theta,\varphi) &= R_1(\alpha',\beta',\theta',\varphi')R_2(\alpha,\beta,\theta,\varphi)\\
&= R_1(\beta,\alpha,\theta+\alpha-\beta,\varphi+\beta-\alpha)R_2(\alpha,\beta,\theta,\varphi)\\
&= \frac{1}{\sin(\theta+\alpha-\beta)\sin(\varphi+\beta-\alpha)}\cdot\\
&\cdot\begin{bmatrix}
\sin\alpha\sin\theta' e^{i(\alpha-\varphi)} & \sin(\alpha-\varphi)\sin\theta' e^{i\alpha} & -\sin(\alpha-\varphi)\sin\theta' e^{i\alpha}\\
\sin\alpha\sin\varphi' e^{i(\alpha+\theta)} & \frac{\sin\varphi'\sin\beta\sin\alpha}{\sin(\beta-\theta)}e^{i\alpha} & -\sin\alpha\sin\varphi' e^{i(\alpha+\theta)}\\
\sin(\theta+\varphi)\sin\alpha e^{i\beta} & \sin(\theta+\varphi)\sin\beta e^{i\alpha} & A
\end{bmatrix},
\end{aligned}
\tag{4.2.7}
$$

where, as before, $\varphi' = \varphi+\beta-\alpha$, $\theta' = \theta+\alpha-\beta$ and A is as in (4.2.5).

On the other hand, $J = PA_1$ is easier to calculate, since A_1 does not change

the type of the configuration. Hence

$$J(\alpha,\beta,\theta,\varphi) = P(\alpha,\beta,\theta,\varphi)A_1(\alpha,\beta,\theta,\varphi) = \frac{1}{\sin(\theta+\alpha-\beta)\sin(\varphi+\beta-\alpha)}\cdot$$
$$\cdot \begin{bmatrix} \sin\alpha\sin\theta' e^{i(\alpha+\varphi)} & \sin(\alpha-\varphi)\sin\theta' e^{i\alpha} & -\sin(\alpha-\varphi)\sin\theta' e^{i\alpha} \\ \sin\alpha\sin\varphi' e^{i(\alpha+\theta+2\varphi)} & \frac{\sin\varphi'\sin\beta\sin\alpha}{\sin(\beta-\theta)} e^{i\alpha} & -\sin\alpha\sin\varphi' e^{i(\alpha+\theta)} \\ \sin(\theta+\varphi)\sin\alpha e^{i(\beta+2\varphi)} & \sin(\theta+\varphi)\sin\beta e^{i\alpha} & A \end{bmatrix}, \tag{4.2.8}$$

where again $\varphi' = \varphi+\beta-\alpha$, $\theta' = \theta+\alpha-\beta$ and A is as in (4.2.5).

We remark that if we define a second set of coordinates as $\mathbf{s} = P^{-1}\mathbf{t}$ (as we will do later), the action of R_2 is equivalent to applying R_1 on the $\mathbf{s}$-coordinates. In other words, $R_2 = PR_1P^{-1} = R_1R_2R_1R_2^{-1}R_1^{-1}$, which is equivalent to the braid relation

$$R_1R_2R_1 = R_2R_1R_2.$$

Again, to calculate this composition, we need to record how the configuration changes when applying the matrices, so we need to prove that the following diagram commutes

$$\begin{array}{ccc} (\alpha,\beta,\theta,\varphi) & \xrightarrow{R_1^{-1}} & (\alpha,\pi+\theta-\beta,\theta,\varphi) \\ \downarrow{\scriptstyle R_2} & & \downarrow{\scriptstyle R_2^{-1}} \\ (\beta,\alpha,\alpha+\theta-\beta,\beta+\varphi-\alpha) & & (\pi+\theta-\beta,\alpha,\alpha+\beta-\pi,\pi+\theta+\varphi-\alpha-\beta) \\ \uparrow{\scriptstyle R_1} & & \downarrow{\scriptstyle R_1} \\ (\beta,\pi+\theta-\beta,\alpha+\theta-\beta,\beta+\varphi-\alpha) & \xleftarrow{R_2} & (\pi+\theta-\beta,\beta,\alpha+\beta-\pi,\pi+\theta+\varphi-\alpha-\beta) \end{array}$$

which is easy to verify by a simple calculation.

4.3 The polyhedron

4.3.1 Complex lines and vertices

As mentioned, the metric completion of the moduli space is the cone manifold that we want to study. Following the discussion in Remark 3.2.6 this means that we want to see what happens when two cone points get closer and closer until they coalesce. We define L_{ij} to be the complex line obtained when v_i and v_j coalesce, for $i,j \in \{0,1,2,3,*\}$. Its polar vector will be denoted as $\mathbf{n}_{ij}$. We remark that

in calculating the equations of some of the lines involving v_1, v_2 and v_4 we are making a choice on whether to collapse using v_i or v_{-i}. The choice is recorded in the second column. The lines have equations as follow:

L_{ij}	$v_i \equiv v_j$	Equations in terms of the $\mathbf{t}$-coordinates
L_{*0}	$v_* \equiv v_0$	$t_1 = \frac{\sin(\alpha-\varphi)\sin\theta}{\sin\alpha\sin(\theta+\varphi)}$
L_{*1}	$v_* \equiv v_{-1}$	$t_1 = e^{-i\varphi}\frac{\sin\theta}{\sin(\theta+\varphi)}$
L_{*2}	$v_* \equiv v_{-2}$	$t_2 = e^{i\theta}\frac{\sin\varphi}{\sin(\theta+\varphi)}$
L_{*3}	$v_* \equiv v_3$	$t_2 = \frac{\sin(\beta-\theta)\sin\varphi}{\sin\beta\sin(\theta+\varphi)}$
L_{01}	$v_0 \equiv v_1$	$t_1 = 0$
L_{02}	$v_0 \equiv v_2$	$\frac{\sin\alpha}{\sin(\alpha-\varphi)}e^{i\varphi}t_1 + t_2 = 1$
L_{03}	$v_0 \equiv v_3$	$\frac{\sin\alpha}{\sin(\alpha-\varphi)}e^{i\varphi}t_1 + e^{-i\theta}\frac{\sin\beta}{\sin(\beta-\theta)}t_2 = 1$
L_{12}	$v_1 \equiv v_2$	$t_1 + t_2 = 1$
L_{13}	$v_1 \equiv v_3$	$t_1 + e^{-i\theta}\frac{\sin\beta}{\sin(\beta-\theta)}t_2 = 1$
L_{23}	$v_2 \equiv v_3$	$t_2 = 0$

Table 4.1: The equations defining the complex lines of two cone points collapsing.

Moreover, one can study the points in $\mathbf{H}^2_{\mathbb{C}}$ given by two pairs of points coalescing, i.e. obtained by intersecting pairs of these complex lines. They will be the vertices of the polyhedron and they have coordinates as follows.

Lines	$\mathbf{t}_k$	t_1	t_2
$L_{01} \cap L_{23}$	$\mathbf{t}_1$	0	0
$L_{03} \cap L_{12}$	$\mathbf{t}_2$	$\frac{\sin(\alpha-\varphi)(\sin(\beta-\theta)-e^{-i\theta}\sin\beta)}{e^{i\varphi}\sin\alpha\sin(\beta-\theta)-e^{-i\theta}\sin\beta\sin(\alpha-\varphi)}$	$\frac{e^{i\alpha}\sin(\beta-\theta)\sin\varphi}{e^{i\varphi}\sin\alpha\sin(\beta-\theta)-e^{-i\theta}\sin\beta\sin(\alpha-\varphi)}$
$L_{*0} \cap L_{23}$	$\mathbf{t}_3$	$\frac{\sin(\alpha-\varphi)\sin\theta}{\sin\alpha\sin(\theta+\varphi)}$	0
$L_{*0} \cap L_{12}$	$\mathbf{t}_4$	$\frac{\sin(\alpha-\varphi)\sin\theta}{\sin\alpha\sin(\theta+\varphi)}$	$\frac{\sin(\alpha+\theta)\sin\varphi}{\sin\alpha\sin(\theta+\varphi)}$
$L_{*0} \cap L_{13}$	$\mathbf{t}_5$	$\frac{\sin(\alpha-\varphi)\sin\theta}{\sin\alpha\sin(\theta+\varphi)}$	$e^{i\theta}\frac{\sin(\alpha+\theta)\sin(\beta-\theta)\sin\varphi}{\sin\alpha\sin\beta\sin(\theta+\varphi)}$
$L_{*1} \cap L_{23}$	$\mathbf{t}_6$	$e^{-i\varphi}\frac{\sin\theta}{\sin(\theta+\varphi)}$	0
$L_{*1} \cap L_{02}$	$\mathbf{t}_7$	$e^{-i\varphi}\frac{\sin\theta}{\sin(\theta+\varphi)}$	$\frac{\sin(\alpha-\theta-\varphi)\sin\varphi}{\sin(\alpha-\varphi)\sin(\theta+\varphi)}$
$L_{*1} \cap L_{03}$	$\mathbf{t}_8$	$e^{-i\varphi}\frac{\sin\theta}{\sin(\theta+\varphi)}$	$e^{i\theta}\frac{\sin(\alpha-\theta-\varphi)\sin(\beta-\theta)\sin\varphi}{\sin(\alpha-\varphi)\sin\beta\sin(\theta+\varphi)}$
$L_{*3} \cap L_{01}$	$\mathbf{t}_9$	0	$\frac{\sin(\beta-\theta)\sin\varphi}{\sin\beta\sin(\theta+\varphi)}$

$L_{*3} \cap L_{12}$	$\mathbf{t}_{10}$	$\frac{\sin(\beta+\varphi)\sin\theta}{\sin\beta\sin(\theta+\varphi)}$	$\frac{\sin(\beta-\theta)\sin\varphi}{\sin\beta\sin(\theta+\varphi)}$
$L_{*3} \cap L_{02}$	$\mathbf{t}_{11}$	$e^{-i\varphi}\frac{\sin(\alpha-\varphi)\sin(\beta+\varphi)\sin\theta}{\sin\alpha\sin\beta\sin(\theta+\varphi)}$	$\frac{\sin(\beta-\theta)\sin\varphi}{\sin\beta\sin(\theta+\varphi)}$
$L_{*2} \cap L_{01}$	$\mathbf{t}_{12}$	0	$e^{i\theta}\frac{\sin\varphi}{\sin(\theta+\varphi)}$
$L_{*2} \cap L_{13}$	$\mathbf{t}_{13}$	$\frac{\sin(\beta-\theta-\varphi)\sin\theta}{\sin(\beta-\theta)\sin(\theta+\varphi)}$	$e^{i\theta}\frac{\sin\varphi}{\sin(\theta+\varphi)}$
$L_{*2} \cap L_{03}$	$\mathbf{t}_{14}$	$e^{-i\varphi}\frac{\sin(\alpha-\varphi)\sin(\beta-\theta-\varphi)\sin\theta}{\sin\alpha\sin(\beta-\theta)\sin(\theta+\varphi)}$	$e^{i\theta}\frac{\sin\varphi}{\sin(\theta+\varphi)}$

Table 4.2: The coordinates of the vertices.

4.3.2 Second set of coordinates

It will be useful to define another set of coordinates in order to define the polyhedron explicitly. This is given by

$$\mathbf{s} = \begin{bmatrix} s_1 \\ s_2 \\ 1 \end{bmatrix} = P^{-1} \begin{bmatrix} t_1 \\ t_2 \\ 1 \end{bmatrix}. \tag{4.3.1}$$

To calculate the $\mathbf{s}$-coordinates, the first thing to do is to calculate the matrix of $P^{-1}(\alpha,\beta,\theta,\varphi)$, with a similar argument as in Section 4.2. We recall that this means that P^{-1} is applied to the configuration $(\alpha,\beta,\theta,\varphi)$. As shown in Figure 4.5, P^{-1} acts as follows:

$$\begin{aligned}(\alpha,\beta,\theta,\varphi) &\xmapsto{R_1^{-1}} (\alpha',\beta',\theta',\varphi') = (\alpha,\pi+\theta-\beta,\theta,\varphi) \xmapsto{R_2^{-1}} \\ &\xmapsto{R_2^{-1}} (\alpha'',\beta'',\theta'',\varphi'') = (\pi+\theta-\beta,\alpha,\alpha+\beta-\pi,\pi+\theta+\varphi-\alpha-\beta),\end{aligned} \tag{4.3.2}$$

so

$$P^{-1}(\alpha,\beta,\theta,\varphi) = R_2^{-1}(\alpha,\pi+\theta-\beta,\theta,\varphi) \circ R_1^{-1}(\alpha,\beta,\theta,\varphi).$$

Explicitly, we have

$$P^{-1}(\alpha,\beta,\theta,\varphi) = \begin{bmatrix} -\sin\alpha\sin\theta' e^{-i(\alpha-\varphi)} & -\frac{\sin(\alpha-\varphi)\sin\theta'\sin\beta}{\sin(\beta-\theta)} e^{-i(\alpha+\theta)} & \sin(\alpha-\varphi)\sin\theta' e^{-i\alpha} \\ \sin\beta\sin\varphi' e^{i(\beta-\theta)} & \sin\beta\sin\varphi' e^{i(\beta-\theta)} & -\sin\beta\sin\varphi' e^{i(\beta-\theta)} \\ \sin(\theta+\varphi)\sin\alpha e^{i(\beta-\theta)} & -\sin(\theta+\varphi)\sin\beta e^{-i(\alpha+\theta)} & B \end{bmatrix}, \tag{4.3.3}$$

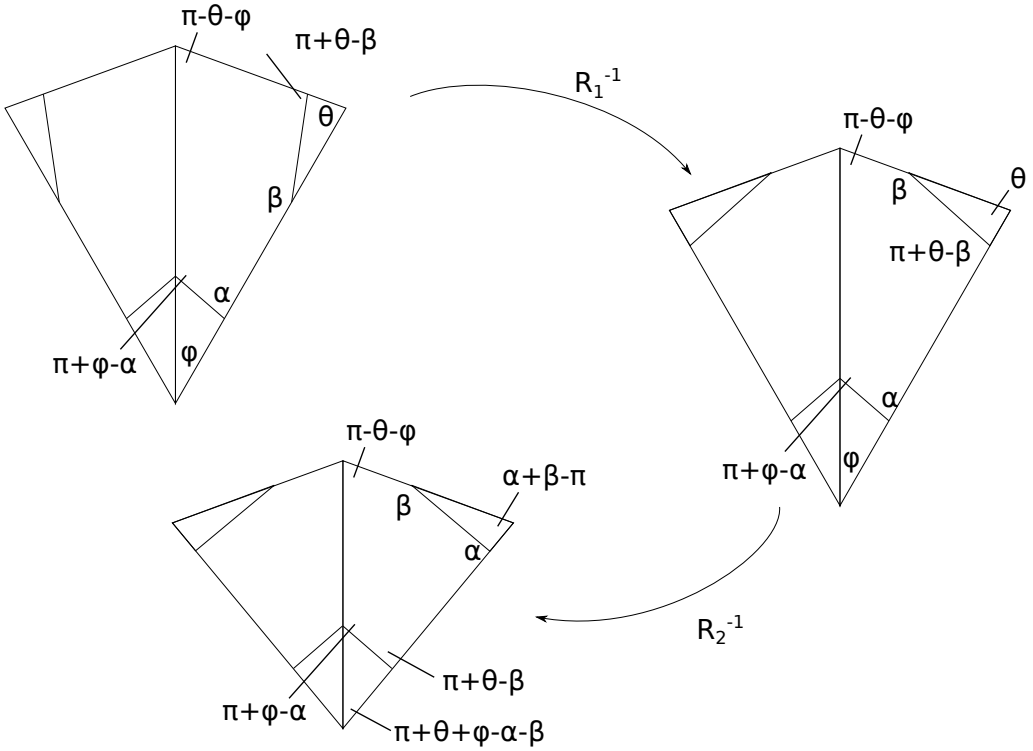

Figure 4.5: The action of P^{-1} on the angles.

where $\varphi' = \pi + \theta + \varphi - \alpha - \beta$, $\theta' = \alpha + \beta - \pi$ and B is

$$\begin{aligned} B &= -\sin\theta' \sin\varphi - \sin(\theta+\varphi)\sin\alpha e^{i(\beta-\theta)} \\ &= -\sin\varphi' \sin\theta + \sin(\theta+\varphi)\sin(\beta-\theta)e^{-i\alpha}. \end{aligned} \tag{4.3.4}$$

One can easily verify that the matrices of $P(\alpha,\beta,\theta,\varphi)$ and $P^{-1}(\alpha,\beta,\theta,\varphi)$ in (4.2.7) and (4.3.3) respectively, satisfy (4.2.2).

We now apply P^{-1} to the lines and vertices described in Tables 4.1 and 4.2 to obtain their s-coordinates.

L_{ij}	Equations in terms of the s-coordinates
L_{*0}	$s_1 = -\frac{\sin(\alpha-\varphi)\sin(\alpha+\beta)}{\sin(\beta-\theta)\sin(\theta+\varphi)}$
L_{*1}	$s_2 = -e^{i(\alpha+\beta)}\frac{\sin(\alpha+\beta-\theta-\varphi)}{\sin(\theta+\varphi)}$
L_{*2}	$s_2 = \frac{\sin(\alpha+\beta-\theta-\varphi)\sin\beta}{\sin\alpha\sin(\theta+\varphi)}$
L_{*3}	$s_1 = e^{-i(\alpha+\beta-\theta-\varphi)}\frac{\sin(\alpha+\beta)}{\sin(\theta+\varphi)}$
L_{01}	$-\frac{\sin(\beta-\theta)}{\sin(\alpha-\varphi)}e^{i(\alpha+\beta-\theta-\varphi)}s_1 + s_2 = 1$

L_{02}	$-\frac{\sin(\beta-\theta)}{\sin(\alpha-\varphi)}e^{i(\alpha+\beta-\theta-\varphi)}s_1 - e^{-i(\alpha+\beta)}\frac{\sin\alpha}{\sin\beta}s_2 = 1$
L_{03}	$s_1 = 0$
L_{12}	$s_2 = 0$
L_{13}	$s_1 + s_2 = 1$
L_{23}	$s_1 - e^{-i(\alpha+\beta)}\frac{\sin\alpha}{\sin\beta}s_2 = 1$

Table 4.3: The equations defining the complex lines of two cone points collapsing in terms of the **s**-coordinates.

$\mathbf{t}_k$	s_1	s_2
$\mathbf{t}_1$	$\frac{e^{-i\alpha}\sin(\alpha-\varphi)\sin(\alpha+\beta)}{\sin(\alpha-\varphi)\sin\beta - e^{-i(\theta+\varphi)}\sin\alpha\sin(\beta-\theta)}$	$\frac{e^{i(\beta-\theta)}\sin\beta\sin(\alpha+\beta-\theta-\varphi)}{\sin(\alpha-\varphi)\sin\beta - e^{-i(\theta+\varphi)}\sin\alpha\sin(\beta-\theta)}$
$\mathbf{t}_2$	0	0
$\mathbf{t}_3$	$-\frac{\sin(\alpha-\varphi)\sin(\alpha+\beta)}{\sin(\beta-\theta)\sin(\theta+\varphi)}$	$-e^{i(\alpha+\beta)}\frac{\sin(\alpha+\theta)\sin\beta\sin(\alpha+\beta-\theta-\varphi)}{\sin(\beta-\theta)\sin\alpha\sin(\theta+\varphi)}$
$\mathbf{t}_4$	$-\frac{\sin(\alpha-\varphi)\sin(\alpha+\beta)}{\sin(\beta-\theta)\sin(\theta+\varphi)}$	0
$\mathbf{t}_5$	$-\frac{\sin(\alpha-\varphi)\sin(\alpha+\beta)}{\sin(\beta-\theta)\sin(\theta+\varphi)}$	$\frac{\sin(\alpha+\theta)\sin(\alpha+\beta-\theta-\varphi)}{\sin(\beta-\theta)\sin(\theta+\varphi)}$
$\mathbf{t}_6$	$\frac{\sin(\alpha+\beta)\sin(\theta+\varphi-\alpha)}{\sin\beta\sin(\theta+\varphi)}$	$-e^{i(\alpha+\beta)}\frac{\sin(\alpha+\beta-\theta-\varphi)}{\sin(\theta+\varphi)}$
$\mathbf{t}_7$	$-e^{-i(\alpha+\beta-\theta-\varphi)}\frac{\sin(\alpha-\varphi)\sin(\alpha+\beta)\sin(\theta+\varphi-\alpha)}{\sin(\beta-\theta)\sin\beta\sin(\theta+\varphi)}$	$-e^{i(\alpha+\beta)}\frac{\sin(\alpha+\beta-\theta-\varphi)}{\sin(\theta+\varphi)}$
$\mathbf{t}_8$	0	$-e^{i(\alpha+\beta)}\frac{\sin(\alpha+\beta-\theta-\varphi)}{\sin(\theta+\varphi)}$
$\mathbf{t}_9$	$e^{-i(\alpha+\beta-\theta-\varphi)}\frac{\sin(\alpha+\beta)}{\sin(\theta+\varphi)}$	$\frac{\sin(\beta+\varphi)\sin(\alpha+\beta-\theta-\varphi)}{\sin(\alpha-\varphi)\sin(\theta+\varphi)}$
$\mathbf{t}_{10}$	$e^{-i(\alpha+\beta-\theta-\varphi)}\frac{\sin(\alpha+\beta)}{\sin(\theta+\varphi)}$	0
$\mathbf{t}_{11}$	$e^{-i(\alpha+\beta-\theta-\varphi)}\frac{\sin(\alpha+\beta)}{\sin(\theta+\varphi)}$	$-e^{i(\alpha+\beta)}\frac{\sin(\beta+\varphi)\sin\beta\sin(\alpha+\beta-\theta-\varphi)}{\sin(\alpha-\varphi)\sin\alpha\sin(\theta+\varphi)}$
$\mathbf{t}_{12}$	$-e^{-i(\alpha+\beta-\theta-\varphi)}\frac{\sin(\alpha-\varphi)\sin(\theta+\varphi-\beta)\sin(\alpha+\beta)}{\sin(\beta-\theta)\sin\alpha\sin(\theta+\varphi)}$	$\frac{\sin\beta\sin(\alpha+\beta-\theta-\varphi)}{\sin\alpha\sin(\theta+\varphi)}$
$\mathbf{t}_{13}$	$\frac{\sin(\theta+\varphi-\beta)\sin(\alpha+\beta)}{\sin\alpha\sin(\theta+\varphi)}$	$\frac{\sin\beta\sin(\alpha+\beta-\theta-\varphi)}{\sin\alpha\sin(\theta+\varphi)}$
$\mathbf{t}_{14}$	0	$\frac{\sin\beta\sin(\alpha+\beta-\theta-\varphi)}{\sin\alpha\sin(\theta+\varphi)}$

Table 4.4: The **s**-coordinates of the vertices.

Remark 4.3.1. The equations of the lines are of the same form as the ones for the **t**-coordinates, except for the sign of the exponential for the t_1-coordinate and up to substituting $(\alpha, \beta, \theta, \varphi)$ with the new angles as in Figure 4.5, i.e. up to substituting $(\alpha, \beta, \theta, \varphi)$ with $(\alpha', \beta', \theta', \varphi') = (\pi + \theta - \beta, \alpha, \alpha + \beta - \pi, \pi + \theta + \varphi - \alpha - \beta)$. The same is true for the coordinates of the vertices. In other words, up to remembering

that $\alpha' = \pi + \theta - \beta$, $\beta' = \alpha$, $\theta' = \alpha + \beta - \pi$ and $\varphi' = \pi + \theta + \varphi - \alpha - \beta$ as in Figure 4.5, the s-coordinates can be equivalently listed as in the following tables.

L_{ij}	Equations in terms of the s-coordinates
L_{*0}	$s_1 = \frac{\sin(\alpha'-\varphi')\sin\theta'}{\sin\alpha'\sin(\theta'+\varphi')}$
L_{*1}	$s_2 = e^{i\theta'}\frac{\sin\varphi'}{\sin(\theta'+\varphi')}$
L_{*2}	$s_2 = \frac{\sin(\beta'-\theta')\sin\varphi'}{\sin\beta'\sin(\theta'+\varphi')}$
L_{*3}	$s_1 = e^{i\varphi'}\frac{\sin\theta'}{\sin(\theta'+\varphi')}$
L_{01}	$\frac{\sin\alpha'}{\sin(\alpha'-\varphi')}e^{-i\varphi'}s_1 + s_2 = 1$
L_{02}	$\frac{\sin\alpha'}{\sin(\alpha'-\varphi')}e^{-i\varphi'}s_1 + e^{-i\theta'}\frac{\sin\beta'}{\sin(\beta'-\theta')}s_2 = 1$
L_{03}	$s_1 = 0$
L_{12}	$s_2 = 0$
L_{13}	$s_1 + s_2 = 1$
L_{23}	$s_1 + e^{-i\theta'}\frac{\sin\beta'}{\sin(\beta'-\theta')}s_2 = 1$

Table 4.5: The equations of the complex lines in terms of the s-coordinates and of the angles in the target configuration.

t_k	s_1	s_2
t_1	$-\frac{e^{-i\beta'}\sin(\alpha'-\varphi')\sin\theta'}{\sin(\alpha'-\varphi')\sin(\beta'-\theta')-e^{-i(\theta'+\varphi')}\sin\alpha'\sin\beta'}$	$-\frac{e^{-i\alpha'}\sin\varphi'\sin(\beta'-\theta')}{\sin(\alpha'-\varphi')\sin(\beta'-\theta')-e^{-i(\theta'+\varphi')}\sin\alpha'\sin\beta'}$
t_2	0	0
t_3	$\frac{\sin(\alpha'-\varphi')\sin\theta'}{\sin\alpha'\sin(\theta'+\varphi')}$	$e^{i\theta'}\frac{\sin(\alpha'+\theta')\sin(\beta'-\theta')\sin\varphi'}{\sin\alpha'\sin\beta'\sin(\theta'+\varphi')}$
t_4	$\frac{\sin(\alpha'-\varphi')\sin\theta'}{\sin\alpha'\sin(\theta'+\varphi')}$	0
t_5	$\frac{\sin(\alpha'-\varphi')\sin\theta'}{\sin\alpha'\sin(\theta'+\varphi')}$	$\frac{\sin(\alpha'+\theta')\sin\varphi'}{\sin\alpha'\sin(\theta'+\varphi')}$
t_6	$\frac{\sin\theta'\sin(\beta'-\theta'-\varphi')}{\sin(\beta'-\theta')\sin(\theta'+\varphi')}$	$e^{i\theta'}\frac{\sin\varphi'}{\sin(\theta'+\varphi')}$
t_7	$e^{i\varphi'}\frac{\sin(\alpha'-\varphi')\sin\theta'\sin(\beta'-\theta'-\varphi')}{\sin\alpha'\sin(\beta'-\theta')\sin(\theta'+\varphi')}$	$e^{i\theta'}\frac{\sin\varphi'}{\sin(\theta'+\varphi')}$
t_8	0	$e^{i\theta'}\frac{\sin\varphi'}{\sin(\theta'+\varphi')}$
t_9	$e^{i\varphi'}\frac{\sin\theta'}{\sin(\theta'+\varphi')}$	$\frac{\sin(\alpha'-\theta'-\varphi')\sin\varphi'}{\sin(\alpha'-\varphi')\sin(\theta'+\varphi')}$
t_{10}	$e^{i\varphi'}\frac{\sin\theta'}{\sin(\theta'+\varphi')}$	0
t_{11}	$e^{i\varphi'}\frac{\sin\theta'}{\sin(\theta'+\varphi')}$	$e^{i\theta'}\frac{\sin(\alpha'-\theta'-\varphi')\sin(\beta'-\theta')\sin\varphi'}{\sin(\alpha'-\varphi')\sin\beta'\sin(\theta'+\varphi')}$
t_{12}	$e^{i\varphi'}\frac{\sin(\alpha'-\varphi')\sin(\beta'+\varphi')\sin\theta'}{\sin\alpha'\sin\beta'\sin(\theta'+\varphi')}$	$\frac{\sin(\beta'-\theta')\sin\varphi'}{\sin\beta'\sin(\theta'+\varphi')}$
t_{13}	$\frac{\sin(\beta'+\varphi')\sin\theta'}{\sin\beta'\sin(\theta'+\varphi')}$	$\frac{\sin(\beta'-\theta')\sin\varphi'}{\sin\beta'\sin(\theta'+\varphi')}$

$\mathbf{t}_{14}$	0	$\frac{\sin(\beta'-\theta')\sin\varphi'}{\sin\beta'\sin(\theta'+\varphi')}$

Table 4.6: The **s**-coordinates of the vertices in terms of the angles in the target configuration.

4.3.3 The polyhedron

As we can easily see just by looking at Tables 4.2 and 4.4, if we consider one column of either table, i.e. fixing one of t_1, t_2, s_1, s_2, most vertices have that particular coordinate either as a real number or a real number multiplied by a unit complex number of the same argument along the column (respectively $e^{-i\varphi}$, $e^{i\theta}$, $e^{i\varphi'}$ or $e^{i\theta'}$). The only ones not following this rule are $\mathbf{t}_1$ for the **s**-coordinates and $\mathbf{t}_2$ for the **t**-coordinates. It is hence natural to define the subspaces where the arguments of the coordinates have one of these special values, as in the table below. It is now natural to consider the portion of complex hyperbolic space consisting of all points with arguments of the coordinates included in the ranges bounded by these values, i.e. the region bounded by these subspaces. We hence define our polyhedron to be this region. At the end of Section 2.3, we mentioned that the sides of our polyhedron will be contained in bisectors. Now we will prove that these subspaces are bisectors and we will use them to cut out a polyhedron, which will be called D.

On the boundary of the polyhedron we have cells of different dimensions. The codimension 1 cells (3-dimensional cells) are called *sides*. The 2-dimensional cells are called *ridges* and the 1-dimensional cells are the *edges*. The *vertices* are the 0-dimensional cells in the boundary of the polyhedron. The sides of the polyhedron will be contained in bisectors, described in this section.

Bisector	Equation	Vertices in the bisector
$B(P)$	$\mathrm{Im}(t_1) = 0$	$\mathbf{t}_1, \mathbf{t}_3, \mathbf{t}_4, \mathbf{t}_5, \mathbf{t}_9, \mathbf{t}_{10}, \mathbf{t}_{12}, \mathbf{t}_{13}$
$B(P^{-1})$	$\mathrm{Im}(s_1) = 0$	$\mathbf{t}_2, \mathbf{t}_3, \mathbf{t}_4, \mathbf{t}_5, \mathbf{t}_6, \mathbf{t}_8, \mathbf{t}_{13}, \mathbf{t}_{14}$
$B(J)$	$\mathrm{Im}(e^{i\varphi}t_1) = 0$	$\mathbf{t}_1, \mathbf{t}_6, \mathbf{t}_7, \mathbf{t}_8, \mathbf{t}_9, \mathbf{t}_{11}, \mathbf{t}_{12}, \mathbf{t}_{14}$
$B(J^{-1})$	$\mathrm{Im}(e^{-i\varphi'}s_1) = 0$	$\mathbf{t}_2, \mathbf{t}_7, \mathbf{t}_8, \mathbf{t}_9, \mathbf{t}_{10}, \mathbf{t}_{11}, \mathbf{t}_{12}, \mathbf{t}_{14}$
$B(R_1)$	$\mathrm{Im}(t_2) = 0$	$\mathbf{t}_1, \mathbf{t}_3, \mathbf{t}_4, \mathbf{t}_6, \mathbf{t}_7, \mathbf{t}_9, \mathbf{t}_{10}, \mathbf{t}_{11}$
$B(R_1^{-1})$	$\mathrm{Im}(e^{-i\theta}t_2) = 0$	$\mathbf{t}_1, \mathbf{t}_3, \mathbf{t}_5, \mathbf{t}_6, \mathbf{t}_8, \mathbf{t}_{12}, \mathbf{t}_{13}, \mathbf{t}_{14}$
$B(R_2)$	$\mathrm{Im}(s_2) = 0$	$\mathbf{t}_2, \mathbf{t}_4, \mathbf{t}_5, \mathbf{t}_9, \mathbf{t}_{10}, \mathbf{t}_{12}, \mathbf{t}_{13}, \mathbf{t}_{14}$
$B(R_2^{-1})$	$\mathrm{Im}(e^{-i\theta'}s_2) = 0$	$\mathbf{t}_2, \mathbf{t}_3, \mathbf{t}_4, \mathbf{t}_6, \mathbf{t}_7, \mathbf{t}_8, \mathbf{t}_{10}, \mathbf{t}_{11}$

The reason for the bisectors to be denoted as $B(T)$ is that we want the map T to send the side contained in $B(T)$ to the one contained in $B(T^{-1})$, for T one of the maps $\{P, P^{-1}, J, J^{-1}, R_1, R_1^{-1}, R_2, R_2^{-1}\}$. The following lemma shows that this is the case.

Lemma 4.3.2. *In* $\mathbf{t}$- *and* $\mathbf{s}$-*coordinates and writing* $\theta' = \alpha + \beta - \pi$ *and* $\varphi' = \pi + \theta + \varphi - \alpha - \beta$, *we have*

- $\mathrm{Im}(t_1) \leq 0$ *if and only if* $|\langle \mathbf{t}, \mathbf{n}_{*1}\rangle| \leq \left|\langle \mathbf{t}, P^{-1}(\mathbf{n}_{*3})\rangle\right|$,
- $\mathrm{Im}(s_1) \geq 0$ *if and only if* $|\langle \mathbf{s}, \mathbf{n}_{*3}\rangle| \leq |\langle \mathbf{s}, P(\mathbf{n}_{*1})\rangle|$,
- $\mathrm{Im}(e^{i\varphi}t_1) \geq 0$ *if and only if* $|\langle \mathbf{t}, \mathbf{n}_{*0}\rangle| \leq \left|\langle \mathbf{t}, J^{-1}(\mathbf{n}_{*0})\rangle\right|$,
- $\mathrm{Im}(e^{-i\varphi'}s_1) \leq 0$ *if and only if* $|\langle \mathbf{s}, \mathbf{n}_{*0}\rangle| \leq |\langle \mathbf{s}, J(\mathbf{n}_{*0})\rangle|$,
- $\mathrm{Im}(t_2) \geq 0$ *if and only if* $|\langle \mathbf{t}, \mathbf{n}_{*2}\rangle| \leq \left|\langle \mathbf{t}, R_1^{-1}(\mathbf{n}_{*3})\rangle\right|$,
- $\mathrm{Im}(e^{-i\theta}t_2) \leq 0$ *if and only if* $|\langle \mathbf{t}, \mathbf{n}_{*3}\rangle| \leq |\langle \mathbf{t}, R_1(\mathbf{n}_{*2})\rangle|$,
- $\mathrm{Im}(s_2) \geq 0$ *if and only if* $|\langle \mathbf{s}, \mathbf{n}_{*1}\rangle| \leq \left|\langle \mathbf{s}, R_2^{-1}(\mathbf{n}_{*2})\rangle\right|$,
- $\mathrm{Im}(e^{-i\theta'}s_2) \leq 0$ *if and only if* $|\langle \mathbf{s}, \mathbf{n}_{*2}\rangle| \leq |\langle \mathbf{s}, R_2(\mathbf{n}_{*1})\rangle|$.

Remark 4.3.3. By definition, a point is in the polyhedron D if and only if it satisfies all the conditions on the left hand side in the lemma.

Note that the notation in the statement is a shortcut to avoid specifying the configuration every time. One can write down the right configuration by

remembering the configuration corresponding to the $\mathbf{t}$- and $\mathbf{s}$-coordinates and remembering the action of the maps on the coordinates as explained in Section 4.2. The key remark is that we always want to multiply vectors when applied to the same configuration. So, for example, for the first line we have $\mathbf{t}$-coordinates, which correspond to the configuration $(\alpha, \beta, \theta, \varphi)$ and hence $\mathbf{n}_{*1}$ is applied to the same configuration. Meanwhile, we want $P^{-1}(\mathbf{n}_{*3})$ to be also in configuration $(\alpha, \beta, \theta, \varphi)$. Since $(\alpha, \beta, \theta, \varphi) \overset{P}{\longmapsto} (\beta, \pi + \theta - \beta, \theta + \alpha - \beta, \varphi + \beta - \alpha)$, the first line of the lemma is

$$|\langle \mathbf{t}, \mathbf{n}_{*1}(\alpha, \beta, \theta, \varphi)\rangle| \leq \left|\langle \mathbf{t}, P^{-1}(\mathbf{n}_{*3}(\beta, \pi + \theta - \beta, \theta + \alpha - \beta, \varphi + \beta - \alpha))\rangle\right|.$$

The proof is along the lines of the one in Lemma 4.6 in [Par06], Lemma 4.2 in [BP15] and Lemma 7.2 of [Pas16]. We will prove the first line of the lemma and the others can be proved in a similar way.

Proof. Omitting the configurations above,

$$\mathbf{n}_{*1} = \begin{bmatrix} e^{-i\varphi}\frac{\sin(\alpha-\varphi)}{\sin\alpha} \\ 0 \\ 1 \end{bmatrix}, \qquad \mathbf{n}_{*3} = \begin{bmatrix} 0 \\ 1 \\ 1 \end{bmatrix}, \qquad P^{-1}(\mathbf{n}_{*3}) = \begin{bmatrix} \frac{\sin(\alpha-\varphi)}{\sin\alpha}e^{i\varphi} \\ 0 \\ 1 \end{bmatrix}.$$

Then

$$|\langle \mathbf{t}, \mathbf{n}_{*1}\rangle| = \left|\frac{\sin\theta\sin\varphi}{\sin(\theta+\varphi)} - \sin\varphi e^{i\varphi}t_1\right|,$$
$$\left|\langle \mathbf{t}, P^{-1}\mathbf{n}_{*3}\rangle\right| = \left|\frac{\sin\theta\sin\varphi}{\sin(\theta+\varphi)} - \sin\varphi e^{-i\varphi}t_1\right|,$$

and the first term is smaller than the second one if and only if $-\operatorname{Re}(e^{i\varphi}t_1) < -\operatorname{Re}(e^{-i\varphi}t_1)$ which is equivalent to $\operatorname{Im} t_1 < 0$. ∎

As we mentioned, the lemma explains the name given to the bisectors. In fact, for example the bisector $B(P)$ is, by definition, given by $\operatorname{Im}(t_1) = 0$, which corresponds, by the lemma, to the points satisfying

$$|\langle \mathbf{t}, \mathbf{n}_{*1}\rangle| = \left|\langle \mathbf{t}, P^{-1}(\mathbf{n}_{*3})\rangle\right|.$$

Applying P to both sides of the equality, we get a point in the bisector defined by

$$|\langle \mathbf{s}, P(\mathbf{n}_{*1})\rangle| = |\langle \mathbf{s}, \mathbf{n}_{*3}\rangle|,$$

which happens when $\mathrm{Im}(s_1) = 0$, which is indeed $B(P^{-1})$.

Now the polyhedron $D = D(\alpha, \beta, \theta, \varphi)$ is defined as the intersection of all the half spaces in the lemma. More precisely, it will be

$$D(\alpha,\beta,\theta,\varphi) = \left\{ \mathbf{t} = P(\mathbf{s}) \colon \begin{array}{ll} \arg(t_1) \in (-\varphi, 0), & \arg(t_2) \in (0, \theta), \\ \arg(s_1) \in (0, \varphi'), & \arg(s_2) \in (0, \theta') \end{array} \right\}, \quad (4.3.5)$$

where, as before, we have $\theta' = \alpha + \beta - \pi$ and $\varphi' = \pi + \theta + \varphi - \alpha - \beta$.

The sides (codimension 1 cells) of the polyhedron will be defined as $S(T) = \overline{D} \cap B(T)$. Each of them is contained in one of the bisectors in the table.

4.4 The combinatorial structure of the polyhedron

We now want to study the combinatorics of the polyhedron $D(\alpha, \beta, \theta, \varphi)$.

First we will see how the combinatorics change with the values of the angles. A more in depth analysis can be found for the specific 3-fold symmetry case in Section 5.7.1. Later we will study all possible side (3-dimensional facets) intersections in order to be able to list all possible ridges (2-dimensional facets) and edges (1-dimensional facets).

According to the values of the parameters, we will have occasions where the the three vertices on L_{*i} collapse to a single vertex, for $i = 0, 1, 2, 3$. This means that instead of having the three choices of vertices, we have only one, which will have new coordinates. A more in depth analysis is done in the next section for the 3-fold symmetry case.

Proposition 4.4.1. *We have*

- *the vertices on L_{*0} collapse when $\alpha - \varphi \geq \pi - \theta - \varphi$, i.e. when $\pi - \alpha - \theta \leq 0$,*
- *the vertices on L_{*1} collapse when $\pi - \alpha \geq \pi - \theta - \varphi$, i.e. $\alpha - \theta - \varphi \leq 0$,*
- *the vertices on L_{*2} collapse when $\sin(\beta - \theta)/\sin\beta \leq \sin\varphi/\sin(\theta + \varphi)$, i.e. $\beta - \theta - \varphi \leq 0$,*
- *the vertices on L_{*3} collapse when $\pi - \beta \leq \varphi$, i.e. $\pi - \beta - \varphi \leq 0$.*

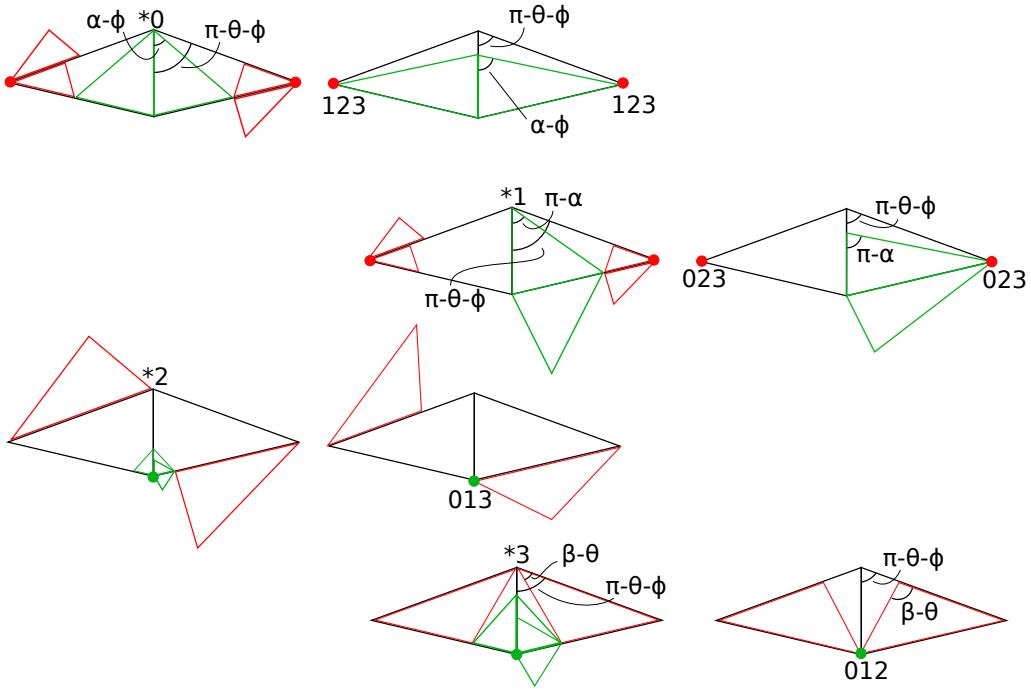

Figure 4.6: The collapsing vertices.

Figure 4.6 summarises the possible degenerations: each of the four pairs of configurations corresponds to an instance of the proposition. In each pair, the left configuration is a superposition of the three possible vertices when they do not collapse (in fact, the three vertices only differ by one of T_1 or T_2 having three different positions) and the configuration on the right hand side is the single vertex that appears when the collapsing happens.

Proof. We will prove the first instance of the proposition, since the others can be done in a similar way. Take vertices $\mathbf{t}_3$, $\mathbf{t}_4$ and $\mathbf{t}_5$ on L_{*0}. These are characterised by the fact that, when increasing the modulus of z_1 (i.e. making T_1 as big as possible), the vertex v_0 hits v_* before v_1 hits the vertex of T_3 with angle θ (see Figure 4.1). In other words, the vertices collapse if, before we can have $v_0 \equiv v_*$, we get $v_1 \equiv v_2 \equiv v_3$. This implies that there is no other choice for z_2 but to be zero, instead of having the three choices that give the three possible vertices with $v_0 \equiv v_*$. In terms of the parameters, this means that the three vertices collapse

when the angle of T_1 opposite z_1 is bigger than the angle of T_3 opposite z_3, i.e. when $\alpha - \varphi \geq \pi - \theta - \varphi$. ■

We remark that the sides all have the same combinatorial structure when they are not degenerate. In particular, they will look like in Figure 4.7. This is the same structure as 2 of the 10 sides in [DFP05], where this combinatorial structure first appeared. Later, in [Pas16], we showed how this structure is more general and all other fundamental domains for Deligne-Mostow lattices can be seen as a deformation of this structure given by Proposition 4.4.1. Each side will correspond to fixing the argument of one of the coordinates. Then there will be one triangular ridge (e.g. the bottom one) where the coordinate is equal to zero and a second triangular ridge (e.g. the top one) where the coordinate has another fixed value. The complex lines interpolating between the two will be the slices of the foliation (see Section 2.3). The edge connecting the two triangles is contained in the spine of the bisector and always contains one of the vertices $\mathbf{t}_1$ or $\mathbf{t}_2$. The pentagonal lateral ridges containing the vertical edge are contained in totally geodesic Lagrangian planes and are the extremities of the foliation by meridians. In the next lemma, we claim that in each side the modulus of the coordinate whose argument defines the bisector containing the side varies between the two values it assumes on the top and bottom triangular ridges. To check this, for example, in $S(J)$, we need to check that $|t_1|$ in $\mathbf{t}_{11}$ and $\mathbf{t}_{14}$ is smaller than $|t_1|$ in $\mathbf{t}_6$, $\mathbf{t}_7$ and $\mathbf{t}_8$ ($|t_1|$ has the same value in these three vertices, since they are contained in the complex line L_{*1}) and so on. It is an easy calculation (see proof of Lemma 4.4.2 below) to check that this is true for each side, as long as

$$\begin{aligned} &\sin(\alpha+\beta-\pi) \geq 0 && \sin(\pi+\alpha+\beta-\theta-\varphi) \geq 0 \\ &\sin(\alpha+\theta-\beta) \geq 0 && \sin(\beta+\varphi-\alpha) \geq 0. \end{aligned} \tag{4.4.1}$$

Remembering the action of P and P^{-1} on the angles, this means that we are just asking for the configuration, after applying these two maps, to make sense in our coordinates.

This gives us the following lemma:

Lemma 4.4.2. *If the parameters satisfy* (4.4.1)*, then*

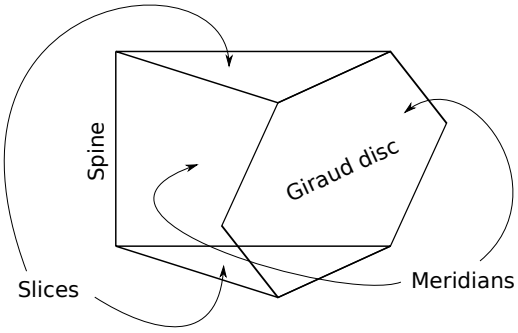

Figure 4.7: The combinatorial structure of a side.

- *In* $S(P)$, *we have* $|t_1| \leq \frac{\sin(\alpha-\varphi)\sin\theta}{\sin\alpha\sin(\theta+\varphi)}$,
- *In* $S(J)$, *we have* $|t_1| \leq \frac{\sin\theta}{\sin(\theta+\varphi)}$,
- *In* $S(R_1)$, *we have* $|t_2| \leq \frac{\sin(\beta-\theta)\sin\varphi}{\sin\beta\sin(\theta+\varphi)}$,
- *In* $S(R_1^{-1})$, *we have* $|t_2| \leq \frac{\sin\varphi}{\sin(\theta+\varphi)}$,
- *In* $S(P^{-1})$, *we have* $|s_1| \leq -\frac{\sin(\alpha-\varphi)\sin(\alpha+\beta)}{\sin(\beta-\theta)\sin(\theta+\varphi)}$,
- *In* $S(J^{-1})$, *we have* $|s_1| \leq -\frac{\sin(\alpha+\beta)}{\sin(\theta+\varphi)}$,
- *In* $S(R_2)$, *we have* $|s_2| \leq \frac{\sin(\alpha+\beta-\theta-\varphi)\sin\beta}{\sin\alpha\sin(\theta+\varphi)}$,
- *In* $S(R_2^{-1})$, *we have* $|s_2| \leq \frac{\sin(\alpha+\beta-\theta-\varphi)\sin\beta}{\sin\alpha\sin(\theta+\varphi)}$.

We will show the first instance of the lemma and all the others are done in a very similar way.

Proof. Let us take $\mathbf{t} \in S(P)$. This means that $\operatorname{Im} t_1 = 0$ and hence $t_1 = u \in \mathbb{R}$. Since the bisector is foliated by complex lines corresponding to the value of t_1, we just need to know that for each vertex $\mathbf{t}_i \in S(P)$ (i.e. $i = 1, 3, 4, 5, 9, 10, 12, 13$), we have $|u| \leq \frac{\sin(\alpha-\varphi)\sin\theta}{\sin\alpha\sin(\theta+\varphi)}$. Now, for $i = 1, 9, 12$, $u = 0$ and the condition is always satisfied. For $i = 3, 4, 5$, $u = \frac{\sin(\alpha-\varphi)\sin\theta}{\sin\alpha\sin(\theta+\varphi)}$ and the condition is always satisfied. For $i = 10$, we want

$$u = \frac{\sin(\beta+\theta)\sin\theta}{\sin\beta\sin(\theta+\varphi)} \leq \frac{\sin(\alpha-\varphi)\sin(\theta)}{\sin\alpha\sin(\theta+\varphi)},$$

which is true as long as the two following equivalent inequalities hold.

$$\sin(\beta+\varphi)\sin\alpha - \sin(\alpha-\varphi)\sin\beta \leq 0 \Longleftrightarrow \sin\varphi\sin(\alpha+\beta) \leq 0.$$

Since $\sin\varphi$ is always positive, the condition we want only requires $\sin(\alpha+\beta) \leq 0$, which means that $\sin(\alpha+\beta-\pi) \geq 0$.

Similarly, for $i = 13$, $u \leq \frac{\sin(\alpha-\varphi)\sin\theta}{\sin\alpha\sin(\theta+\varphi)}$ is equivalent to asking that

$$\frac{\sin(\beta-\theta-\varphi)\sin\theta}{\sin(\beta-\theta)\sin(\theta+\varphi)} \leq \frac{\sin(\alpha-\varphi)\sin(\theta)}{\sin\alpha\sin(\theta+\varphi)},$$

which is equivalent to

$$-\sin\varphi\sin(\alpha-\beta+\theta) \leq 0,$$

which is true since $\sin\varphi$ is always positive and the angles satisfy (4.4.1). ■

We now want to consider all possible side intersections to find the combinatorics of the polyhedron. We will denote by $\gamma_{i,j}$ the geodesic segment between the vertices $\mathbf{t}_i$ and $\mathbf{t}_j$. We will first analyse certain bisector intersections which are made of the union of two edges of the polyhedron. In all of the cases there will be three vertices inside the intersection and we will prove that the intersection actually consist in each case of the union of the only two edges connecting two of these points to a central one. We remark that we are always considering the parts of the intersection that are inside or on the boundary of our polyhedron.

Proposition 4.4.3. *The following side intersections consist of the union of two edges:*

$$\begin{aligned}
S(P)\cap S(J^{-1}) &= \gamma_{10,9}\cup\gamma_{9,12}, & S(R_1^{-1})\cap S(J^{-1}) &= \gamma_{8,14}\cup\gamma_{14,12},\\
S(P)\cap S(R_2^{-1}) &= \gamma_{3,4}\cup\gamma_{4,10}, & S(J)\cap S(R_2) &= \gamma_{9,12}\cup\gamma_{12,14},\\
S(R_1)\cap S(R_2) &= \gamma_{4,10}\cup\gamma_{10,9}, & S(J)\cap S(P^{-1}) &= \gamma_{6,8}\cup\gamma_{8,14},\\
S(R_1)\cap S(P^{-1}) &= \gamma_{4,3}\cup\gamma_{3,6}, & S(R_1^{-1})\cap S(R_2^{-1}) &= \gamma_{3,6}\cup\gamma_{6,8}.
\end{aligned}$$

Proof. We will prove the first point of the proposition and the rest can be proved using the same strategy. Let $\mathbf{t} \in D$ be contained in both $B(P)\cap B(J^{-1})$. By inspection on the table of vertices, one can see that $\mathbf{t}$ also belongs to $B(R_2)$. Then we can write $s_1 = ue^{i\varphi'}$, where $\varphi' = \pi+\theta-\alpha-\beta$ and $t_1 = x$. Since

here $P^{-1}\colon (\alpha,\beta,\theta,\varphi) \mapsto (\pi+\theta-\beta,\alpha,\alpha+\beta-\pi,\pi+\theta+\varphi-\alpha-\beta)$, we have $\mathbf{t} = P(\pi+\theta-\beta,\alpha,\alpha+\beta-\pi,\pi+\theta+\varphi-\alpha-\beta)(\mathbf{s})$ which we can use to calculate x in terms of s_2 and $s_1 = ue^{i\varphi'}$. We get

$$\begin{aligned}
&\Big(-\sin(\theta+\varphi)\sin(\beta-\theta)e^{i\alpha}e^{i\varphi'}u - \sin(\theta+\varphi)\sin\alpha e^{-i(\beta-\theta)}s_2 \\
&-\sin(\alpha+\beta)\sin\varphi + \sin(\theta+\varphi)\sin\alpha e^{-i(\beta-\theta)}\Big)x = \\
&= -\sin(\beta-\theta)\sin\theta e^{i(\alpha-\varphi)}e^{i\varphi'}u - \sin(\alpha-\varphi)\sin\theta e^{-i(\beta-\theta)}s_2 \\
&+\sin(\alpha-\varphi)\sin\theta e^{-i(\beta-\theta)},
\end{aligned}$$

so

$$\begin{aligned}
&s_2\left(\sin(\alpha-\varphi)\sin\theta - \sin(\theta+\varphi)\sin\alpha x\right) = \\
&\quad = -\sin(\beta-\theta)\sin\theta u - \sin(\alpha-\varphi)\sin\theta + \sin(\theta+\varphi)\sin(\beta-\theta)e^{i\varphi}ux \\
&\quad - x\left(\sin(\alpha+\beta)\sin\varphi e^{i(\beta-\theta)} + \sin(\theta+\varphi)\sin\alpha\right).
\end{aligned}$$

Then

$$0 = \operatorname{Im} s_2 = \frac{x(\sin(\theta+\varphi)\sin(\beta-\theta)\sin\varphi u - \sin(\alpha+\beta)\sin\varphi\sin(\beta-\theta))}{\sin(\alpha-\varphi)\sin\theta - \sin(\theta+\varphi)\sin\alpha x}$$

so, either $x=0$ or $u = \frac{\sin(\alpha+\beta)}{\sin(\theta+\varphi)}$. If $x=0$, then $\mathbf{t} \in B(J)$ and we are on $\gamma_{9,12}$. Otherwise, $\mathbf{t} \in L_{*3}$, so t_2 is real and $\mathbf{t} \in B(R_1)$, which means that we are on $\gamma_{10,9}$.

■

In some of the ridges contained in a complex line the intersection actually consists of the union of a triangle, which is the ridge itself, and an extra edge connected to one of the vertices of the ridge and not belonging to it. We will now see this for the remaining intersections. The proposition will state that if we have a point in the bisector intersection, but not belonging to the complex line containing the ridge, then it is on an edge with one vertex on the ridge and one outside.

Proposition 4.4.4. *The bisector intersections satisfy:*

- *A point* $\mathbf{t}$ *in the side intersection* $S(P)\cap S(P^{-1})$*, with* $t_1 \neq \frac{\sin\theta\sin(\alpha-\varphi)}{\sin\alpha\sin(\theta+\varphi)}$ *and* $s_1 \neq -\frac{\sin(\alpha+\beta)\sin(\alpha-\varphi)}{\sin(\beta-\theta)\sin(\theta+\varphi)}$*, belongs to the edge* $\gamma_{5,13}$.

- *A point* $\mathfrak{t}$ *in the side intersection* $S(J)\cap S(R_2^{-1})$*, with* $t_1 \neq e^{-i\varphi}\frac{\sin\theta}{\sin(\theta+\varphi)}$ *and* $s_2 \neq -e^{i(\alpha+\beta)}\frac{\sin(\alpha+\beta-\theta-\varphi)}{\sin(\theta+\varphi)}$*, belongs to the edge* $\gamma_{7,11}$*.*

- *Moreover, a point* $\mathfrak{t}$ *in the side intersection* $S(R_2)\cap S(R_1^{-1})$*, with* $t_2 \neq e^{i\theta}\frac{\sin\varphi}{\sin(\theta+\varphi)}$ *and* $s_2 \neq \frac{\sin(\alpha+\beta-\theta-\varphi)\sin\beta}{\sin\alpha\sin(\theta+\varphi)}$*, belongs to the edge* $\gamma_{5,13}$*.*

- *Finally, a point* $\mathfrak{t}$ *in the side intersection* $S(R_1)\cap S(J^{-1})$*, with* $t_2 \neq \frac{\sin(\beta-\theta)\sin\varphi}{\sin\beta\sin(\theta+\varphi)}$ *and* $s_1 \neq e^{-i(\alpha+\beta-\theta-\varphi)}\frac{\sin(\alpha+\beta)}{\sin(\theta+\varphi)}$*, belongs to the edge* $\gamma_{7,11}$*.*

We will prove the first point and the others are proved in the exact same way.

Proof. Let us take $\mathfrak{t}\in S(P)\cap S(P^{-1})$. Then

$$t_1 = x, \qquad\qquad s_1 = u$$

and by hypothesis, and using Lemma 4.4.2, we have

$$x \leq \frac{\sin\theta\sin(\alpha-\varphi)}{\sin\alpha\sin(\theta+\varphi)}, \qquad u \leq -\frac{\sin(\alpha+\beta)\sin(\alpha-\varphi)}{\sin(\beta-\theta)\sin(\theta+\varphi)}. \tag{4.4.2}$$

Then using (4.3.1) one can express t_2 and s_2 in terms of x and u as follows:

$$\begin{aligned}(\sin(\theta+\varphi)\sin\alpha x - \sin(\alpha-\varphi)\sin\theta)s_2 = \\ -\sin(\beta-\theta)\sin\theta e^{i(\alpha+\beta-\theta-\varphi)}u + \sin(\theta+\varphi)\sin(\beta-\theta)e^{i(\alpha+\beta-\theta)}ux \\ +(\sin(\alpha+\beta)\sin\varphi e^{i(\beta-\theta)} + \sin(\theta+\varphi)\sin\alpha)x - \sin(\alpha-\varphi)\sin\theta,\end{aligned}$$

$$\begin{aligned}(-\sin(\theta+\varphi)\sin(\beta-\theta)u - \sin(\alpha-\varphi)\sin(\alpha+\beta))\,t_2 = \\ \frac{\sin(\beta-\theta)}{\sin\beta}e^{-i\theta}(\sin\theta\sin(\alpha+\beta-\theta-\varphi)e^{i\alpha}u - \sin(\theta+\varphi)\sin\alpha e^{i(\alpha+\beta-\theta)}ux \\ +(\sin\alpha\sin(\alpha+\beta)e^{-i\varphi} - \sin(\alpha-\varphi)\sin(\alpha+\beta))x - \sin(\theta+\varphi)\sin(\beta-\theta)).\end{aligned}$$

Now, we know by Lemma 4.3.2 that inside D we have

$$\begin{aligned}0 \geq \operatorname{Im} e^{-i\theta}t_2 = \frac{\sin(\beta-\theta)\sin\alpha}{\sin\beta}\cdot \\ \cdot\frac{\sin(\alpha+\beta)\sin\varphi x + \sin(\theta+\varphi)\sin(\alpha+\beta-\theta)ux - \sin\theta\sin(\alpha+\beta-\theta-\varphi)u}{\sin(\theta+\varphi)\sin(\beta-\theta)u + \sin(\alpha-\varphi)\sin(\alpha+\beta)},\end{aligned}$$

but by (4.4.2) we know that the denominator is strictly negative and so the numerator must be positive.

Again by Lemma 4.3.2, $\mathbf{t}$ satisfies

$$0 \leq \operatorname{Im} s_2 = \sin(\beta - \theta) \cdot \\ \cdot \frac{\sin(\alpha+\beta)\sin\varphi x + \sin(\theta+\varphi)\sin(\alpha+\beta-\theta)ux - \sin\theta\sin(\alpha+\beta-\theta-\varphi)u}{\sin(\theta+\varphi)\sin\alpha x - \sin(\alpha-\varphi)\sin\theta},$$

and since by (4.4.2) the denominator must be strictly negative, then the numerator must be negative.

But since the two numerators coincide, then they must both equal 0. This means that the point we are considering must also be in $S(R_1^{-1})$ and in $S(R_2)$, which means that we are on edge $\gamma_{5,13}$. ■

Remark 4.4.5. The proof relies on Lemma 4.4.2. As we will see in Section 6.3.3, there are cases in which (4.4.1) is not satisfied. In term of configurations, this means that one needs to consider a slightly different configuration of triangles (see Section 6.3.3). Using the new configuration one can prove an equivalent statement using the exact same strategy of proof as in [Par06] and [Pas16].

Chapter 5

Lattices with 3-fold symmetry

Let us now consider a cone metric on the sphere with 5 cone singularities such that 3 of the cone angles are the same. The lattices obtained from these are the lattices with 3-fold symmetry. The contents of the first part of this chapter consist in showing how all the analysis in the previous chapter applies to the case of 3-fold symmetry. We will first show how to parametrise the configuration space and explain what the moves are like in this case. The main difference with the previous chapter is that now the moves will swap cone points with same cone angle and so the configuration type will never change. In other words, we will have $\alpha = \beta = \pi + \theta - \beta = \frac{\pi - \theta}{2}$. The second part of the chapter will prove that the polyhedron constructed in Section 4.3 is a fundamental domain for the group generated by the moves.

5.1 Cone structures

Let us now consider a cone metric on the sphere with cone angles

$$(\pi - \theta + 2\varphi, \pi + \theta, \pi + \theta, \pi + \theta, 2\pi - 2\theta - 2\varphi)\,. \tag{5.1.1}$$

This is the same as in (4.1.2) when we consider that $\alpha = \beta = \pi + \theta - \beta = \frac{\pi - \theta}{2}$. As before, these will be the angles at the cone points v_0, v_1, v_2, v_3, v_* respectively. From (3.4.1) one can see that the angles θ and φ correspond respectively to $\frac{2\pi}{p}$ and $\frac{\pi}{k}$, with p and k in Table 3.1.

Let us now take a path through v_1, v_2, v_3, v_* in order, cut through this path

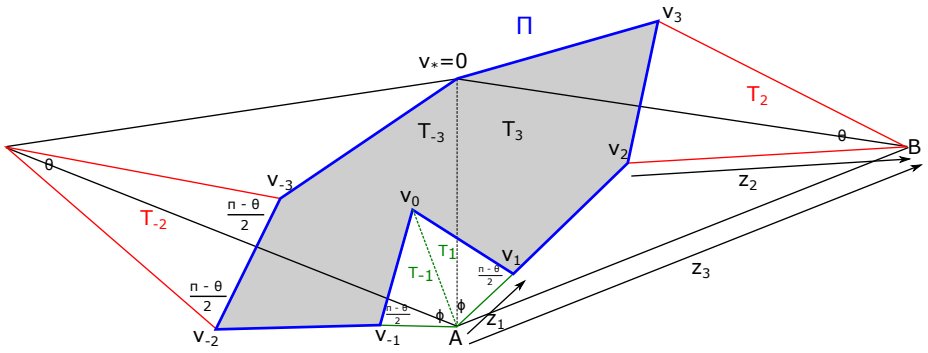

Figure 5.1: Octagon Π when the parameters are complex.

and open up the surface, obtaining an octagon like the one in Figure 5.1, called Π. Again, we choose the vertex v_* to be in the origin of our coordinates and we place Π such that v_0 is on the negative imaginary axis when the cone points are all along the equator of the sphere. We take the parameters z_1, z_2 and z_3 like in Chapter 4.

Then the vertices have the following coordinates.

$$\begin{aligned}
v_0 &= -i\frac{\sin\theta}{\sin(\theta+\varphi)}z_3 + i\frac{\sin\theta}{\sin\varphi+\sin(\theta-\varphi)}z_1,\\
v_1 &= ie^{-i\varphi}z_1 - i\frac{\sin\theta}{\sin(\theta+\varphi)}z_3,\\
v_2 &= -ie^{-i\varphi}z_2 + i\frac{e^{-i\theta-i\varphi}\sin\varphi}{\sin(\theta+\varphi)}z_3,\\
v_3 &= -ie^{-i\theta-i\varphi}z_2 + i\frac{e^{-i\theta-i\varphi}\sin\varphi}{\sin(\theta+\varphi)}z_3,\\
A &= -i\frac{\sin\theta}{\sin(\theta+\varphi)}z_3.
\end{aligned}$$

The area of the right half of the octagon can be obtained taking the area of T_3 and subtracting the area of T_1 and the area of T_2. The total area of Π will hence be twice this quantity. A simple calculation shows that

$$\begin{aligned}
\text{Area}(T_1) &= \frac{\sin\theta\sin\varphi}{2(\sin\varphi+\sin(\theta-\varphi))}|z_1|^2,\\
\text{Area}(T_2) &= \frac{\sin\theta}{2}|z_2|^2,\\
\text{Area}(T_3) &= \frac{\sin\theta\sin\varphi}{2\sin(\theta+\varphi)}|z_3|^2
\end{aligned}$$

and so

$$\begin{aligned}\operatorname{Area}\Pi &= 2\left(\operatorname{Area}T_3 - \operatorname{Area}T_1 - \operatorname{Area}T_2\right)\\ &= \frac{\sin\theta\sin\varphi}{\sin(\theta+\varphi)}|z_3|^2 - \sin\theta|z_2|^2 - \frac{\sin\theta\sin\varphi}{(\sin\varphi+\sin(\theta-\varphi))}|z_1|^2. \qquad (5.1.2)\end{aligned}$$

Following Section 4.1, one can put a complex hyperbolic structure on the moduli space we just parametrised.

Consider the Hermitian matrix

$$H = \sin\theta\begin{bmatrix} -\frac{\sin\varphi}{\sin\varphi+\sin(\theta-\varphi)} & 0 & 0\\ 0 & -1 & 0\\ 0 & 0 & \frac{\sin\varphi}{\sin(\theta+\varphi)}\end{bmatrix}. \qquad (5.1.3)$$

Since the area is given by Equation (5.1.2), this is equivalent to saying

$$\operatorname{Area}(\Pi) = \mathbf{z}^* H\mathbf{z}.$$

In this sense, the area gives an Hermitian form of signature (1,2) on $\mathbb{C}^3$.

We define hence our model of complex hyperbolic space as

$$\mathbf{H}^2_{\mathbb{C}} = \{\mathbf{z}\colon \langle\mathbf{z},\mathbf{z}\rangle = \mathbf{z}^* H\mathbf{z} > 0\}.$$

Then, asking for the area to be positive means that our complex hyperbolic structure is given by

$$\mathbf{H}^2_{\mathbb{C}} = \left\{\begin{bmatrix} z_1\\ z_2\\ z_3\end{bmatrix} \;:\; -\frac{\sin\theta\sin\varphi}{\sin\varphi+\sin(\theta-\varphi)}|z_1|^2 - \sin\theta|z_2|^2 + \frac{\sin\theta\sin\varphi}{\sin(\theta+\varphi)} > 0\right\}. \qquad (5.1.4)$$

5.2 Moves on the cone structures

We know that the second, third and fourth vertices have the same angle. This means that there is no canonical way of ordering them while choosing a path through the five points. Therefore the moves in Section 4.2 are now automorphisms of the sphere swapping cone points.

The first move R_1 fixes the vertices v_*, v_0 and v_1, and exchanges v_2 and v_3. This is equivalent to saying that the path on the sphere along which we will open

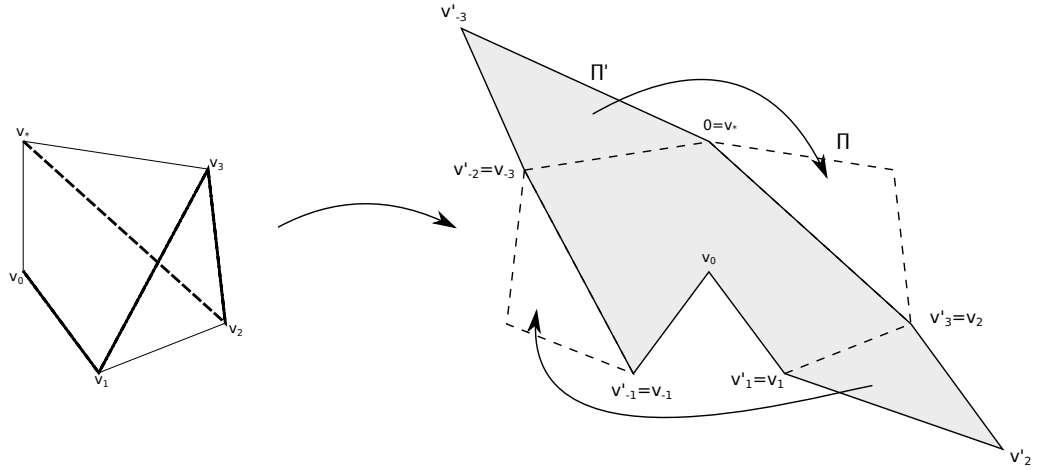

Figure 5.2: The cut for R_1 and the octagon we obtain. Vertices v_i''s are the images under R_1 of v_i's.

up the surface to give the polygon Π will be done starting in v_0, continuing in v_1 as before, but then passing, in order, through v_3 and v_2 and ending in v_*. In Figure 5.2 we show the new cut in the glued pentagons case and the octagon that we obtain.

The new octagon can be obtained from the previous one by a cut and paste. In fact, the new cut from v_* goes directly where v_2 was previously, as this is the image of v_3. Hence the triangle v_*, v_3, v_2 has to be glued on the segment between v_* and v_{-3} according to the identification of the sides. Similarly, the triangle v_{-1}, v_{-2}, v_{-3} has to be glued on the edge v_1, v_2, as in Figure 5.2. This means that the move R_1 does not change the area of the octagon.

One way to find the matrix of R_1 is by describing geometrically the position of the new variables, image of the z_i's. In fact, if we leave z_3 and z_1 as before and we multiply z_2 by $e^{i\theta}$, it geometrically means that we are rotating T_2 and T_{-2} by θ, fixing the vertex corresponding to angle θ, by definition of the variables. It is easy to see that this gives the configuration on the right hand side of Figure 5.2.

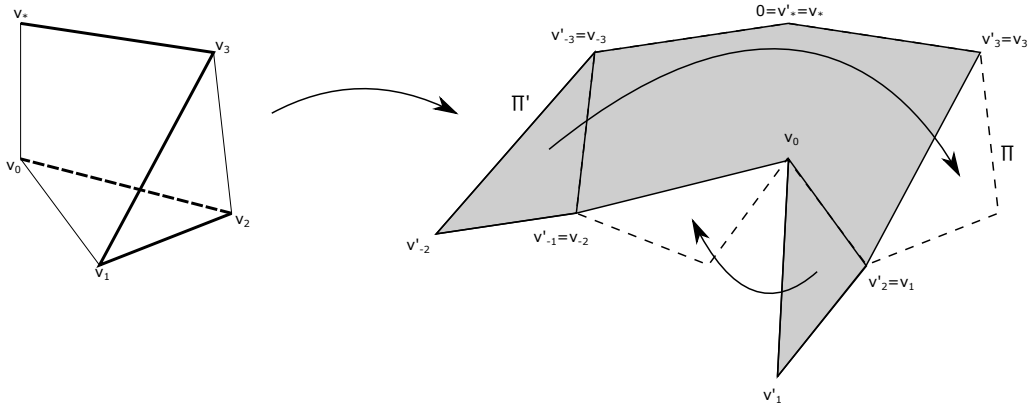

Figure 5.3: The cut for R_2. Again, v_i' is the image under R_2 of v_i.

The matrix of R_1 will hence be:

$$R_1 = \begin{bmatrix} 1 & 0 & 0 \\ 0 & e^{i\theta} & 0 \\ 0 & 0 & 1 \end{bmatrix}.$$

Let us now define the second move R_2. This new move fixes v_*, v_0 and v_3, while it interchanges v_1 and v_2. As before, this means that the cut that we do goes first through v_0, then to v_2 and v_1 and finally it ends as before by cutting through v_3 and v_*. The cut and the octagon are shown is Figure 5.3.

As before, in the figure we also showed the cut and paste map that we need to recover the initial shape. In particular, the triangle between v_3, v_2 and v_1 has to be glued on the edge v_{-2}, v_{-3}, as this time the cut goes from v_3 directly to the image of v_2, that coincides now with the position of v_1. Similarly, the triangle v_0, v_{-1}, v_{-2} has to be glued on edge v_0, v_1. Both gluings are done according to the side identifications we described when recovering the come metric from the octagon. We remark again that the existence of such a cut and paste implies that the area is preserved after applying the move R_2.

To find the matrix of the transformation one needs to see its action on the variables that determine the coordinates of the vertices. According to Figure 5.3, we therefore ask that $v_0' = v_0$, $v_2' = v_1$, $v_{-1}' = v_{-2}$ and $v_3' = v_3$.

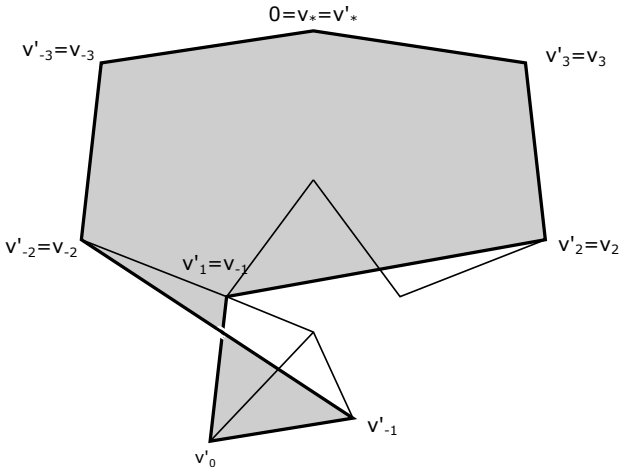

Figure 5.4: The octagon obtained after applying A_1.

The matrix for R_2 is:

$$R_2 = \frac{1}{(1-e^{-i\theta})\sin\varphi}\begin{bmatrix} -\sin\theta e^{-i\varphi} & -\sin\varphi - \sin(\theta-\varphi) & \sin\varphi + \sin(\theta-\varphi) \\ -\sin\varphi & -\sin\varphi e^{-i\theta} & \sin\varphi \\ -\sin(\theta+\varphi) & -\sin(\theta+\varphi) & \sin\varphi + \sin\theta e^{i\varphi} \end{bmatrix}.$$

The two moves R_1 and R_2 correspond, as automorphisms of the sphere with 5 cone singularities, to a Dehn twist along a curve through the two points we are swapping, not separating the other singularities.

The third move, A_1, will be exactly like in Section 4.2, making the triangle T_1 rotate so that vertices v_*, v_2, v_3 remain fixed, while v_1' coincides this time with v_{-1}.

Once again, the triangles T_2 and T_3 remain fixed and hence so are the variables z_2 and z_3. The third triangle is rotated of an angle of 2φ. This gives us the matrix of the move, which will be

$$A_1 = \begin{bmatrix} e^{2i\varphi} & 0 & 0 \\ 0 & 1 & 0 \\ 0 & 0 & 1 \end{bmatrix}.$$

As before, we can also see how it acts on the vertices and deduce from there the same matrix.

At this point, we want to consider the group $\Gamma = \langle R_1, R_2, A_1 \rangle$. Since the moves preserve the area, they are unitary with respect to the Hermitian form, i.e. $R_1^* H R_1 = H$ and same for R_2 and A_1. This can also easily checked by calculation. Hence they are elements of $PU(2,1)$ for the Hermitian form given in (5.1.3). For the values of φ and θ that we are considering (see Section 5.1), Γ is discrete and is in the list of Deligne-Mostow lattices described in Section 3.4.1. In fact, here we are implementing Thurston's procedure described in [Thu98], which, as he explains, is related with the groups previously constructed by Deligne and Mostow in [DM86] and [Mos80].

In the group $\Gamma = \langle R_1, R_2, A_1 \rangle$, we will often use some special elements, as already explained in Section 4.2. Here it will be easier to calculate them, since the moves do not change the configuration.

The first one is J, defined as $J = R_1 R_2 A_1$. Its matrix is

$$J = \frac{1}{\sin\varphi(1-e^{-i\theta})} \begin{bmatrix} -\sin\theta e^{i\varphi} & -\sin\varphi - \sin(\theta-\varphi) & \sin\varphi + \sin(\theta-\varphi) \\ -\sin\varphi e^{i(2\varphi+\theta)} & -\sin\varphi & \sin\varphi e^{i\theta} \\ -\sin(\theta+\varphi)e^{2i\varphi} & -\sin(\theta+\varphi) & \sin\varphi + \sin\theta e^{i\varphi} \end{bmatrix}.$$

We remark that J has zero trace and hence it has order 3. Most of the time we will consider projective equalities and drop the initial factor $\frac{1}{\sin\varphi(1-e^{-i\theta})}$. Projective equivalence will be denoted by the symbol $\sim$.

The second one is P, defined by $P = R_1 R_2$. Its matrix is:

$$P = \frac{1}{\sin\varphi(1-e^{-i\theta})} \begin{bmatrix} -\sin\theta e^{-i\varphi} & -\sin\varphi - \sin(\theta-\varphi) & \sin\varphi + \sin(\theta-\varphi) \\ -\sin\varphi e^{i\theta} & -\sin\varphi & \sin\varphi e^{i\theta} \\ -\sin(\theta+\varphi) & -\sin(\theta+\varphi) & \sin\varphi + \sin\theta e^{i\varphi} \end{bmatrix}.$$

Note that J previously defined can also be written as $J = PA_1$. The transformation P will be used here to give a new set of coordinates different from the $\mathbf{z}$-coordinates used until now. These are the same as the $\mathbf{s}$-coordinates introduced in Section 4.3.2.

The new coordinates are defined by

$$\mathbf{w} = \left[P^{-1}(\mathbf{z})\right].$$

This gives us the formulae

$$w_1 = \frac{-\sin\theta e^{i\varphi} z_1 - (\sin\varphi + \sin(\theta-\varphi))e^{-i\theta} z_2 + \sin\varphi + \sin(\theta-\varphi)}{-\sin(\theta+\varphi)z_1 - \sin(\theta+\varphi)e^{-i\theta} z_2 + \sin\varphi + \sin\theta e^{-i\varphi}}, \tag{5.2.1}$$

$$w_2 = \frac{-\sin\varphi z_1 - \sin\varphi z_2 + \sin\varphi}{-\sin(\theta+\varphi)z_1 - \sin(\theta+\varphi)e^{-i\theta} z_2 + \sin\varphi + \sin\theta e^{-i\varphi}}, \tag{5.2.2}$$

with inverses

$$z_1 = \frac{-\sin\theta e^{-i\varphi} w_1 - (\sin\varphi + \sin(\theta-\varphi))w_2 + \sin\varphi + \sin(\theta-\varphi)}{-\sin(\theta+\varphi)w_1 - \sin(\theta+\varphi)w_2 + \sin\varphi + \sin\theta e^{i\varphi}}, \tag{5.2.3}$$

$$z_2 = \frac{-\sin\varphi e^{i\theta} w_1 - \sin\varphi w_2 + \sin\varphi e^{i\theta}}{-\sin(\theta+\varphi)w_1 - \sin(\theta+\varphi)w_2 + \sin\varphi + \sin\theta e^{i\varphi}}. \tag{5.2.4}$$

The new set of coordinates makes it easier to describe the polyhedron, that will be defined by imposing that the arguments of the coordinates z_1, z_2, w_1, w_2 vary in a certain range.

We will denote $A_1' = J^{-1}R_1^{-1}R_2^{-1}$, coherently with the notations in [Par09]. We will often consider another transformation, which is the antiholomorphic isometry ι defined by $\iota(\mathbf{z}) = R_1R_2R_1(\overline{\mathbf{z}})$. Equivalently, $\iota(\mathbf{z}) = PR_1(\overline{\mathbf{z}})$. By definition,

$$\iota \begin{bmatrix} z_1 \\ z_2 \\ 1 \end{bmatrix} \sim \begin{bmatrix} \overline{w}_1 \\ \overline{w}_2 e^{i\theta} \\ 1 \end{bmatrix}. \tag{5.2.5}$$

This transformation will give us a symmetry of the polyhedron that we will construct (see Lemma 5.3.1).

Remark 5.2.1. A simple computation shows that ι is consistent with the maps defined previously. In other words, we have

$$J\iota = \iota J^{-1}, \qquad P\iota = \iota P^{-1} \qquad R_1\iota = \iota R_2^{-1} \qquad R_2\iota = \iota R_1^{-1}.$$

5.3 The polyhedron

In this section we will show how the polyhedron D constructed in Chapter 4 adapts to the lattices of 3-fold symmetry. We will also prove that it is a fundamental domain for the action of Γ on $\mathbf{H}^2_{\mathbb{C}}$. This is a general construction which contains all cases of lattices with three fold symmetry on Deligne and Mostow's list. The polyhedron as we will describe it here will be a fundamental domain in

some of the cases described in Section 3.4.1. In the other cases, the fundamental polyhedron will be obtained from this one by collapsing some triplets of vertices. Section 5.7.1 will be dedicated to the analysis of these cases, adapting Proposition 4.4.1 to the 3-fold symmetry case.

5.3.1 The vertices

Following Section 4.3, we will explain which points of $\mathbf{H}^2_{\mathbb{C}}$ are the special points which will represent the vertices of the polyhedron. For each of them we will give both $\mathbf{z}$-coordinates and $\mathbf{w}$-coordinates. As before, $\mathbf{w} = P^{-1}(\mathbf{z})$.

As before, these points will be obtained by making some cone points approach, until, in the limit, they coalesce. In this case, each vertex will be obtained by separately coalescing two distinct pairs of cone points. On the octagon Π, this corresponds to fixing the triangle T_3 and considering the cone metrics on the sphere corresponding to configurations when T_1 and T_2 are as small and as big as possible, in different directions, until pairs of vertices coincide. This is shown in Figure 5.5. Every time that we make two points coalesce, we turn two cone points into a new one.

In the following tables we describe the vertices of the polyhedron. The first one tells us, for each vertex, which cone points coalesced.

Vert.	Cone points		Vert.	Cone points		Vert.	Cone points	
$\mathbf{z}_1$	$v_0, v_{\pm 1}$	$v_{\pm 2}, v_{\pm 3}$	$\mathbf{z}_6$	$v_*, v_{\pm 1}$	$v_{\pm 2}, v_{\pm 3}$	$\mathbf{z}_{11}$	$v_*, v_{\pm 3}$	$v_0, v_{\pm 2}$
$\mathbf{z}_2$	$v_0, v_{\pm 3}$	$v_{\pm 1}, v_{\pm 2}$	$\mathbf{z}_7$	$v_*, v_{\pm 1}$	$v_0, v_{\pm 2}$	$\mathbf{z}_{12}$	$v_*, v_{\pm 2}$	$v_0, v_{\pm 1}$
$\mathbf{z}_3$	v_*, v_0	$v_{\pm 2}, v_{\pm 3}$	$\mathbf{z}_8$	$v_*, v_{\pm 1}$	$v_0, v_{\pm 3}$	$\mathbf{z}_{13}$	$v_*, v_{\pm 2}$	$v_{\pm 1}, v_{\pm 3}$
$\mathbf{z}_4$	v_*, v_0	$v_{\pm 1}, v_{\pm 2}$	$\mathbf{z}_9$	$v_*, v_{\pm 3}$	$v_0, v_{\pm 1}$	$\mathbf{z}_{14}$	$v_*, v_{\pm 2}$	$v_0, v_{\pm 3}$
$\mathbf{z}_5$	v_*, v_0	$v_{\pm 1}, v_{\pm 3}$	$\mathbf{z}_{10}$	$v_*, v_{\pm 3}$	$v_{\pm 1}, v_{\pm 2}$			

As mentioned, when two cone points collapse, we get a complex line in $\mathbf{H}^2_{\mathbb{C}}$. These complex lines are described by the following equations.

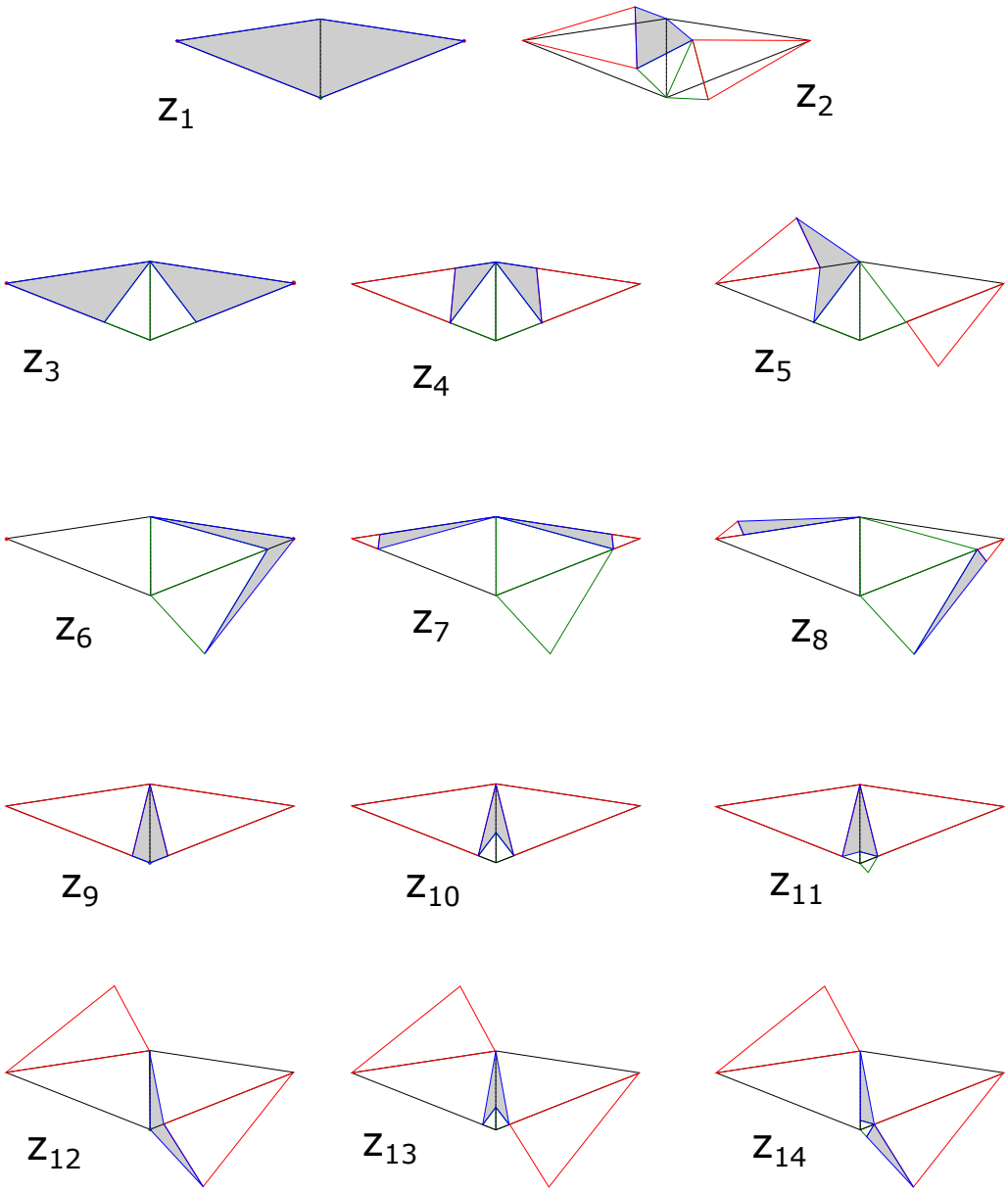

Figure 5.5: The degenerate configurations giving the vertices of the polyhedron.

L_{ij}	$\mathbf{z}$-coordinates equation	$\mathbf{w}$-coordinates equation
L_{*0}	$z_1 = \frac{\sin\varphi+\sin(\theta-\varphi)}{\sin(\theta+\varphi)}$	$w_1 = \frac{\sin\varphi+\sin(\theta-\varphi)}{\sin(\theta+\varphi)}$
L_{*1}	$z_1 = e^{-i\varphi}\frac{\sin\theta}{\sin(\theta+\varphi)}$	$w_2 = e^{i\theta}\frac{\sin\varphi}{\sin(\theta+\varphi)}$
L_{*2}	$z_2 = e^{i\theta}\frac{\sin\varphi}{\sin(\theta+\varphi)}$	$w_2 = \frac{\sin\varphi}{\sin(\theta+\varphi)}$
L_{*3}	$z_2 = \frac{\sin\varphi}{\sin(\theta+\varphi)}$	$w_1 = e^{i\varphi}\frac{\sin\theta}{\sin(\theta+\varphi)}$
L_{01}	$z_1 = 0$	$\frac{\sin\theta}{\sin\varphi+\sin(\theta-\varphi)}e^{-i\varphi}w_1 + w_2 = 1$
L_{02}	$\frac{\sin\theta}{\sin\varphi+\sin(\theta-\varphi)}e^{i\varphi}z_1 + z_2 = 1$	$\frac{\sin\theta}{\sin\varphi+\sin(\theta-\varphi)}e^{-i\varphi}w_1 + e^{-i\theta}w_2 = 1$
L_{03}	$\frac{\sin\theta}{\sin\varphi+\sin(\theta-\varphi)}e^{i\varphi}z_1 + e^{-i\theta}z_2 = 1$	$w_1 = 0$
L_{12}	$z_1 + z_2 = 1$	$w_2 = 0$
L_{23}	$z_2 = 0$	$w_1 + e^{-i\theta}w_2 = 1$
L_{13}	$z_1 + e^{-i\theta}z_2 = 1$	$w_1 + w_2 = 1$

With these equations, we can calculate the coordinates of the vertices by making the complex lines intersect or, equivalently, two pairs of points coalesce at the same time (see, again, the tables in Section 4.3). The first table will give us the $\mathbf{z}$ coordinates of all the vertices, while the second one will give us their $\mathbf{w}$ coordinates.

Vertex	coordinate z_1	coordinate z_2
$\mathbf{z}_1$	0	0
$\mathbf{z}_2$	$\frac{\sin\varphi+\sin(\theta-\varphi)}{\sin\varphi+e^{i\varphi}\sin\theta}$	$\frac{e^{i\theta}\sin\varphi}{\sin\varphi+e^{i\varphi}\sin\theta}$
$\mathbf{z}_3$	$\frac{\sin\varphi+\sin(\theta-\varphi)}{\sin(\theta+\varphi)}$	0
$\mathbf{z}_4$	$\frac{\sin\varphi+\sin(\theta-\varphi)}{\sin(\theta+\varphi)}$	$\frac{\sin\varphi(2\cos\theta-1)}{\sin(\theta+\varphi)}$
$\mathbf{z}_5$	$\frac{\sin\varphi+\sin(\theta-\varphi)}{\sin(\theta+\varphi)}$	$e^{i\theta}\frac{\sin\varphi(2\cos\theta-1)}{\sin(\theta+\varphi)}$
$\mathbf{z}_6$	$e^{-i\varphi}\frac{\sin\theta}{\sin(\theta+\varphi)}$	0
$\mathbf{z}_7$	$e^{-i\varphi}\frac{\sin\theta}{\sin(\theta+\varphi)}$	$1-\frac{\sin^2\theta}{\sin(\theta+\varphi)(\sin\varphi+\sin(\theta-\varphi))}$
$\mathbf{z}_8$	$e^{-i\varphi}\frac{\sin\theta}{\sin(\theta+\varphi)}$	$e^{i\theta}\left(1-\frac{\sin^2\theta}{\sin(\theta+\varphi)(\sin\varphi+\sin(\theta-\varphi))}\right)$
$\mathbf{z}_9$	0	$\frac{\sin\varphi}{\sin(\theta+\varphi)}$
$\mathbf{z}_{10}$	$\frac{\sin(\theta+\varphi)-\sin\varphi}{\sin(\theta+\varphi)}$	$\frac{\sin\varphi}{\sin(\theta+\varphi)}$
$\mathbf{z}_{11}$	$e^{-i\varphi}\frac{\sin\varphi+\sin(\theta-\varphi)}{\sin\theta}\left(1-\frac{\sin\varphi}{\sin(\theta+\varphi)}\right)$	$\frac{\sin\varphi}{\sin(\theta+\varphi)}$
$\mathbf{z}_{12}$	0	$e^{i\theta}\frac{\sin\varphi}{\sin(\theta+\varphi)}$
$\mathbf{z}_{13}$	$\frac{\sin(\theta+\varphi)-\sin\varphi}{\sin(\theta+\varphi)}$	$e^{i\theta}\frac{\sin\varphi}{\sin(\theta+\varphi)}$

$\mathbf{z}_{14}$	$e^{-i\varphi}\frac{\sin\varphi+\sin(\theta-\varphi)}{\sin\theta}\left(1-\frac{\sin\varphi}{\sin(\theta+\varphi)}\right)$	$e^{i\theta}\frac{\sin\varphi}{\sin(\theta+\varphi)}$

Vertex	coordinate w_1	coordinate w_2
$\mathbf{z}_1$	$\frac{\sin\varphi+\sin(\theta-\varphi)}{\sin\varphi+e^{-i\varphi}\sin\theta}$	$\frac{\sin\varphi}{\sin\varphi+e^{-i\varphi}\sin\theta}$
$\mathbf{z}_2$	0	0
$\mathbf{z}_3$	$\frac{\sin\varphi+\sin(\theta-\varphi)}{\sin(\theta+\varphi)}$	$e^{i\theta}\frac{\sin\varphi(2\cos\theta-1)}{\sin(\theta+\varphi)}$
$\mathbf{z}_4$	$\frac{\sin\varphi+\sin(\theta-\varphi)}{\sin(\theta+\varphi)}$	0
$\mathbf{z}_5$	$\frac{\sin\varphi+\sin(\theta-\varphi)}{\sin(\theta+\varphi)}$	$\frac{\sin\varphi(2\cos\theta-1)}{\sin(\theta+\varphi)}$
$\mathbf{z}_6$	$\frac{\sin(\theta+\varphi)-\sin\varphi}{\sin(\theta+\varphi)}$	$e^{i\theta}\frac{\sin\varphi}{\sin(\theta+\varphi)}$
$\mathbf{z}_7$	$e^{i\varphi}\frac{\sin\varphi+\sin(\theta-\varphi)}{\sin\theta}\left(1-\frac{\sin\varphi}{\sin(\theta+\varphi)}\right)$	$e^{i\theta}\frac{\sin\varphi}{\sin(\theta+\varphi)}$
$\mathbf{z}_8$	0	$e^{i\theta}\frac{\sin\varphi}{\sin(\theta+\varphi)}$
$\mathbf{z}_9$	$e^{i\varphi}\frac{\sin\theta}{\sin(\theta+\varphi)}$	$1-\frac{\sin^2\theta}{\sin(\theta+\varphi)(\sin\varphi+\sin(\theta-\varphi))}$
$\mathbf{z}_{10}$	$e^{i\varphi}\frac{\sin\theta}{\sin(\theta+\varphi)}$	0
$\mathbf{z}_{11}$	$e^{i\varphi}\frac{\sin\theta}{\sin(\theta+\varphi)}$	$e^{i\theta}\left(1-\frac{\sin^2\theta}{\sin(\theta+\varphi)(\sin\varphi+\sin(\theta-\varphi))}\right)$
$\mathbf{z}_{12}$	$e^{i\varphi}\frac{\sin\varphi+\sin(\theta-\varphi)}{\sin\theta}\left(1-\frac{\sin\varphi}{\sin(\theta+\varphi)}\right)$	$\frac{\sin\varphi}{\sin(\theta+\varphi)}$
$\mathbf{z}_{13}$	$\frac{\sin(\theta+\varphi)-\sin\varphi}{\sin(\theta+\varphi)}$	$\frac{\sin\varphi}{\sin(\theta+\varphi)}$
$\mathbf{z}_{14}$	0	$\frac{\sin\varphi}{\sin(\theta+\varphi)}$

These vertices present a symmetry given by the transformation ι. In fact, as we can immediately verify on the coordinates in the table, the following lemma holds:

Lemma 5.3.1. *The isometry ι defined by* (5.2.5) *has order 2 and acts on the vertices in the following way:*

$$\iota(\mathbf{z}_1)=\mathbf{z}_2, \qquad \iota(\mathbf{z}_3)=\mathbf{z}_4, \qquad \iota(\mathbf{z}_5)=\mathbf{z}_5, \qquad \iota(\mathbf{z}_6)=\mathbf{z}_{10},$$
$$\iota(\mathbf{z}_7)=\mathbf{z}_{11}, \qquad \iota(\mathbf{z}_8)=\mathbf{z}_9, \qquad \iota(\mathbf{z}_{12})=\mathbf{z}_{14}, \qquad \iota(\mathbf{z}_{13})=\mathbf{z}_{13}.$$

Following Section 4.3.3 (see (4.3.5)), we define our polyhedron to be:

$$D=\left\{\mathbf{z}=P(\mathbf{w})\colon \begin{array}{ll}\arg(z_1)\in(-\varphi,0), & \arg(z_2)\in(0,\theta),\\ \arg(w_1)\in(0,\varphi), & \arg(w_2)\in(0,\theta)\end{array}\right\}. \tag{5.3.1}$$

In other words, D is defined to be the intersection of the two wedges

$$W_1=\{\mathbf{z}\colon \arg(z_1)\in(-\varphi,0) \text{ and } \arg(z_2)\in(0,\theta)\}$$

and

$$W_2 = \{\mathbf{w}\colon \arg(w_1) \in (0,\varphi) \text{ and } \arg(w_2) \in (0,\theta)\}.$$

5.3.2 The sides

Following 4.3.3, the sides of the polyhedron will then be contained in bisectors, which are defined as in the following table.

Bisector	Equation	Points in the bisector
$B(P)$	$\mathrm{Im}(z_1) = 0$	$\mathbf{z}_1, \mathbf{z}_3, \mathbf{z}_4, \mathbf{z}_5, \mathbf{z}_9, \mathbf{z}_{10}, \mathbf{z}_{12}, \mathbf{z}_{13}$
$B(P^{-1})$	$\mathrm{Im}(w_1) = 0$	$\mathbf{z}_2, \mathbf{z}_3, \mathbf{z}_4, \mathbf{z}_5, \mathbf{z}_6, \mathbf{z}_8, \mathbf{z}_{13}, \mathbf{z}_{14}$
$B(J)$	$\mathrm{Im}(e^{i\varphi} z_1) = 0$	$\mathbf{z}_1, \mathbf{z}_6, \mathbf{z}_7, \mathbf{z}_8, \mathbf{z}_9, \mathbf{z}_{11}, \mathbf{z}_{12}, \mathbf{z}_{14}$
$B(J^{-1})$	$\mathrm{Im}(e^{-i\varphi} w_1) = 0$	$\mathbf{z}_2, \mathbf{z}_7, \mathbf{z}_8, \mathbf{z}_9, \mathbf{z}_{10}, \mathbf{z}_{11}, \mathbf{z}_{12}, \mathbf{z}_{14}$
$B(R_1)$	$\mathrm{Im}(z_2) = 0$	$\mathbf{z}_1, \mathbf{z}_3, \mathbf{z}_4, \mathbf{z}_6, \mathbf{z}_7, \mathbf{z}_9, \mathbf{z}_{10}, \mathbf{z}_{11}$
$B(R_1^{-1})$	$\mathrm{Im}(e^{-i\theta} z_2) = 0$	$\mathbf{z}_1, \mathbf{z}_3, \mathbf{z}_5, \mathbf{z}_6, \mathbf{z}_8, \mathbf{z}_{12}, \mathbf{z}_{13}, \mathbf{z}_{14}$
$B(R_2)$	$\mathrm{Im}(w_2) = 0$	$\mathbf{z}_2, \mathbf{z}_4, \mathbf{z}_5, \mathbf{z}_9, \mathbf{z}_{10}, \mathbf{z}_{12}, \mathbf{z}_{13}, \mathbf{z}_{14}$
$B(R_2^{-1})$	$\mathrm{Im}(e^{-i\theta} w_2) = 0$	$\mathbf{z}_2, \mathbf{z}_3, \mathbf{z}_4, \mathbf{z}_6, \mathbf{z}_7, \mathbf{z}_8, \mathbf{z}_{10}, \mathbf{z}_{11}$

Finally, the following lemma proves that the subspaces defined are bisectors and that we named them following the convention just described and is the same as Lemma 4.3.2.

Lemma 5.3.2. *In* $\mathbf{z}$ *and* $\mathbf{w}$ *coordinates, we have*

- $\mathrm{Im}(z_1) < 0$ *if and only if* $|\langle \mathbf{z}, \mathbf{n}_{*1}\rangle| < |\langle \mathbf{z}, P^{-1}(\mathbf{n}_{*3})\rangle|$,
- $\mathrm{Im}(w_1) > 0$ *if and only if* $|\langle \mathbf{w}, \mathbf{n}_{*3}\rangle| < |\langle \mathbf{w}, P(\mathbf{n}_{*1})\rangle|$,
- $\mathrm{Im}(e^{i\varphi} z_1) > 0$ *if and only if* $|\langle \mathbf{z}, \mathbf{n}_{*0}\rangle| < |\langle \mathbf{z}, J^{-1}(\mathbf{n}_{*0})\rangle|$,
- $\mathrm{Im}(e^{-i\varphi} w_1) < 0$ *if and only if* $|\langle \mathbf{w}, \mathbf{n}_{*0}\rangle| < |\langle \mathbf{w}, J(\mathbf{n}_{*0})\rangle|$,
- $\mathrm{Im}(z_2) > 0$ *if and only if* $|\langle \mathbf{z}, \mathbf{n}_{*2}\rangle| < |\langle \mathbf{z}, R_1^{-1}(\mathbf{n}_{*3})\rangle|$,
- $\mathrm{Im}(e^{-i\theta} z_2) < 0$ *if and only if* $|\langle \mathbf{z}, \mathbf{n}_{*3}\rangle| < |\langle \mathbf{z}, R_1(\mathbf{n}_{*2})\rangle|$,
- $\mathrm{Im}(w_2) > 0$ *if and only if* $|\langle \mathbf{w}, \mathbf{n}_{*1}\rangle| < |\langle \mathbf{w}, R_2^{-1}(\mathbf{n}_{*2})\rangle|$,
- $\mathrm{Im}(e^{-i\theta} w_2) < 0$ *if and only if* $|\langle \mathbf{w}, \mathbf{n}_{*2}\rangle| < |\langle \mathbf{w}, R_2(\mathbf{n}_{*1})\rangle|$.

5.3.3 The ridges and edges

5.3.3.1 Useful inequalities

In this section we will present some trigonometric inequalities that will be used all through the following sections.

Lemma 5.3.3. *Let* $\mathbf{z} \in \mathbf{H}^2_{\mathbb{C}}$. *Then*

$$|z_1|^2, |w_1|^2 \leq \frac{\sin\varphi + \sin(\theta-\varphi)}{\sin(\theta+\varphi)}, \qquad \textit{and} \qquad |z_2|^2, |w_2|^2 \leq \frac{\sin\varphi}{\sin(\theta+\varphi)}.$$

Proof. Let us assume that this is not the case, hence $|z_1|^2 > \frac{\sin\varphi+\sin(\theta-\varphi)}{\sin(\theta+\varphi)}$. Now, by the area formula (5.1.4), we have

$$\begin{aligned}
0 &< -\frac{\sin\theta\sin\varphi}{\sin\varphi+\sin(\theta-\varphi)}|z_1|^2 - \sin\theta|z_2|^2 + \frac{\sin\theta\sin\varphi}{\sin(\theta+\varphi)} \\
&< -\frac{\sin\varphi+\sin(\theta-\varphi)}{\sin(\theta+\varphi)} \cdot \frac{\sin\theta\sin\varphi}{\sin\varphi+\sin(\theta-\varphi)} - \sin\theta|z_2|^2 + \frac{\sin\theta\sin\varphi}{\sin(\theta+\varphi)} \\
&= -\sin\theta|z_2|^2 \leq 0,
\end{aligned}$$

which is a contradiction. Therefore we must have $|z_1|^2 \leq \frac{\sin\varphi+\sin(\theta-\varphi)}{\sin(\theta+\varphi)}$.

Similarly, let us assume that $|z_2|^2 > \frac{\sin\varphi}{\sin(\theta+\varphi)}$. Then

$$\begin{aligned}
0 &< -\frac{\sin\theta\sin\varphi}{\sin\varphi+\sin(\theta-\varphi)}|z_1|^2 - \sin\theta|z_2|^2 + \frac{\sin\theta\sin\varphi}{\sin(\theta+\varphi)} \\
&< -\frac{\sin\theta\sin\varphi}{\sin\varphi+\sin(\theta-\varphi)}|z_1|^2 - \sin\theta \cdot \frac{\sin\varphi}{\sin(\theta+\varphi)} + \frac{\sin\theta\sin\varphi}{\sin(\theta+\varphi)} \\
&= -\frac{\sin\theta\sin\varphi}{\sin\varphi+\sin(\theta-\varphi)}|z_1|^2 \leq 0.
\end{aligned}$$

Hence we must have $|z_2|^2 \leq \frac{\sin\varphi}{\sin(\theta+\varphi)}$.

The proofs for w_1 and w_2 go in the same way. ∎

The second useful lemma is the following, divided in two cases according to the values of p and l, the latter as defined in Section 3.4.1 (see (3.4.3)) in terms of p and k.

Lemma 5.3.4. *Let* $\mathbf{z} \in \mathbf{H}^2_{\mathbb{C}}$. *Then we have*

1. *If* $p > 6$, *then*

$$|z_1|, |w_1| < 1,$$

2. If $l \geq 0$, then

$$|z_2|, |w_2| \leq 1.$$

Proof. Obviously if the square of the modulus of a coordinate is smaller than 1, so is the modulus of the coordinate itself. We then just need to prove that the square of such moduli are smaller than 1. By the previous Lemma 5.3.3, we have

$$|z_1|^2, |w_1|^2 \leq \frac{\sin\varphi + \sin(\theta - \varphi)}{\sin(\theta + \varphi)}.$$

For the first part, we then just need to show that

$$\frac{\sin\varphi + \sin(\theta - \varphi)}{\sin(\theta + \varphi)} < 1.$$

But we have

$$\frac{\sin\varphi + \sin(\theta - \varphi)}{\sin(\theta + \varphi)} = \frac{\sin\varphi - 2\sin\varphi\cos\theta}{\sin(\theta + \varphi)} + 1 = 1 - \frac{\sin\varphi}{\sin(\theta + \varphi)}(2\cos\theta - 1) < 1,$$

where the last inequality comes from the fact that $\frac{\sin\varphi}{\sin(\theta+\varphi)}(2\cos\theta - 1)$ is positive when $0 < \theta < \frac{\pi}{3}$. Since $\theta = \frac{2\pi}{p}$, this is the case when $p > 6$, as required.

For the second inequality, by the same Lemma 5.3.3, we just need to prove that

$$\frac{\sin\varphi}{\sin(\theta + \varphi)} \leq 1.$$

But this is true as long as $\sin\varphi \leq \sin(\theta+\varphi)$. Moreover, this condition is equivalent to the statement

$$\theta + \varphi \leq \pi - \varphi \iff 0 \leq \pi - 2\varphi - \theta \iff 0 \leq \frac{2\pi}{2} - \frac{2\pi}{k} - \frac{2\pi}{p} \iff 0 \leq l,$$

where the second equivalence comes from the fact that $\theta = \frac{2\pi}{p}$, $\varphi = \frac{\pi}{k}$ and $\frac{1}{l} = \frac{1}{2} - \frac{1}{p} - \frac{1}{k}$. This implies that the condition in the second inequality corresponds to $l \geq 0$ and hence we are done. ∎

5.3.3.2 Ridges

In this section we will present the dimension 2 facets of our polyhedron, i.e. the ridges. We will divide the ridges in two types. The first type of ridge is obtained by intersecting two bisectors containing either the vertex $\mathbf{z}_1$ or $\mathbf{z}_2$ in their intersection. We will get from these intersections some pentagonal ridges

and some triangular ones. The former will be contained in Lagrangian planes, while the latter are contained in complex lines.

The second type of ridge comes from the intersections of bisectors defined by one condition on the **z**-coordinates and one on the **w**-coordinates. We will again get some triangular ridges, contained in complex lines, but this time we will also get hexagonal ridges, contained in Giraud discs.

We will name the ridges according to the following convention. The ridge named $F(T,S)$, for $T,S \in \{P, P^{-1}, J, J^{-1}, R_1, R_1^{-1}, R_2, R_2^{-1}\}$, will be the ridge contained in the intersection of the bisector $B(T)$ and $B(S)$.

The following table summarizes the ridges of the first type. In the first group there are ridges in the intersection of two bisectors, both containing the vertex $\mathbf{z}_1$ (in other words, bisectors defined by conditions on the **z**-coordinates). In the second group are ridges contained in two bisectors defined by conditions on the **w**-coordinates. The last column says if the ridge is contained in a complex line, marked with S as it is a common slice of the two bisector, or in a Lagrangian plane, marked with M because it is a common meridian of the two bisectors.

Ridge	Vertices in the ridge	Coordinates	
$F(P,J)$	$\mathbf{z}_1, \mathbf{z}_9, \mathbf{z}_{12}$	$z_1 = 0$	S
$F(R_1, R_1^{-1})$	$\mathbf{z}_1, \mathbf{z}_3, \mathbf{z}_6$	$z_2 = 0$	S
$F(P,R_1)$	$\mathbf{z}_1, \mathbf{z}_3, \mathbf{z}_4, \mathbf{z}_9, \mathbf{z}_{10}$	$\mathrm{Im}(z_1) = \mathrm{Im}(z_2) = 0$	M
$F(P,R_1^{-1})$	$\mathbf{z}_1, \mathbf{z}_3, \mathbf{z}_5, \mathbf{z}_{12}, \mathbf{z}_{13}$	$\mathrm{Im}(z_1) = \mathrm{Im}(e^{-i\theta} z_2) = 0$	M
$F(J,R_1)$	$\mathbf{z}_1, \mathbf{z}_6, \mathbf{z}_7, \mathbf{z}_9, \mathbf{z}_{11}$	$\mathrm{Im}(e^{i\varphi} z_1) = \mathrm{Im}(z_2) = 0$	M
$F(J,R_1^{-1})$	$\mathbf{z}_1, \mathbf{z}_6, \mathbf{z}_8, \mathbf{z}_{12}, \mathbf{z}_{14}$	$\mathrm{Im}(e^{i\varphi} z_1) = \mathrm{Im}(e^{-i\theta} z_2) = 0$	M
$F(P^{-1},J^{-1})$	$\mathbf{z}_2, \mathbf{z}_8, \mathbf{z}_{14}$	$w_1 = 0$	S
$F(R_2, R_2^{-1})$	$\mathbf{z}_2, \mathbf{z}_4, \mathbf{z}_{10}$	$w_2 = 0$	S
$F(P^{-1},R_2)$	$\mathbf{z}_2, \mathbf{z}_4, \mathbf{z}_5, \mathbf{z}_{13}, \mathbf{z}_{14}$	$\mathrm{Im}(w_1) = \mathrm{Im}(w_2) = 0$	M
$F(P^{-1},R_2^{-1})$	$\mathbf{z}_2, \mathbf{z}_3, \mathbf{z}_4, \mathbf{z}_6, \mathbf{z}_8$	$\mathrm{Im}(w_1) = \mathrm{Im}(e^{-i\theta} w_2) = 0$	M
$F(J^{-1},R_2)$	$\mathbf{z}_2, \mathbf{z}_9, \mathbf{z}_{10}, \mathbf{z}_{12}, \mathbf{z}_{14}$	$\mathrm{Im}(e^{-i\varphi} w_1) = \mathrm{Im}(w_2) = 0$	M
$F(J^{-1},R_2^{-1})$	$\mathbf{z}_2, \mathbf{z}_7, \mathbf{z}_8, \mathbf{z}_{10}, \mathbf{z}_{11}$	$\mathrm{Im}(e^{-i\varphi} w_1) = \mathrm{Im}(e^{-i\theta} z_2) = 0$	M

The second type of ridges are the ones not containing the vertices $\mathbf{z}_1$ or $\mathbf{z}_2$ and they are listed in the following table. In this case the ridges are contained

either in a Giraud disc or in a complex line. The last column of the table will hence have a G in the first case and, as before, an S in the latter.

Ridge	Vertices in the ridge	Coordinates	
$F(P, R_2)$	$\mathbf{z}_4, \mathbf{z}_5, \mathbf{z}_9, \mathbf{z}_{10}, \mathbf{z}_{12}, \mathbf{z}_{13}$	$\mathrm{Im}(z_1) = \mathrm{Im}(w_2) = 0$	G
$F(J, J^{-1})$	$\mathbf{z}_7, \mathbf{z}_8, \mathbf{z}_9, \mathbf{z}_{11}, \mathbf{z}_{12}, \mathbf{z}_{14}$	$\mathrm{Im}(e^{i\varphi} z_1) = \mathrm{Im}(e^{-i\varphi} w_1) = 0$	G
$F(R_1, R_2^{-1})$	$\mathbf{z}_3, \mathbf{z}_4, \mathbf{z}_6, \mathbf{z}_7, \mathbf{z}_{10}, \mathbf{z}_{11}$	$\mathrm{Im}(z_2) = \mathrm{Im}(e^{-i\theta} w_2) = 0$	G
$F(R_1^{-1}, P^{-1})$	$\mathbf{z}_3, \mathbf{z}_5, \mathbf{z}_6, \mathbf{z}_8, \mathbf{z}_{13}, \mathbf{z}_{14}$	$\mathrm{Im}(e^{-i\theta} z_2) = \mathrm{Im}(w_1) = 0$	G
$F(P, P^{-1})$	$\mathbf{z}_3, \mathbf{z}_4, \mathbf{z}_5$	$\mathrm{Im}(z_1) = \mathrm{Im}(w_1) = 0$	S
$F(J, R_2^{-1})$	$\mathbf{z}_6, \mathbf{z}_7, \mathbf{z}_8$	$\mathrm{Im}(e^{i\varphi} z_1) = \mathrm{Im}(e^{-i\theta} w_2) = 0$	S
$F(R_1, J^{-1})$	$\mathbf{z}_9, \mathbf{z}_{10}, \mathbf{z}_{11}$	$\mathrm{Im}(z_2) = \mathrm{Im}(e^{-i\varphi} w_1) = 0$	S
$F(R_1^{-1}, R_2)$	$\mathbf{z}_{12}, \mathbf{z}_{13}, \mathbf{z}_{14}$	$\mathrm{Im}(e^{-i\theta} z_2) = \mathrm{Im}(w_2) = 0$	S

From now on the ridges contained in a common slice will be called S-ridges, the ones contained in a meridian will be the M-ridges and the ones contained in a Giraud disc will be the G-ridges.

5.3.3.3 Edges

So far, we discussed most facets of the polyhedron: the vertices, the ridges, the sides. In this section we will present the last missing ones, the 1-dimensional facets of D, called edges. Remember that the edge between two vertices $\mathbf{z}_i$ and $\mathbf{z}_j$ will be denoted by $\gamma_{i,j} = \gamma_{j,i}$. The edges of the polyhedron D arise as 1-dimensional intersection of three or more sides. In the following table we will list them, pointing out in which ridges they are contained.

Edge	S-ridge	M-ridge	M-ridge	G-ridge	G-ridge
$\gamma_{1,3}$	$F(R_1, R_1^{-1})$	$F(P, R_1)$	$F(P, R_1^{-1})$		
$\gamma_{1,6}$	$F(R_1, R_1^{-1})$	$F(J, R_1)$	$F(J, R_1^{-1})$		
$\gamma_{1,9}$	$F(P, J)$	$F(P, R_1)$	$F(J, R_1)$		
$\gamma_{1,12}$	$F(P, J)$	$F(P, R_1^{-1})$	$F(J, R_1^{-1})$		
$\gamma_{2,4}$	$F(R_2, R_2^{-1})$	$F(P^{-1}, R_2^{-1})$	$F(P^{-1}, R_2)$		
$\gamma_{2,8}$	$F(P^{-1}, J^{-1})$	$F(P^{-1}, R_2^{-1})$	$F(J^{-1}, R_2^{-1})$		
$\gamma_{2,10}$	$F(R_2, R_2^{-1})$	$F(J^{-1}, R_2)$	$F(J^{-1}, R_2^{-1})$		

$\gamma_{2,14}$	$F(P^{-1}, J^{-1})$	$F(P^{-1}, R_2)$	$F(J^{-1}, R_2)$		
$\gamma_{5,13}$		$F(P, R_1^{-1})$	$F(P^{-1}, R_2)$	$F(P, R_2)$	$F(R_1^{-1}, P^{-1})$
$\gamma_{7,11}$		$F(J, R_1)$	$F(J^{-1}, R_2^{-1})$	$F(J, J^{-1})$	$F(R_1, R_2^{-1})$
$\gamma_{9,10}$	$F(R_1, J^{-1})$	$F(P, R_1)$	$F(J^{-1}, R_2)$	$F(P, R_2)$	
$\gamma_{3,4}$	$F(P, P^{-1})$	$F(P, R_1)$	$F(P^{-1}, R_2^{-1})$	$F(R_1, R_2^{-1})$	
$\gamma_{6,8}$	$F(J, R_2^{-1})$	$F(J, R_1^{-1}$	$F(P^{-1}, R_2)$	$F(R_1^{-1}, P^{-1})$	
$\gamma_{12,14}$	$F(R_1^{-1}, R_2)$	$F(J, R_1^{-1})$	$F(J^{-1}, R_2)$	$F(J, J^{-1})$	
$\gamma_{4,10}$	$F(R_2, R_2^{-1})$	$F(P, R_1)$		$F(P, R_2)$	$F(R_1, R_2^{-1})$
$\gamma_{8,14}$	$F(P^{-1}, J^{-1})$	$F(J, R_1^{-1})$		$F(J, J^{-1})$	$F(R_1^{-1}, P^{-1})$
$\gamma_{9,12}$	$F(P, J)$	$F(J^{-1}, R_2)$		$F(P, R_2)$	$F(J, J^{-1})$
$\gamma_{3,6}$	$F(R_1, R_1^{-1})$	$F(P^{-1}, R_2^{-1})$		$F(R_1, R_2^{-1})$	$F(R_1^{-1}, P^{-1})$
$\gamma_{13,14}$	$F(R_1^{-1}, R_2)$	$F(P^{-1}, R_2)$		$F(R_1^{-1}, P^{-1})$	
$\gamma_{12,13}$	$F(R_1^{-1}, R_2)$	$F(P, R_1^{-1})$		$F(P, R_2)$	
$\gamma_{10,11}$	$F(R_1, J^{-1})$	$F(J^{-1}, R_2^{-1})$		$F(R_1, R_2^{-1})$	
$\gamma_{9,11}$	$F(R_1, J^{-1})$	$F(J, R_1)$		$F(J, J^{-1})$	
$\gamma_{7,8}$	$F(J, R_2^{-1})$	$F(J^{-1}, R_2^{-1})$		$F(J, J^{-1})$	
$\gamma_{6,7}$	$F(J, R_2^{-1})$	$F(J, R_1)$		$F(R_1, R_2^{-1})$	
$\gamma_{4,5}$	$F(P, P^{-1})$	$F(P^{-1}, R_2)$		$F(P, R_2)$	
$\gamma_{3,5}$	$F(P, P^{-1})$	$F(P, R_1^{-1})$		$F(R_1^{-1}, P^{-1})$	

The edges satisfy the following proposition:

Proposition 5.3.5. *Each edge $\gamma_{i,j}$ of the polyhedron is a geodesic segment joining the two vertices $\mathbf{z}_i$ and $\mathbf{z}_j$.*

Proof. We claim that each edge is contained in the common intersection of at least two totally geodesic subspaces of two bisectors. This implies that this edge is a geodesic arc. Remember, from Section 2.3, that slices and meridians are totally geodesic subspaces of bisectors.

To prove the claim, let us consider for each edge the ridges it is contained in, as in the previous table. Just looking at the list we can easily remark the following information:

- Each edge containing either $\mathbf{z}_1$ or $\mathbf{z}_2$ is contained in two M-ridges and one S-ridge;
- Two edges, namely $\gamma_{7,11}$ and $\gamma_{5,13}$, are contained in two M-ridges and two G-ridges;
- All other edges are contained in an S-ridge, an M-ridge and a G-ridge; some of them are contained also in one more ridge, that is either an M-ridge or a G-ridge.

■

Remark 5.3.6. For the edges containing either $\mathbf{z}_1$ or $\mathbf{z}_2$ we have additional information. Each of these edges is contained in two M-ridges of the same bisector. This implies that such edges are in the spine of the bisectors.

5.3.3.4 Other bisector intersections

We will now analyse all the other intersections between pairs of bisectors, following Section 4.4. The next two propositions are the equivalent for the 3-fold symmetry case of Propositions 4.4.3 and 4.4.4.

Proposition 5.3.7. *The following bisector intersections consist of the union of two edges:*

$$B(P) \cap B(J^{-1}) = \gamma_{10,9} \cup \gamma_{9,12}, \qquad B(J^{-1}) \cap B(R_1^{-1}) = \gamma_{8,14} \cup \gamma_{14,12},$$
$$B(P) \cap B(R_2^{-1}) = \gamma_{3,4} \cup \gamma_{4,10}, \qquad B(J) \cap B(R_2) = \gamma_{9,12} \cup \gamma_{12,14},$$
$$B(R_1) \cap B(R_2) = \gamma_{4,10} \cup \gamma_{10,9}, \qquad B(J) \cap B(P^{-1}) = \gamma_{6,8} \cup \gamma_{8,14},$$
$$B(R_1) \cap B(P^{-1}) = \gamma_{4,3} \cup \gamma_{3,6}, \qquad B(R_1^{-1}) \cap B(R_2^{-1}) = \gamma_{3,6} \cup \gamma_{6,8}.$$

Proposition 5.3.8. *The bisectors satisfy:*

- *A point* $\mathbf{z}$ *in the bisectors intersection* $B(P) \cap B(P^{-1})$*, with coordinates satisfying* $z_1 \neq \frac{\sin\varphi + \sin(\theta-\varphi)}{\sin(\theta+\varphi)}$ *and* $w_1 \neq \frac{\sin\varphi + \sin(\theta-\varphi)}{\sin(\theta+\varphi)}$*, belongs to the edge* $\gamma_{5,13}$*.*
- *A point* $\mathbf{z}$ *in the bisectors intersection* $B(J) \cap B(R_2^{-1})$*, with coordinates satisfying* $z_1 \neq e^{-i\varphi}\frac{\sin\theta}{\sin(\theta+\varphi)}$ *and* $w_2 \neq e^{i\theta}\frac{\sin\varphi}{\sin(\theta+\varphi)}$*, belongs to the edge* $\gamma_{7,11}$*.*

- *A point* $\mathbf{z}$ *in the bisectors intersection* $B(R_2) \cap B(R_1^{-1})$*, with coordinates satisfying* $z_2 \neq e^{i\theta}\frac{\sin\varphi}{\sin(\theta+\varphi)}$ *and* $w_2 \neq \frac{\sin\varphi}{\sin(\theta+\varphi)}$*, belongs to the edge* $\gamma_{5,13}$*.*

- *A point* $\mathbf{z}$ *in the bisectors intersection* $B(R_1) \cap B(J^{-1})$*, with coordinates satisfying* $z_2 \neq \frac{\sin\varphi}{\sin(\theta+\varphi)}$ *and* $w_1 \neq e^{i\varphi}\frac{\sin\theta}{\sin(\theta+\varphi)}$*, belongs to the edge* $\gamma_{7,11}$*.*

In the proof of this proposition (done adapting the proof for the general case 4.4.4), we use Lemma 5.3.4. In Section 5.7.1 it will be clear why only for the values in the lemma that precise analysis of bisectors intersection makes sense, due to the collapsing of some ridges.

5.4 Main theorem

We are now ready to show that the polyhedron D constructed is a fundamental domain for Γ. We will use the Poincaré polyhedron theorem to prove that $\Gamma = \langle R_1, R_2, A_1 \rangle$ is discrete, give a presentation for it and prove that D is a fundamental domain. More precisely, we will prove the following:

Theorem 5.4.1. *Let* Γ *be the subgroup of* $PU(H)$ *characterised by* p *and* k *as explained in Section 3.4.1 and such that the two parameters have any of the values in Table 3.1. Then the polyhedron* D *of the previous section is a fundamental domain for* Γ*, up to making some vertices collapse according to the following rule:*

Value of p	*Value of* k	*Fundamental polyhedron*
$0 < p \leq 6$ $(d < 0)$	$k \leq \frac{2p}{p-2}$ $(l < 0)$ *(large phase shift)*	*The polyhedron* D *constructed in Section 5.3 with triples of vertices* z_3, z_4, z_5*;* z_6, z_7, z_8*;* z_9, z_{10}, z_{11} *and* z_{12}, z_{13}, z_{14} *each collapsed to a single vertex is a fundamental domain. This is the same as the polyhedron constructed in [BP15].*

$0 < p \leq 6$ $(d < 0)$	$k > \frac{2p}{p-2}$ $(l > 0)$ *(small phase shift)*	*The polyhedron D constructed in Section 5.3 with triples of vertices z_3, z_4, z_5 each collapsed to a single vertex is a fundamental domain. This is the same polyhedron obtained in [DFP05], as we will explain in Section 5.7.2.*
$p > 6$ $(d > 0)$	$k \leq \frac{2p}{p-2}$ $(l < 0)$ *(large phase shift)*	*The polyhedron D constructed in Section 5.3 with triples of vertices z_6, z_7, z_8; z_9, z_{10}, z_{11} and z_{12}, z_{13}, z_{14} each collapsed to a single vertex is a fundamental domain. This is the same as the polyhedron constructed in [Par06].*
$p > 6$ $(d > 0)$	$k > \frac{2p}{p-2}$ $(l > 0)$ *(small phase shift)*	*The polyhedron D constructed in Section 5.3 is a fundamental domain.*

The table in the theorem is strictly related to Table 3.1. The first three groups, in fact, correspond exactly to the values of the Deligne-Mostow lattices of first, second and third (Livné lattices) type presented in the table. Lattices of the fourth and fifth type are in the fourth line of the table in the theorem.

Remark 5.4.2. The condition $k \lesseqgtr \frac{2p}{p-2}$ is equivalent to saying that the phase shift parameter, as described in Section 3.4.1, is smaller or greater than $\frac{1}{2} - \frac{1}{p}$.

We also remark that the equality cases have to be treated a bit more carefully. For $p = 6$ the vertex obtained collapsing $\mathbf{z}_3, \mathbf{z}_4, \mathbf{z}_5$ is on the boundary of the complex hyperbolic space. These values are discussed in [BP15] and can be included in the case of the lower values. The same discussion is true for the critical value of k and the first group is the only case where such an equality actually holds.

To prove Theorem 5.4.1 we will use the Poincaré polyhedron theorem. Its power lies not only in the fact that it allows to prove that D is a fundamental

domain for Γ, but because it also gives a presentation for the group.

Theorem 5.4.3. *Suppose (p,k) is one of the pairs in Table 3.1. Then the group Γ generated by the side pairing maps of D, i.e. P, J, R_1, R_2 as described, has presentation*

$$\Gamma = \left\langle J, P, R_1, R_2 : \begin{array}{l} J^3 = P^{3d} = R_1^p = R_2^p = (P^{-1}J)^k = (R_2R_1J)^l = I, \\ R_2 = PR_1P^{-1} = JR_1J^{-1},\ P = R_1R_2 \end{array} \right\rangle,$$

with each relation in the first line holding only when the order of the map is positive and finite.

A proof of this theorem comes out automatically while using the Poincaré polyhedron theorem to prove Theorem 5.4.1 and is given in Section 5.5.2.

5.5 Proof of Theorem 5.4.1

In this section we will prove that all the hypothesis of the Poincaré polyhedron theorem hold and explain how to use it to prove Theorem 5.4.1.

5.5.1 Side pairing maps

Let us consider the maps J, P, R_1 and R_2. These maps pair the eight sides of the polyhedron, as shown in Figure 5.6. In this section we want to show that these side pairing maps satisfy the conditions (S.1)–(S.6).

Conditions (S.1), (S.2), (S.5) follow clearly from our construction of the sides. Also, (S.6) is an empty condition, because each pair of sides of our polyhedron intersects. The following proposition shows that conditions (S.3) and (S.4) are verified by the sides of D.

Proposition 5.5.1. *Let T be one of $J^{\pm 1}, P^{\pm 1}, R_1^{\pm 1}$ and $R_2^{\pm 1}$. Then $T^{-1}(D) \cap D = \emptyset$. Moreover, $T^{-1}(\overline{D}) \cap \overline{D} = S(T)$.*

Proof. Let us take a side $S(T)$. By definition it is contained in a bisector $B(T)$. By Lemma 5.3.2, there exist two vertices $\mathbf{z}_i$ and $\mathbf{z}_j$ such that $B(T)$ is the set of points equidistant from $\mathbf{z}_i$ and $T^{-1}(\mathbf{z}_j)$. By applying T we get that $T(B(T))$ is $B(T^{-1})$, which is the bisector equidistant from $T(\mathbf{z}_i)$ and $\mathbf{z}_j$. By Remark 4.3.3,

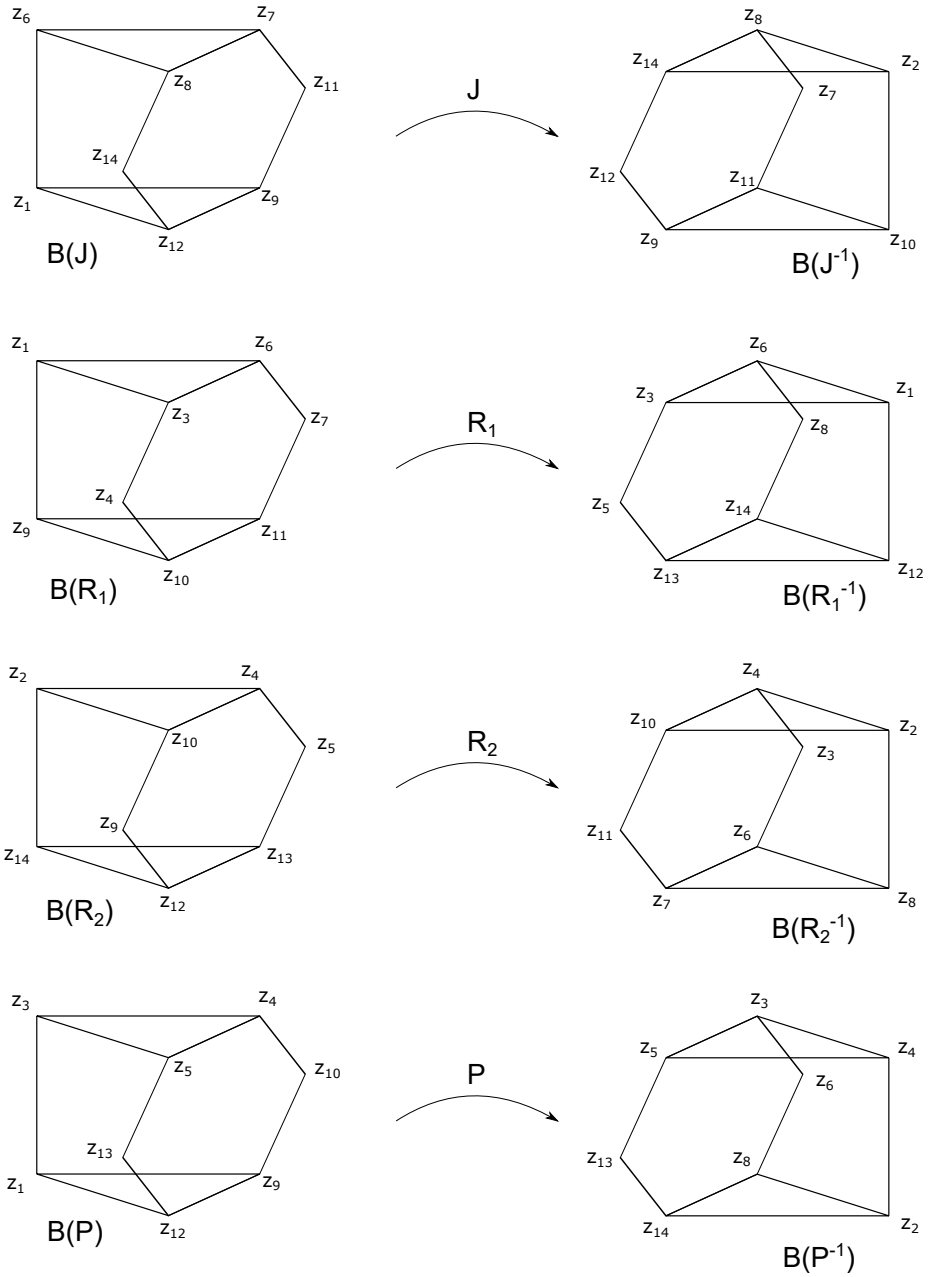

Figure 5.6: The sides of the polyhedron with the corresponding side pairing maps.

the points of the polyhedron are closer to $\mathbf{z}_i$ than to $T^{-1}(\mathbf{z}_j)$, while the ones of $T(D)$ are closer to $T(\mathbf{z}_i)$ than to $\mathbf{z}_j$. This implies that $T^{-1}(D) \cap D = \emptyset$.

If we now also consider the boundary of the polyhedron and we pass to

$T^{-1}(\overline{D}) \cap \overline{D} = S(T)$, we are considering the equality cases in Lemma 5.3.2. But the lemma itself guarantees that the intersections, which corresponds to the equality cases of the lemma, are always contained in $B(T)$. Since by definition $S(T) = \overline{D} \cap B(T)$, we are done. ■

5.5.2 Cycle relations

It remains now to show that the ridges of the polyhedron D satisfy conditions (F.1)–(F.3). This will be done in this and next section. The first condition is straightforward in this case. In fact the edges in a ridge intersect so that they bound a polygon, giving hence a ridge homeomorphic to a ball. In the following table we summarise the cycle relations coming from Properties (F.2) and (F.3). Proving them is a simple calculation of the action of the transformations on the bisectors. In fact by definition the ridge $F(T, S)$ is contained in bisectors $B(T)$ and $B(S)$. This means that we can apply side pairings T or S, corresponding to going in one or the other direction of the cycle. The maps within each cycle are given (one per type of ridges) in the next section at the end of each proof.

Ridges in the cycle	Transform.	ℓ	m
$F(P, J), \quad F(P^{-1}, J^{-1})$	$P^{-1}J$	1	k
$F(R_1, R_1^{-1})$	R_1	1	p
$F(R_2, R_2^{-1})$	R_2	1	p
$F(P, R_1), \quad F(P, R_1^{-1}), \quad F(P^{-1}, R_2), \quad F(P^{-1}, R_2^{-1})$	$R_1^{-1}P^{-1}R_2P$	1	1
$F(J, R_1), \quad F(J, R_1^{-1}), \quad F(J^{-1}, R_2), \quad F(J^{-1}, R_2^{-1})$	$R_1^{-1}J^{-1}R_2J$	1	1
$F(P, R_2), \quad F(R_1, R_2^{-1}), \quad F(R_1^{-1}, P^{-1})$	$R_2P^{-1}R_1$	1	1
$F(J, R_2^{-1}), \quad F(R_1, J^{-1}), \quad F(R_1^{-1}, R_2)$	R_2R_1J	1	l
$F(J, J^{-1})$	J	3	1
$F(P, P^{-1})$	P	3	d

This table gives immediately a proof the presentation as given in Theorem 5.4.3, as they correspond to the cycle relations in the Poincaré polyhedron theorem

and the reflection relations are empty. The second part of property (F.3) will be proved in the next section.

5.5.3 Tessellation around the ridges

We now want to prove that the images of the polyhedron under the side paring maps tessellate around neighbourhoods of the interior of the ridges. This is proved in different ways, depending on whether the ridges described in Section 5.3.3.2 are contained in a Giraud disc, in a Lagrangian plane or in a complex line.

Tessellation around ridges contained in a Giraud disc

The easiest case to treat is the tessellation around the ridges contained in Giraud discs, which are $F(J, J^{-1}), F(R_1, R_2^{-1}), F(P, R_2)$ and $F(P^{-1}, R_1^{-1})$. The main tool for this is Lemma 5.3.2.

Proposition 5.5.2. *We have the following:*

- *The polyhedron D and its images under the maps J and J^{-1} tessellate around the ridge $F(J, J^{-1})$.*
- *The polyhedron D and its images under the maps R_1^{-1} and R_2 tessellate around the ridge $F(R_1, R_2^{-1})$.*
- *Moreover, the polyhedron D and its images under the maps R_2^{-1} and P^{-1} tessellate around the ridge $F(P, R_2)$.*
- *Finally, the polyhedron D and its images under the maps R_1 and P tessellate around the ridge $F(P^{-1}, R_1^{-1})$.*

Proof. The proof consists in dividing the space into points that are closer to one of L_{*0}, $J(L_{*0})$ or $J^{-1}(L_{*0})$ and showing that D and its images under J are contained each in a different one of these domains and coincide with them around the ridge $F(J, J^{-1})$.

More formally, by Lemma 5.3.2 we know that D is contained in the part of space closer to L_{*0} than to its images under J and J^{-1}. We can hence write

$$D \subset \{\mathbf{z} \in \mathbf{H}^2_{\mathbb{C}} \colon |\langle \mathbf{z}, \mathbf{n}_{*0}\rangle| < |\langle \mathbf{z}, J(\mathbf{n}_{*0})\rangle|, \quad |\langle \mathbf{z}, \mathbf{n}_{*0}\rangle| < |\langle \mathbf{z}, J^{-1}(\mathbf{n}_{*0})\rangle|\}. \quad (5.5.1)$$

For a point $\mathbf{z} \in J^{\pm 1}(D)$, we also have $J^{\mp 1}(\mathbf{z}) \in D$. Applying the conditions in (5.5.1) to $J^{\mp}(\mathbf{z})$, we get

$$|\langle J^{\mp 1}(\mathbf{z}), \mathbf{n}_{*0}\rangle| < |\langle J^{\mp 1}(\mathbf{z}), J(\mathbf{n}_{*0})\rangle|, \quad |\langle J^{\mp 1}(\mathbf{z}), \mathbf{n}_{*0}\rangle| < |\langle J^{\mp 1}(\mathbf{z}), J^{-1}(\mathbf{n}_{*0})\rangle|.$$

By applying $J^{\pm 1}$ to all terms of (5.5.1), we obtain

$$J^{\pm 1}(D) \subset \{\mathbf{z} \in \mathbf{H}^2_{\mathbb{C}} : |\langle \mathbf{z}, J^{\pm 1}(\mathbf{n}_{*0})\rangle| < |\langle \mathbf{z}, \mathbf{n}_{*0}\rangle|, \quad |\langle \mathbf{z}, J^{\pm 1}(\mathbf{n}_{*0})\rangle| < |\langle \mathbf{z}, J^{\mp 1}\mathbf{n}_{*0}\rangle|\}.$$

Clearly, we used the fact that J has order 3, so $J^2 = J^{-1}$. It is obvious that $D, J(D)$ and $J^{-1}(D)$ are disjoint.

The ridge we are considering is characterized by $\mathrm{Im}(e^{i\varphi}z_1) = \mathrm{Im}(e^{-i\varphi}w_1) = 0$. We take a neighbourhood of the interior small enough, so that it does not meet the other sides of D. Then a point of U is in $\overline{D}$ if and only if it is closer to L_{*0} than to its images. This is because if we consider the z_1 and w_1 coordinates small enough, D actually coincides with the set described in (5.5.1) and same for the images. From this, it is easy to see that D, $J(D)$ and $J^{-1}(D)$ tessellate around U.

The cycle transformation is

$$F(J, J^{-1}) \xrightarrow{J} F(J, J^{-1}).$$

The other points of the proof are done in the same way, by taking the different images mentioned in the statement and using the same proof strategy. ■

Tessellation around ridges contained in Lagrangian planes

The second type are the ridges $F(P, R_1)$, $F(P, R_1^{-1})$, $F(J, R_1)$ and $F(J, R_1^{-1})$, contained in Lagrangian planes.

They contain either vertex $\mathbf{z}_1$ or $\mathbf{z}_2$ and they are defined by conditions only on the $\mathbf{z}$-coordinates or on the $\mathbf{w}$-coordinates. It is enough to show that the polyhedron and its images under the side pairing maps tessellate around the ridges containing the vertex $\mathbf{z}_1$. By applying ι we will have the same for ridges containing $\mathbf{z}_2$.

Proposition 5.5.3. *The polyhedron D and its images under R_1^{-1}, P^{-1} and $R_1^{-1}P^{-1}$ tessellate around the ridge $F(P, R_1)$.*

Proof. Considering that $\mathbf{w} = P^{-1}(\mathbf{z})$ and that applying R_1 means to add θ to the argument of z_2, we can prove the signs in the following table.

Image of D	$\mathrm{Im}(z_1)$	$\mathrm{Im}(e^{i\varphi}z_1)$	$\mathrm{Im}(z_2)$	$\mathrm{Im}(e^{-i\theta}z_2)$
D	-	+	+	-
$R_1^{-1}(D)$	-	+	-	-
$P^{-1}(D)$	+	+	+	-
$R_1^{-1}P^{-1}(D)$	+	+	-	-

We can see from the table that each pair of images have some coordinates whose imaginary part has different sign. This clearly implies that they are disjoint.

Now, the ridge $F(P, R_1)$ is characterised by $\mathrm{Im}(z_1) = \mathrm{Im}(z_2) = 0$. Let us now consider a neighbourhood U of the ridge and a point $\mathbf{z} \in U$. If $\mathbf{z}$ has argument of z_1 smaller than 0, then D and R_1^{-1} cover U, in the respective cases when the argument of z_2 and positive or negative. Similarly, when $\mathbf{z}$ has first coordinate of argument bigger than 0, then $P^{-1}(D)$ and $R_1^{-1}P^{-1}(D)$ cover U, when $\arg(z_2)$ is positive or negative respectively.

The corresponding cycle transformation is

$$F(P, R_1) \xrightarrow{P} F(P^{-1}, R_2) \xrightarrow{R_2} F(P^{-1}, R_2^{-1}) \xrightarrow{P^{-1}} F(P, R_1^{-1}) \xrightarrow{R_1^{-1}} F(P, R_1).$$

■

By applying R_1, PR_1 and $P = R_2^{-1}PR_1$ we get similar results for the other ridges in the cycle, namely $F(P, R_1^{-1})$, $F(P^{-1}, R_2^{-1})$ and $F(P^{-1}, R_2)$ respectively.

In a similar way, we can also prove

Proposition 5.5.4. *The polyhedron D and its images under $R_1^{-1}, J^{-1} = A_1^{-1}P^{-1}$ and $R_1^{-1}A_1^{-1}P^{-1}$ tessellate around the ridge $F(J, R_1)$.*

Again, by applying the maps in the cycle transformation, which is

$$F(J, R_1) \xrightarrow{J} F(J^{-1}, R_2) \xrightarrow{R_2} F(J^{-1}, R_2^{-1}) \xrightarrow{J^{-1}} F(J, R_1^{-1}) \xrightarrow{R_1^{-1}} F(J, R_1),$$

we can get that the tessellation property (F.3) holds also for the ridges $F(J^{-1}, R_2)$, $F(J^{-1}, R_2^{-1})$ and $F(J, R_1^{-1})$.

Tessellation around ridges contained in complex lines

In this section we will show that the images of D tessellate around the ridges contained in complex lines. We will divide them in two parts for which we will use slightly different methods.

We will start with the ridges contained in complex lines and defined by conditions either on the **z**-coordinates or on the **w**-coordinates. These are ridges $F(P, J)$, $F(R_1, R_1^{-1})$, $F(P^{-1}, J^{-1})$ and $F(R_2, R_2^{-1})$. From the first two, the others follow by applying ι. The proofs, which we will omit as they are similar to the ones in [Par06], strongly rely on the fact that p and k are integers. In some of the cases that we are considering, though, k is of the form $p/2$, with p odd. The proof can be adapted, as we will explain in Section 5.6.

Proposition 5.5.5. *The polyhedron D and its images under P^{-1}, A_1 and A_1P^{-1} tessellate around the ridge $F(P, J)$. Moreover, the polyhedron D and its images under R_1 tessellate around the ridge $F(R_1, R_1^{-1})$.*

By applying ι we have equivalent results around $F(P^{-1}, J^{-1})$ and $F(R_2, R_2^{-1})$.

Moreover, in exactly the same way as in Proposition 4.13 of [Par06] we can prove that D and appropriate images tessellate around $F(P, P^{-1})$. The proof is done by showing that in some coordinates P^3 rotates $\mathbf{n}_{*0}$ by $e^{i\psi}$, with $\psi = \frac{2\pi}{d}$ and $d = \frac{2p}{p-6}$, as in (3.4.3). At the same time, P^3 fixes the ridge itself. Then the polyhedron and its images under P and P^{-1} will be contained in different sectors for the arguments of at least one of the new coordinates and they will cover a sector of length ψ. Applying P^3 this sector will cover a whole neighbourhood of the ridge by rationality of ψ, since d is always an integer.

The corresponding cycle transformation is

$$F(P, P^{-1}) \xrightarrow{P} F(P, P^{-1}).$$

Finally, we have the last set of ridges.

Proposition 5.5.6. *The polyhedron D and its images under J, JR_2, R_1R_2J and their compositions tessellate around the ridge $F(R_1, J^{-1})$.*

Proof. The proof works similarly to those for ridges $F(P, J)$ and $F(P, P^{-1})$. We can in fact change coordinates as in the latter case, so to have an analogous

situation to the one in the former. In this case though, we will define $\psi = \frac{2\pi}{l}$, for l defined in (3.4.3).

First of all, we recall that $F(J^{-1}, R_1)$ is contained in L_{*3}. Furthermore, the map JR_2R_1 rotates the normal vector $\mathbf{n}_{*3}$ by $-\psi$ and it fixes pointwise the ridge. We then change basis to new coordinates, so that the first coordinate is along the normal vector to the complex line (up to a minus sign, which will be useful in the calculations) and the other two are along two vectors spanning the complex line once we pass to projective coordinates.

The vector in the new basis will hence be

$$\begin{pmatrix} z_1 \\ z_2 \\ 1 \end{pmatrix} = \frac{\sin\varphi - \sin(\theta+\varphi)z_2}{\sin(\theta+\varphi) - \sin\varphi} \begin{pmatrix} 0 \\ -1 \\ -1 \end{pmatrix} + z_1 \begin{pmatrix} 1 \\ 0 \\ 0 \end{pmatrix} + \frac{1 - z_2}{\sin(\theta+\varphi) - \sin\varphi} \begin{pmatrix} 0 \\ \sin\varphi \\ \sin(\theta+\varphi) \end{pmatrix}.$$

We define then the ξ-coordinates to be

$$\begin{aligned} \xi_1 &= \frac{\sin\varphi - \sin(\theta+\varphi)z_2}{1 - z_2}, \\ \xi_2 &= \frac{z_1(\sin(\theta+\varphi) - \sin\varphi)}{1 - z_2}. \end{aligned} \tag{5.5.2}$$

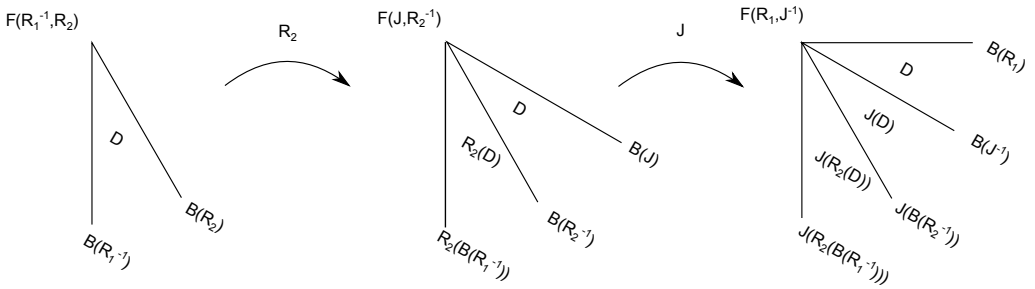

Figure 5.7: The tessellation around $F(R_1, J^{-1})$.

Let us now look at Figure 5.7. By definition the ridge $F(R_1, J^{-1})$ is contained in the intersection of $B(R_1)$ and $B(J^{-1})$. It is clear that on $B(R_1)$, since z_2 is real, also ξ_1 will be real.

If we take the ridge $F(R_1^{-1}, R_2)$, we know that the polyhedron D is as in the first image of Figure 5.7. By definition of the bisectors, $R_2(B(R_2)) = B(R_2^{-1})$.

Also, R_2 sends $F(R_1^{-1}, R_2)$ to $F(J, R_2^{-1})$ (see cycle relation below). Then we can apply the map to the first image and get the second configuration, since $F(J, R_2^{-1})$ is in $B(J)$ and $B(R_2^{-1})$ by definition but also in $R_2(B(R_1^{-1}))$ by construction. We can do the same thing applying J and we get the third configuration in the figure.

We now want to prove that in the argument of the coordinate ξ_1, D, $J(D)$ and $JR_2(D)$ make a sector of angle ψ. Once we prove this, we can use the same argument as in the proof of Theorem 5.5.5. In other words, we can apply the map R_1R_2J which acts on the ξ coordinates (ξ_1, ξ_2) by sending to $(e^{-i\psi}\xi_1, \xi_2)$, and hence it carries the configuration all around the ridge and tessellates the space because of rationality of ψ, which comes from the fact that l is always an integer.

To prove that the size of the sector is ψ, we will prove that the argument of the ξ_1 coordinate of a point on $JR_2(B(R_1^{-1}))$ is $-\psi$. This is just a calculation, as it turns out that

$$JR_2\mathbf{z} = JR_2 \begin{pmatrix} z_1 \\ z_2 \\ 1 \end{pmatrix} = J \begin{pmatrix} -\sin\theta e^{-i\varphi} z_1 + (\sin\varphi + \sin(\theta-\varphi))(1-z_2) \\ \sin\varphi(1 - z_1 - e^{-i\theta} z_2) \\ -\sin(\theta+\varphi)(z_1+z_2) + \sin\varphi + \sin\theta e^{i\varphi} \end{pmatrix}$$

$$= \begin{pmatrix} 2z_1 \sin^2\varphi(1-\cos\theta) \\ 2z_2 \sin^2\varphi e^{i\varphi}(\cos(\theta+\varphi) - \cos\varphi) + \sin^2\varphi(1-e^{i\theta})(e^{2i\varphi}-1) \\ z_2(1-e^{-i\theta})\sin\varphi\sin(\theta+\varphi)(e^{2i\varphi}-1) + \sin^2\varphi(1-e^{-i\theta})(1-e^{i(2\varphi+\theta)}) \end{pmatrix}.$$

Then we can calculate its ξ_1 coordinate and we have

$$\xi_1 = \frac{-e^{i(\theta+2\varphi)}\sin^2\varphi(2(1-\cos\theta)(\sin\varphi - e^{-i\theta}z_2\sin(\theta+\varphi)))}{-2\sin^2\varphi(1-\cos\theta)e^{-i\theta}z_2 + 2\sin^2\varphi(1-\cos\theta)} =$$

$$= e^{-i\psi}\frac{\sin\varphi - \sin(\theta+\varphi)e^{-i\theta}z_2}{1-e^{-i\theta}z_2}. \tag{5.5.3}$$

If a point $\mathbf{z}$ is in $B(R_1^{-1})$, then its z_2 coordinate is $z_2 = e^{i\theta}u$ and hence the previous expression is

$$\xi_1 = e^{-i\psi}\frac{\sin\varphi - \sin(\theta+\varphi)u}{1-u}.$$

Clearly, the argument of the new coordinate is $-\psi$.

The last thing we need to show is that the three images are disjoint. We already saw that D is disjoint from $J(D)$ and $R_2(D)$ in 5.5.2 and in the equivalent statement of 5.5.5 for R_2, respectively. But then also $J(D)$ and $JR_2(D)$ are

disjoint because J is an isometry. To prove the disjointness of D and $JR_2(D)$, we look at the expression for the ξ_1 coordinate of a point in D, as in (5.5.2), and of a point in $JR_2(D)$, as in (5.5.3).

To show disjointness, we will show that D and $JR_2(D)$ are contained in the sector where the argument of ξ_1 is respectively bigger and smaller than $-\frac{\psi}{2}$. To do that we just need to show that $B(J^{-1})$ and $J(B(R_2^{-1})) = JR_2(B(R_2))$ are as said.

Since both these bisectors are defined by equations on the $\mathbf{w}$-coordinates, it is useful to rewrite the two equations in terms of these, using Formulae (5.2.3) and (5.2.4). They will be as following. If $\mathbf{z} \in D$, then

$$\xi_1 = 2\sin\frac{\theta}{2}\sin\varphi e^{-i\frac{\psi}{2}}\frac{\sin\theta - \sin(\theta+\varphi)e^{-i\varphi}w_1}{-\sin\theta e^{-i\varphi}w_1 + (\sin\varphi - \sin(\theta+\varphi))w_2 + \sin\varphi + \sin(\theta-\varphi)},$$

with w_1 and w_2 coordinates of $\mathbf{z}$. We will consider points in $B(J^{-1})$, so $w_1 = e^{i\varphi}u$, with u real and we want to show that $\mathrm{Im}(e^{-i\frac{\psi}{2}}\xi_1) > 0$.

Taking the imaginary part of the expression above, this means requiring that

$$(\sin\theta - \sin(\theta+\varphi)u)(\sin(\theta+\varphi) - \sin\varphi)\,\mathrm{Im}(w_2) > 0.$$

The third term is positive for points in D, while the second one is positive as long as l is positive, which is the case where the ridge we are tessellating around does not collapse. The last thing we need is then to prove that in $B(J^{-1})$ the modulus of w_2 remains smaller than $\frac{\sin\theta}{\sin(\theta+\varphi)}$. But looking at the structure of the side, as in Figure 5.6, we can see that the side is bounded by the complex lines L_{03} and L_{*3}, so the modulus of w_2 is between 0 and $\frac{\sin\theta}{\sin(\theta+\varphi)}$ (see Lemma 4.4.2).

On the other hand, if $\mathbf{z}$ is in $JR_2(B(R_2))$, its coordinate will be

$$\xi_1 = 2\sin\frac{\theta}{2}\sin\varphi e^{-i\frac{\psi}{2}}\frac{\sin\varphi - \sin(\theta+\varphi)w_2}{(\sin\varphi - \sin(\theta+\varphi))e^{-i\varphi}w_1 - \sin\theta w_2 + \sin\theta},$$

with w_1 and w_2 coordinates of a point in D. As they vary through the possible values, $\mathbf{z}$ varies in $JR_2(B(D))$. Here we consider points in $JR_2(B(R_2))$, so where $w_2 = x$, with x real and we want to show this time that $\mathrm{Im}(e^{-i\frac{\psi}{2}}\xi_1) < 0$.

We now take the imaginary part of the expression for ξ_1 and we obtain that such a condition is equivalent to requiring that

$$(\sin\varphi - \sin(\theta+\varphi)x)(\sin(\theta+\varphi) - \sin\varphi)\,\mathrm{Im}(e^{-i\varphi}w_1) < 0.$$

As before, this reduces to show that the first term is positive and this is true because of the structure of $B(R_2)$, which is contained between L_{12} and L_{*2}. This concludes the proof.

The corresponding cycle transformation is

$$F(R_1, J^{-1}) \xrightarrow{R_1} F(R_1^{-1}, R_2) \xrightarrow{R_2} F(J, R_2^{-1}) \xrightarrow{J} F(R_1, J^{-1}).$$

■

By applying the isometries that compose the cycle transformation, we obtain the tessellation around the last ridges, $F(R_1^{-1}, R_2)$, $F(J, R_2^{-1})$ and $F(R_1, J^{-1})$.

5.6 Polyhedra with extra symmetry

In this section we will describe the particular case when either l or k is equal $\frac{p}{2}$. Considering k or l is equivalent, since swapping them corresponds to swapping μ_1 and μ_5 in the ball quintuple, which geometrically corresponds to choosing whether to have v_* or v_0 in the origin of the coordinates and will hence give us the same construction. In this case the polyhedron has an extra symmetry, because by definition the condition implies that $\varphi = \theta$. The pairs (p, k) in our list and satisfying this condition, are $(5, 5/2)$, $(6, 3)$, $(7, 7/2)$, $(8, 4)$, $(9, 9/2)$, $(10, 5)$, $(12, 4)$ and $(18, 3)$. By Theorem 6.2 in [Sau90] (see Corollary 3.5.2), the lattice $(p, \frac{p}{2})$ is isomorphic to the one of the form $(p, 2)$ (see Chapter 7 for more details on the commensurability classes).

This includes the cases when k is not an integer, which have not been treated previously because previous proofs for tessellation rely on the fact that k was always an integer. When tessellating a neighbourhood of $F(P, J)$, in fact, D and $P^{-1}(D)$ are contained in sectors where the argument of z_1 is between 0 and φ and between φ and 2φ respectively. Then, one can apply A_1 to the polyhedra and translate of 2φ the sector. In order to cover exactly all the possible values of the argument of z_1 one then needs k to be an integer.

To avoid this problem, one can use a slightly different version of the same theorem, namely the Poincaré polyhedron theorem for coset decompositions. The statement is given in the second half of Section 2.4 and can be found in [Mos80]

and in [DPP16]. The basic difference is the presence of a finite group $\Upsilon < \mathrm{Is}\,\mathbf{H}^2_{\mathbb{C}}$ preserving the polyhedron and compatible with the side pairing maps.

Then one just needs tessellation around one facet in each orbit of the action of Υ and the cosets of the polyhedron will tessellate the space. This also gives a different presentation for the group generated by Υ and the side pairings, with the additional relations given by a presentation of Υ and by the compatibility relations. Here the group Υ will be a finite cyclic group of order 4 and the polyhedron will hence contain 4 copies of the fundamental domain.

The main difference is that we do not need then a butterfly move A_1, because we can introduce a move that swaps points v_0 and v_1 (which now have same cone angle). The new move, squared, is the same as A_1 we used so far. This solves the problem because the new move acts on the z_1 coordinate by rotating by φ instead of 2φ as before, so we just need $2k$ to be an integer.

From now on, we will assume we are in the case where $k = \frac{p}{2}$, hence $\varphi = \theta = \frac{2\pi}{p}$. Clearly, the calculations to find vertices, area and moves could be simplified by adding the relation $\varphi = \theta$ in the equations, but for simplicity we will leave them as they are. We will have the moves R_1 and R_2 defined as before, but we will also have an extra move corresponding to swapping the vertices v_0 and v_1, as we already mentioned. This new move, that we will call S_1, can be found by requiring that the images under S_1 of the v_i's, which we denote by v_i', satisfy the equations $v_3' = v_3, v_2' = v_2, v_1' = v_0$ and $v_0' = v_{-1}$. The move is illustrated in Figure 5.8.

Solving the equations or looking at the geometric meaning of the move, one can deduce the matrix of S_1. The three moves will hence be

$$R_1 = \begin{bmatrix} 1 & 0 & 0 \\ 0 & e^{i\theta} & 0 \\ 0 & 0 & 1 \end{bmatrix}, \qquad R_2 = \frac{1}{1-e^{-i\theta}} \begin{bmatrix} -e^{-i\theta} & -1 & 1 \\ -1 & -e^{-i\theta} & 1 \\ -2\cos\theta & -2\cos\theta & 1+e^{i\theta} \end{bmatrix}$$

and

$$S_1 = \begin{bmatrix} e^{i\theta} & 0 & 0 \\ 0 & 1 & 0 \\ 0 & 0 & 1 \end{bmatrix}.$$

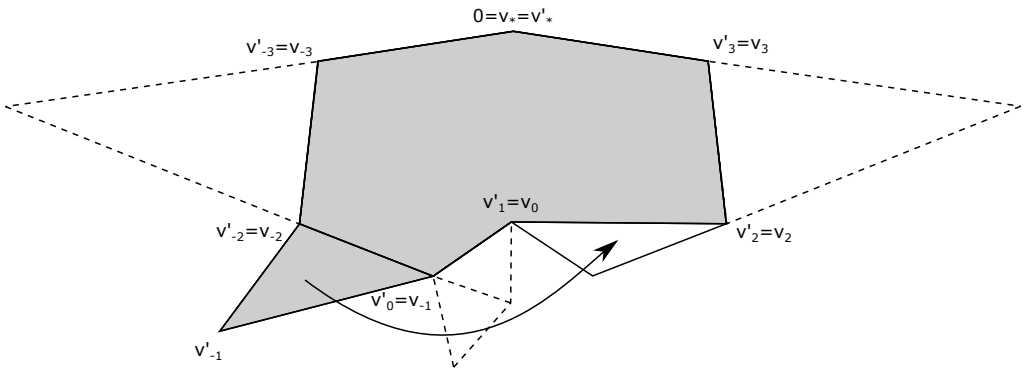

Figure 5.8: The move S_1.

Remark 5.6.1. We remark that S_1 commutes with R_1 and satisfies the braid relation with R_2.

By looking at the coordinates of the vertices of the polyhedron and keeping in mind that $\varphi = \theta$, it is easy to see that the action of S_1 on the vertices is the following:

$$S_1 \colon \mathbf{z}_1 \to \mathbf{z}_1, \qquad S_1 \colon \mathbf{z}_6 \to \mathbf{z}_3, \qquad S_1 \colon \mathbf{z}_7 \to \mathbf{z}_4, \qquad S_1 \colon \mathbf{z}_8 \to \mathbf{z}_5,$$
$$S_1 \colon \mathbf{z}_9 \to \mathbf{z}_9, \qquad S_1 \colon \mathbf{z}_{11} \to \mathbf{z}_{10}, \qquad S_1 \colon \mathbf{z}_{12} \to \mathbf{z}_{12}, \qquad S_1 \colon \mathbf{z}_{14} \to \mathbf{z}_{13}.$$

In other words, this means that $S_1 \colon B(J) \to B(P)$.

It is then natural to use S_1 as a side pairing map and to find another map which will map $B(J^{-1})$ and $B(P^{-1})$ to each other. With $P = R_1 R_2$ as before, we can define $S_2 = P S_1 P^{-1}$, which will act on the $\mathbf{w}$-coordinates in the same way as S_1 does on the $\mathbf{z}$-coordinates. In this sense they have an analogous relation to the one between R_1 and R_2. By inspection on the table of coordinates of the vertices, one can see that the action of S_2 is

$$S_2 \colon \mathbf{z}_2 \to \mathbf{z}_2, \qquad S_2 \colon \mathbf{z}_3 \to \mathbf{z}_{11}, \qquad S_2 \colon \mathbf{z}_4 \to \mathbf{z}_{10}, \qquad S_2 \colon \mathbf{z}_5 \to \mathbf{z}_9,$$
$$S_2 \colon \mathbf{z}_6 \to \mathbf{z}_7, \qquad S_2 \colon \mathbf{z}_8 \to \mathbf{z}_8, \qquad S_2 \colon \mathbf{z}_{13} \to \mathbf{z}_{12}, \qquad S_2 \colon \mathbf{z}_{14} \to \mathbf{z}_{14}.$$

This means that S_2 sends $B(P^{-1})$ to $B(J^{-1})$ as required.

The new side pairing maps will then be

$$R_1\colon B(R_1) \to B(R_1^{-1}), \qquad R_2\colon B(R_2) \to B(R_2^{-1}),$$
$$S_1\colon B(J) \to B(P), \qquad S_2\colon B(P^{-1}) \to B(J^{-1}).$$

In order to apply the Poincaré polyhedron theorem for cosets, we now need a group Υ that leaves the polyhedron invariant and is compatible with the action of the side pairing maps. Let us then define $K = R_1R_2S_1$. This is similar to the definition of J, but using S_1 instead of A_1. Multiplying the matrices gives

$$K = \frac{1}{1-e^{-i\theta}} \begin{bmatrix} -1 & -1 & 1 \\ -e^{2i\theta} & -1 & e^{i\theta} \\ -2\cos\theta e^{i\theta} & -2\cos\theta & 1+e^{i\theta} \end{bmatrix}.$$

Remark 5.6.2. One can see that projectively K has order 4. In fact, $e^{i\theta}K$ has both determinant and trace equal 1. The one can write the characteristic polynomial of $A \in PU(2,1)$ as $\chi_A(x) = x^3 - \operatorname{Tr} A + \overline{\operatorname{Tr} A} - \det A$ and for $e^{i\theta}K$ is becomes $x^3 - x^2 + x - 1$ and so the eigenvalues are 1, i and $-i$. Hence $e^{i\theta}K$ has order 4 and hence so does K projectively.

One can apply K to the vertices of the polyhedron and verify that its action is the following:

$$K\colon \mathbf{z}_1 \to \mathbf{z}_2, \quad K\colon \mathbf{z}_2 \to \mathbf{z}_1, \quad K\colon \mathbf{z}_3 \to \mathbf{z}_{10}, \quad K\colon \mathbf{z}_4 \to \mathbf{z}_9,$$
$$K\colon \mathbf{z}_5 \to \mathbf{z}_{11}, \quad K\colon \mathbf{z}_6 \to \mathbf{z}_4, \quad K\colon \mathbf{z}_7 \to \mathbf{z}_5, \quad K\colon \mathbf{z}_8 \to \mathbf{z}_3$$
$$K\colon \mathbf{z}_9 \to \mathbf{z}_{14}, \quad K\colon \mathbf{z}_{10} \to \mathbf{z}_{12}, \quad K\colon \mathbf{z}_{11} \to \mathbf{z}_{13}, \quad K\colon \mathbf{z}_{12} \to \mathbf{z}_8,$$
$$K\colon \mathbf{z}_{13} \to \mathbf{z}_7, \quad K\colon \mathbf{z}_{14} \to \mathbf{z}_6.$$

This means that K preserves the polyhedron and acts on the sides as

$$B(R_1) \xrightarrow{K} B(R_2) \xrightarrow{K} B(J) \xrightarrow{K} B(P^{-1}) \xrightarrow{K} B(R_1),$$
$$B(R_1^{-1}) \xrightarrow{K} B(R_2^{-1}) \xrightarrow{K} B(P) \xrightarrow{K} B(J^{-1}) \xrightarrow{K} B(R_1^{-1}),$$

namely it cyclically permutes them, preserving the two columns in Figure 5.6. Using Remark 5.6.1, and the braid relation between R_1 and R_2, it is easy to see that

$$R_2 = KR_1K^{-1}, \quad S_1 = K^2R_1K^{-2}, \quad S_2 = K^3R_1K^{-3}, \quad R_1 = K^4R_1K^{-4},$$

which proves that the action of K is compatible with the side pairing maps.

We now define $\Upsilon = \langle K \rangle$ and we are in the framework of the Poincaré polyhedron theorem for coset decompositions. The theorem ensures that we need to check the tessellation only for one ridge per cycle (which we already knew) and for one ridge per orbit under the action of K. This means that we need to analyse only the ridges contained in $B(R_1)$, which are $F(R_1, R_1^{-1})$, $F(R_1, P)$, $F(R_1, J)$, $F(R_1, R_2^{-1})$ and $F(R_1, J^{-1})$, for which we already proved the tessellation property.

We just need to check how the ridge cycles change with the new side pairing maps, so to give a presentation for these groups according to the theorem. The cycles for the ridges we mentioned are the following:

$$
\begin{aligned}
&F(R_1, R_1^{-1}) \xrightarrow{R_1} F(R_1, R_1^{-1}),\\
&F(R_1, P) \xrightarrow{R_1} F(P, R_1^{-1}) \xrightarrow{S_1^{-1}} F(R_1^{-1}, J) \xrightarrow{R_1^{-1}} F(J, R_1) \xrightarrow{S_1} F(R_1, P),\\
&F(R_1, R_2^{-1}) \xrightarrow{R_1} F(P^{-1}, R_1^{-1}) \xrightarrow{K} F(R_1, R_2^{-1}),\\
&F(R_1, J^{-1}) \xrightarrow{R_1} F(R_2, R_1^{-1}) \xrightarrow{K^{-1}} F(R_1, J^{-1}).
\end{aligned}
$$

Note that we stop when we come back in the same cycle or when we arrive in the same ridge orbit under the action of K.

The presentation obtained from the Poincaré polyhedron theorem for coset decompositions is then

$$
\Gamma = \left\langle K, R_1 : \begin{array}{l} R_1^p = K^4 = (K^{-1}R_1)^{3d} = (KR_1)^3 = K^2 S_1^{-1} R_1 = I, \\ (K^2 R_1)^2 = (R_1 K^2)^2 \end{array} \right\rangle.
$$

We want to remark that since $k = \frac{p}{2}$, by rewriting (3.4.3) or simply by inspection in Table 3.1, we have that $l = d$. It is then not surprising that the relation in the presentation where l appeared, here it becomes $(K^{-1})^{3d} = I$.

5.7 Previously known cases

Following 4.4.1, we have cases when three of the vertices collapse to a single one. This is determined by the values of the cone angles and hence by the valued of p and k. Of the four cases in the proposition, three coincide in the 3-fold symmetry

case. Hence we will have 2 possible degeneration and four possible combination of whether each degeneration happens or not. These four cases correspond to the four types described in Section 3.4.1 and to the four cases of Theorem 5.4.1. In this section we will explain in details these four cases.

For three of the four cases a fundamental polyhedron had already been constructed. For lattices of first and third type it is immediate to see how the suitable degeneration of our polyhedron D give exactly the one constructed in [BP15] and [Par06], since the same procedure has been used to construct the fundamental polyhedron. For lattices of second type a little more explanations are needed. The second part of this section is devoted to show how the suitable deformation of our fundamental polyhedron relates to the construction from [DFP05], in the description given in [Par09].

5.7.1 Degenerate cases

The first thing to remark is that the parametrisation we chose in (4.1.2) is completely general and can be used to parametrise all possible lattices in our list when we define $\theta = \frac{2\pi}{p}$ and $\varphi = \frac{\pi}{k}$ as before.

In [Par06], the same angle parametrisation holds after imposing $\varphi = \frac{\pi}{2}$, since for all lattices of that group $k = 2$. In [BP15], this parametrisation has explicitly been used. Other cases on the list could be treated with an extra condition. The lattices of fourth type, for example, always have $\varphi = \frac{\pi}{3}$. All of the ones of type 5, instead, satisfy $\theta = \varphi$ since $k = \frac{p}{2}$, as mentioned after interchanging k and l if necessary. The construction presented in this work though includes all the other cases up to imposing the values of p and k that we want to consider.

The difference comes out when we start making the singularities collapse in order to find the vertices of the polyhedron. This is because when we make T_1 and T_2 shrink or enlarge, the vertices of D change according to the size of the angles. Let us consider a generic configuration as in Figure 5.1.

The angles that we will have to consider are marked in Figure 5.9. In particular, the vertices of the polyhedron will depend on the values of

- the angle in T_1 at the vertex v_0, which we will call α,

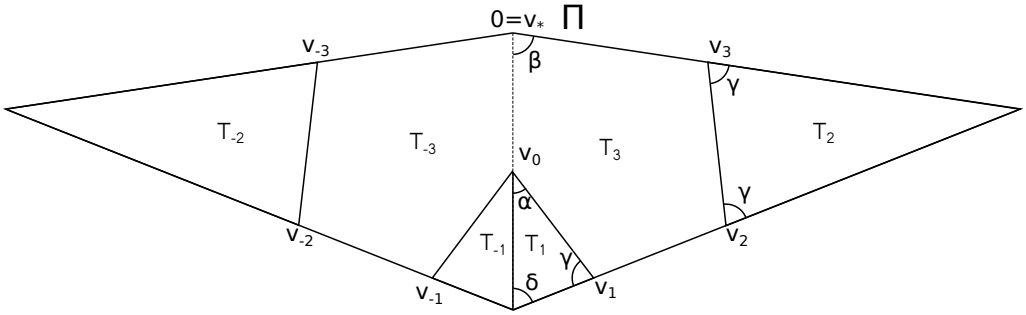

Figure 5.9: The angles whose values determines which polyhedron we shall consider.

- the angle in T_3 at v_*, which we will call β,
- the two equal angles in T_2, which we will call γ,
- the angle in T_1 at v_1, which by construction is equal to the angle γ defined previously,
- the third angle in T_1, which we will call δ.

In this section, following Proposition 4.4.1 we will explain the conditions on this angles to determine which are the vertices of our polyhedron. Then we will substitute their values, that can be easily calculated in terms of p and k.

What we need to show is that, for the particular values we are considering, the vertices that we can obtain by making cone points collapse are the ones described in the theorem.

Let us then consider the configuration in Figure 5.1 and start studying the cone points that can collapse. We have the following situation:

1. The configurations giving vertices $\mathbf{z}_1$ and $\mathbf{z}_2$ always give positive area and they do not depend on the angles at all. They will hence always be in the polyhedron.

2. If we let z_1 be as big as possible, keeping it real and such that T_1 is in the interior of T_3, there are two possibilities, illustrated in Figure 5.10. As the

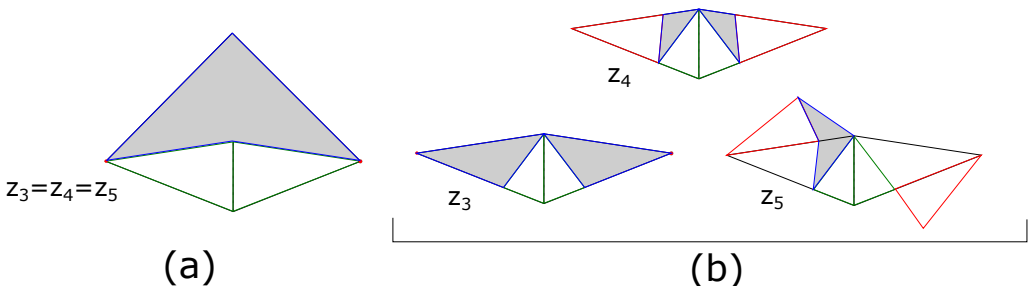

Figure 5.10: The two possibilities for the vertices in case 2.

coordinate grows, either v_1 will coincide with the apex vertex of T_2, or v_0 will coalesce with v_*.

In the first case (a) there is no other possibility for T_2 but to collapse to a point, giving a single vertex defined by $v_1 \equiv v_2 \equiv v_3$. This is the case when $\beta \leq \alpha$.

In the second case (b) we have instead that $v_0 \equiv v_*$. Also, T_2 has still some degrees of freedom, so we can make z_2 either to be 0, either to be as large as possible but still real, or to be as large as possible but after rotating it as in Figure 5.10. The three options give respectively that also $v_2 \equiv v_3$, $v_1 \equiv v_2$ or $v_1 \equiv v_3$. This is the case when $\beta \geq \alpha$.

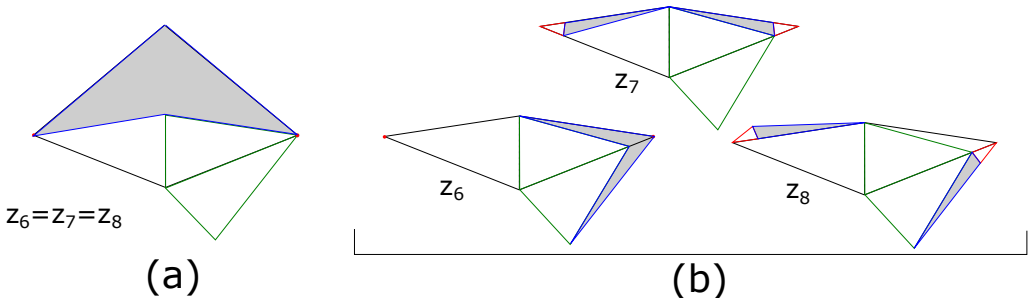

Figure 5.11: The two possibilities for the vertices in case 3.

3. With a similar argument, by imposing $z_1 = re^{-i\varphi}$ with r as big as possible, but such that T_{-1} is inside T_3, we can get the two possibilities in Figure 5.11.

Case (a) will correspond to when the cone points collapsing are $v_0 \equiv v_2 \equiv v_3$ and it corresponds to the case when $\gamma \geq \beta$.

Case (b) is when we have $v_* \equiv v_{-1}$. The three choices will be when also $v_2 \equiv v_3$, $v_0 \equiv v_2$ or $v_0 \equiv v_3$ and it occurs when $\gamma \leq \beta$.

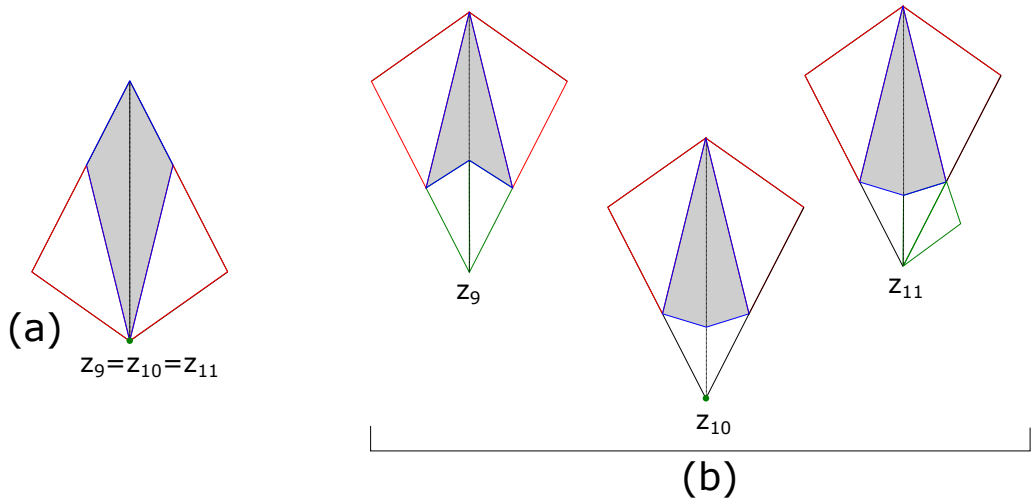

Figure 5.12: The two possibilities for the vertices in case 4.

4. Similarly, when z_2 is real, as big as possible and such that T_2 is inside T_3, we can get the configurations in Figure 5.12.

   Case (a) occurs when $\gamma \leq \delta$ and the point will be defined by $v_2 \equiv v_1 \equiv v_0$.

   In Case (b) we always have the condition $v_* \equiv v_3$, with the three possibilities as $v_0 \equiv v_1$, $v_1 \equiv v_2$ or $v_0 \equiv v_2$. This happens when $\gamma \geq \delta$.

5. Once more, when $z_2 = re^{i\theta}$, for r as big as possible but still maintaining a positive area, we can have the configurations as in Figure 5.13.

   We will hence have Case (a), when $\delta \geq \beta$ and where $v_0 \equiv v_1 \equiv v_3$.

   When $\delta \leq \beta$ we will have Case (b) instead, with $v_* \equiv v_{-2}$ for all the three vertices and $v_0 \equiv v_1$, $v_1 \equiv v_3$ or $v_0 \equiv v_3$ in the each of them.

Since in each case we have either one or three vertices, from a combinatorial point of view the cases with fewer vertices will be obtained by the case with more vertices by making triplets of vertices collapse to just one. On the other hand,

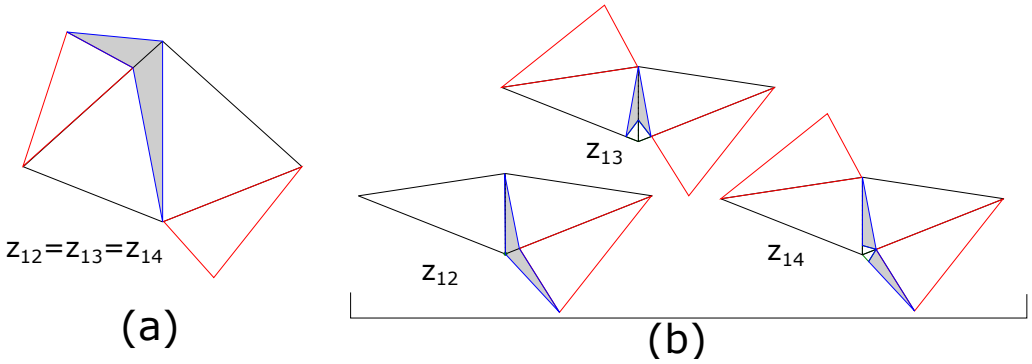

Figure 5.13: The two possibilities for the vertices in case 5.

the case with many vertices can be obtained from the other by cutting through a corner so to make one vertex become three. We will see in Section 5.7.2 that this is exactly the case, for the values of p and k that have already been treated.

Putting together Figure 5.1 and Figure 5.9, it is easy to see that

$$\alpha = \frac{\pi}{2} + \frac{\theta}{2} - \varphi, \qquad \beta = \pi - \theta - \varphi, \qquad \gamma = \frac{\pi}{2} - \frac{\theta}{2}, \qquad \delta = \varphi.$$

Substituting the values of the angles in terms of p and k, we can summarise the cases with the following table.

Case		Relation on the angles	Relation on p and k
2	(a)	$\beta \leq \alpha$	$p \leq 6$
	(b)	$\beta \geq \alpha$	$p \geq 6$
3	(a)	$\beta \leq \gamma$	$k \leq \frac{2p}{p-2}$
	(b)	$\beta \geq \gamma$	$k \geq \frac{2p}{p-2}$
4	(a)	$\gamma \geq \delta$	$k \geq \frac{2p}{p-2}$
	(b)	$\gamma \leq \delta$	$k \leq \frac{2p}{p-2}$
5	(a)	$\beta \leq \delta$	$k \leq \frac{2p}{p-2}$
	(b)	$\beta \geq \delta$	$k \geq \frac{2p}{p-2}$

As we can see, three of these conditions correspond to the same values for p and k, so we will either have all cases of the three vertices or all cases of a single vertex. Consequently, there are four possible cases and they are the four values of p and k given in the Theorem 5.4.1.

It is clear that the case of D described in the previous section is the one where all 14 vertices remain distinct. The other cases of the theorem follow immediately by our analysis. In fact, we will have one case where only one triplet collapses, one case where three triplets collapse and one case where all four do. By considering the theorem and the figures to see which vertices are collapsing, we just need to consider that the name of the configurations given in Figures 5.10–5.13 are the same as the ones given for D in the previous sections.

We remark that when the angles we are considering are equal, while making the points collapse to get a vertex, we obtain some configurations with zero area, so on the boundary of the complex hyperbolic space. This corresponds to the order of some special maps to be infinite. A more precise discussion of what happens in these cases can be found in [Par06] and [BP15]. Moreover, since, like for the case with negative parameters, we do not have the choice of three configurations (hence three vertices) but we have only one possible configuration (hence one vertex), it is more natural to include them in the case of the lower values of the parameters (i.e. with negative parameters as order of the special maps) as we did in Theorem 5.4.1.

Another way to see this is to notice that the cases where three vertices collapse correspond to when the values of l and d are negative. We saw that these two values are the order of the cycle maps R_2R_1J and P^3 respectively. As explained in [Par09], when l or d is negative, the corresponding map becomes a complex reflection in a point instead of a complex reflection in a line. The ridge on the mirror indeed becomes a single point. When they are not finite, the corresponding map becomes a parabolic element.

Already in [Par09] it has been explained that the fundamental polyhedron for the lattices of first type can be obtained from the one of third type by truncating a vertex with a triangle contained in a complex line. In that case, one vertex becomes three and we will see that it corresponds to the case (a) and (b) in point 2 of our analysis of the vertices. Comparing the sides for these cases and the ones for ours it is easy to see that the same thing can be done from our polyhedron.

5.7.2 Lattices of second type

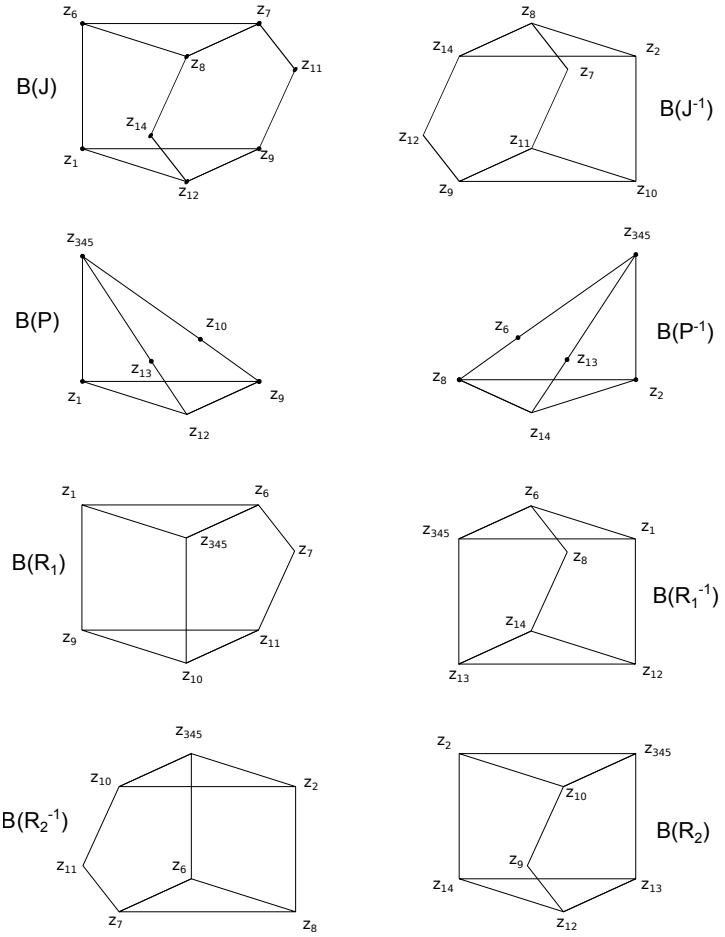

Figure 5.14: The sides compared for our polyhedron and the previous one for type 2 lattices.

In this section we will analyse the relation between this method and the previous fundamental polyhedra found for Deligne-Mostow lattices with three fold symmetry of second type. As mentioned, a fundamental polyhedron for this case was already constructed in [DFP05]. Since the approach there is a bit different from ours, Parker in [Par09] showed how to see in their procedure an approach similar to ours. What we do here though, gives a different presentation for the group and an easier construction of the polyhedron, more coherent with the known construction for the other cases.

The main difference comes from the fact that the sides and the side-pairing maps considered there are slightly different from ours. We now want to explain how to reconcile the two presentations. First of all, for the case we are talking about we need to make the vertices $\mathbf{z}_3, \mathbf{z}_4$ and $\mathbf{z}_5$ collapse to a single vertex as we saw in Theorem 5.4.1 and we will call this new vertex $\mathbf{z}_{345}$. The sides of the polyhedron D after collapsing vertices as described for the second case of our main theorem, will be as in Figure 5.14.

We want now to compare our construction with the sides of the polyhedron considered in [DFP05] as shown in Figure 11 of [Par09]. To refer to sides in our construction, we will use $B(T)$, for $T \in \{J^{\pm 1}, P^{\pm 1}, R_1^{\pm 1}, R_2^{\pm 1}\}$, while for the sides used before we will be coherent with their notation and call them $S(T)$, for $T \in \{J^{\pm 1}, P_1^{\pm 1}, P_2^{\pm 1}, R_1^{\pm 1}, R_2^{\pm 1}\}$.

The maps J considered in each case coincide and so do the sides $B(J) = S(J)$ and the sides $B(J^{-1}) = S(J^{-1})$. The same thing is true for $P = P_1 = R_1 R_2$ and the corresponding sides. On the other hand, the four sides $B(R_1^{\pm 1})$ and $B(R_2^{\pm 1})$ and the side pairing R_1 and R_2 include in their action the six remaining sides $S(R_1^{\pm 1})$, $S(R_2^{\pm 1})$ and $S(P_2^{\pm 1})$. In fact, the previous procedure splits the sides $B(R_1)$ and $B(R_1^{-1})$ in two blocks each, by cutting along a line through vertices $\mathbf{z}_9, \mathbf{z}_{11}, \mathbf{z}_{345}$ and a line through $\mathbf{z}_{12}, \mathbf{z}_{14}, \mathbf{z}_{345}$ respectively. Then, for each of $B(R_1)$ and $B(R_1^{-1})$, of the two pieces of side obtained we consider the one not containing vertex $\mathbf{z}_{10}$ and vertex $\mathbf{z}_{13}$ respectively. These are exactly the sides $S(R_1)$ and $S(R_1^{-1})$, and R_1 sends the first to the latter. Similarly, for $B(R_2)$ and $B(R_2^{-1})$, we divide the sides in two blocks by cutting with a line through $\mathbf{z}_{12}, \mathbf{z}_{14}, \mathbf{z}_{345}$ and a line through $\mathbf{z}_7, \mathbf{z}_8, \mathbf{z}_{345}$ respectively. We then consider the block not containing vertex $\mathbf{z}_{13}$ and $\mathbf{z}_6$ respectively and these are sides $S(R_2)$ and $S(R_2^{-1})$ respectively, the first sent to the second by R_2.

We have then four more block to consider. The first remark is that there are, in fact, only three blocks, because the parts of $B(R_1^{-1})$ and of $B(R_2)$ containing vertex $\mathbf{z}_{13}$ are the same block. For simplicity, we will call it $S(T)$. The other two blocks are exactly sides $S(P_2)$ and $S(P_2^{-1})$. We also know by our construction that R_1 sends $S(P_2)$ to $S(T)$, while R_2 sends $S(T)$ to $S(P_2^{-1})$. Since $P_2 = R_2 R_1$ by definition, that is the side pairing map that sends the two new blocks $S(P_2)$

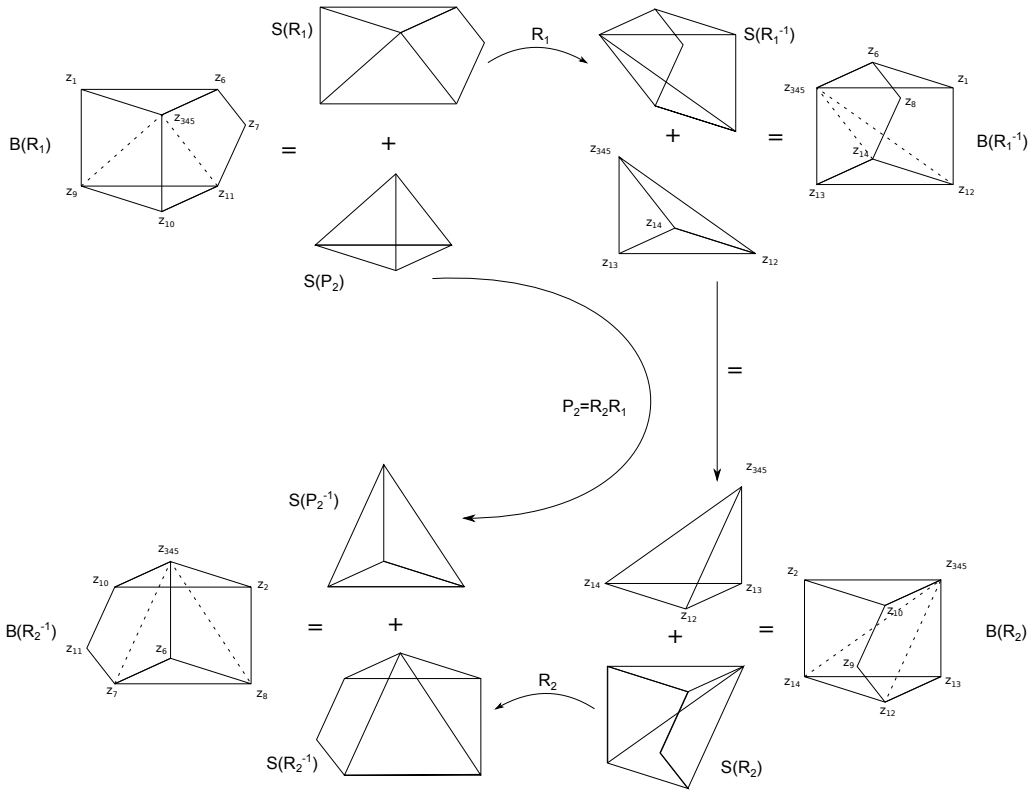

Figure 5.15: The side pairing maps compared for our polyhedron and the previous one.

to $S(P_2^{-1})$, as described in [Par09]. This is illustrated in Figure 5.15.

Chapter 6

Lattices with 2-fold symmetry

We will now consider the lattices with 2-fold symmetry, i.e. the ones obtained from cone metrics on the sphere where two of the five cone points have the same cone angles. The values of the angles that give lattices are described in Section 3.4.2. In this section we will show how to use the polyhedron in Section 4.3 to build a fundamental domain for them.

Remember, from Section 4.1 (see (4.1.2)) that we were considering a sphere with five cone points of cone angles θ_0, θ_1, θ_2, θ_3, θ_4 with values

$$(2(\pi+\varphi-\alpha), 2\alpha, 2\beta, 2(\pi+\theta-\beta), 2(\pi-\theta-\varphi)).$$

Now, following Section 3.4.2, we also want two equal angles at the vertices v_1 and v_2. This means that $\alpha = \beta$. We can also reinterpret the parameters p, p', k, k', l, l', d in terms of the angles α, β, θ, φ as follows.

$$\begin{aligned} &\frac{\pi}{p} = \theta, && \frac{\pi}{k} = \varphi, && \frac{\pi}{l} = \alpha-\theta-\varphi, && \frac{\pi}{d} = \pi-\alpha-\theta, \\ &\frac{\pi}{p'} = \alpha-\frac{\pi}{2}, && \frac{\pi}{k'} = \pi+\theta+\varphi-2\alpha, && \frac{\pi}{l'} = \pi-\alpha-\varphi. \end{aligned} \quad (6.0.1)$$

These parameters will be the orders of some maps in the group. In particular, this means that the parameters (p, k, p') we used in Section 3.4.2 denote the configuration $(\alpha, \alpha, \theta, \varphi)$. We remark that in the 2-2-fold symmetry case (i.e. when we also have $\theta_0 = \theta_3$), we have $\theta = \varphi$ and so the lattice is of the form (p, p, p'). Notice also that in the 3-fold symmetry case one would have $k = k'$, $l = l'$ and $p = 2p'$. In fact k and k' will be the orders of $A_1(\alpha, \beta, \theta, \varphi)$ for two of the

different configurations we will consider (see (4.2.6)) which coincide in the 3-fold symmetry case. A similar thing happens for l and l'. The values p' and p here are the orders of $R_1(\pi+\theta-\alpha, \alpha, 2\alpha-\pi, \pi+\theta+\varphi-2\alpha)$ and $R_1 \circ R_1(\alpha, \pi+\theta-\alpha, \theta, \varphi)$ respectively (remember that the composition is done as in (4.2.1)), and notice that they are applied to different configurations. Since in the 3-fold symmetry case the three configurations we consider coincide, p will be the order of the square of R_1, which has order p' and hence $p = 2p'$.

6.1 Configuration types

Since the case that we treated before is when the three angles at v_1, v_2 and v_3 were equal, by analogy we also want to consider the configurations where the two equal angles are at v_1 and v_2, at v_2 and v_3 or at v_1 and v_3. We will call these configurations of type ①, ② and ③ respectively. Note that configuration of type ① corresponds to having the cone angles satisfying $\theta_i = \theta_{i+1}$, for indices $i = 1, 2, 3$ taken mod 3.

We will build a polyhedron for each of these cases and use their union to build a fundamental domain for the lattices. On the parameters $(\alpha, \beta, \theta, \varphi)$ (see Section 4.1), type ① corresponds to $(\alpha, \alpha, \theta, \varphi)$, type ② corresponds to $(\pi + \theta - \alpha, \alpha, 2\alpha - \pi, \pi + \theta + \varphi - 2\alpha)$ and type ③ corresponds to $(\alpha, \pi + \theta - \alpha, \theta, \varphi)$. For each type, we will consider the **t**-coordinates and **s**-coordinates. We will have **x**-, **y**- and **z**-coordinates as **t**-coordinates of the configuration of type ①, ② and ③ respectively. We will also have **u**-, **v**- and **w**-coordinates, representing copies of type ①, ② and ③ respectively and being the **s**-coordinates of one of the previous ones. More precisely, the relation between **x**-, **y**-, **z**- and **u**-, **v**-, **w**-coordinates is as follows. Since P^{-1} acts on the copies as explained in Figure 4.5, then, for example, a configuration of type ① will be sent to one of type ②. This means that the coordinates defined as $P^{-1}(\mathbf{x})$ will be the **v**-coordinates. With a similar argument, one gets

$$\mathbf{u} = P^{-1}(\mathbf{z}), \qquad \mathbf{v} = P^{-1}(\mathbf{x}), \qquad \mathbf{w} = P^{-1}(\mathbf{y}). \tag{6.1.1}$$

In other words, the **u**-, **v**- and **w**-coordinates will be the coordinates for the

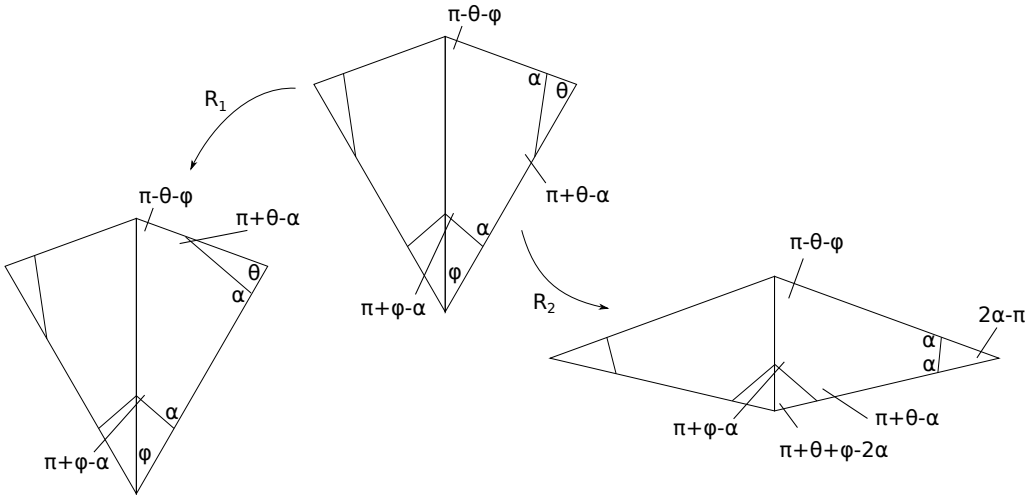

Figure 6.1: The representative for each configuration type.

configuration of type ①, ② and ③ respectively, obtained after applying P to the standard configuration of type ③, ① and ② respectively.

We will start from the configuration of type ③, with its **z**-coordinates as the **t**-coordinates of configuration $(\alpha, \pi+\theta-\alpha, \theta, \varphi)$. The **x**- and **y**-coordinates will be determined by the action of the moves R_1 and R_2^{-1} respectively (see Figure 6.1 for more details). As mentioned, each configuration will give us a polyhedron of the same type as D in (4.3.5).

We will first explain what the relation between the **x**-, **y**- and **z**-coordinates is. Since copies of type ① and ③ are swapped by R_1, it is natural to define

$$\mathbf{x} = R_1(\alpha, \pi+\theta-\alpha, \theta, \varphi)\mathbf{z}. \tag{6.1.2}$$

Since the **w**- and **u**-coordinates are also of type ③ and ① respectively, one would also want

$$\mathbf{u} = R_1(\alpha, \pi+\theta-\alpha, \theta, \varphi)\mathbf{w}. \tag{6.1.3}$$

Using the definition of **u**- and **w**-coordinates, together with the previous formula, the **y**-coordinates are defined as

$$\mathbf{z} = R_2(\pi+\theta-\alpha, \alpha, 2\alpha-\pi, \pi+\theta+\varphi-2\alpha)\mathbf{y}. \tag{6.1.4}$$

Using Equations (6.1.1), (6.1.2) and (6.1.4), one can also see that

$$\mathbf{v} = P^{-1}\mathbf{x} = P^{-1}R_1\mathbf{z} = P^{-1}R_1R_2\mathbf{y} = \mathbf{y}. \tag{6.1.5}$$

The following digram summarises the relations between the coordinates.

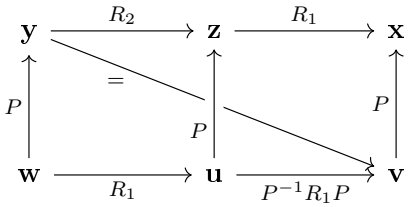

6.2 The fundamental polyhedron

For each coordinate type, we can define a polyhedron as in (4.3.5). This will give us three components of our fundamental polyhedron D and we will write

$$D = D_1 \cup D_2 \cup D_3, \text{ with } \begin{cases} D_1 = D(\alpha, \alpha, \theta, \varphi) = R_1^{-1}(D_3), \\ D_2 = D(\pi + \theta - \alpha, \alpha, 2\alpha - \pi, \pi + \theta + \varphi - 2\alpha) = R_2(D_3), \\ D_3 = D(\alpha, \pi + \theta - \alpha, \theta, \varphi). \end{cases} \tag{6.2.1}$$

In coordinates, the polyhedron D_1 is defined as

$$D_1 = \left\{ \mathbf{x} = P(\mathbf{v}) \colon \begin{array}{ll} \arg(x_1) \in (-\varphi, 0), & \arg(x_2) \in (0, \theta), \\ \arg(v_1) \in (0, \pi + \theta + \varphi - 2\alpha), & \arg(v_2) \in (0, 2\alpha - \pi) \end{array} \right\},$$

the polyhedron D_2 is

$$D_2 = \left\{ \mathbf{y} = P(\mathbf{w}) \colon \begin{array}{ll} \arg(y_1) \in (-(\pi + \theta + \varphi - 2\alpha, 0), & \arg(y_2) \in (0, 2\alpha - \pi), \\ \arg(w_1) \in (0, \varphi), & \arg(w_2) \in (0, \theta) \end{array} \right\}$$

and the polyhedron D_3 is defined as

$$D_3 = \left\{ \mathbf{z} = P(\mathbf{u}) \colon \begin{array}{ll} \arg(z_1) \in (-\varphi, 0), & \arg(z_2) \in (0, \theta), \\ \arg(u_1) \in (0, \varphi), & \arg(u_2) \in (0, \theta) \end{array} \right\}.$$

Due to the fact that the matrix for R_1 is extremely simple, we will keep track only of three sets of coordinates, namely **z**-, **w**- and **y**-coordinates and use the relations in (6.1.2), (6.1.3) and (6.1.5) to give the other coordinates in term of these.

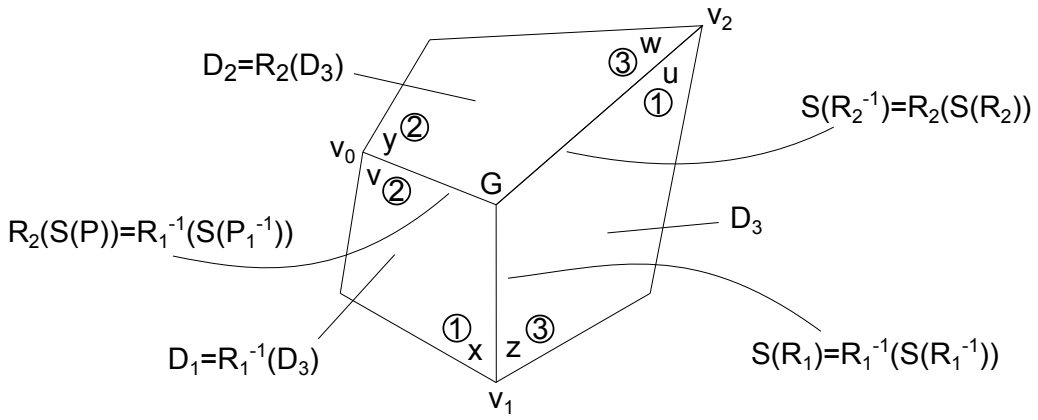

Figure 6.2: The interaction of the polyhedra and their coordinates.

Then we can describe the polyhedron as follows.

$$D = \left\{ \mathbf{z} = R_2(\mathbf{y}) = R_2P(\mathbf{w}) \colon \begin{array}{ll} \arg(z_1) \in (-\varphi, 0), & \arg(z_2) \in (-\theta, \theta), \\ \arg(w_1) \in (0, \varphi), & \arg(w_2) \in (-\theta, \theta), \\ \arg(y_1) \in (-\varphi', \varphi'), & \arg(y_2) \in (0, \theta') \end{array} \right\},$$

with $\varphi' = \pi + \theta + \varphi - 2\alpha$ and $\theta' = 2\alpha - \pi$.

In Figure 6.2 one can see how the polyhedra and the coordinates interact. As we will specify in the next section, the three polyhedra have disjoint interiors, they intersect pairwise in a side and all three have a common Giraud disc G (see (6.2.2), (6.2.3) and (6.2.4)). Passing from $\mathbf{t}$- to $\mathbf{s}$-coordinates changes the type of configuration from ⓚ to ⓘ within the same polyhedron D_k, where $i = k - 2$, taken mod 3. Three special vertices of the polyhedron (see section below) $\mathbf{v}_0$, $\mathbf{v}_1$ and $\mathbf{v}_2$ are the origin of one of the coordinates.

6.2.1 Vertices of D

The vertices of D will be of three types. Some will come from D_1 and they will be called $\mathbf{x}_i$, for $i = 1, \ldots, 14$, some will be the vertices of D_2 and we will denote them $\mathbf{y}_i$, for $i = 1, \ldots, 14$ and finally there will be the vertices $\mathbf{z}_i$'s for $i = 1, \ldots, 14$, coming from D_3. Since the three polyhedra intersect there will be some vertices that are repeated. The following table describes all the vertices. In

the first column there will be the label we choose for the vertex, in the second, third and fourth column its name in D_3, D_1 and D_2 respectively (if there is one), and in the final columns we will record which coordinates have a "nice" form.

D	D_3	D_1	D_2	$\arg z_1$	$\arg z_2$	$\arg w_1$	$\arg w_2$	$\arg y_1$	$\arg y_2$
$\mathbf{v}_0$		$\mathbf{x}_2$	$\mathbf{y}_1$					$y_1 = 0$	$y_2 = 0$
$\mathbf{v}_1$	$\mathbf{z}_1$	$\mathbf{x}_1$		$z_1 = 0$	$z_2 = 0$				
$\mathbf{v}_2$	$\mathbf{z}_2$		$\mathbf{y}_2$			$w_1 = 0$	$w_2 = 0$		
$\mathbf{v}_3$	$\mathbf{z}_3$	$\mathbf{x}_3$	$\mathbf{y}_5$	0	$z_2 = 0$	0	0	0	θ'
$\mathbf{v}_4$	$\mathbf{z}_4$	$\mathbf{x}_5$	$\mathbf{y}_4$	0	0	0	$w_2 = 0$	0	0
$\mathbf{v}_5$	$\mathbf{z}_5$			0	θ	0	$-\theta$		
$\mathbf{v}_6$	$\mathbf{z}_6$	$\mathbf{x}_6$	$\mathbf{y}_{13}$	$-\varphi$	$z_2 = 0$	0	0	0	θ'
$\mathbf{v}_7$	$\mathbf{z}_7$	$\mathbf{x}_8$	$\mathbf{y}_{12}$	$-\varphi$	0	φ	0	$y_1 = 0$	θ'
$\mathbf{v}_8$	$\mathbf{z}_8$		$\mathbf{y}_{14}$	$-\varphi$	θ	$w_1 = 0$	0	$-\varphi'$	θ'
$\mathbf{v}_9$	$\mathbf{z}_9$	$\mathbf{x}_{12}$		$z_1 = 0$	0	φ	$-\theta$	φ'	0
$\mathbf{v}_{10}$	$\mathbf{z}_{10}$	$\mathbf{x}_{13}$	$\mathbf{y}_{10}$	0	0	φ	$w_2 = 0$	0	0
$\mathbf{v}_{11}$	$\mathbf{z}_{11}$	$\mathbf{x}_{14}$	$\mathbf{y}_9$	$-\varphi$	0	φ	0	$y_1 = 0$	0
$\mathbf{v}_{12}$	$\mathbf{z}_{12}$			$z_1 = 0$	θ	φ	$-\theta$		
$\mathbf{v}_{13}$	$\mathbf{z}_{13}$			0	θ	0	$-\theta$		
$\mathbf{v}_{14}$	$\mathbf{z}_{14}$			$-\varphi$	θ	0	$-\theta$		
$\mathbf{v}_{16}$		$\mathbf{x}_4$	$\mathbf{y}_3$	0	$-\theta$	0	θ	0	$y_2 = 0$
$\mathbf{v}_{17}$		$\mathbf{x}_7$		$-\varphi$	$-\theta$			φ'	θ'
$\mathbf{v}_{18}$		$\mathbf{x}_9$		$z_1 = 0$	$-\theta$			φ'	0
$\mathbf{v}_{19}$		$\mathbf{x}_{10}$		0	$-\theta$			φ'	$y_2 = 0$
$\mathbf{v}_{20}$		$\mathbf{x}_{11}$		$-\varphi$	$-\theta$			φ'	θ'
$\mathbf{v}_{21}$			$\mathbf{y}_6$			0	θ	$-\varphi'$	$y_2 = 0$
$\mathbf{v}_{22}$			$\mathbf{y}_7$			φ	θ	$-\varphi'$	0
$\mathbf{v}_{23}$			$\mathbf{y}_8$			$w_1 = 0$	θ	$-\varphi'$	θ'
$\mathbf{v}_{24}$			$\mathbf{y}_{11}$			φ	θ	$-\varphi'$	0

Table 6.1: The vertices of D.

This reflects how the D_i's glue together. In particular, the polyhedra D_1 and D_3 glue along

$$\{\operatorname{Im} z_2 = 0\} \cap D_3 = \{\operatorname{Im} e^{-i\theta} x_2 = 0\} \cap D_1, \tag{6.2.2}$$

while D_2 and D_3 are glued along

$$\{\operatorname{Im} e^{-i\theta} u_2 = 0\} \cap D_3 = \{\operatorname{Im} w_2 = 0\} \cap D_2 \tag{6.2.3}$$

and D_1 and D_2 intersect along

$$\{\operatorname{Im} v_1 = 0\} \cap D_1 = \{\operatorname{Im} y_1 = 0\} \cap D_2. \tag{6.2.4}$$

Moreover, all three will intersect along the Giraud disc G containing the ridge bounded by vertices $\mathbf{v}_3, \mathbf{v}_4, \mathbf{v}_6, \mathbf{v}_7, \mathbf{v}_{10}$ and $\mathbf{v}_{11}$ (see Figure 6.2).

Remark 6.2.1. Using Table 4.1, one can obtain the equations of the complex lines for our three configurations and see that the following lines coincide:

1. $L_{*0}(\alpha, \pi + \theta - \alpha, \theta, \varphi) = L_{*0}(\pi + \theta - \alpha, \alpha, 2\alpha - \pi, \pi + \theta + \varphi - 2\alpha) = L_{*0}(\alpha, \alpha, \theta, \varphi)$,
2. $L_{*3}(\alpha, \pi + \theta - \alpha, \theta, \varphi) = L_{*3}(\pi + \theta - \alpha, \alpha, 2\alpha - \pi, \pi + \theta + \varphi - 2\alpha) = L_{*2}(\alpha, \alpha, \theta, \varphi)$,
3. $L_{*1}(\alpha, \pi + \theta - \alpha, \theta, \varphi) = L_{*2}(\pi + \theta - \alpha, \alpha, 2\alpha - \pi, \pi + \theta + \varphi - 2\alpha) = L_{*1}(\alpha, \alpha, \theta, \varphi)$.

6.2.2 Sides and side pairing maps

In view of applying the Poincaré polyhedron theorem in Section 6.3, we need to analyse the sides of D and explain how we have some maps pairing them.

Clearly, the sides of D will be the union of all sides in D_i, with $i = 1, 2, 3$, except for the three sides along which two of the copies glue. Some of the sides combine to create a single larger side. Remembering (6.2.1), the sides (illustrated in Figure 6.3 with their side pairings) will be as follows.

$$\begin{array}{llll}
S(J), & S(P), & S(R_1), & S(R_2), \\
S(J^{-1}), & S(P^{-1}), & S(R_1^{-1}), & S(R_2^{-1}), \\
R_1^{-1}S(J), & R_1^{-1}S(P), & R_1^{-1}S(R_1), & R_1^{-1}S(R_2), \\
R_1^{-1}S(J^{-1}), & R_1^{-1}S(P^{-1}), & R_1^{-1}S(R_1^{-1}), & R_1^{-1}S(R_2^{-1}), \\
R_2S(J), & R_2S(P), & R_2S(R_1), & R_2S(R_2), \\
R_2S(J^{-1}), & R_2S(P^{-1}), & R_2S(R_1^{-1}), & R_2S(R_2^{-1}).
\end{array}$$

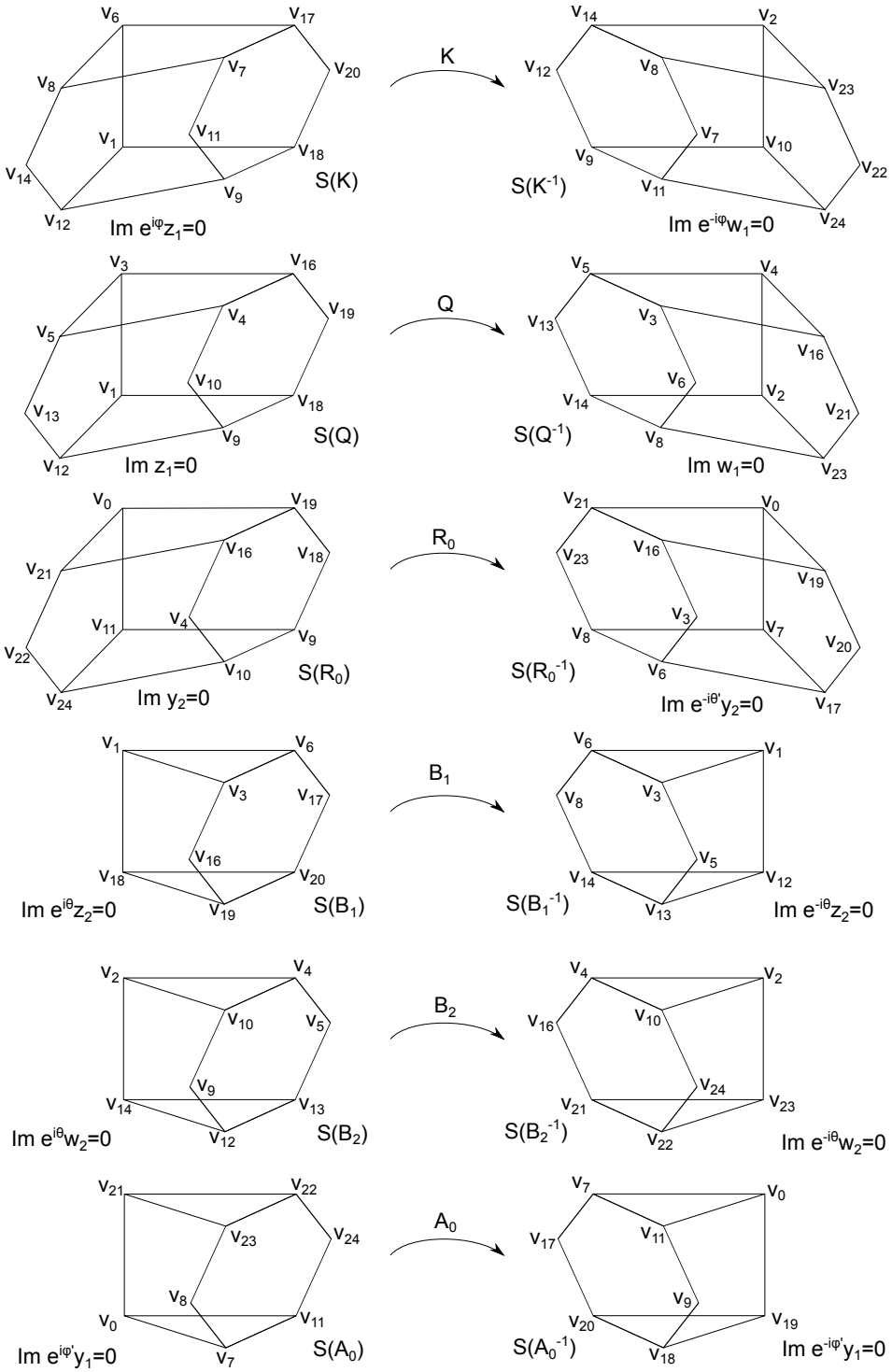

Figure 6.3: The sides of D.

Now the glueing of the three polyhedra (see Equations (6.2.2), (6.2.3) and (6.2.4)) tells us that

$$R_1^{-1}S(R_1^{-1}) = S(R_1), \quad R_2S(R_2) = S(R_2^{-1}), \quad R_1^{-1}S(P^{-1}) = R_2S(P),$$

so these sides are now internal (see Figure 6.2).

The side pairings will be obtained by adapting to the union of the three polyhedra the equivalent on each D_i of the side pairings in previous works (see Section 4.3 of [Par06], Section 5.3 of [BP15] and Section 8.3.1 of [Pas16]). In other words, in each copy we need to consider R_1, R_2, P and J and adapt them to act on the sides of D. We will describe all of them, treating the $\mathbf{z}$-coordinates as the main coordinates. In other words, we will give the matrix as applied to the $\mathbf{z}$-coordinates of the point.

First consider R_1 and R_2. Since applying $R_2(\alpha, \alpha, \theta, \varphi)$ to a point in its $\mathbf{x}$-coordinates is equivalent to applying $R_1(\pi + \theta - \alpha, \alpha, 2\alpha - \pi, \pi + \theta + \varphi - 2\alpha)$ to its $\mathbf{v} = \mathbf{y}$-coordinates, these combine to a single side pairing

$$R_1(\pi + \theta - \alpha, \alpha, 2\alpha - \pi, \pi + \theta + \varphi - 2\alpha) = \begin{bmatrix} 1 & 0 & 0 \\ 0 & -e^{2i\alpha} & 0 \\ 0 & 0 & 1 \end{bmatrix}.$$

This is the side pairing as applied on the $\mathbf{y}$-coordinates. We will hence consider

$$R_0 = R_2R_1R_2^{-1} = R_2(\pi + \theta - \alpha, \alpha, 2\alpha - \pi, \pi + \theta + \varphi - 2\alpha) \circ$$
$$\circ R_1(\pi + \theta - \alpha, \alpha, 2\alpha - \pi, \pi + \theta + \varphi - 2\alpha) \circ R_2^{-1}(\alpha, \pi + \theta - \alpha, \theta, \varphi), \quad (6.2.5)$$

which includes the change of coordinates.

Now consider $R_1(\alpha, \alpha, \theta, \varphi)$ and $R_1(\alpha, \pi + \theta - \alpha, \theta, \varphi)$. The target side of the former coincides with the source side of the latter and is the (now internal) side $D_1 \cap D_3$. This means that we can compose the two maps and have a new side pairing

$$B_1 = R_1(\alpha, \pi + \theta - \alpha, \theta, \varphi)R_1(\alpha, \alpha, \theta, \varphi) = \begin{bmatrix} 1 & 0 & 0 \\ 0 & e^{2i\theta} & 0 \\ 0 & 0 & 1 \end{bmatrix}.$$

We remark that even though it looks like this is the matrix we use when applying the map to a point in its $\mathbf{x}$-coordinates, composing it with the change of

coordinates from our coordinates (the **z**-coordinates), one gets that in terms of matrices

$$B_1(\alpha, \pi+\theta-\alpha, \theta, \varphi) = R_1^{-1}(\alpha, \alpha, \theta, \varphi) B_1(\alpha, \alpha, \theta, \varphi) R_1(\alpha, \pi+\theta-\alpha, \theta, \varphi) \tag{6.2.6}$$

$$= B_1(\alpha, \alpha, \theta, \varphi). \tag{6.2.7}$$

Similarly, the common side of D_2 and D_3 is the target side of $R_2(\alpha, \pi+\theta-\alpha, \theta, \varphi)$ and the starting side of $R_2(\pi+\theta-\alpha, \alpha, 2\alpha-\pi, \pi+\theta+\varphi-2\alpha)$. We can then define

$$B_2 = R_2(\pi+\theta-\alpha, \alpha, 2\alpha-\pi, \pi+\theta+\varphi-2\alpha) R_2(\alpha, \pi+\theta-\alpha, \theta, \varphi).$$

The map B_2 is already defined to act on the **z**-coordinates. As we said for R_2 and R_1, B_2 acts as B_1, but on the **u**-coordinates.

In the 3-fold symmetry case, the side pairings P and J related the **t**- and **s**-coordinates of the polyhedron, but the side pairing property relied on the fact that the source and target configurations were of the same type. Adapting this to our case means that we want to consider the maps relating **z**- and **w**-coordinates, **x**- and **u**-coordinates and **y**- and **v**-coordinates. The map relating **y**- and **v**-coordinates is the identity and it indeed maps the common side between D_1 and D_2 to itself. Since this side is in the interior of D, we can ignore it. Composing the map obtained with $A_1(\pi+\theta-\alpha, \alpha, 2\alpha-\pi, \pi+\theta+\varphi-2\alpha)$ to compute the equivalent of J and applying the change of coordinates to our main coordinates, we obtain the side pairing

$$A_0 = R_2 A_1 R_2^{-1}.$$

Now, we have

$$\mathbf{w} = P^{-1}\mathbf{y} = P^{-1}R_2^{-1}\mathbf{z} = Q^{-1}\mathbf{z}$$

and

$$\mathbf{u} = R_2^{-1}R_1^{-1}R_1^{-1}\mathbf{x},$$

which translates to the **z**-coordinates as Q^{-1} again. Then $Q = R_1R_2R_1$ will be our new side pairing. Moreover, we will consider $K = QA_1$.

Putting all this information together and remarking that $J^3 = \mathrm{Id}$, one gets that the side pairings are

$$\begin{aligned}
K = JR_1 = R_2J &: R_1^{-1}S(J) \cup S(J) \longmapsto S(J^{-1}) \cup R_2S(J^{-1}),\\
Q = PR_1 = R_2P &: R_1^{-1}S(P) \cup S(P) \longmapsto S(P^{-1}) \cup R_2S(P),\\
R_0 = R_1^{-1}R_2R_1 = R_2R_1R_2^{-1} &: R_1^{-1}S(R_2) \cup R_2S(R_1) \longmapsto R_1^{-1}S(R_2^{-1}) \cup R_2S(R_1^{-1}),\\
B_1 = R_1R_1 &: R_1^{-1}S(R_1) \longmapsto S(R_1^{-1}),\\
B_2 = R_2R_2 &: S(R_2) \longmapsto R_2S(R_2^{-1}),\\
A_0 = R_1^{-1}J^{-1}J^{-1}R_2^{-1} &: R_2S(J) \longmapsto R_1^{-1}S(J^{-1}).
\end{aligned}$$

As mentioned for the general case, the sides are contained in bisectors. One can rewrite Lemma 4.3.2 for each copy and eliminate the inequalities related to the sides along which the polyhedra glue. Translating the inequalities on the right hand side into $\mathbf{z}$-coordinates and giving all the $\mathbf{n}_{*i}$ in terms of the configuration $(\alpha, \pi + \theta - \alpha, \theta, \varphi)$ (using Remark 6.2.1), we get the following lemma.

Lemma 6.2.2. *We have*

- $\mathrm{Im}(z_1) \leq 0$ *if and only if* $|\langle \mathbf{z}, \mathbf{n}_{*1}\rangle| \leq |\langle \mathbf{z}, P^{-1}(\mathbf{n}_{*3})\rangle|$,
- $\mathrm{Im}(e^{i\varphi}z_1) \geq 0$ *if and only if* $|\langle \mathbf{z}, \mathbf{n}_{*0}\rangle| \leq |\langle \mathbf{z}, K^{-1}(\mathbf{n}_{*0})\rangle|$,
- $\mathrm{Im}(e^{-i\theta}z_2) \leq 0$ *if and only if* $|\langle \mathbf{z}, \mathbf{n}_{*3}\rangle| \leq |\langle \mathbf{z}, B_1(\mathbf{n}_{*3})\rangle|$,
- $\mathrm{Im}(e^{i\theta}z_2) \geq 0$ *if and only if* $|\langle \mathbf{z}, \mathbf{n}_{*3}\rangle| \leq |\langle \mathbf{z}, B_1^{-1}(\mathbf{n}_{*3})\rangle|$,
- $\mathrm{Im}(e^{i\varphi'}y_1) \geq 0$ *if and only if* $|\langle \mathbf{z}, \mathbf{n}_{*0}\rangle| \leq |\langle \mathbf{z}, K^2(\mathbf{n}_{*0})\rangle|$,
- $\mathrm{Im}(y_2) \geq 0$ *if and only if* $|\langle \mathbf{z}, \mathbf{n}_{*1}\rangle| \leq |\langle \mathbf{z}, Q^{-1}B_1(\mathbf{n}_{*3})\rangle|$,
- $\mathrm{Im}(e^{-i\theta'}y_2) \leq 0$ *if and only if* $|\langle \mathbf{z}, \mathbf{n}_{*3}\rangle| \leq |\langle \mathbf{z}, B_1^{-1}Q(\mathbf{n}_{*1})\rangle|$,
- $\mathrm{Im}(e^{-i\varphi'}y_1) \leq 0$ *if and only if* $|\langle \mathbf{z}, \mathbf{n}_{*0}\rangle| \leq |\langle \mathbf{z}, K^{-2}(\mathbf{n}_{*0})\rangle|$,
- $\mathrm{Im}(w_1) \geq 0$ *if and only if* $|\langle \mathbf{z}, \mathbf{n}_{*3}\rangle| \leq |\langle \mathbf{z}, Q(\mathbf{n}_{*1})\rangle|$,
- $\mathrm{Im}(e^{-i\varphi}w_1) \leq 0$ *if and only if* $|\langle \mathbf{z}, \mathbf{n}_{*0}\rangle| \leq |\langle \mathbf{z}, K(\mathbf{n}_{*0})\rangle|$,
- $\mathrm{Im}(e^{-i\theta}w_2) \leq 0$ *if and only if* $|\langle \mathbf{z}, \mathbf{n}_{*1}\rangle| \leq |\langle \mathbf{z}, B_2(\mathbf{n}_{*1})\rangle|$,
- $\mathrm{Im}(e^{i\theta}w_2) \geq 0$ *if and only if* $|\langle \mathbf{z}, \mathbf{n}_{*1}\rangle| \leq |\langle \mathbf{z}, B_2^{-1}(\mathbf{n}_{*1})\rangle|$.

6.3 Main theorem

In this section we will state and prove that D (or a suitable modification of D) is a fundamental domain for Deligne-Mostow lattices with 2-fold symmetry as parametrised in Section 3.4.2. To do this we will use the Poincaré polyhedron theorem, in the form given in Section 2.4.

We are now ready to state and show that D or a suitable modification of it is a fundamental domain for the lattices we are considering.

Theorem 6.3.1. *Let Γ be one of the Deligne-Mostow lattices with 2-fold symmetry (see Table 3.2). Then a suitable modification of the polyhedron D defined in Section 6.2 is a fundamental domain for Γ. More precisely the fundamental domain is D up to collapsing some ridges to a point when some parameters are degenerate (negative of infinite) according to the following table.*

Lattice	*Deg. par.*	*Ridges collapsing*
(4,4,6), (4,4,5)		
(3,4,4), (2,4,3), (3,3,4)	l', d	$F(A_0, B_2^{-1}), F(B_2, B_1^{-1}),$ $F(A_0^{-1}, B_1),\ F(Q, Q^{-1}).$
(2,6,6)	l, d	$F(Q, Q^{-1}), F(K, R_0^{-1}),$ $F(K^{-1}, R_0).$
(2,3,3)	l, l', d	$F(Q, Q^{-1}), F(K, R_0^{-1}),$ $F(K^{-1}, R_0), F(A_0, B_2^{-1}),$ $F(B_2, B_1^{-1}),\ F(A_0^{-1}, B_1).$
(3,6,3), (4,4,3), (6,6,3)	k', l', d	$F(A_0, A_0^{-1}), F(Q, Q^{-1}),$ $F(B_2, B_1^{-1}),\ F(A_0^{-1}, B_1).$
(2,3,3)	k'	$F(A_0, A_0^{-1}).$

Moreover, a presentation for Γ *is given by*

$$\Gamma = \left\langle \begin{array}{l} K, Q, B_1, \\ B_2, R_0, A_0 \end{array} \; : \; \begin{array}{l} B_1^p = B_2^p = R_0^{p'} = A_0^{k'} = (Q^{-1}K)^k = (R_0K)^l = I, \\ (A_0B_2B_1)^{l'} = Q^{2d} = I, \quad Q = B_1R_0 = R_0B_2 = B_2^{-1}QB_1, \\ R_0^{-1}A_0R_0 = A_0 = K^{-2}, \quad B_2K = KB_1 \end{array} \right\rangle,$$

where each of the relations involving k', l, l' *and* d *hold as long as the corresponding parameter is finite and positive.*

The reason for the ridges to collapse to a point (except for k', which is treated in Section 6.3.3) relies on Proposition 4.4.1 applied to each of the polyhedra D_1, D_2 and D_3. In fact:

- First, consider the case when $d < 0$ or $d = \infty$. By definition (see (6.0.1)), this is equivalent to say that $\pi - \alpha - \theta \leq 0$. Remembering Proposition 4.4.1 and using the notation of Remark 6.2.1, one can see that the vertices on L_{*0} collapse when $\pi - \alpha - \theta \leq 0$. Since these three vertices form the ridge $F(Q, Q^{-1})$, this ridge collapses when $d < 0$ or $d = \infty$.

- Similarly, when $l < 0$ or $l = \infty$, by definition, we have $\alpha - \theta - \varphi \leq 0$. Now the vertices on L_{*3} collapse when $\alpha - \theta - \varphi \leq 0$ and so do the ones on L_{*1}. Since $F(K^{-1}, R_0)$ is formed of the vertices contained in L_{*3} and $F(K, R_0^{-1})$ of the ones contained in L_{*1}, they degenerate when $l < 0$ or $l = \infty$.

- Now assume $l' < 0$ or $l' = \infty$, i.e. $\pi - \alpha - \varphi \leq 0$. By Proposition 4.4.1, the vertices on $L_{*2}(\alpha, \pi + \theta - \alpha, \theta, \varphi)$, $L_{*3}(\alpha, \alpha, \theta, \varphi)$ and $L_{*1}(\pi + \theta - \alpha, 2\alpha - \pi, \pi + \theta + \varphi - 2\alpha)$ all degenerate when $\pi - \alpha - \varphi \leq 0$. Then the claim of the theorem follows from the fact that $F(B_1, A_0^{-1})$, $F(B_1^{-1}, B_2)$ and $F(B_2^{-1}, A_0)$ are bounded by the vertices contained in $L_{*3}(\alpha, \alpha, \theta, \varphi)$, $L_{*2}(\alpha, \pi + \theta - \alpha, \theta, \varphi)$ and $L_{*1}(\pi + \theta - \alpha, 2\alpha - \pi, \pi + \theta + \varphi - 2\alpha)$ respectively.

- Finally, the case of k' negative is treated in Section 6.3.3.

An alternative presentation for the lattices can be obtained by remembering that $K = QA_1$ and substituting $Q = B_1R_0$, $K = B_1R_0A_1$, $B_2 = R_0^{-1}B_1R_0$ and

$A_0 = (B_1R_0A_1)^{-2}$. Then

$$\Gamma = \left\langle \begin{array}{ll} & B_1^p = R_0^{p'} = (B_1R_0A_1)^{2k'} = A_1^k = (R_0B_1R_0A_1)^l = I, \\ B_1, R_0, A_1 \ : & (A_1R_0)^{2l'} = (B_1R_0)^{2d} = I, \quad br_4(B_1, R_0), \\ & br_2((B_1R_0A_1)^{-2}, R_0), \quad br_2(A_1, B_1) \end{array} \right\rangle,$$

where, following [DPP], $br_n(T, S)$ is the braid relation of length n on T and S, i.e. $(TS)^{n/2} = (ST)^{n/2}$, where the power $n/2$ with n odd means that the product has n factors (e.g. $(TS)^{3/2} = TST$). Note that the generators can be found in (6.2.6), (6.2.5) and (4.2.6). They are all applied to configuration of type ③, i.e. to $(\alpha, \pi + \theta - \alpha, \theta, \varphi)$ and preserve the Hermitian form $H(\alpha, \pi + \theta - \alpha, \theta, \varphi)$ in (4.1.4).

6.3.1 Cycles

The cycles given by the Poincaré polyhedron theorem are the following.

$$F(K, Q) \xrightarrow{K} F(K^{-1}, Q^{-1}) \xrightarrow{Q^{-1}} F(K, Q),$$
$$F(K^{-1}, R_0) \xrightarrow{R_0} F(K, R_0^{-1}) \xrightarrow{K} F(K^{-1}, R_0),$$
$$F(B_1, A_0^{-1}) \xrightarrow{B_1} F(B_1^{-1}, B_2) \xrightarrow{B_2} F(B_2^{-1}, A_0) \xrightarrow{A_0} F(B_1, A_0^{-1}),$$
$$F(R_0, R_0^{-1}) \xrightarrow{R_0} F(R_0, R_0^{-1}),$$
$$F(Q, Q^{-1}) \xrightarrow{Q} F(Q, Q^{-1}),$$
$$F(B_1, B_1^{-1}) \xrightarrow{B_1} F(B_1, B_1^{-1}),$$
$$F(B_2, B_2^{-1}) \xrightarrow{B_2} F(B_2, B_2^{-1}),$$
$$F(A_0, A_0^{-1}) \xrightarrow{A_0} F(A_0, A_0^{-1}),$$
$$F(K, B_1) \xrightarrow{B_1} F(K, B_1^{-1}) \xrightarrow{K} F(K^{-1}, B_2^{-1}) \xrightarrow{B_2^{-1}} F(K^{-1}, B_2) \xrightarrow{K^{-1}} F(K, B_1),$$
$$F(B_1, Q) \xrightarrow{Q} F(B_2, Q^{-1}) \xrightarrow{B_2} F(B_2^{-1}, Q^{-1}) \xrightarrow{Q^{-1}} F(B_1^{-1}, Q) \xrightarrow{B_1^{-1}} F(B_1, Q),$$
$$F(A_0, R_0) \xrightarrow{A_0} F(A_0^{-1}, R_0) \xrightarrow{R_0} F(A_0^{-1}, R_0^{-1}) \xrightarrow{A_0^{-1}} F(A_0, R_0^{-1}) \xrightarrow{R_0^{-1}} F(A_0, R_0),$$
$$F(K, K^{-1}) \xrightarrow{K} F(K^{-1}, A_0) \xrightarrow{A_0} F(K, A_0^{-1}) \xrightarrow{K} F(K, K^{-1}),$$
$$F(B_1, R_0^{-1}) \xrightarrow{B_1} F(B_1^{-1}, Q^{-1}) \xrightarrow{Q^{-1}} F(Q, R_0) \xrightarrow{R_0} F(B_1, R_0^{-1}),$$
$$F(R_0^{-1}, Q^{-1}) \xrightarrow{Q^{-1}} F(Q, B_2) \xrightarrow{B_2} F(B_2^{-1}, R_0) \xrightarrow{R_0} F(R_0^{-1}, Q^{-1}).$$

These cycles give the following cycle transformations, where ℓ is the power of T which fixes the ridge pointwise and ℓm is the order of T. Note that for all of

the 2-fold symmetry values that we are considering, k, k', p, p', l, l' and d are all integers (positive or negative) or infinite.

Cycle transformation T	ℓ	m	Cycle transformation T	ℓ	m
$Q^{-1}K$	1	k	A_0	1	k'
R_0	1	p'	$B_1A_0B_2 = (B_2^{-1}K)^2$	1	l'
B_2	1	p	B_1	1	p
Q	2	d	R_0K	1	l
$R_0Q^{-1}B_1 = \mathrm{Id}$	1	1	$B_2Q^{-1}R_0 = \mathrm{Id}$	1	1
$B_1K^{-1}B_2^{-1}K = \mathrm{Id}$	1	1	$B_1^{-1}Q^{-1}B_2Q = \mathrm{Id}$	1	1
$A_0R_0^{-1}A_0^{-1}R_0 = \mathrm{Id}$	1	1	$KA_0K = \mathrm{Id}$	1	1

Table 6.4: The cycle transformations and their orders.

When the order of a cycle transformation is negative, we know that the corresponding ridge collapses to a point and so the transformation is a complex reflection to a point. When the order is ∞, then the cycle transformation is parabolic.

6.3.2 Tessellation

The proof of Theorem 6.3.1 consists of proving that D and our side pairings satisfy the hypothesis of the Poincaré polyhedron theorem. The proof is similar to that of Theorem 5.4.1. In particular, we only need to include the proof of the tessellation condition, since the rest is done in the same way.

We will divide the ridges in three groups. Looking at the structure of sides in Figure 4.7, one can see that the ridges are contained in either a Giraud disc, a Lagrangian plane or a complex line. We will include the proof of the tessellation condition for one ridge from each type. For the others it can be done in exactly the same way.

Ridges contained in a Giraud disc. The ridges contained in a Giraud disc are $F(K, K^{-1})$, $F(K, A_0^{-1})$, $F(A_0, K^{-1})$, $F(B_1, R_0^{-1})$, $F(B_1^{-1}, Q^{-1})$, $F(Q, R_0)$, $F(R_0^{-1}, Q^{-1})$, $F(Q, B_2)$ and $F(B_2^{-1}, R_0)$. To prove the tessellation condition for

them, we will use Lemma 6.2.2.

Proposition 6.3.2. *The polyhedra D, $K(D)$ and $KA_0(D) = K^{-1}(D)$ tessellate around the ridge $F(K, K^{-1})$.*

Proof. Take $\mathbf{z} \in D$. By the second point of Lemma 6.2.2, $\mathbf{z}$ is closer to $\mathbf{n}_{*0}$ than to $K^{-1}(\mathbf{n}_{*0})$. By the tenth point of the lemma, it is closer to $\mathbf{n}_{*0}$ than to $K(\mathbf{n}_{*0})$. Similarly, take a point $\mathbf{z} \in K(D)$. This means that $K^{-1}(\mathbf{z}) \in D$. By the second point of the lemma applied to $K^{-1}(\mathbf{z})$, $\mathbf{z}$ is closer to $K(\mathbf{n}_{*0})$ than to $\mathbf{n}_{*0}$. By the eighth point of the lemma, it is closer to $K(\mathbf{n}_{*0})$ than to $K^{-1}(\mathbf{n}_{*0})$. Finally, take a point $\mathbf{z} \in K^{-1}(D)$. This means that $K(\mathbf{z}) \in D$. By the fifth point of the lemma applied to $K(\mathbf{z})$, $\mathbf{z}$ is closer to $K^{-1}(\mathbf{n}_{*0})$ than to $K(\mathbf{n}_{*0})$. By the tenth point of the lemma, it is closer to $K^{-1}(\mathbf{n}_{*0})$ than to $\mathbf{n}_{*0}$.

This clearly implies that the three images are disjoint and since $F(K, K^{-1})$ is defined by $\mathrm{Im}(e^{i\varphi} z_1) = 0$ and $\mathrm{Im}(e^{-i\varphi} w_1) = 0$, a small enough neighbourhood of the ridge is covered by the three images. ■

Ridges contained in a Lagrangian plane. The ridges contained in a Lagrangian plane are $F(K, B_1)$, $F(K^{-1}, B_2^{-1})$, $F(K^{-1}, B_2)$, $F(K, B_1^{-1})$, $F(B_1, Q)$, $F(B_2, Q^{-1})$, $F(B_2^{-1}, Q^{-1})$, $F(B_1^{-1}, Q)$, $F(A_0^{-1} R_0)$, $F(A_0^{-1}, R_0^{-1})$, $F(A_0, R_0^{-1})$ and $F(A_0, R_0)$. The proof of the tessellation property is done by studying the sign of some of the coordinates. We will prove the property for the first ridge mentioned. The others are done in a similar way.

Proposition 6.3.3. *The polyhedra D, $B_1^{-1}(D)$, $K^{-1}(D)$ and $B_1^{-1}K^{-1}(D)$ tessellate around the ridge $F(K, B_1)$.*

Proof. Let us consider points in D, $B_1^{-1}(D)$, $K^{-1}(D)$ and $B_1^{-1}K^{-1}(D)$ and record the sign of the values of $\mathrm{Im}(z_1)$, $\mathrm{Im}(e^{i\varphi} z_1)$, $\mathrm{Im}(e^{i\theta} z_2)$ and $\mathrm{Im}(e^{-i\theta} z_2)$ for them. They are shown in the following table.

	$\mathrm{Im}(z_1)$	$\mathrm{Im}(e^{i\varphi} z_1)$	$\mathrm{Im}(e^{i\theta} z_2)$	$\mathrm{Im}(e^{-i\theta} z_2)$
D	-	+	+	-
$B_1^{-1}(D)$	-	+	-	-
$K^{-1}(D)$	-	-	+	-
$B_1^{-1}K^{-1}(D)$	-	-	-	-

The first row can be deduced using the definition of D in terms of the arguments of the coordinates. The second row can be deduced by considering that the action of B_1 only consists in multiplying the coordinate z_2 by $e^{2i\theta}$. The third row can be deduced by the fact that applying K corresponds to first applying A_1, which multiplies the coordinate z_1 by $e^{2i\varphi}$ and then applying Q, which relates the $\mathbf{z}$ coordinates to the $\mathbf{w}$ coordinates.

The ridge $F(K, B_1)$ is defined by $\mathrm{Im}(e^{i\varphi}z_1) = 0$ and $\mathrm{Im}(e^{i\theta}z_2) = 0$ and in a neighbourhood of the ridge the images considered coincide with the sectors where the values are either positive or negative. Combining the information of the table one gets the tessellation as required. ■

Ridges contained in complex lines. The ridges contained in complex lines are $F(K,Q)$, $F(K^{-1},Q^{-1})$, $F(K,R_0^{-1})$, $F(K^{-1},R_0)$, $F(R_0,R_0)$, $F(Q,Q^{-1})$, $F(B_2,A_0^{-1})$, $F(B_1^{-1},B_2)$, $F(B_1^{-1},A_0)$, $F(B_1,B_1^{-1})$, $F(B_2,B_2^{-1})$ and $F(A_0,A_0^{-1})$. The strategy for proving the tessellation property consists of showing that the polyhedron (and suitable images) cover a sector of amplitude ψ and that the cycle transformation acts on the orthogonal of the complex line as a rotation through angle ψ. Then each power of the cycle transformation covers a sector and since ψ is always $\frac{2\pi}{a}$ with a integer, we cover the whole space around the ridge.

The cases of $F(B_1,A_0^{-1})$, $F(Q,Q^{-1})$ and $F(K^{-1},R_0)$ (and the ones in their cycles) are an exception because the procedure is the same but after applying a suitable change of coordinates. For completeness, we will include the proof of one of these ridges.

Proposition 6.3.4. *The polyhedra D, $A_0(D)$ and $A_0B_2(D)$ and their images under $A_0B_2B_1$ tessellate around the ridge $F(B_1,A_0^{-1})$.*

Proof. The ridge $F(B_1,A_0^{-1})$ is contained in $L_{*3}(\alpha,\alpha,\theta,\varphi)$. We remark that the map $e^{-2i(\theta-\alpha)}A_0B_2B_1$ fixes the ridge pointwise and rotates its normal vector $\mathbf{n}_{*3}(\alpha,\alpha,\theta,\varphi)$ by $e^{2i(\alpha+\varphi-\pi)}$.

The proof consists of changing the coordinates to have a similar situation as for the other ridges contained in a complex line. The new coordinates will be in

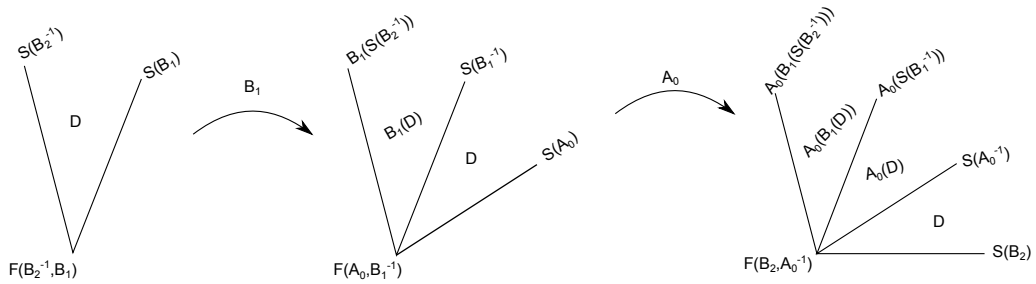

Figure 6.4: The polyhedra around $F(A_0^{-1}, B_2)$.

terms of two vectors spanning the complex line and the vector normal to it, since the complex line is the mirror of the transformation $A_0B_2B_1$. More precisely, writing

$$\begin{pmatrix} x_1 \\ x_2 \\ 1 \end{pmatrix} = \frac{\sin\varphi\sin(\alpha-\theta) - \sin\alpha\sin(\theta+\varphi)x_2}{\sin\theta\sin(\alpha+\varphi)} \begin{pmatrix} 0 \\ -1 \\ -1 \end{pmatrix} + x_1 \begin{pmatrix} 1 \\ 0 \\ 0 \end{pmatrix} + \frac{1-x_2}{\sin\theta\sin(\alpha+\varphi)} \begin{pmatrix} 0 \\ \sin\varphi\sin(\alpha-\theta) \\ \sin(\theta+\varphi)\sin\alpha \end{pmatrix}, \quad (6.3.1)$$

the new coordinates are

$$\begin{aligned} \xi_1 &= \frac{\sin\varphi\sin(\alpha-\theta) - \sin\alpha\sin(\theta+\varphi)x_2}{1-x_2}, \\ \xi_2 &= \frac{\sin\theta\sin(\alpha+\varphi)x_1}{1-x_2}. \end{aligned} \quad (6.3.2)$$

This means that $A_0B_2B_1$ acts on the new coordinates by sending (ξ_1, ξ_2) to the point $(e^{2i(\alpha+\varphi-\pi)}\xi_1, \xi_2)$. Since the configurations are as in Figure 6.4, if we prove that D, $A_0(D)$ and $A_0B_2(D)$ cover the sector defined by the argument of ξ_1 being between 0 and $2(\alpha+\varphi-\pi)$, then the appropriate images under $A_0B_2B_1$ will cover a neighbourhood of $F(A_0^{-1}, B_2)$.

First notice that if we are in $S(B_1)$, then $x_2 \in \mathbb{R}$ and so $\arg\xi_1 = 0$. Moreover, if we take a point $\mathbf{z} \in S(B_1^{-1})$, then $z_2 = e^{i\theta}u$ with $u \in \mathbb{R}$ and the coordinate ξ_1 of $A_0B_2\mathbf{z}$ is

$$\xi_1 = e^{2i(\alpha+\varphi-\pi)}\frac{\sin(\theta+\varphi)u + \sin\varphi}{\sin(\alpha-\theta)u - \sin\alpha}$$

and so $\arg \xi_1 = 2(\alpha + \varphi - \pi)$.

The last thing we need to prove is that such images are disjoint. The pairs D, A_0D and A_0D, B_2A_0D are disjoint because of tessellation property around $F(A_0, A_0^{-1})$ and $F(B_2, B_2^{-1})$. To prove that D and B_2A_0D are disjoint, it is enough to prove that the argument of the coordinate ξ_1 of points in D is smaller than $\alpha + \varphi - \pi$, while the one of points in B_2A_0D is bigger than $\alpha + \varphi - \pi$.

If one writes the coordinate ξ_1 in terms of the $\mathbf{v}$-coordinates, then a point in $S(A_0)$ has coordinate $v_1 = e^{i\varphi'}u$, with $\mathbb{R} \ni u \leq \frac{-\sin(2\alpha)}{\sin(\theta+\varphi)}$ by Lemma 4.4.2 and

$$\xi_1 = e^{i(\alpha+\varphi-\pi)} \frac{\sin\varphi \sin(\alpha-\theta)(-\sin(2\alpha) - \sin(\theta+\varphi)u)}{\sin(\alpha-\theta)u - \sin(\alpha+\varphi)v_2 + \sin(\alpha-\varphi)}.$$

Then

$$\operatorname{Im} e^{i(\alpha+\varphi-\pi)}\xi_1 = \sin\varphi \sin(\alpha-\theta)(-\sin(2\alpha) - \sin(\theta+\varphi)u)\sin(\alpha+\varphi)\operatorname{Im} v_2 \geq 0.$$

Similarly, if we take a point $\mathbf{z} \in S(B_2^{-1})$, then we have $w_2 = e^{-i\theta}v$, with $\mathbb{R} \ni v \leq \frac{\sin\varphi}{\sin(\theta+\varphi)}$ and the coordinate ξ_1 of $A_0\mathbf{z}$ is

$$\xi_1 = e^{-i(\alpha+\varphi-\pi)} \frac{\sin\varphi}{\sin\alpha} \cdot \frac{\sin(\theta+\varphi)u - \sin\varphi}{\sin(\alpha+\varphi)e^{-i\varphi}w_1 + \sin(\alpha-\theta)u - \sin\alpha}$$

and

$$\operatorname{Im} e^{i(\alpha+\varphi-\pi)}\xi_1 = \frac{\sin\varphi}{\sin\alpha}(\sin\varphi - \sin(\theta+\varphi)u)\sin(\alpha+\varphi)\operatorname{Im} e^{-i\varphi}w_2 \leq 0.$$

Note that we are using the fact that $\sin(\alpha+\varphi) > 0$, which is always the case when the ridge does not collapse (i.e. $l' > 0$ and finite). ■

6.3.3 The case k' negative

When k' is negative, after applying P^{-1} to the configuration $(\alpha, \alpha, \theta, \varphi)$ we obtain a configuration where φ is negative. This means that we cannot describe the configuration with the same coordinates and triangles as before. This does not stop us from doing everything in the same way, up to taking a slightly different configuration of triangles. By construction (see Figure 4.1), once we developed the cone metric on the plane, φ was the angle between the line passing through v_* and v_0 and the line passing through v_1 and v_2 on the side of v_0 and v_1. When

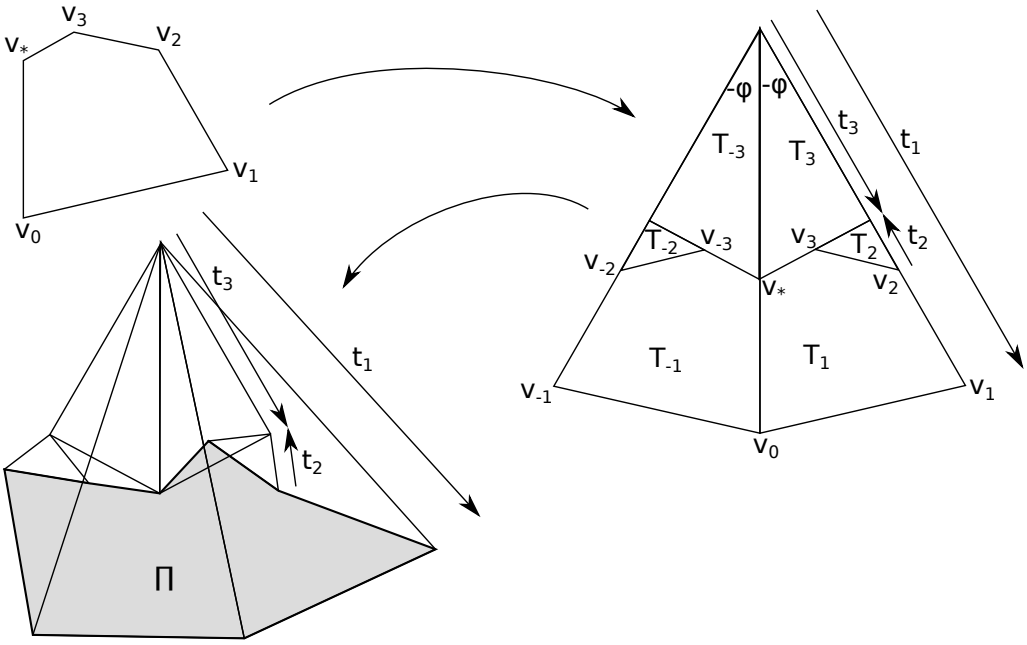

Figure 6.5: The configuration of triangles when k' is negative.

this angle is negative, we will take $-\varphi$ to be the angle between the same two lines, but on the side of v_2 and v_* (see Figure 6.5).

The area of the cone metric is the area of the shaded region Π. Using the coordinates as in the figure, this is

$$\text{Area} = \frac{-\sin\varphi\sin\alpha}{\sin(\alpha-\varphi)}|t_1|^2 - \frac{\sin\theta\sin\beta}{\sin(\beta-\theta)}|t_2|^2 - \frac{-\sin\varphi\sin\theta}{\sin(\theta+\varphi)}|t_3|^2.$$

Remembering that $-\sin\varphi$ is positive, this is still a Hermitian form of the same signature, except that the roles of t_1 and t_3 are exchanged. This makes sense, since now the triangles T_2 and T_3 are "inside" the triangle T_1.

When looking at the vertices, this tells us that the we cannot have the line L_{01}, since to make v_0 and v_1 collapse, one should take $t_1 = 0$ and the whole figure would collapse. We will hence have a new vertex $\mathbf{v}_{*23}$ obtained by taking $t_1 = t_3 = 0$ and so by making $v_* \equiv v_2 \equiv v_3$ instead of the three vertices $\mathbf{y}_1, \mathbf{y}_9, \mathbf{y}_{12}$. In terms of our polyhedron D, this means that $\mathbf{v}_0$, $\mathbf{v}_7$ and $\mathbf{v}_{11}$ collapse to this new point $\mathbf{v}_{*23}$, which is on the boundary (i.e. it makes the area be 0) if k' is infinite. All the other vertices remain the same and everything else in the study

of the combinatorial structure of the polyhedron can be done in the exact same way. In particular, as in Proposition 4.4.1, we still have that the vertices on L_{*0} collapse to a single vertex if $\pi - \alpha' - \theta' \leq 0$ (i.e. if $d \leq 0$) and the vertices on L_{*1} collapse to a single vertex if $\alpha' - \theta' - \varphi' \leq 0$ (i.e. if $l' \leq 0$). Note that the vertices on L_{*2} and L_{*3} never collapse, as $l > 0$ in all our cases. This analysis gives the cases in Theorem 6.3.1.

Chapter 7

Volumes and commensurability

In this chapter we will calculate the volumes of the polyhedra using the orbifold Euler characteristic. We will do this for the fundamental polyhedra built in the 2- and 3-fold symmetry cases and also in all the possible degenerations that we mentioned in the main theorems. Finally we will show how the values found are coherent with the commensurability theorems described in Section 3.5.

The volume of the quotient is a multiple of the orbifold Euler characteristic $\chi\left(\Gamma\backslash\mathbf{H}^n_{\mathbb{C}}\right)$. Seeing Section 8 of [McM17] for example, one can see that for a closed complex hyperbolic manifold $M = \Gamma\backslash\mathbf{H}^n_{\mathbb{C}}$, one has $\mathrm{Vol}(M) = C_n\chi(M)$, where $C_n = \frac{(-4\pi)^n}{(n+1)!}$, when the metric is normalised as we chose in Chapter 2. Since $n = 2$ here, the constant is $\frac{8\pi^2}{3}$. The orbifold Euler characteristic is calculated by taking the sum (with alternating signs with the dimension of the facets) of the reciprocal of the order of the stabiliser of each orbit of cells.

7.1 Volumes of polyhedra arising from lattices with 3-fold symmetry

In this section we will consider the lattices with 3-fold symmetry. Following Theorem 5.4.1 we will have four cases according to the sign of l and d. We will refer to the different cases as lattices of type one, two, three and four as explained in Section 3.4.1.

The following table refers to the lattices of fourth type and hence to the

polyhedron D, where no facets collapse.

Orbit of the facet	Stabiliser	Order
$\mathbf{z}_1, \mathbf{z}_2$	$\langle A_1, R_1 \rangle$	kp
$\mathbf{z}_3, \mathbf{z}_4, \mathbf{z}_5$	$\langle P^3, R_1 \rangle$	pd
$\mathbf{z}_6, \mathbf{z}_{10}, \mathbf{z}_{13}$	$\langle A_1', R_1 \rangle$	pl
$\mathbf{z}_8, \mathbf{z}_7, \mathbf{z}_9, \mathbf{z}_{11}, \mathbf{z}_{12}, \mathbf{z}_{14}$	$\langle A_1, A_1' \rangle$	kl
$\gamma_{1,3}, \gamma_{2,4}$	$\langle R_1 \rangle$	p
$\gamma_{1,6}, \gamma_{2,10}$	$\langle R_1 \rangle$	p
$\gamma_{3,6}, \gamma_{5,13}, \gamma_{4,10}$	$\langle R_1 \rangle$	p
$\gamma_{2,8}, \gamma_{1,9}, \gamma_{1,12}, \gamma_{2,14}$	$\langle A_1 \rangle$	k
$\gamma_{7,11}, \gamma_{9,12}, \gamma_{8,14}$	$\langle JR_1 \rangle$	$2k$
$\gamma_{9,10}, \gamma_{12,13}, \gamma_{6,7}, \gamma_{13,14}, \gamma_{6,8}, \gamma_{10,11}$	$\langle A_2' \rangle$	l
$\gamma_{7,8}, \gamma_{12,14}, \gamma_{9,11}$	$\langle JR_1^{-1} \rangle$	$2l$
$\gamma_{4,5}, \gamma_{3,5}, \gamma_{3,4}$	$\langle R_2 P \rangle$	$2d$
$F(P, J), \quad F(P^{-1}, J^{-1})$	A_1	k
$F(R_1, R_1^{-1})$	R_1	p
$F(R_2, R_2^{-1})$	R_2	p
$F(P, R_1), \quad F(P, R_1^{-1}), \quad F(P^{-1}, R_2), \quad F(P^{-1}, R_2^{-1})$	1	1
$F(J, R_1), \quad F(J, R_1^{-1}), \quad F(J^{-1}, R_2), \quad F(J^{-1}, R_2^{-1})$	1	1
$F(P, R_2), \quad F(R_1, R_2^{-1}), \quad F(R_1^{-1}, P^{-1})$	1	1
$F(J, R_2^{-1}), \quad F(R_1, J^{-1}), \quad F(R_1^{-1}, R_2)$	A_1'	l
$F(J, J^{-1})$	J	3
$F(P, P^{-1})$	P	$3d$
$S(J), S(J^{-1})$	1	1
$S(R_1), S(R_1^{-1})$	1	1
$S(R_2), S(R_2^{-1})$	1	1
$S(P), S(P^{-1})$	1	1
D	1	1

Table 7.1: The stabilisers for l and d positive and finite.

In this case, the vertices are all contained in two orthogonal complex lines. This implies that the stabiliser is a direct product of two cyclic groups, each generated by the complex reflections in these lines. The ridges are stabilised by the cycle relations, while the sides are fixed only by the identity, as the side pairing maps send the sides one in the other.

To find the stabiliser of the edges requires slightly more work. If the map T stabilises an edge, then either it will fix the endpoints or it will swap them. If we can find a map that swaps them, then it will generate the maps that fix them. If the endpoints are not in the same orbit, then there is no map that swaps them and by analysing the action of the side pairing maps (i.e. the generators of the group) on the vertices, we can verify that the stabilisers are as in the table. If the vertices are in the same orbit, the same analysis will tell us if there are maps swapping the endpoints or just fixing them. In this way it is easy to check that the stabilisers are the above.

From the table it follows that the Euler orbifold characteristic is

$$\begin{aligned}
\chi\left(\Gamma\backslash\mathbf{H}^2_{\mathbb{C}}\right) = \quad & \frac{1}{kp}+\frac{1}{pd}+\frac{1}{pl}+\frac{1}{kl}-\frac{1}{p}-\frac{1}{p}-\frac{1}{p}-\frac{1}{k}-\frac{1}{2k}-\frac{1}{l}-\frac{1}{2l}-\frac{1}{2d} \\
& +\frac{1}{k}+\frac{1}{p}+\frac{1}{p}+1+1+1+\frac{1}{l}+\frac{1}{3}+\frac{1}{3d} \\
= \quad & \frac{1}{kp}+\frac{1}{2p}-\frac{3}{p^2}+\frac{1}{2p}-\frac{1}{p^2}-\frac{1}{pk}+\frac{1}{2k}-\frac{1}{pk}-\frac{1}{k^2} \\
& -\frac{1}{p}-\frac{1}{2k}-\frac{1}{4}+\frac{1}{2p}+\frac{1}{2k}-\frac{1}{4}+\frac{3}{2p}+\frac{1}{3}+\frac{1}{6}-\frac{1}{p} \\
= \quad & -\frac{4}{p^2}-\frac{1}{pk}-\frac{1}{k^2}+\frac{1}{2k}+\frac{1}{p} \\
= \quad & \frac{p^2+12p-60}{16p^2}-\frac{t^2}{4}, \qquad (7.1.1)
\end{aligned}$$

where for the second equality we used $\frac{1}{l}=\frac{1}{2}-\frac{1}{p}-\frac{1}{k}$ and $\frac{1}{d}=\frac{1}{2}-\frac{3}{p}$, while in the last one we used $t=-\frac{1}{2}+\frac{1}{p}+\frac{2}{k}$.

The following tables correspond to the degenerations of the polyhedron for the other types and are calculated in [Par09]. We will omit the details of the methods used to calculate the orders of the stabilisers in the degenerate cases, since they are similar to the ones that we will use in the next section to calculate orders for the degenerate 2-fold symmetry case.

Orbit of the facet	Stabiliser	Order
$\mathbf{z}_1, \mathbf{z}_2$	$\langle A_1, R_1 \rangle$	kp
$\mathbf{z}_3$	$\langle R_1, R_2 \rangle$	$6d^2$
$\mathbf{z}_6, \mathbf{z}_9, \mathbf{z}_{12}$	$\langle A_1, R_1 \rangle$	$2l^2$
$\gamma_{1,3}, \gamma_{2,3}$	$\langle R_1 \rangle$	p
$\gamma_{1,6}, \gamma_{2,9}$	$\langle R_1 \rangle$	p
$\gamma_{3,6}, \gamma_{5,12}, \gamma_{3,9}$	$\langle R_1 \rangle$	p
$\gamma_{2,6}, \gamma_{1,9}, \gamma_{1,12}, \gamma_{2,12}$	$\langle A_1 \rangle$	k
$\gamma_{6,9}, \gamma_{9,12}, \gamma_{6,12}$	$\langle JR_1 \rangle$	$2k$
$F(P,J), \quad F(P^{-1}, J^{-1})$	A_1	k
$F(R_1, R_1^{-1})$	R_1	p
$F(R_2, R_2^{-1})$	R_2	p
$F(P,R_1), \quad F(P,R_1^{-1}), \quad F(P^{-1},R_2), \quad F(P^{-1},R_2^{-1})$	1	1
$F(J,R_1), \quad F(J,R_1^{-1}), \quad F(J^{-1},R_2), \quad F(J^{-1},R_2^{-1})$	1	1
$F(P,R_2), \quad F(R_1,R_2^{-1}), \quad F(R_1^{-1},P^{-1})$	1	1
$F(J,J^{-1})$	J	3
$S(J), S(J^{-1})$	1	1
$S(R_1), S(R_1^{-1})$	1	1
$S(R_2), S(R_2^{-1})$	1	1
$S(P), S(P^{-1})$	1	1
D	1	1

Table 7.2: The stabilisers for l and d negative or infinite.

The orbifold Euler characteristic in this case is

$$\chi\left(\Gamma \backslash \mathbf{H}^2_{\mathbb{C}}\right) = \frac{1}{2}\left(2\left(\frac{1}{2} - \frac{1}{p}\right) - \frac{1}{k}\right)^2. \tag{7.1.2}$$

Orbit of the facet	Stabiliser	Order
$\mathbf{z}_1, \mathbf{z}_2$	$\langle A_1, R_1 \rangle$	kp
$\mathbf{z}_3$	$\langle R_1, R_2 \rangle$	$6d^2$
$\mathbf{z}_6, \mathbf{z}_{10}, \mathbf{z}_{13}$	$\langle A_1', R_1 \rangle$	pl

$\mathbf{z}_8, \mathbf{z}_7, \mathbf{z}_9, \mathbf{z}_{11}, \mathbf{z}_{12}, \mathbf{z}_{14}$	$\langle A_1, A_1' \rangle$	kl
$\gamma_{1,3}, \gamma_{2,3}$	$\langle R_1 \rangle$	p
$\gamma_{1,6}, \gamma_{2,10}$	$\langle R_1 \rangle$	p
$\gamma_{3,6}, \gamma_{3,13}, \gamma_{3,10}$	$\langle R_1 \rangle$	p
$\gamma_{2,8}, \gamma_{1,9}, \gamma_{1,12}, \gamma_{2,14}$	$\langle A_1 \rangle$	k
$\gamma_{7,11}, \gamma_{9,12}, \gamma_{8,14}$	$\langle JR_1 \rangle$	$2k$
$\gamma_{9,10}, \gamma_{12,13}, \gamma_{6,7}, \gamma_{13,14}, \gamma_{6,8}, \gamma_{10,11}$	$\langle A_2' \rangle$	l
$\gamma_{7,8}, \gamma_{12,14}, \gamma_{9,11}$	$\langle JR_1^{-1} \rangle$	$2l$
$F(P, J), \quad F(P^{-1}, J^{-1})$	A_1	k
$F(R_1, R_1^{-1})$	R_1	p
$F(R_2, R_2^{-1})$	R_2	p
$F(P, R_1), \quad F(P, R_1^{-1}), \quad F(P^{-1}, R_2), \quad F(P^{-1}, R_2^{-1})$	1	1
$F(J, R_1), \quad F(J, R_1^{-1}), \quad F(J^{-1}, R_2), \quad F(J^{-1}, R_2^{-1})$	1	1
$F(P, R_2), \quad F(R_1, R_2^{-1}), \quad F(R_1^{-1}, P^{-1})$	1	1
$F(J, R_2^{-1}), \quad F(R_1, J^{-1}), \quad F(R_1^{-1}, R_2)$	A_1'	l
$F(J, J^{-1})$	J	3
$S(J), S(J^{-1})$	1	1
$S(R_1), S(R_1^{-1})$	1	1
$S(R_2), S(R_2^{-1})$	1	1
$S(P), S(P^{-1})$	1	1
D	1	1

Table 7.3: The stabilisers for l positive and finite and d negative or infinite.

The orbifold Euler characteristic in this case is

$$\chi\left(\Gamma \backslash \mathbf{H}^2_{\mathbb{C}}\right) = \frac{1}{2}\left(\frac{1}{2} - \frac{1}{p}\right)^2 + \frac{1}{k}\left(\frac{1}{2} - \frac{1}{p} - \frac{1}{k}\right). \tag{7.1.3}$$

Orbit of the facet	Stabiliser	Order
$\mathbf{z}_1, \mathbf{z}_2$	$\langle A_1, R_1 \rangle$	kp
$\mathbf{z}_3, \mathbf{z}_4, \mathbf{z}_5$	$\langle P^3, R_1 \rangle$	pd
$\mathbf{z}_6, \mathbf{z}_9, \mathbf{z}_{12}$	$\langle A_1', R_1 \rangle$	$2l^2$

$\gamma_{1,3}, \gamma_{2,4}$	$\langle R_1 \rangle$	p
$\gamma_{1,6}, \gamma_{2,9}$	$\langle R_1 \rangle$	p
$\gamma_{3,6}, \gamma_{5,12}, \gamma_{4,9}$	$\langle R_1 \rangle$	p
$\gamma_{2,6}, \gamma_{1,9}, \gamma_{1,12}, \gamma_{2,12}$	$\langle A_1 \rangle$	k
$\gamma_{6,9}, \gamma_{9,12}, \gamma_{6,12}$	$\langle JR_1 \rangle$	$2k$
$\gamma_{4,5}, \gamma_{3,5}, \gamma_{3,4}$	$\langle R_2 P \rangle$	$2d$
$F(P,J), \quad F(P^{-1}, J^{-1})$	A_1	k
$F(R_1, R_1^{-1})$	R_1	p
$F(R_2, R_2^{-1})$	R_2	p
$F(P,R_1), \quad F(P,R_1^{-1}), \quad F(P^{-1},R_2), \quad F(P^{-1},R_2^{-1})$	1	1
$F(J,R_1), \quad F(J,R_1^{-1}), \quad F(J^{-1},R_2), \quad F(J^{-1},R_2^{-1})$	1	1
$F(P,R_2), \quad F(R_1,R_2^{-1}), \quad F(R_1^{-1},P^{-1})$	1	1
$F(J,J^{-1})$	J	3
$F(P,P^{-1})$	P	$3d$
$S(J), S(J^{-1})$	1	1
$S(R_1), S(R_1^{-1})$	1	1
$S(R_2), S(R_2^{-1})$	1	1
$S(P), S(P^{-1})$	1	1
D	1	1

Table 7.4: The stabilisers for l negative or infinite and d positive and finite.

The orbifold Euler characteristic in this case is

$$\chi\left(\Gamma \backslash \mathbf{H}^2_{\mathbb{C}}\right) = \frac{p-5}{2p^2}. \tag{7.1.4}$$

Finally, one needs to look at the case where $k = \frac{p}{2}$ as in Section 5.6. In this case, one has $l = d$ and hence they must either be both positive or both negative. In fact, from Table 3.1 one can see that these 4-fold symmetry lattices are in the fifth class of the table, except for one which is in the first class.

Remark 7.1.1. From Section 5.6, we recall that the fundamental domain we built (and of which we calculated the volume here) contains four copies of a fundamental

domain for the group with extra symmetry. Moreover, in the respective formulae ((7.1.2) for $(5, 5/2)$ and (7.1.1) for the others) we need to substitute k with $\frac{p}{2}$ and hence t with $\frac{5}{p} - \frac{1}{2}$. Then one can see that the orbifold Euler characteristics will be

$$\chi\left(\Gamma \backslash \mathbf{H}^2_{\mathbb{C}}\right) = \frac{(p-4)^2}{8p^2} \quad \text{for } (5, 5/2) \quad \text{and} \quad \chi\left(\Gamma \backslash \mathbf{H}^2_{\mathbb{C}}\right) = \frac{p-5}{2p^2} \quad \text{for the others.}$$

We remark that all the values calculated here are coherent with the ones from Sauter (see [Sau90]). To see this, let us start by looking at the lattices of first and second type. In [Sau90], the volume is calculated in Theorems 5.1 and 5.2 respectively. The value found there is 3 times the value presented in this section. This is because Sauter calculates the volume of Ω, which is a fundamental domain for Γ modulo the subgroup generated by J, which has order 3. This is explained later in Theorem 5.1′. For Livné lattices, the volume calculated by Sauter in Theorem 5.3 is 6 times the one in this section. This is because Sauter calculates the volume of $\Gamma_\mu \backslash \mathbf{H}^2_{\mathbb{C}}$, while we are calculating the volume of $\Gamma_{\mu\Sigma} \backslash \mathbf{H}^2_{\mathbb{C}}$. This is, in fact, the value in Theorem 5.7. Similarly, for the lattices of fourth type, Sauter calculates the volume of $\Gamma_\mu \backslash \mathbf{H}^2_{\mathbb{C}}$ in Theorem 5.3 and this is 6 times the volume in this section, which is the same as the volume of $\Gamma_{\mu\Sigma} \backslash \mathbf{H}^2_{\mathbb{C}}$ calculated in Theorem 5.5 of Sauter. The values for the 4-fold symmetry case can be found in [Sau90] in Theorem 5.8 for $(5, 5/2)$ and and Theorem 5.6 for the others. Here, his value coincides with ours, since it is calculated for $\Gamma_{\mu\Sigma} \backslash \mathbf{H}^2_{\mathbb{C}}$ also in [Sau90].

In order to relate Sauter's notations to ours, one needs to consider the following information. The lattices of fourth type all have $k = 3$ and hence correspond to ball 5-tuples

$$\left(\frac{1}{2} - \frac{1}{p}, \frac{1}{2} - \frac{1}{p}, \frac{1}{2} - \frac{1}{p}, \frac{1}{6} + \frac{1}{p}, \frac{1}{3} + \frac{2}{p}\right).$$

The Livné lattices all have $k = 2$ and hence correspond to ball 5-tuples

$$\left(\frac{1}{2} - \frac{1}{p}, \frac{1}{2} - \frac{1}{p}, \frac{1}{2} - \frac{1}{p}, \frac{1}{p}, \frac{1}{2} + \frac{2}{p}\right).$$

The lattices with 4-fold symmetry correspond to ball 5-tuples

$$\left(\frac{1}{2} - \frac{1}{p}, \frac{1}{2} - \frac{1}{p}, \frac{1}{2} - \frac{1}{p}, \frac{1}{2} - \frac{1}{p}, \frac{4}{p}\right).$$

Note that Sauter presents the ball 5-tuples as having the first 3 elements to be equal, while here we have $\mu_2 = \mu_3 = \mu_4$ instead. Moreover, the condition $\mu_i + \mu_j < 1$ for all $i \neq j$ corresponds to saying that d and l are positive and finite. Moreover, the condition $\mu_4 + \mu_5 \geq 1$ in Sauter (which, in our ordering of the ball 5-tuple, translates to saying that $\mu_1 + \mu_5 \geq 1$) corresponds to saying that d is negative or infinite, while the condition $\mu_1 + \mu_5 \geq 1$ in Sauter (which, in our ordering of the ball 5-tuple, translates to saying that $\mu_2 + \mu_5 \geq 1$) corresponds to saying that l is negative. The other two conditions ($\mu_1 + \mu_2 < 1$ and $2\mu_2 < 1$ in our notation) always happen for the lattices we are considering, since p and k are positive and finite.

7.2 Volumes of polyhedra arising from lattices with 2-fold symmetry

The same tables need to be done to calculate the volume of the 2-fold symmetry lattices (see Section 3.4.2) using the polyhedron D constructed in Section 6.2.

As in Theorem 6.3.1, we will have six cases, according to which parameters are negative or infinite. Following the order in the theorem, the cases are

1. when all values are positive and finite,
2. when l' and d are negative or infinite,
3. when l and d are negative or infinite,
4. when l, l' and d are negative or infinite,
5. when k', l' and d are negative or infinite,
6. when k' is negative or infinite.

In the following tables we list the orbits of facets by dimension, calculate the stabiliser of the first element in the orbit and give its order. The first table represents Case 1. Later, we will explain how the table changes when considering the degenerations of D and write down the corresponding tables.

Case 1 contains $(4,4,6)$ and $(4,4,5)$. Its volume is calculated using the following table.

Orbit of the facet	Stabiliser	Order
$\mathbf{v}_1, \mathbf{v}_2$	$\langle A_1, B_1 \rangle$	kp
$\mathbf{v}_3, \mathbf{v}_4$	$\langle Q^2, B_1 \rangle$	pd
$\mathbf{v}_{16}, \mathbf{v}_5$	$\langle Q^2, R_0 \rangle$	$p'd$
$\mathbf{v}_6, \mathbf{v}_{10}$	$\langle R_0K, B_1 \rangle$	pl
$\mathbf{v}_7, \mathbf{v}_{11}$	$\langle R_0K, A_0 \rangle$	$k'l$
$\mathbf{v}_8, \mathbf{v}_9, \mathbf{v}_{17}, \mathbf{v}_{24}$	$\langle QK^{-1}, R_0K \rangle$	kl
$\mathbf{v}_{18}, \mathbf{v}_{14}, \mathbf{v}_{20}, \mathbf{v}_{22}, \mathbf{v}_{23}, \mathbf{v}_{12}$	$\langle A_0B_2B_1, A_1 \rangle$	$l'k$
$\mathbf{v}_{19}, \mathbf{v}_{13}, \mathbf{z}_{21}$	$\langle A_0B_2B_1, R_0 \rangle$	$p'l'$
$\mathbf{v}_0$	$\langle R_0, A_0 \rangle$	$k'p'$
$\gamma_{1,3}, \gamma_{2,4}$	$\langle B_1 \rangle$	p
$\gamma_{1,6}, \gamma_{2,10}$	$\langle B_1 \rangle$	p
$\gamma_{1,12}, \gamma_{2,23}, \gamma_{2,14}, \gamma_{1,18}$	$\langle A_1 \rangle$	k
$\gamma_{3,5}, \gamma_{4,16}, \gamma_{4,5}, \gamma_{3,16}$	$\langle Q^2 \rangle$	d
$\gamma_{3,6}, \gamma_{4,10}$	$\langle B_1 \rangle$	p
$\gamma_{5,13}, \gamma_{16,19}, \gamma_{16,21}$	$\langle R_0 \rangle$	p'
$\gamma_{6,8}, \gamma_{10,24}, \gamma_{9,10}, \gamma_{6,17}$	$\langle R_0K \rangle$	l
$\gamma_{7,8}, \gamma_{11,24}, \gamma_{9,11}, \gamma_{7,17}$	$\langle R_0K \rangle$	l
$\gamma_{7,11}$	$\langle K \rangle$	$2k'$
$\gamma_{7,15}, \gamma_{11,15}$	$\langle A_0 \rangle$	k'
$\gamma_{8,14}, \gamma_{22,24}, \gamma_{17,20}, \gamma_{9,18}, \gamma_{23,8}, \gamma_{9,12}$	$\langle A_1 \rangle$	k
$\gamma_{12,13}, \gamma_{21,22}, \gamma_{18,19}, \gamma_{21,23}, \gamma_{19,20}, \gamma_{13,14}$	$\langle B_1A_0B_2 \rangle$	l'
$\gamma_{12,14}, \gamma_{22,23}, \gamma_{18,20}$	$\langle B_2^{-1}K \rangle$	$2l'$
$\gamma_{15,19}, \gamma_{15,21}$	$\langle R_0 \rangle$	p'
$F(K,Q), \quad F(K^{-1},Q^{-1})$	$\langle A_1 \rangle$	k
$F(K^{-1},R_0), \quad F(K,R_0^{-1})$	$\langle KR_0 \rangle$	l
$F(R_0,R_0^{-1})$	$\langle R_0 \rangle$	p'
$F(Q,Q^{-1})$	$\rangle Q \langle$	$2d$
$F(B_1,A_0^{-1}), \quad F(B_1^{-1},B_2), \quad F(B_2^{-1},A_0)$	$\langle A_0B_2B_1 \rangle$	l'

$F(B_1, B_1^{-1})$	$\langle B_1 \rangle$	p
$F(B_2, B_2^{-1})$	$\langle B_2 \rangle$	p
$F(A_0, A_0^{-1})$	$\langle A_1' \rangle$	k'
$F(K, B_1), \quad F(K, B_1^{-1}), \quad F(K^{-1}, B_2^{-1}), \quad F(K^{-1}, B_2)$	1	1
$F(B_1, Q), \quad F(B_2, Q^{-1}), \quad F(B_2^{-1}, Q^{-1}), \quad F(B_1^{-1}, Q)$	1	1
$F(A_0, R_0), \quad F(A_0^{-1}, R_0), \quad F(A_0^{-1}, R_0^{-1}), \quad F(A_0, R_0^{-1})$	1	1
$F(K, K^{-1}), \quad F(K^{-1}, A_0), \quad F(K, A_0^{-1})$	1	1
$F(B_1, R_0^{-1}), \quad F(B_1^{-1}, Q^{-1}), \quad F(Q, R_0)$	1	1
$F(R_0^{-1}, Q^{-1}), \quad F(Q, B_2), \quad F(B_2^{-1}, R_0)$	1	1
$S(K), S(K^{-1})$	1	1
$S(Q), S(Q^{-1})$	1	1
$S(B_2), S(B_2^{-1})$	1	1
$S(B_1), S(B_1^{-1})$	1	1
$S(R_0), S(R_0^{-1})$	1	1
$S(A_0), S(A_0^{-1})$	1	1
D	1	1

Table 7.5: The stabilisers when all values are positive and finite.

Then the orbifold Euler characteristic of D is given by

$$\chi\left(\Gamma\backslash\mathbf{H}^2_{\mathbb{C}}\right) = \frac{1}{kp} + \frac{1}{pd} + \frac{1}{dp'} + \frac{1}{pl} + \frac{1}{k'l} + \frac{1}{kl} + \frac{1}{l'k} + \frac{1}{p'l'} + \frac{1}{k'p'} - \frac{1}{2d} - \frac{1}{p} - \frac{1}{l} - \frac{1}{2k'} - \frac{1}{k} - \frac{1}{2l'} - \frac{1}{p'} + 1 \tag{7.2.1}$$

and the volume is $\frac{8\pi^2}{3}\chi\left(\Gamma\backslash\mathbf{H}^2_{\mathbb{C}}\right)$.

While it is easy to see that the stabiliser of each facet contains the group in the second column of the table, the converse inclusion requires slightly more work and follows from the cycles in the Poincaré polyhedron theorem. More specifically, to find the stabiliser, one needs to consider all the cycle transformations of the cycles and keep track of each facet. For example, let us try to find the stabiliser of $\mathbf{v}_1$. Examining the action of the side pairings, one can see that the only other vertex

in the orbit of $\mathbf{v}_1$ is $\mathbf{v}_2$. The parts of cycles involving this orbit give the following graph.

$$B_1 \circlearrowright \mathbf{v}_1 \underset{J'}{\overset{P'}{\rightrightarrows}} \mathbf{v}_2 \circlearrowright B_2$$

Then one considers all the transformations inside cycles that stabilise the facet. In the example, one has B_1, $P'^{-1}J'$ and $P'^{-1}B_2J'$, with their compositions, inverses and powers. Now one needs to find the map or maps that generate all these maps. Here, since $P'^{-1}J' = A_1$ and $P'^{-1}B_2J' = B_1A_1$, B_1 and A_1 generate all the maps. Since the cycles are composed of side pairings, which are generators for the group, the Poincaré polyhedron theorem guarantees that all the maps in the stabiliser belong to this group and so in the example the stabiliser is exactly $\langle B_1, A_1\rangle$. All the other stabilisers can be found using the same procedure.

Now we need to explain how to modify the table when calculating the orbifold Euler characteristic for one of the degenerations of D.

- First consider the case when d is negative or infinite. Then the vertices $\mathbf{v}_3$, $\mathbf{v}_4$, $\mathbf{v}_5$ and $\mathbf{v}_{16}$ collapse to a single point. This means that the two orbits containing them will collapse to only one orbit. The new vertex is stabilised by $\langle B_1, R_0\rangle$ and we need to calculate its order. This is similar to the proof of Proposition 2.3 of [DPP] (adapting the argument to complex reflections with different orders) and to the proof of 4.4, 4.5 and 4.6 in [Par09]. Now, R_0 has eigenvalues $e^{i\theta'}, 1, 1$, while B_1 has eigenvalues $e^{2i\theta}, 1, 1$. In other words, remembering $\theta' = \frac{2\pi}{p'}$ and $\theta = \frac{\pi}{p}$, R_0 and B_1 have eigenvalues $e^{2i\pi/p'}, 1, 1$ and $e^{2i\pi/p}, 1, 1$ respectively. Now consider B_1R_0. It has eigenvalues $1, e^{i(\alpha+\theta)}, -e^{i(\alpha+\theta)}$, which we can write as $1, e^{i(\frac{\pi}{p'}+\frac{\pi}{p}+\frac{\pi}{2})}, e^{i(\frac{\pi}{p'}+\frac{\pi}{p}-\frac{\pi}{2})}$ because $\theta' = 2\alpha - \pi$. In this way the part acting on the sphere orthogonal to the common eigenspace is in $SU(2)$. This means that $\langle R_0, B_1\rangle$ is a central extension of a $(2, p, p')$-triangle group. Recalling that a $(2, a, b)$-triangle group has order $\frac{4ab}{2a+2b-ab}$ and that the parameters are defined by (6.0.1), the order of the triangle group is $-2d$. Since $\pi - \alpha - \theta = \frac{\pi}{d}$, the eigenvalues of $(R_0A_1)^2$ are $e^{\frac{2\pi}{d}}, e^{\frac{2\pi}{d}}, 1$ and hence the order of the centre is $-d$. Therefore the order of the stabiliser is $2d^2$. Moreover, the line of the table corresponding to the edges between these three points (so the line of

the orbit of $\gamma_{3,5}$) needs to be eliminated and so does the line corresponding to the ridge $F(Q, Q^{-1})$.

- Now consider the case of l' negative or infinite. We have three triples of vertices collapsing to the three vertices $\mathbf{v}_{12}$, $\mathbf{v}_{18}$ and $\mathbf{v}_{21}$, where $\mathbf{v}_i$, $\mathbf{v}_j$ and $\mathbf{v}_k$ are said to collapse to $\mathbf{v}_i$. They are in a unique orbit and $\mathbf{v}_{18}$ is stabilised by $\langle R_0, Q^{-1}K\rangle = \langle R_0, A_1\rangle$. We need to calculate its order. Now, R_0 has eigenvalues $e^{i\theta'}, 1, 1$, while A_1 has eigenvalues $e^{2i\varphi}, 1, 1$. In other words, remembering $\theta' = \frac{2\pi}{p'}$ and $\varphi = \frac{\pi}{k}$, R_0 and A_1 have eigenvalues $e^{2i\pi/p'}, 1, 1$ and $e^{2i\pi/k}, 1, 1$ respectively. Now consider R_0A_1. It has eigenvalues $1, e^{i(\alpha+\varphi)}, -e^{i(\alpha+\varphi)}$, which we can write as $1, e^{i(\frac{\pi}{p'}+\frac{\pi}{k}+\frac{\pi}{2})}, e^{i(\frac{\pi}{p'}+\frac{\pi}{k}-\frac{\pi}{2})}$. This means that $\langle R_0, A_1\rangle$ is a central extension of a $(2, p', k)$-triangle group, which has order $\frac{4p'k}{2p'+2k-p'k} = -2l'$. Since $\alpha + \varphi - \pi = \frac{\pi}{l'}$, the eigenvalues of $(R_0A_1)^2$ are $e^{\frac{2\pi}{l'}}, e^{\frac{2\pi}{l'}}, 1$ and hence the order of the centre is $-l'$. This means that the order of $\langle R_0, A_1\rangle$ is $2l'^2$. Moreover, the two lines of the table corresponding to edges between the three collapsing points need to be eliminated. In other words, the lines of the orbits of $\gamma_{12,13}$ and $\gamma_{12,14}$ disappear from the table, together with the orbit of the three ridges that collapse.

- Now let us consider the parameter l. From Table 3.3 one can see that it is never negative. Hence the only degeneration comes when it is infinite. This means that the two vertices obtained by triples collapsing are on the boundary and hence their stabilisers have infinite order. Hence the orbit of these vertices disappears in the calculation of the orbifold Euler characteristic. Similarly, the two orbits of edges between collapsing vertices disappear from the calculation (the orbits of $\gamma_{6,8}$ and $\gamma_{7,8}$) and so does the orbit containing the two ridges that collapse to the two new boundary points.

- When k' is negative, the vertices $\mathbf{v}_0$, $\mathbf{v}_7$ and $\mathbf{v}_{11}$ collapse to a single point $\mathbf{v}_0$ (see Section 6.3.3). This means that the two orbits of these three points collapse to a single one. It is easy to see that the new point is stabilised by K, A_0 and R_0, so the stabiliser is $\langle R_0, K\rangle$. We now need to calculate the order of this group. Since $K^2 = A_0^{-1}$ and A_0 commutes with R_0, the centre is generated by K^2, which has order $-k'$. Now, we know that R_0K

has order l, so $\langle R_0, K\rangle$ modulo the centre is a $(2, p', l)$-triangle group, which has order $-2k'$. Therefore the order of $\langle R_0, K\rangle$ is $2k'^2$. Moreover, the lines of the table corresponding to the two orbits of edges between these three points (i.e. the orbit of $\gamma_{7,11}$ and $\gamma_{7,0}$) disappear in the calculation and so does the line relative to $F(A_0, A_0^{-1})$.

Below are the tables obtained modifying Table 7.5 in this way.

Case 2 contains $(3,4,4)$, $(2,4,3)$ and $(3,3,4)$ and their volumes are calculated using the following table.

Orbit of the facet	Stabiliser	Order
$\mathbf{v}_1, \mathbf{v}_2$	$\langle A_1, B_1\rangle$	kp
$\mathbf{v}_3$	$\langle R_0, B_1\rangle$	$2d^2$
$\mathbf{v}_6, \mathbf{v}_{10}$	$\langle R_0K, B_1\rangle$	pl
$\mathbf{v}_7, \mathbf{v}_{11}$	$\langle R_0K, A_0\rangle$	$k'l$
$\mathbf{v}_8, \mathbf{v}_9, \mathbf{v}_{17}, \mathbf{v}_{24}$	$\langle KA_1K^{-1}, R_0K\rangle$	kl
$\mathbf{v}_{18}, \mathbf{v}_{12}, \mathbf{z}_{21}$	$\langle A_1, R_0\rangle$	$2l'^2$
$\mathbf{v}_0$	$\langle R_0, A_0\rangle$	$k'p'$
$\gamma_{1,3}, \gamma_{2,3}$	$\langle B_1\rangle$	p
$\gamma_{1,6}, \gamma_{2,10}$	$\langle B_1\rangle$	p
$\gamma_{1,12}, \gamma_{2,21}, \gamma_{2,12}, \gamma_{1,18}$	$\langle A_1\rangle$	k
$\gamma_{3,6}, \gamma_{3,10}$	$\langle B_1\rangle$	p
$\gamma_{3,12}, \gamma_{3,18}, \gamma_{3,21}$	$\langle R_0\rangle$	p'
$\gamma_{6,8}, \gamma_{10,24}, \gamma_{9,10}, \gamma_{6,17}$	$\langle R_0K\rangle$	l
$\gamma_{7,8}, \gamma_{11,24}, \gamma_{9,11}, \gamma_{7,17}$	$\langle R_0K\rangle$	l
$\gamma_{7,11}$	$\langle K\rangle$	$2k'$
$\gamma_{7,15}, \gamma_{11,15}$	$\langle A_0\rangle$	k'
$\gamma_{8,12}, \gamma_{21,24}, \gamma_{17,18}, \gamma_{9,18}, \gamma_{21,8}, \gamma_{9,12}$	$\langle A_1\rangle$	k
$\gamma_{15,18}, \gamma_{15,21}$	$\langle R_0\rangle$	p'
$F(K, Q), \quad F(K^{-1}, Q^{-1})$	A_1	k
$F(K^{-1}, R_0), \quad F(K, R_0^{-1})$	KR_0	l
$F(R_0, R_0^{-1})$	R_0	p'
$F(B_1, B_1^{-1})$	B_1	p

$F(B_2, B_2^{-1})$	B_2	p
$F(A_0, A_0^{-1})$	A_1'	k'
$F(K, B_1), \quad F(K, B_1^{-1}), \quad F(K^{-1}, B_2^{-1}), \quad F(K^{-1}, B_2)$	1	1
$F(B_1, Q), \quad F(B_2, Q^{-1}), \quad F(B_2^{-1}, Q^{-1}), \quad F(B_1^{-1}, Q)$	1	1
$F(A_0, R_0), \quad F(A_0^{-1}, R_0), \quad F(A_0^{-1}, R_0^{-1}), \quad F(A_0, R_0^{-1})$	1	1
$F(K, K^{-1}), \quad F(K^{-1}, A_0), \quad F(K, A_0^{-1})$	1	1
$F(B_1, R_0^{-1}), \quad F(B_1^{-1}, Q^{-1}), \quad F(Q, R_0)$	1	1
$F(R_0^{-1}, Q^{-1}), \quad F(Q, B_2), \quad F(B_2^{-1}, R_0)$	1	1
$S(K), S(K^{-1})$	1	1
$S(Q), S(Q^{-1})$	1	1
$S(B_2), S(B_2^{-1})$	1	1
$S(B_1), S(B_1^{-1})$	1	1
$S(R_0), S(R_0^{-1})$	1	1
$S(A_0), S(A_0^{-1})$	1	1
D	1	1

Table 7.6: The stabilisers for l' and d negative or infinite.

Then the orbifold Euler characteristic of D is given by

$$\chi\left(\Gamma\backslash\mathbf{H}^2_{\mathbb{C}}\right) = \frac{1}{kp} + \frac{1}{2d^2} + \frac{1}{pl} + \frac{1}{k'l} + \frac{1}{kl} + \frac{1}{2l'^2} + \frac{1}{k'p'} - \frac{1}{k} - \frac{1}{p} - \frac{1}{p'} - \frac{1}{l} - \frac{1}{2k'} + 1. \tag{7.2.2}$$

Case 3 contains $(2, 6, 6)$ and its volume is calculated using the following table.

Orbit of the facet	Stabiliser	Order
$\mathbf{v}_1, \mathbf{v}_2$	$\langle A_1, B_1 \rangle$	kp
$\mathbf{v}_3, \mathbf{v}_4$	$\langle R_0, B_1 \rangle$	$2d^2$
$\mathbf{v}_6, \mathbf{v}_9$	$\langle A_0, A_1, B_1 \rangle$	∞
$\mathbf{v}_{18}, \mathbf{v}_{14}, \mathbf{v}_{20}, \mathbf{v}_{22}, \mathbf{v}_{23}, \mathbf{v}_{12}$	$\langle A_0 B_2 B_1, A_1 \rangle$	$l'k$
$\mathbf{v}_{19}, \mathbf{v}_{13}, \mathbf{z}_{21}$	$\langle A_0 B_2 B_1, R_0 \rangle$	$p'l'$
$\mathbf{v}_0$	$\langle R_0, A_0 \rangle$	$k'p'$
$\gamma_{1,3}, \gamma_{2,3}$	$\langle B_1 \rangle$	p

$\gamma_{1,6}, \gamma_{2,9}$	$\langle B_1 \rangle$	p
$\gamma_{1,12}, \gamma_{2,23}, \gamma_{2,14}, \gamma_{1,18}$	$\langle A_1 \rangle$	k
$\gamma_{3,6}, \gamma_{3,9}$	$\langle B_1 \rangle$	p
$\gamma_{5,13}, \gamma_{16,19}, \gamma_{16,21}$	$\langle R_0 \rangle$	p'
$\gamma_{6,9}$	$\langle K \rangle$	$2k'$
$\gamma_{6,15}, \gamma_{9,15}$	$\langle A_0 \rangle$	k'
$\gamma_{6,14}, \gamma_{22,9}, \gamma_{6,20}, \gamma_{9,18}, \gamma_{23,8}, \gamma_{9,12}$	$\langle A_1 \rangle$	k
$\gamma_{12,13}, \gamma_{21,22}, \gamma_{18,19}, \gamma_{21,23}, \gamma_{19,20}, \gamma_{13,14}$	$\langle B_1 A_0 B_2 \rangle$	l'
$\gamma_{12,14}, \gamma_{22,23}, \gamma_{18,20}$	$\langle B_2^{-1} K \rangle$	$2l'$
$\gamma_{15,19}, \gamma_{15,21}$	$\langle R_0 \rangle$	p'
$F(K,Q), \quad F(K^{-1},Q^{-1})$	A_1	k
$F(R_0, R_0^{-1})$	R_0	p'
$F(B_1, A_0^{-1}), \quad F(B_1^{-1}, B_2), \quad F(B_2^{-1}, A_0)$	$A_0 B_2 B_1$	l'
$F(B_1, B_1^{-1})$	B_1	p
$F(B_2, B_2^{-1})$	B_2	p
$F(A_0, A_0^{-1})$	A_1'	k'
$F(K, B_1), \quad F(K, B_1^{-1}), \quad F(K^{-1}, B_2^{-1}), \quad F(K^{-1}, B_2)$	1	1
$F(B_1, Q), \quad F(B_2, Q^{-1}), \quad F(B_2^{-1}, Q^{-1}), \quad F(B_1^{-1}, Q)$	1	1
$F(A_0, R_0), \quad F(A_0^{-1}, R_0), \quad F(A_0^{-1}, R_0^{-1}), \quad F(A_0, R_0^{-1})$	1	1
$F(K, K^{-1}), \quad F(K^{-1}, A_0), \quad F(K, A_0^{-1})$	1	1
$F(B_1, R_0^{-1}), \quad F(B_1^{-1}, Q^{-1}), \quad F(Q, R_0)$	1	1
$F(R_0^{-1}, Q^{-1}), \quad F(Q, B_2), \quad F(B_2^{-1}, R_0)$	1	1
$S(K), S(K^{-1})$	1	1
$S(Q), S(Q^{-1})$	1	1
$S(B_2), S(B_2^{-1})$	1	1
$S(B_1), S(B_1^{-1})$	1	1
$S(R_0), S(R_0^{-1})$	1	1
$S(A_0), S(A_0^{-1})$	1	1
D	1	1

Table 7.7: The stabilisers when l and d are negative or infinite.

Then the orbifold Euler characteristic of D is given by

$$\chi\left(\Gamma\backslash\mathbf{H}^2_{\mathbb{C}}\right) = \frac{1}{kp} + \frac{1}{2d^2} + \frac{1}{l'k} + \frac{1}{p'l'} + \frac{1}{k'p'} - \frac{1}{k} - \frac{1}{p} - \frac{1}{p'} - \frac{1}{2k'} - \frac{1}{2l'} + 1. \tag{7.2.3}$$

Case 4 contains $(2,3,3)$ and its volume is calculated using the following table.

Orbit of the facet	Stabiliser	Order
$\mathbf{v}_1, \mathbf{v}_2$	$\langle A_1, B_1\rangle$	kp
$\mathbf{v}_3$	$\langle R_0, B_1\rangle$	$2d^2$
$\mathbf{v}_6, \mathbf{v}_9$	$\langle A_0, A_1, B_1\rangle$	∞
$\mathbf{v}_{18}, \mathbf{v}_{12}, \mathbf{v}_{21}$	$\langle R_0, A_1\rangle$	$2l'^2$
$\mathbf{v}_0$	$\langle R_0, A_0\rangle$	$k'p'$
$\gamma_{1,3}, \gamma_{2,3}$	$\langle B_1\rangle$	p
$\gamma_{1,6}, \gamma_{2,10}$	$\langle B_1\rangle$	p
$\gamma_{1,12}, \gamma_{2,21}, \gamma_{2,12}, \gamma_{1,18}$	$\langle A_1\rangle$	k
$\gamma_{3,6}, \gamma_{3,9}$	$\langle B_1\rangle$	p
$\gamma_{3,12}, \gamma_{3,18}, \gamma_{3,20}$	$\langle R_0\rangle$	p'
$\gamma_{6,9}$	$\langle K\rangle$	$2k'$
$\gamma_{6,15}, \gamma_{9,15}$	$\langle A_0\rangle$	k'
$\gamma_{6,12}, \gamma_{21,9}, \gamma_{6,18}, \gamma_{9,18}, \gamma_{21,6}, \gamma_{9,12}$	$\langle A_1\rangle$	k
$\gamma_{15,19}, \gamma_{15,21}$	$\langle R_0\rangle$	p'
$F(K,Q), \quad F(K^{-1},Q^{-1})$	A_1	k
$F(R_0,R_0^{-1})$	R_0	p'
$F(B_1,B_1^{-1})$	B_1	p
$F(B_2,B_2^{-1})$	B_2	p
$F(A_0,A_0^{-1})$	A_1'	k'
$F(K,B_1), \quad F(K,B_1^{-1}), \quad F(K^{-1},B_2^{-1}), \quad F(K^{-1},B_2)$	1	1
$F(B_1,Q), \quad F(B_2,Q^{-1}), \quad F(B_2^{-1},Q^{-1}), \quad F(B_1^{-1},Q)$	1	1
$F(A_0,R_0), \quad F(A_0^{-1},R_0), \quad F(A_0^{-1},R_0^{-1}), \quad F(A_0,R_0^{-1})$	1	1
$F(K,K^{-1}), \quad F(K^{-1},A_0), \quad F(K,A_0^{-1})$	1	1
$F(B_1,R_0^{-1}), \quad F(B_1^{-1},Q^{-1}), \quad F(Q,R_0)$	1	1
$F(R_0^{-1},Q^{-1}), \quad F(Q,B_2), \quad F(B_2^{-1},R_0)$	1	1

$S(K), S(K^{-1})$	1	1
$S(Q), S(Q^{-1})$	1	1
$S(B_2), S(B_2^{-1})$	1	1
$S(B_1), S(B_1^{-1})$	1	1
$S(R_0), S(R_0^{-1})$	1	1
$S(A_0), S(A_0^{-1})$	1	1
D	1	1

Table 7.8: The stabilisers when l, l' and d are negative or infinite.

Then the orbifold Euler characteristic of D is given by

$$\chi\left(\Gamma\backslash\mathbf{H}^2_{\mathbb{C}}\right) = \frac{1}{kp} + \frac{1}{2d^2} + \frac{1}{2l'^2} + \frac{1}{k'p'} - \frac{1}{p} - \frac{1}{2k'} - \frac{1}{k} - \frac{1}{p'} + 1. \tag{7.2.4}$$

Case 5 contains $(3,6,3)$, $(4,4,3)$ and $(6,6,3)$ and their volumes are calculated using the following table.

Orbit of the facet	Stabiliser	Order
$\mathbf{v}_1, \mathbf{v}_2$	$\langle A_1, B_1\rangle$	kp
$\mathbf{v}_3$	$\langle R_0, B_1\rangle$	$2d^2$
$\mathbf{v}_6, \mathbf{v}_{10}$	$\langle R_0K, B_1\rangle$	pl
$\mathbf{v}_8, \mathbf{v}_9, \mathbf{v}_{17}, \mathbf{v}_{24}$	$\langle KA_1K^{-1}, R_0K\rangle$	kl
$\mathbf{v}_{18}, \mathbf{v}_{12}, \mathbf{z}_{21}$	$\langle A_1, R_0\rangle$	$2l'^2$
$\mathbf{v}_0$	$\langle R_0, K\rangle$	$2k'^2$
$\gamma_{1,3}, \gamma_{2,3}$	$\langle B_1\rangle$	p
$\gamma_{1,6}, \gamma_{2,10}$	$\langle B_1\rangle$	p
$\gamma_{1,12}, \gamma_{2,21}, \gamma_{2,12}, \gamma_{1,18}$	$\langle A_1\rangle$	k
$\gamma_{3,6}, \gamma_{3,10}$	$\langle B_1\rangle$	p
$\gamma_{3,12}, \gamma_{3,18}, \gamma_{3,21}$	$\langle R_0\rangle$	p'
$\gamma_{6,8}, \gamma_{10,24}, \gamma_{9,10}, \gamma_{6,17}$	$\langle R_0K\rangle$	l
$\gamma_{7,8}, \gamma_{11,24}, \gamma_{9,11}, \gamma_{7,17}$	$\langle R_0K\rangle$	l

$\gamma_{8,12}, \gamma_{21,24}, \gamma_{17,18}, \gamma_{9,18}, \gamma_{21,8}, \gamma_{9,12}$ $\gamma_{15,18}, \gamma_{15,21}$	$\langle A_1 \rangle$ $\langle R_0 \rangle$	k p'
$F(K,Q), \quad F(K^{-1},Q^{-1})$	A_1	k
$F(K^{-1},R_0), \quad F(K,R_0^{-1})$	KR_0	l
$F(R_0,R_0^{-1})$	R_0	p'
$F(B_1,B_1^{-1})$	B_1	p
$F(B_2,B_2^{-1})$	B_2	p
$F(K,B_1), \quad F(K,B_1^{-1}), \quad F(K^{-1},B_2^{-1}), \quad F(K^{-1},B_2)$	1	1
$F(B_1,Q), \quad F(B_2,Q^{-1}), \quad F(B_2^{-1},Q^{-1}), \quad F(B_1^{-1},Q)$	1	1
$F(A_0,R_0), \quad F(A_0^{-1},R_0), \quad F(A_0^{-1},R_0^{-1}), \quad F(A_0,R_0^{-1})$	1	1
$F(K,K^{-1}), \quad F(K^{-1},A_0), \quad F(K,A_0^{-1})$	1	1
$F(B_1,R_0^{-1}), \quad F(B_1^{-1},Q^{-1}), \quad F(Q,R_0)$	1	1
$F(R_0^{-1},Q^{-1}), \quad F(Q,B_2), \quad F(B_2^{-1},R_0)$	1	1
$S(K), S(K^{-1})$	1	1
$S(Q), S(Q^{-1})$	1	1
$S(B_2), S(B_2^{-1})$	1	1
$S(B_1), S(B_1^{-1})$	1	1
$S(R_0), S(R_0^{-1})$	1	1
$S(A_0), S(A_0^{-1})$	1	1
D	1	1

Table 7.9: The stabilisers for k', l' and d negative or infinite.

Then the orbifold Euler characteristic of D is given by

$$\chi\left(\Gamma\backslash\mathbf{H}^2_{\mathbb{C}}\right) = \frac{1}{kp} + \frac{1}{2d^2} + \frac{1}{pl} + \frac{1}{kl} + \frac{1}{2l'^2} + \frac{1}{2k'^2} - \frac{1}{k} - \frac{1}{p} - \frac{1}{p'} - \frac{1}{l} + 1. \tag{7.2.5}$$

Similarly, Case 6 contains lattices $(18,18,9)$, $(12,12,6)$ and $(10,10,5)$ and their volumes are calculated using the following table.

Orbit of the facet	Stabiliser	Order
$\mathbf{v}_1, \mathbf{v}_2$	$\langle A_1, B_1 \rangle$	kp
$\mathbf{v}_3, \mathbf{v}_4$	$\langle Q^2, B_1 \rangle$	pd
$\mathbf{v}_{16}, \mathbf{v}_5$	$\langle Q^2, R_0 \rangle$	$p'd$
$\mathbf{v}_6, \mathbf{v}_{10}$	$\langle R_0 K, B_1 \rangle$	pl
$\mathbf{v}_8, \mathbf{v}_9, \mathbf{v}_{17}, \mathbf{v}_{24}$	$\langle QK^{-1}, R_0 K \rangle$	kl
$\mathbf{v}_{18}, \mathbf{v}_{14}, \mathbf{v}_{20}, \mathbf{v}_{22}, \mathbf{v}_{23}, \mathbf{v}_{12}$	$\langle A_0 B_2 B_1, A_1 \rangle$	$l'k$
$\mathbf{v}_{19}, \mathbf{v}_{13}, \mathbf{z}_{21}$	$\langle A_0 B_2 B_1, R_0 \rangle$	$p'l'$
$\mathbf{v}_0$	$\langle R_0, K \rangle$	$2k'^2$
$\gamma_{1,3}, \gamma_{2,4}$	$\langle B_1 \rangle$	p
$\gamma_{1,6}, \gamma_{2,10}$	$\langle B_1 \rangle$	p
$\gamma_{1,12}, \gamma_{2,23}, \gamma_{2,14}, \gamma_{1,18}$	$\langle A_1 \rangle$	k
$\gamma_{3,5}, \gamma_{4,16}, \gamma_{4,5}, \gamma_{3,16}$	$\langle Q^2 \rangle$	d
$\gamma_{3,6}, \gamma_{4,10}$	$\langle B_1 \rangle$	p
$\gamma_{5,13}, \gamma_{16,19}, \gamma_{16,21}$	$\langle R_0 \rangle$	p'
$\gamma_{6,8}, \gamma_{10,24}, \gamma_{9,10}, \gamma_{6,17}$	$\langle R_0 K \rangle$	l
$\gamma_{7,8}, \gamma_{11,24}, \gamma_{9,11}, \gamma_{7,17}$	$\langle R_0 K \rangle$	l
$\gamma_{8,14}, \gamma_{22,24}, \gamma_{17,20}, \gamma_{9,18}, \gamma_{23,8}, \gamma_{9,12}$	$\langle A_1 \rangle$	k
$\gamma_{12,13}, \gamma_{21,22}, \gamma_{18,19}, \gamma_{21,23}, \gamma_{19,20}, \gamma_{13,14}$	$\langle B_1 A_0 B_2 \rangle$	l'
$\gamma_{12,14}, \gamma_{22,23}, \gamma_{18,20}$	$\langle B_2^{-1} K \rangle$	$2l'$
$\gamma_{15,19}, \gamma_{15,21}$	$\langle R_0 \rangle$	p'
$F(K, Q), \quad F(K^{-1}, Q^{-1})$	A_1	k
$F(K^{-1}, R_0), \quad F(K, R_0^{-1})$	KR_0	l
$F(R_0, R_0^{-1})$	R_0	p'
$F(Q, Q^{-1})$	Q	$2d$
$F(B_1, A_0^{-1}), \quad F(B_1^{-1}, B_2), \quad F(B_2^{-1}, A_0)$	$A_0 B_2 B_1$	l'
$F(B_1, B_1^{-1})$	B_1	p
$F(B_2, B_2^{-1})$	B_2	p
$F(K, B_1), \quad F(K, B_1^{-1}), \quad F(K^{-1}, B_2^{-1}), \quad F(K^{-1}, B_2)$	1	1
$F(B_1, Q), \quad F(B_2, Q^{-1}), \quad F(B_2^{-1}, Q^{-1}), \quad F(B_1^{-1}, Q)$	1	1

$F(A_0, R_0), \quad F(A_0^{-1}, R_0), \quad F(A_0^{-1}, R_0^{-1}), \quad F(A_0, R_0^{-1})$	1	1
$F(K, K^{-1}), \quad F(K^{-1}, A_0), \quad F(K, A_0^{-1})$	1	1
$F(B_1, R_0^{-1}), \quad F(B_1^{-1}, Q^{-1}), \quad F(Q, R_0)$	1	1
$F(R_0^{-1}, Q^{-1}), \quad F(Q, B_2), \quad F(B_2^{-1}, R_0)$	1	1
$S(K), S(K^{-1})$	1	1
$S(Q), S(Q^{-1})$	1	1
$S(B_2), S(B_2^{-1})$	1	1
$S(B_1), S(B_1^{-1})$	1	1
$S(R_0), S(R_0^{-1})$	1	1
$S(A_0), S(A_0^{-1})$	1	1
D	1	1

Table 7.10: The stabilisers when k' is negative or infinite.

Then the orbifold Euler characteristic of D is given by

$$\chi\left(\Gamma\backslash\mathbf{H}^2_{\mathbb{C}}\right) = \frac{1}{kp} + \frac{1}{pd} + \frac{1}{dp'} + \frac{1}{pl} + \frac{1}{2k'^2} + \frac{1}{kl} + \frac{1}{l'k} + \frac{1}{p'l'} - \frac{1}{k} - \frac{1}{2d} - \frac{1}{p} - \frac{1}{p'} - \frac{1}{l} - \frac{1}{2l'} + 1. \tag{7.2.6}$$

Remark 7.2.1. We remark that the calculation of the Euler orbifold characteristic is done for lattices with 2-fold symmetry but forgetting that some of them have 2-2-fold symmetry. These are the lattices in the first class of Table 3.2. In other words, we are calculating the volume of $\Gamma_{\mu\Sigma_1}$, with $\Sigma_1 = \langle(3,4)\rangle \cong \mathbb{Z}_2$, rather than $\Gamma_{\mu\Sigma_2}$, with $\Sigma_2 = \langle(1,2),(3,4)\rangle \cong \mathbb{Z}_2 \times \mathbb{Z}_2$, which is the full symmetry group of the ball 5-tuple. When we have the extra symmetry, our polyhedron will contain two copies of a fundamental domain for the lattices (see Remark 7.1.1 for a similar discussion). The Euler orbifold characteristic of the fundamental domain for $\Gamma_{\mu\Sigma}$, with Σ being the full symmetry group of the ball 5-tuple as usual, will hence be half the one found with the formulae.

7.3 Commensurability and volumes

In Section 3.5 we reproduced some commensurability theorems given by Sauter in [Sau90] and by Deligne and Mostow in [DM93] (that can be also found in [Par09]), together with a commensurability theorem from [DPP]. Here we will show how the volumes found in the previous sections of this chapter are coherent with the theorems. We will only explain the commensurability relations involving 2-fold symmetry lattices in detail, since the others can be found in the final pages of [Sau90]. At the end of this section we will give a full table summarising all the commensurability theorems known between the lattices that we are treating, including the 3-fold symmetry ones.

Each of the following tables is obtained using one of the theorems in Section 3.5. On the right hand side and on the left hand side of the vertical line one can find the pair of lattices that are commensurable. We will identify the lattice by using the parameters (p, k) for 3-fold lattices and the parameters (p, k, p') for the 2-fold symmetry ones, as usual. Moreover, in the two central columns, we will give the value of the orbifold Euler characteristic χ, as calculated with the formulae in the first sections of this chapter. Then it will be clear that the values exactly differ only by the index of commensurability.

From Theorem 3.5.1 we get the following isomorphisms

Lattice	χ	χ	Lattice
(2,6,6)	$\frac{1}{2^3}$	$\frac{1}{3\cdot 2^2}$	(6,6)
(2,3,3)	$\frac{1}{3\cdot 2^3}$	$\frac{1}{3\cdot 2^2}$	(3,6,3)
(2,4,3)	$\frac{7}{2^5\cdot 3}$	$\frac{7}{2^4\cdot 3}$	(3,3,4)

Note that it looks like the χ's do not coincide. For the 2-2-fold symmetry case, this is because the isomorphism in the theorem keeps into account the 2-2-fold symmetry, while, as mentioned in Remark 7.2.1, our formulae only consider the 2-fold symmetry. This gives the extra factor of 2.

For the case on the first line of the table, Theorem 3.5.1 considers $(a, a, b, b, 2-2a-2b)$. However, $(6, 6)$ *also* has a 3-fold symmetry. Meanwhile, our calculation ignores that the ball 5-tuple also has a 4-fold symmetry. In other words, the

factor of 3 comes from Theorem 3.5.1 ignoring the 3-fold symmetry that arises when $a = b$ and the factor of 2 comes from the fact that we ignore the extra symmetry given by $a = b$ (i.e. by the 4-fold symmetry).

From Corollary 3.5.2 one gets the following commensurability:

Lattice	χ	χ	Lattice
(6,6,3)	$\frac{1}{3\cdot 2^3}$	$\frac{1}{3^2\cdot 2^3}$	(6,2)
(10,10,5)	$\frac{3}{2^3\cdot 5}$	$\frac{1}{2^3\cdot 5}$	(10,2)
(12,12,6)	$\frac{7}{2^5\cdot 3}$	$\frac{7}{2^5\cdot 3^2}$	(12,2)
(18,18,9)	$\frac{13}{2^3\cdot 3^3}$	$\frac{13}{2^3\cdot 3^4}$	(18,2)

These have index 3 because the theorem from which we deduced the corollary does not take into account the 3-fold symmetry (see above). The value of p to use in the corollary is indeed the p in (p, k) and in (p, k, p').

Similarly, from Corollary 3.5.3 one gets the following commensurability:

Lattice	χ	χ	Lattice
(4,4,3)	$\frac{1}{3\cdot 2^3}$	$\frac{1}{3^2\cdot 2^3}$	(4,3)
(4,4,5)	$\frac{11\cdot 3^2}{2^5\cdot 5^2}$	$\frac{11\cdot 3}{2^5\cdot 5^2}$	(4,5)
(4,4,6)	$\frac{13}{2^5\cdot 3}$	$\frac{13}{2^5\cdot 3^2}$	(4,6)

The value of k to use in the corollary is indeed the k in (p, k) (which is equal to the k' in (p, k, p')).

From Proposition 3.5.5 and recalling that the lattice associated to the ball 5-tuple $\mu = (3, 3, 5, 6, 7)/12$ is the one we called $(3, 4, 4)$, one gets the following commensurability:

Lattice	χ	χ	Lattice
(3,4,4)	$\frac{17}{3\cdot 2^5}$	$\frac{17}{2^5}$	$\mathcal{T}(4, E_2)$

Below is a summary of all the commensurability theorems known for the lattices we are treating in this work. The number above the arrow denotes the theorem from which the commensurability is deduced. The number below the arrow indicates the index of the intersection in each of the groups.

$$
\begin{array}{lllllllll}
(2,6,6) & \overset{3.5.1}{\underset{3:2}{\longleftrightarrow}} & (6,6) & & & & & & \\
(2,3,3) & \overset{3.5.1}{\underset{1:2}{\longleftrightarrow}} & (3,6,3) & & & & & & \\
(2,4,3) & \overset{3.5.1}{\underset{1:2}{\longleftrightarrow}} & (3,3,4) & & & & & & \\
(6,6,3) & \overset{3.5.2}{\underset{3:1}{\longleftrightarrow}} & (6,2) & \overset{3.5.2}{\underset{1:4}{\longleftrightarrow}} & (6,3) & \overset{3.5.4}{\underset{4:1}{\longleftrightarrow}} & (3,6) & & \\
(10,10,5) & \overset{3.5.2}{\underset{3:1}{\longleftrightarrow}} & (10,2) & \overset{3.5.2}{\underset{1:1}{\longleftrightarrow}} & (10,5) & & & & \\
(12,12,6) & \overset{3.5.2}{\underset{3:1}{\longleftrightarrow}} & (12,2) & \overset{3.5.2}{\underset{1:1}{\longleftrightarrow}} & (12,6) & & & & \\
(18,18,9) & \overset{3.5.2}{\underset{3:1}{\longleftrightarrow}} & (18,2) & \overset{3.5.2}{\underset{1:4}{\longleftrightarrow}} & (18,3) & \overset{3.5.4}{\underset{4:1}{\longleftrightarrow}} & (3,9) & \overset{3.5.4}{\underset{1:4}{\longleftrightarrow}} & (9,3) \\
(4,4,3) & \overset{3.5.3}{\underset{3:1}{\longleftrightarrow}} & (4,3) & \overset{3.5.4}{\underset{4:1}{\longleftrightarrow}} & (3,4) & & & & \\
(4,4,5) & \overset{3.5.3}{\underset{3:1}{\longleftrightarrow}} & (4,5) & & & & & & \\
(4,4,6) & \overset{3.5.3}{\underset{3:1}{\longleftrightarrow}} & (4,6) & & & & & & \\
(3,4,4) & \overset{3.5.5}{\underset{1:3}{\longleftrightarrow}} & \mathcal{T}(4,E_2) & & & & & & \\
(3,5) & \overset{3.5.4}{\underset{1:4}{\longleftrightarrow}} & (5,3) & & & & & & \\
(3,7) & \overset{3.5.4}{\underset{1:4}{\longleftrightarrow}} & (7,3) & & & & & & \\
(3,8) & \overset{3.5.4}{\underset{1:4}{\longleftrightarrow}} & (8,3) & & & & & & \\
(3,10) & \overset{3.5.4}{\underset{1:4}{\longleftrightarrow}} & (10,3) & & & & & & \\
(3,12) & \overset{3.5.4}{\underset{1:4}{\longleftrightarrow}} & (12,3) & & & & & & \\
(5,5/2) & \overset{3.5.2}{\underset{1:1}{\longleftrightarrow}} & (5,2) & & & & & & \\
(7,7/2) & \overset{3.5.2}{\underset{1:1}{\longleftrightarrow}} & (7,2) & & & & & & \\
(9,9/2) & \overset{3.5.2}{\underset{1:1}{\longleftrightarrow}} & (9,2) & & & & & & \\
(4,8) & \overset{3.5.3}{\underset{2:1}{\longleftrightarrow}} & (8,4) & \overset{3.5.2}{\underset{1:1}{\longleftrightarrow}} & (8,2) & & & & \\
(4,4) & & & & & & & & \\
(5,4) & & & & & & & & \\
(5,5) & & & & & & & & \\
(6,4) & & & & & & & &
\end{array}
$$

We remark that the commensurability between lattices with 3-fold symmetry coming from Corollary 3.5.2 can give index 1 or index 4 according to whether we are considering the 4-fold symmetry given by $k = \frac{p}{2}$ or not. Commensurability coming from Theorem 3.5.4 always has index 4. The only commensurability

coming from Corollary 3.5.3 which has not been explained earlier in this section is the one for $(4, 8)$ and $(8, 4)$. In these cases, the index is 2 because the ball 5-tuple associated to $(4, 8)$ has a 3-2-fold symmetry that we do not consider in the calculation.

Chapter 8

Future work

Our future research plans go in two different directions.

On one hand, we would like to use the same construction to consider the lattices in $PU(3,1)$, found by Deligne-Mostow and Thurston. In fact, one of the two non-arithmetic lattices known in $PU(3,1)$ arises from cone metrics on a sphere with 6 cone singularities and it would be very interesting to build a fundamental domain for it. This would also allow us to calculate the volume and have an explicit presentation for it. Preliminary works for this case are in Section 8.1.

Moreover, Veech proved (see [Vee93] and Theorem 8.2.1 below) that the moduli space of a torus with cone singularities of a certain type has a complex hyperbolic structure. Recently, Ghazouani and Pirio (see [GP17] and Theorem 8.2.2 below) analysed the cone manifold arising as metric completion of this moduli space, using a similar procedure as Thurston's. We hope to use a similar geometrical representation to get good coordinates and eventually find some new (potentially non-arithmetic) lattices by building explicitly the cone manifold describing the moduli space. More details on the preliminary works for this case are in Section 8.2.

8.1 Dimension 3

In this section we will first introduce the Deligne-Mostow lattices we would like to treat and explain how to parametrise them using complex coordinates. Then

we will present the moves we are considering as potential generators of the lattices and we will start studying what happens when pairs of cone points coalesce.

8.1.1 Lattices and configurations

We are considering some of the Deligne-Mostow lattices that can be found in the appendix of [Thu98]. Among these, we take the ones of dimension 3 (ball 6-tuples). Later, we will work specifically on the ones which have a 4-fold symmetry (i.e. the ball 6-tuples which have at least 4 equal values).

In the following table we give the ball 6-tuple in the first 6 columns and the corresponding values of the angles defined as

$$\varphi = \pi(1 - \mu_1 - \mu_2), \qquad \theta = \pi(1 - \mu_3 - \mu_4), \qquad \psi = \pi(1 - \mu_5 - \mu_6).$$

Their geometric meaning can be deduced by Figure 8.1.

μ_1	μ_2	μ_3	μ_4	μ_5	μ_6	θ	φ	ψ	A/NA
1/3	1/3	1/3	1/3	1/3	1/3	$\pi/3$	$\pi/3$	$\pi/3$	A
3/4	1/4	1/4	1/4	1/4	1/4	$\pi/2$	0	$\pi/2$	A
1/2	1/4	1/4	1/4	1/4	1/2	$\pi/2$	$\pi/4$	$\pi/4$	A
5/6	1/6	1/6	1/6	1/6	1/2	$2\pi/3$	0	$\pi/3$	A
2/3	1/6	1/6	1/6	1/6	2/3	$2\pi/3$	$\pi/6$	$\pi/6$	A
1/2	1/3	1/3	1/3	1/3	1/6	$\pi/3$	$\pi/6$	$\pi/2$	A
3/8	3/8	3/8	3/8	3/8	1/8	$\pi/4$	$\pi/4$	$\pi/2$	A
3/5	3/10	3/10	3/10	3/10	1/5	$2\pi/5$	$\pi/10$	$\pi/2$	A
5/10	3/10	3/10	3/10	3/10	3/10	$2\pi/5$	$2\pi/5$	$\pi/5$	A
3/4	1/6	1/6	1/6	1/6	7/12	$2\pi/3$	$\pi/12$	$\pi/4$	A
7/12	1/4	1/4	1/4	1/4	5/12	$\pi/2$	$\pi/6$	$\pi/3$	NA
5/6	1/3	1/6	1/6	1/6	1/3	$2\pi/3$	$-\pi/6$	$\pi/2$	A
2/3	1/2	1/6	1/6	1/6	1/3	$2\pi/3$	$-\pi/6$	$\pi/2$	A
1/2	1/2	1/6	1/6	1/6	1/2	$2\pi/3$	0	$\pi/3$	A
2/3	1/6	1/3	1/3	1/3	1/6	$\pi/3$	$\pi/6$	$\pi/2$	A
1/2	1/3	1/3	1/6	1/6	1/2	$\pi/2$	$\pi/6$	$\pi/3$	A
5/12	5/12	1/4	1/4	1/4	5/12	$\pi/2$	$\pi/6$	$\pi/3$	A

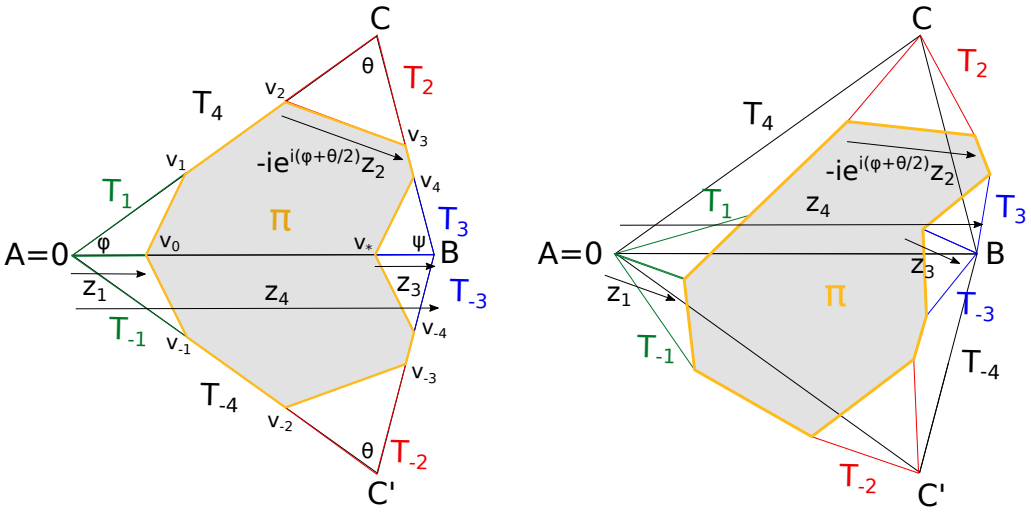

Figure 8.1: The configuration.

7/12	7/12	1/6	1/6	1/6	1/3	$2\pi/3$	$-\pi/6$	$\pi/2$	A

Table 8.1: Lattices in dimension 3.

When φ is negative, we will need to consider a different configuration, in the same way as we did in Section 6.3.3. When φ is 0, we expect to need to use a different parametrisation and this will be done in future research.

From now on we restrict ourselves to the 4-fold symmetry case. The discussion can easily be generalised to the other cases (see Remark 8.1.1).

From the ball 6-tuple $(\mu_1, \ldots, \mu_6)$ we are choosing $\theta_i = 2\pi(1 - \mu_i)$ to be the angles around the singularities of the cone metric on the sphere. Then θ, φ and ψ are defined so that the cone metric on the sphere has angles

$$(\pi - \theta + 2\varphi, \pi + \theta, \pi + \theta, \pi + \theta, \pi + \theta, \pi - \theta + 2\psi)\,.$$

They also satisfy $\theta + \varphi + \psi = \pi$, as the ball 6-tuple verifies $\sum \mu_i = 2$ (see (3.2.1)).

We also notice that the angle φ is always the smallest.

Finally, we point out that the angles θ and ψ are always positive, while φ can be 0. This case will be studied separately in the future.

The decagon Π describing the cone metric can be described as in the left hand side of Figure 8.1, by taking two big black triangles T_4 and T_{-4} and removing from each of them a copy of a green triangle T_1 and T_{-1}, a copy of a red triangle T_2 and T_{-2} and a copy of a blue triangle T_3 and T_{-3}. Then one side of each of the triangles will be our coordinates z_i and we will allow the sides to be complex numbers (i.e. vectors) as in the right hand side of Figure 8.1, just like in previous works.

We can now calculate the Hermitian form that gives the area of the polygon Π. We give it in matrix form as

$$H = \begin{bmatrix} -\frac{\sin\psi(\sin\varphi+\sin(\theta-\psi))}{\sin\theta} & 0 & 0 & 0 \\ 0 & -\frac{1+\cos\theta}{2\sin\theta} & 0 & 0 \\ 0 & 0 & -\frac{\sin\varphi(\sin\varphi+\sin(\theta-\varphi))}{\sin\theta} & 0 \\ 0 & 0 & 0 & \frac{\sin\psi\sin\varphi}{\sin(\psi+\varphi)} \end{bmatrix}.$$

It has signature (3,1), as $\sin\theta$, $\sin\psi$, $\sin\varphi$ and $\sin(\theta+\varphi)$ are positive and so are $\sin\psi+\sin(\theta-\psi) = \sin\theta\cos\psi+\sin\psi(1-\cos\theta)$ and $\sin\varphi+\sin(\theta-\varphi)$.

We will also need the coordinates of the vertices and of some additional points in the configuration in Figure 8.1.

$$
\begin{aligned}
A &= 0,\\
B &= z_4,\\
C &= \frac{\sin\psi}{\sin\theta}e^{i\varphi}z_4,\\
C' &= \frac{\sin\psi}{\sin\theta}e^{-i\varphi}z_4,\\
v_0 &= B - z_1 = z_4 - z_1,\\
v_1 &= z_4 - \frac{\cos(\theta/2-\psi)}{\cos(\theta/2)}e^{-i\psi}z_1,\\
v_{-1} &= z_4 - \frac{\cos(\theta/2-\psi)}{\cos(\theta/2)}e^{i\psi}z_1,\\
v_2 &= \frac{\sin\psi}{\sin\theta}e^{i\varphi}z_4 + \frac{\cos(\theta/2)}{\sin\theta}e^{-i\psi}z_2,\\
v_{-2} &= \frac{\sin\psi}{\sin\theta}e^{-i\varphi}z_4 + \frac{\cos(\theta/2)}{\sin\theta}e^{i\psi}z_2,\\
v_3 &= v_2 - z_2 = \frac{\sin\psi}{\sin\theta}e^{i\varphi}z_4 - \frac{\cos(\theta/2)}{\sin\theta}e^{i\varphi}z_2,\\
v_{-3} &= \frac{\sin\psi}{\sin\theta}e^{-i\varphi}z_4 - \frac{\cos(\theta/2)}{\sin\theta}e^{-i\varphi}z_2,\\
v_4 &= \frac{\cos(\theta/2-\varphi)}{\cos(\theta/2)}e^{i\varphi}z_3,\\
v_{-4} &= \frac{\cos(\theta/2-\varphi)}{\cos(\theta/2)}e^{-i\varphi}z_3,\\
v_* &= z_3.
\end{aligned}
$$

8.1.2 Moves

The moves are the automorphisms of the sphere swapping the vertices. When the cone angles are the same, we will denote the move that swaps v_i and v_j as R_{ij}. When the two angles are not the same, we consider the move swapping the cone points twice in the spirit of Thurston's butterfly move and we will call the move A_{ij}.

The move sending v_1 to v_{-1} (i.e. swapping v_1 and v_0 twice) is given by the

matrix

$$A_{01} = \begin{bmatrix} e^{2i\psi} & 0 & 0 & 0 \\ 0 & 1 & 0 & 0 \\ 0 & 0 & 1 & 0 \\ 0 & 0 & 0 & 1 \end{bmatrix}.$$

The move swapping v_2 and v_3 (by sending v_3 on v_2) is given by the matrix

$$R_{23} = \begin{bmatrix} 1 & 0 & 0 & 0 \\ 0 & e^{i\theta} & 0 & 0 \\ 0 & 0 & 1 & 0 \\ 0 & 0 & 0 & 1 \end{bmatrix}.$$

The move sending v_{-4} to v_4 (i.e. swapping v_4 and v_* twice) is given by the matrix

$$A_{4*} = \begin{bmatrix} 1 & 0 & 0 & 0 \\ 0 & 1 & 0 & 0 \\ 0 & 0 & e^{2i\varphi} & 0 \\ 0 & 0 & 0 & 1 \end{bmatrix}.$$

Now, the move R_{12} swapping v_1 and v_2 can be found by solving the equations

$$\begin{array}{llll} v'_* = v_*, & v'_2 = v_1, & v'_3 = v_3, & v'_4 = v_4, \\ v'_0 = v_0, & v'_{-1} = v_{-2}, & v'_{-3} = v_{-3}, & v'_{-4} = v_{-4}. \end{array}$$

The matrix of the move is

$$R_{12} = \frac{1}{\sin\psi(1-e^{-i\theta})} \cdot \begin{bmatrix} -\sin\theta e^{-i\psi} & -\cos\frac{\theta}{2} & 0 & \sin\varphi \\ -\frac{\sin\psi(\sin\psi+\sin(\theta-\psi))}{\cos\frac{\theta}{2}} & -\sin\psi e^{-i\theta} & 0 & \frac{\sin\varphi\sin\psi}{\cos\frac{\theta}{2}} \\ 0 & 0 & \sin\psi(1-e^{-i\theta}) & 0 \\ -\sin\psi-\sin(\theta-\psi) & -\cos\frac{\theta}{2} & 0 & \sin\psi+\sin\theta e^{i\psi} \end{bmatrix}.$$

In the case of R_{34} we cannot do exactly the same thing. This is because we are changing z_3, so we are changing the position of the origin, seen as the common vertex of T_3 and T_4. To do this, we need to change the coordinates, imposing that the origin of our coordinates is in B instead. This simply means subtracting B

from the coordinates of each vertex. This will allow us to proceed in the same way, because z_1 remains unchanged when applying R_{34}.

We hence ask that, in the new coordinates,

$$v'_* = v_*, \qquad v'_1 = v_1, \qquad v'_2 = v_2, \qquad v'_4 = v_3,$$
$$v'_0 = v_0, \qquad v'_{-1} = v_{-1}, \qquad v'_{-2} = v_{-2}, \qquad v'_{-3} = v_{-4}.$$

By solving the equations we get the matrix

$$R_{34} = \frac{1}{\sin\varphi(1-e^{-i\theta})}\cdot$$
$$\cdot\begin{bmatrix} \sin\varphi(1-e^{-i\theta}) & 0 & 0 & 0 \\ 0 & -\sin\varphi e^{-i\theta} & -\frac{\sin\varphi(\sin\varphi+\sin(\theta-\varphi))}{\cos\frac{\theta}{2}} & \frac{\sin\varphi\sin\psi}{\cos\frac{\theta}{2}} \\ 0 & -\cos\frac{\theta}{2} & -\sin\theta e^{-i\varphi} & \sin\psi \\ 0 & -\cos\frac{\theta}{2} & -\sin\varphi-\sin(\theta-\varphi) & \sin\varphi+\sin\theta e^{i\varphi} \end{bmatrix}.$$

We will also consider $P_1 = R_{23}R_{12}$ and $P_2 = R_{23}R_{34}$ and their inverses. They are as follows.

$$P_1 = \frac{1}{\sin\psi(1-e^{-i\theta})}\cdot$$
$$\cdot\begin{bmatrix} -\sin\theta e^{-i\psi} & -\cos\frac{\theta}{2} & 0 & \sin\varphi \\ -\frac{\sin\psi(\sin\psi+\sin(\theta-\psi))}{\cos\frac{\theta}{2}}e^{i\theta} & -\sin\psi & 0 & \frac{\sin\varphi\sin\psi}{\cos\frac{\theta}{2}}e^{i\theta} \\ 0 & 0 & \sin\psi(1-e^{-i\theta}) & 0 \\ -\sin\psi-\sin(\theta-\psi) & -\cos\frac{\theta}{2} & 0 & \sin\psi+\sin\theta e^{i\psi} \end{bmatrix},$$

$$P_2 = \frac{1}{\sin\varphi(1-e^{-i\theta})}\cdot$$
$$\cdot\begin{bmatrix} \sin\varphi(1-e^{-i\theta}) & 0 & 0 & 0 \\ 0 & -\sin\varphi & -\frac{\sin\varphi(\sin\varphi+\sin(\theta-\varphi))}{\cos\frac{\theta}{2}}e^{i\theta} & \frac{\sin\varphi\sin\psi}{\cos\frac{\theta}{2}}e^{i\theta} \\ 0 & -\cos\frac{\theta}{2} & -\sin\theta e^{-i\varphi} & \sin\psi \\ 0 & -\cos\frac{\theta}{2} & -\sin\varphi-\sin(\theta-\varphi) & \sin\varphi+\sin\theta e^{i\varphi} \end{bmatrix},$$

$$P_1^{-1} = \frac{1}{\sin\psi(1-e^{i\theta})}\cdot$$
$$\cdot\begin{bmatrix} -\sin\theta e^{i\psi} & -\cos\frac{\theta}{2}e^{-i\theta} & 0 & \sin\varphi \\ -\frac{\sin\psi(\sin\psi+\sin(\theta-\psi))}{\cos\frac{\theta}{2}} & -\sin\psi & 0 & \frac{\sin\varphi\sin\psi}{\cos\frac{\theta}{2}} \\ 0 & 0 & \sin\psi(1-e^{i\theta}) & 0 \\ -\sin\psi-\sin(\theta-\psi) & -\cos\frac{\theta}{2}e^{-i\theta} & 0 & \sin\psi+\sin\theta e^{-i\psi} \end{bmatrix},$$

$$P_2^{-1} = \frac{1}{\sin\varphi(1-e^{i\theta})}\cdot$$
$$\cdot\begin{bmatrix} \sin\varphi(1-e^{i\theta}) & 0 & 0 & 0 \\ 0 & -\sin\varphi & -\frac{\sin\varphi(\sin\varphi+\sin(\theta-\varphi))}{\cos\frac{\theta}{2}} & \frac{\sin\varphi\sin\psi}{\cos\frac{\theta}{2}} \\ 0 & -\cos\frac{\theta}{2}e^{-i\theta} & -\sin\theta e^{i\varphi} & \sin\psi \\ 0 & -\cos\frac{\theta}{2}e^{-i\theta} & -\sin\varphi-\sin(\theta-\varphi) & \sin\varphi+\sin\theta e^{-i\varphi} \end{bmatrix}.$$

In the following, we will keep track of the following three sets of coordinates

$$\mathbf{z} = \begin{bmatrix} z_1 \\ z_2 \\ z_3 \\ 1 \end{bmatrix}, \qquad \mathbf{u} = P_1^{-1}\mathbf{z}, \qquad \mathbf{v} = P_2^{-1}\mathbf{z}.$$

8.1.3 Collapsing cone points

The vertices of the polyhedron are made by making pairs of vertices of Π collapse. To have a vertex –i.e. a 0-dimensional facet– we need 6 conditions, hence 3 equations in the $\mathbf{z}$-coordinates. We will now give the equations of the subspaces obtained when a pair of vertices of Π collapses. Intersecting them, we will have the coordinates of the vertices of the polyhedron. The subspace $L_{,j}$ is the one obtained by collapsing vertices v_i and v_j, with $i, j \in \{0, 1, 2, 3, 4, *\}$. Note that $2\sin\frac{\theta}{2}\cos\left(\frac{\theta}{2}-\varphi\right) = \sin\varphi + \sin(\theta-\varphi)$ and $-e^{-i(\theta+\varphi)} = e^{i(\pi-\theta-\varphi)} = e^{i\psi}$.

Subspace	Vertices collapsing	Equation on **z**-coordinates
L_{*0}	$v_0 = v_*$	$z_1 + z_3 = 1$
L_{*1}	$v_* = v_{-1}$	$\frac{\sin\psi+\sin(\theta-\psi)}{\sin\theta}e^{i\psi}z_1 + z_3 = 1$
L_{*2}	$v_* = v_{-2}$	$\frac{\cos\frac{\theta}{2}}{\sin\psi}e^{-i\theta}z_2 + \frac{\sin\theta}{\sin\psi}e^{i\varphi}z_3 = 1$
L_{*3}	$v_* = v_{-3}$	$\frac{\cos\frac{\theta}{2}}{\sin\psi}z_2 + \frac{\sin\theta}{\sin\psi}e^{i\varphi}z_3 = 1$
L_{*4}	$v_* = v_4 = v_{-4}$	$z_3 = 0$
L_{01}	$v_0 = v_1 = v_{-1}$	$z_1 = 0$
L_{02}	$v_0 = v_2$	$\frac{\sin\theta}{\sin\varphi}e^{i\psi}z_1 + \frac{\cos\frac{\theta}{2}}{\sin\varphi}z_2 = 1$
L_{03}	$v_0 = v_3$	$\frac{\sin\theta}{\sin\varphi}e^{i\psi}z_1 + \frac{\cos\frac{\theta}{2}}{\sin\varphi}e^{-i\theta}z_2 = 1$
L_{04}	$v_0 = v_4$	$z_1 + \frac{\sin\varphi+\sin(\theta-\varphi)}{\sin\theta}e^{i\varphi}z_3 = 1$
L_{12}	$v_1 = v_2$	$\frac{\sin\psi+\sin(\theta-\psi)}{\sin\varphi}z_1 + \frac{\cos\frac{\theta}{2}}{\sin\varphi}z_2 = 1$
L_{13}	$v_1 = v_3$	$\frac{\sin\psi+\sin(\theta-\psi)}{\sin\varphi}z_1 + \frac{\cos\frac{\theta}{2}}{\sin\varphi}e^{-i\theta}z_2 = 1$
L_{14}	$v_{-1} = v_4$	$\frac{\sin\psi+\sin(\theta-\psi)}{\sin\theta}e^{i\psi}z_1 + \frac{\sin\varphi+\sin(\theta-\varphi)}{\sin\theta}e^{i\varphi}z_3 = 1$
L_{23}	$v_2 = v_3$	$z_2 = 0$
L_{24}	$v_{-2} = v_{-4}$	$\frac{\cos\frac{\theta}{2}}{\sin\psi}e^{-i\theta}z_2 + \frac{\sin\varphi+\sin(\theta-\varphi)}{\sin\psi}z_3 = 1$
L_{34}	$v_3 = v_4$	$\frac{\cos\frac{\theta}{2}}{\sin\psi}z_2 + \frac{\sin\varphi+\sin(\theta-\varphi)}{\sin\psi}z_3 = 1$

Subspace	Vertices collapsing	Equation on **u**-coordinates
L_{*0}	$v_0 = v_*$	$u_1 + u_3 = 1$
L_{*1}	$v_* = v_{-1}$	$\frac{\cos\frac{\theta}{2}}{\sin\psi}e^{-i\theta}u_2 + \frac{\sin\theta}{\sin\psi}e^{i\varphi}u_3 = 1$
L_{*2}	$v_* = v_{-2}$	$\frac{\cos\frac{\theta}{2}}{\sin\psi}u_2 + \frac{\sin\theta}{\sin\psi}e^{i\varphi}u_3 = 1$
L_{*3}	$v_* = v_{-3}$	$\frac{\sin\psi+\sin(\theta-\psi)}{\sin\theta}e^{-i\psi}u_1 + e^{2i\varphi}u_3 = 1$

L_{*4}	$v_* = v_4 = v_{-4}$	$u_3 = 0$
L_{01}	$v_0 = v_1 = v_{-1}$	$\frac{\sin\theta}{\sin\varphi}e^{-i\psi}u_1 + \frac{\cos\frac{\theta}{2}}{\sin\varphi}u_2 = 1$
L_{02}	$v_0 = v_2$	$\frac{\sin\theta}{\sin\varphi}e^{-i\psi}u_1 + \frac{\cos\frac{\theta}{2}}{\sin\varphi}e^{-i\theta}u_2 = 1$
L_{03}	$v_0 = v_3$	$u_1 = 0$
L_{04}	$v_0 = v_4$	$u_1 + \frac{\sin\varphi+\sin(\theta-\varphi)}{\sin\theta}e^{i\varphi}u_3 = 1$
L_{12}	$v_1 = v_2$	$u_2 = 0$
L_{13}	$v_1 = v_3$	$\frac{\sin\psi+\sin(\theta-\psi)}{\sin\varphi}u_1 + \frac{\cos\frac{\theta}{2}}{\sin\varphi}u_2 = 1$
L_{14}	$v_{-1} = v_4$	$\frac{\cos\frac{\theta}{2}}{\sin\psi}e^{-i\theta}u_2 + \frac{\sin\varphi+\sin(\theta-\varphi)}{\sin\psi}e^{2i\varphi}u_3 = 1$
L_{23}	$v_2 = v_3$	$\frac{\sin\psi+\sin(\theta-\psi)}{\sin\varphi}u_1 + \frac{\cos\frac{\theta}{2}}{\sin\varphi}e^{-i\theta}u_2 = 1$
L_{24}	$v_{-2} = v_{-4}$	$\frac{\cos\frac{\theta}{2}}{\sin\psi}u_2 + \frac{\sin\varphi+\sin(\theta-\varphi)}{\sin\psi}u_3 = 1$
L_{34}	$v_3 = v_4$	$\frac{\sin\psi+\sin(\theta-\psi)}{\sin\theta}e^{-i\psi}u_1 + \frac{\sin\varphi+\sin(\theta-\varphi)}{\sin\theta}e^{i\varphi}u_3 = 1$

Subspace	Vertices collapsing	Equation on **v**-coordinates
L_{*0}	$v_0 = v_*$	$v_1 + v_3 = 1$
L_{*1}	$v_* = v_{-1}$	$\frac{\sin\psi+\sin(\theta-\psi)}{\sin\theta}e^{i\psi}v_1 + v_3 = 1$
L_{*2}	$v_* = v_{-2}$	$v_3 = 0$
L_{*3}	$v_* = v_{-3}$	$\frac{\cos\frac{\theta}{2}}{\sin\psi}e^{-i\theta}v_2 + \frac{\sin\theta}{\sin\psi}e^{-i\varphi}v_3 = 1$
L_{*4}	$v_* = v_4 = v_{-4}$	$\frac{\cos\frac{\theta}{2}}{\sin\psi}v_2 + \frac{\sin\theta}{\sin\psi}e^{-i\varphi}v_3 = 1$
L_{01}	$v_0 = v_1 = v_{-1}$	$v_1 = 0$
L_{02}	$v_0 = v_2$	$e^{2i\psi}v_1 + \frac{\sin\varphi+\sin(\theta-\varphi)}{\sin\theta}e^{-i\varphi}v_3 = 1$
L_{03}	$v_0 = v_3$	$\frac{\sin\theta}{\sin\varphi}e^{i\psi}v_1 + \frac{\cos\frac{\theta}{2}}{\sin\varphi}v_2 = 1$
L_{04}	$v_0 = v_4$	$\frac{\sin\theta}{\sin\varphi}e^{i\psi}v_1 + \frac{\cos\frac{\theta}{2}}{\sin\varphi}e^{-i\theta}v_2 = 1$

L_{12}	$v_1 = v_2$	$\frac{\sin\psi+\sin(\theta-\psi)}{\sin\theta}e^{i\psi}v_1 + \frac{\sin\varphi+\sin(\theta-\varphi)}{\sin\theta}e^{-i\varphi}v_3 = 1$
L_{13}	$v_1 = v_3$	$\frac{\sin\psi+\sin(\theta-\psi)}{\sin\varphi}v_1 + \frac{\cos\frac{\theta}{2}}{\sin\varphi}v_2 = 1$
L_{14}	$v_{-1} = v_4$	$\frac{\sin\psi+\sin(\theta-\psi)}{\sin\varphi}e^{2i\psi}u_1 + \frac{\cos\frac{\theta}{2}}{\sin\psi}e^{-i\theta}v_2 = 1$
L_{23}	$v_2 = v_3$	$\frac{\cos\frac{\theta}{2}}{\sin\psi}e^{-i\theta}v_2 + \frac{\sin\varphi+\sin(\theta-\varphi)}{\sin\psi}v_3 = 1$
L_{24}	$v_{-2} = v_{-4}$	$\frac{\cos\frac{\theta}{2}}{\sin\psi}v_2 + \frac{\sin\varphi+\sin(\theta-\varphi)}{\sin\psi}v_3 = 1$
L_{34}	$v_3 = v_4$	$v_2 = 0$

Note that when calculating the coordinates of these subspaces, we are making a choice each time on whether to choose v_i or v_{-i} for collapsing the coordinates. We keep in mind that potentially this might need to be changed, or both cases might need to be considered.

The next step will be to remark that in each of these subspaces, we are in one of the situations previously analysed in this work, i.e. we have a sphere with five cone singularities and either 3- or 2-fold symmetry. This means that we want to find one of the polyhedra previously constructed as real 4-dimensional facets of the cone manifold that we are trying to build. In other words we need to check that all the vertices of those polyhedra are included in the list of new vertices. Note that the new configurations is parametrised in a slightly different way, in order to have the parameters to be real and positive when they are along the positive real axis, but the same vertices of Π will be collapsing.

For example, on L_{*4}, when $z_3 = 0$, we are exactly in the 3-fold symmetry case, as v_1, v_2 and v_3 have same cone angle. Then $\overrightarrow{Av_{-1}}$, $\overrightarrow{v_{-2}C'}$ and $\overrightarrow{AC'}$ will have the same role as z_1, z_2 and z_3 in Chapter 5 respectively. We hence need all the configurations we had in the 14 vertices of the 3-fold symmetry case to be contained in the subspace L_{*4}.

On L_{23}, when $z_2 = 0$, we have a 2-fold symmetry configuration of type ③. Again, the roles of the coordinates change and involve some vertices not marked in out figure, but it is possible to describe the relation. Moreover, only the

configurations given by one of the three copies the form the fundamental domain in Chapter 6 can be easily seen as degenerations of the triangles, but it is possible to use the moves to find the others.

With a similar analysis for each 2-dimensional subspace, one can find the potential vertices of the new polyhedron describing the cone manifold in the three dimensional case.

Then one will need to better understand the bisectors in higher dimensional complex hyperbolic space in order to use similar arguments like the ones previously described.

Remark 8.1.1. In fact, this is also true for the 3-dimensional lattices without 4-fold symmetry. When collapsing pairs of cone points, we can still find a lower dimensional lattice with 2- or 3-fold symmetry. More specifically, we have one of three cases:

- either the collapsing is not possible and we have a degeneration similar to Proposition 4.4.1,
- or we find one of the lattices in Tables 3.1 and 3.2,
- or we get one of the lattices we had excluded which still satisfy condition ΣINT, i.e. one of the lattices with $p = \infty$.

To cover the third case, we expect that we will need to change the parameters in a similar way as we will have to do for the cases where $\varphi = 0$ previously mentioned. In fact, this means that certain sides of Π are parallel, so they do not close up to form a triangle, but they form a strip that is infinite only on one side (i.e. a "triangle" with two parallel sides). One idea is to use the width of the strip as a new parameter, instead of one of the (now infinite) sides of the triangle. In other words, to use the side of the triangle which remains finite. When $\varphi = 0$ and this parameter is 0 (i.e. we collapse the two cone points v_0 and v_1), the area of the polygon goes to zero and certain other cone points are forced to collapse. Therefore, the set of such configurations where these two cone points have collapsed corresponds to a point in the ideal boundary, just like in

the 2-dimensional case, when one of the orders of generators was ∞ and hence the corresponding angle was 0.

8.2 Tori with cone points

The starting point of this construction is a theorem from Veech which can be found in [Vee93] and generalises some basic results of Thurston to higher genus surfaces. First remark that we can define a *(indefinite when $p > 1$) complex hyperbolic space of type* (p, q) in the same way we defined $\mathbf{H}^n_{\mathbb{C}}$, where the signature of the Hermitian form is (p, q). We will denote such a space as $\mathbb{C}\mathbf{H}^{p+q-1}_p$ and the group of linear maps preserving the Hermitian structure as $PU(p, q)$. When $p = 1$, this is the complex hyperbolic space as defined in Chapter 2. Now Veech's theorem states that moduli spaces of higher genus surfaces has a $(\mathbb{C}\mathbf{H}^{p+q-1}_p, PU(p, q))$-structure (see 3.2.4 for the definition of an (X, G)-structure), provided that we fix the values of the holonomy. This means not only fixing the angle of the cone singularities, as we did for the case of the sphere, but also fixing the holonomy along curves around the genus. Roughly speaking, each part of moduli space with fixed holonomy is called a leaf of the Veech foliation of the moduli space. More precisely, we have the following theorem.

Theorem 8.2.1. *Let S be a surface of genus g with N cone singularities whose angles satisfy the Gauss-Bonnet formula* (3.2.1) *and are not integer multiples of 2π. A leaf of the Veech foliation of S with its area form has a geometric structure modelled on $(\mathbb{C}\boldsymbol{H}^{p+q-1}_p, PU(p, q))$, for p and q two integers such that $p + q = 2g + N - 2$. Moreover, $p = 1$ in exactly two cases:*

- *when $g = 0$ and all cone angles are between 0 and 2π, giving a $(N - 3)$-dimensional complex hyperbolic structure,*
- *when $g = 1$, one cone angle is between 2π and 4π and the others are all between 0 and 2π, giving a $(N-1)$-dimensional complex hyperbolic structure.*

The first case is the one studied by Thurston. Recently, in [GP17], Ghazouani and Pirio showed that the same analysis on the metric completion is also possible

for the second case. In particular, for the second case of the theorem above, they proved the following.

Theorem 8.2.2. *Fixing a rational linear holonomy, the metric completion of a leaf of the Veech foliation is a complex hyperbolic cone manifold of dimension $N-1$ with finite volume, which has a stratified structure. The number of strata is finite and they are finite covers of lower dimensional leaves. Appropriate surgeries explain how to pass between strata and allow calculation the cone angles around each stratum. These surgeries include inverting the collapsing of cone points (as in Thurston's work) as well as pinching along curves around the genus.*

This is a starting point to try and find a similar procedure to the one used in this work to explicitly describe the cone manifold and potentially find (new) complex hyperbolic lattices as holonomy of the cone manifold.

The first case we have been investigating is the one of a torus with three cone singularities.

8.2.1 The configurations

The first step is to choose three parameters that geometrically describe the leaf in the moduli space.

Let the cone angles be $2\theta \in (2\pi, 4\pi)$, 2φ, $2\psi \in (0, 2\pi)$. Note that $2\theta + 2\varphi + 2\psi = 6\pi$, so they satisfy the Gauss-Bonnet formula (3.2.1). Let 2α and 2β be the two holonomy angles along two curves around the genus as in Figure 8.2.

Similarly to the case of the sphere, we cut the torus along straight arcs between cone points in such a way that the result is an octagon with vertices in (positive) cyclic order v_1, v_2, v_3, v_4, v_{-4}, v_{-3}, v_{-2}, v_{-1}. The side pairing map identifies sides $(v_{-j}, v_{-(j+1)})$ with (v_j, v_{j+1}) for $j = 1, 2, 3$ and also identifies (v_{-1}, v_1) with (v_{-4}, v_4). The vertex on the torus obtained by glueing v_2 and v_{-2} is the one of angle 2φ, while the vertex obtained by v_3 and v_{-3} is the one of angle 2ψ. Then the holonomy 2α is also the angle between the line through v_2, v_3 and the line through v_{-2}, v_{-3}, while the holonomy 2β is the angle between the line through v_1, v_{-1} and the line through v_4, v_{-4}. We assume that the first pair of lines meet on the side of v_2 and the second pair of lines meet on the side of v_1 (see Figure

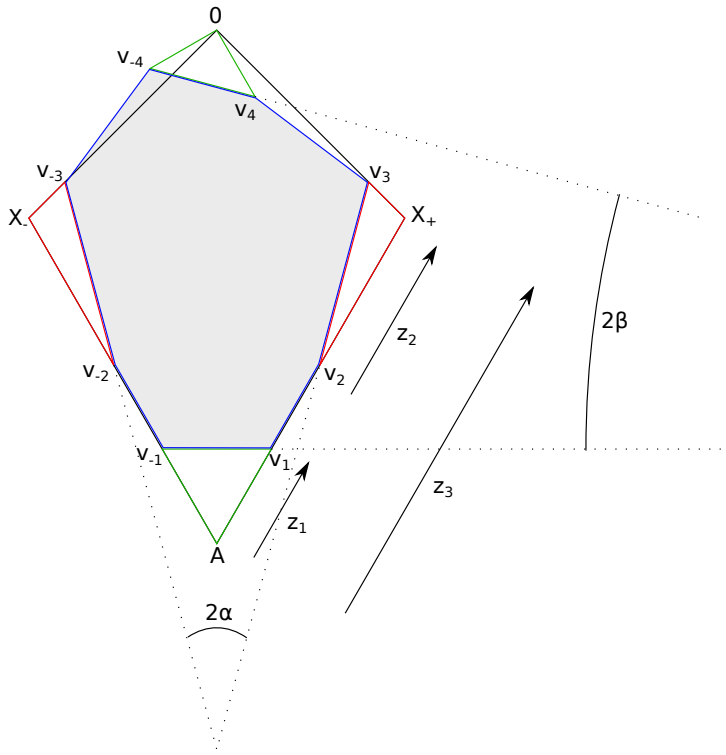

Figure 8.2: The special octagon and the parameters.

8.2).

Let us first assume that the cut from v_1 to v_2 and then to v_3 cuts the cone angle at v_2 in half.

Let $X_\pm$ be the intersection point of the line through $v_{\pm 1}$, $v_{\pm 2}$ and the line through $v_{\pm 3}$, $v_{\pm 4}$. Moreover, let A be the intersection point of the line through v_1, v_2 and the line through v_{-1}, v_{-2} and 0 the intersection point of the line through X_+, v_3 and the line through X_-, v_{-3}. Let 0 be the origin and A be on the negative imaginary axis.

Let z_1, z_2 and z_3 be such that:

$$-ie^{i(\varphi-\alpha)}z_1 = \overrightarrow{Av_1}, \quad -ie^{i(\varphi-\alpha)}z_2 = \overrightarrow{v_2X_+}, \quad -ie^{i(\varphi-\alpha)}z_3 = \overrightarrow{AX_+}. \tag{8.2.1}$$

We remark that the $-ie^{i(\varphi-\alpha)}$ factor means that the z_i are coherent with our coordinates space (i.e. the z_i's are real and positive when horizontal and pointing towards right). Let us call the triangles formed by 0, A, $X_\pm$ as $T_{\pm 3}$, the triangle

formed by v_1, v_{-1}, A as T_1, the triangle formed by v_4, v_{-4}, 0 as T_{-1} and the triangles formed by $v_{\pm 3}$, $v_{\pm 2}$, $X_\pm$ as $T_{\pm 2}$.

Let us now consider the general case. The configuration will look like Figure 8.3. To determine what the z_i's are, we need to first find the points A and $X_\pm$. Then they can be defined as above. Since the angles of the triangles T_2, T_3 and T_1 are all determined by the initial cone angles, one only needs to glue these triangles on the sides v_1v_{-1} and v_2v_3 to obtain the points X_+ and A. Then the z_i's are defined by (8.2.1).

In view of this, we can write the coordinates of the vertices of our triangles as

$$\begin{aligned}
v_1 &= -ie^{i(\varphi-\alpha)}z_1 + i\frac{\sin(\varphi+\psi)}{\sin(\alpha+\psi)}z_3,\\
v_{-1} &= -ie^{-i(\varphi-\alpha)}z_1 + i\frac{\sin(\varphi+\psi)}{\sin(\alpha+\psi)}z_3,\\
v_2 &= ie^{i(\varphi-\alpha)}z_2 + i\frac{\sin(\varphi-\alpha)}{\sin(\alpha+\psi)}e^{-i(\alpha+\psi)}z_3,\\
v_{-2} &= ie^{-i(\varphi-\alpha)}z_2 + i\frac{\sin(\varphi-\alpha)}{\sin(\alpha+\psi)}e^{i(\alpha+\psi)}z_3,\\
v_3 &= -i\frac{\sin(\varphi)}{\sin(\psi)}e^{-i(\alpha+\psi)}z_2 + i\frac{\sin(\varphi-\alpha)}{\sin(\alpha+\psi)}e^{-i(\alpha+\psi)}z_3,\\
v_{-3} &= -i\frac{\sin(\varphi)}{\sin(\psi)}e^{i(\alpha+\psi)}z_2 + i\frac{\sin(\varphi-\alpha)}{\sin(\alpha+\psi)}e^{i(\alpha+\psi)}z_3,\\
v_4 &= i\frac{\sin(\varphi-\alpha)}{\sin(\alpha+\psi)}e^{-i(\alpha+\psi+2\beta)}z_1,\\
v_{-4} &= i\frac{\sin(\varphi-\alpha)}{\sin(\alpha+\psi)}e^{i(\alpha+\psi+2\beta)}z_1,\\
A &= i\frac{\sin(\varphi+\psi)}{\sin(\alpha+\psi)}z_3,\\
X_+ &= i\frac{\sin(\varphi-\alpha)}{\sin(\alpha+\psi)}e^{-i(\alpha+\psi)}z_3.
\end{aligned}$$

The area of the octagon is then

$$\begin{aligned}
\mathcal{A} &= \mathrm{Area}(T_3) + \mathrm{Area}(T_{-3}) - \mathrm{Area}(T_2) - \mathrm{Area}(T_{-2}) - \mathrm{Area}(T_1) - \mathrm{Area}(T_{-1})\\
&= 2\,\mathrm{Area}(T_3) - 2\,\mathrm{Area}(T_2) - \mathrm{Area}(T_1) - \mathrm{Area}(T_{-1})\\
&= -\frac{\sin(\varphi-\alpha)\sin(\varphi+\psi)}{\sin(\alpha+\psi)}|z_3|^2 + \frac{\sin(\varphi)\sin(\varphi+\psi)}{\sin(\psi)}|z_2|^2\\
&+ \frac{\sin(\varphi-\alpha)\sin(\varphi+\psi)}{\sin(\alpha+\psi)}|z_1|^2.
\end{aligned}$$

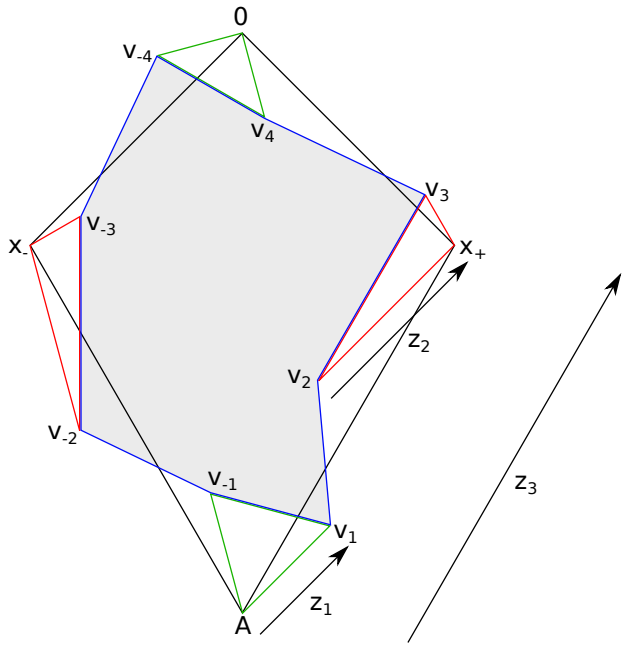

Figure 8.3: The generic octagon and the parameters.

Note that the angle θ can be given in terms of φ and ψ as $\theta = 3\pi - \varphi - \psi$ because of the curvature formula, therefore the quadruple $(\alpha, \beta, \varphi, \psi)$ determine uniquely the configuration. For each prescribed initial datum of cone angles and holonomy $(\alpha, \beta, \varphi, \psi)$, we can parametrise the configuration of points by the triplet (z_1, z_2, z_3) and vice versa, for each triplet of complex parameters which form a configuration with positive area, there is a corresponding cone metric on the torus.

8.2.2 Moves

Some of the moves will be similar to those in the previous case. As before, we will have some moves swapping cone points and we will take the square when the two cone points have different angle. The moves swapping cone points v_i and v_j will be denoted as R_{ij}, while doing this twice will be denoted as A_{ij}. Moreover, there will be additional moves corresponding to the two Dehn twists around the genus.

The move swapping v_2 and v_3. We perform a move where v_2 and v_3 are swapped, called R_{23}. Note that this changes a configuration in the following way

$$(\alpha, \beta, \varphi, \psi) \xmapsto{R_{23}} (\alpha', \beta', \varphi', \psi') = (\alpha + \psi - \varphi, \beta, \psi, \varphi)$$

After the move, $v_{\pm 1}$, $v_{\pm 4}$, $x_{\pm}$ stay fixed and $v'_{-2} = v_{-3}$, $v'_3 = v_2$. Hence

$$z'_1 = z_1, \qquad z'_2 = -\frac{\sin(\psi)}{\sin(\varphi)} e^{i(\varphi+\psi)} z_2, \qquad z'_3 = z_3$$

and

$$R_{23} = \begin{pmatrix} 1 & 0 & 0 \\ 0 & -\frac{\sin(\varphi)}{\sin(\psi)} e^{i(\varphi+\psi)} & 0 \\ 0 & 0 & 1 \end{pmatrix}.$$

When $\varphi \neq \psi$ in order to get an isometry we must perform this move twice. Hence we obtain

$$A_{23} = \begin{pmatrix} 1 & 0 & 0 \\ 0 & e^{2i(\varphi+\psi)} & 0 \\ 0 & 0 & 1 \end{pmatrix}.$$

The shift and the other moves swapping cone points. We want to apply a change of coordinates T that cyclically shifts the order of the cone points. In other words, if the cone angles are (φ, ψ, θ) in this order, the new angles will be (ψ, θ, φ). It will change the configuration in the following way

$$(\alpha, \beta, \varphi, \psi) \xmapsto{T} (\alpha', \beta', \varphi', \psi') = (\alpha + \psi - \pi, \beta, \psi, 3\pi - \varphi - \psi).$$

Now we want to give the new parameters z'_i in terms of the previous ones. If we look at $T_{\pm i}$, for $i = 1, 2, 3$, one can see that their angles are not the same as before. For example, the angle at the origin of T_{-1} was $\pi - \alpha - \psi$, but $\pi - \alpha' - \psi' = -(\pi + \alpha - \varphi) < 0$. This means that T_{-1} is "pointing downwards" and the configuration of the triangles is as shown in the right hand side of Figure 8.4.

Now, we want to find a relation between the new coordinates z'_i and the old ones z_i. To do this, we need to solve the equations

$$v'_1 = v_2, \qquad v'_2 = v_3, \qquad v'_3 = v_4.$$

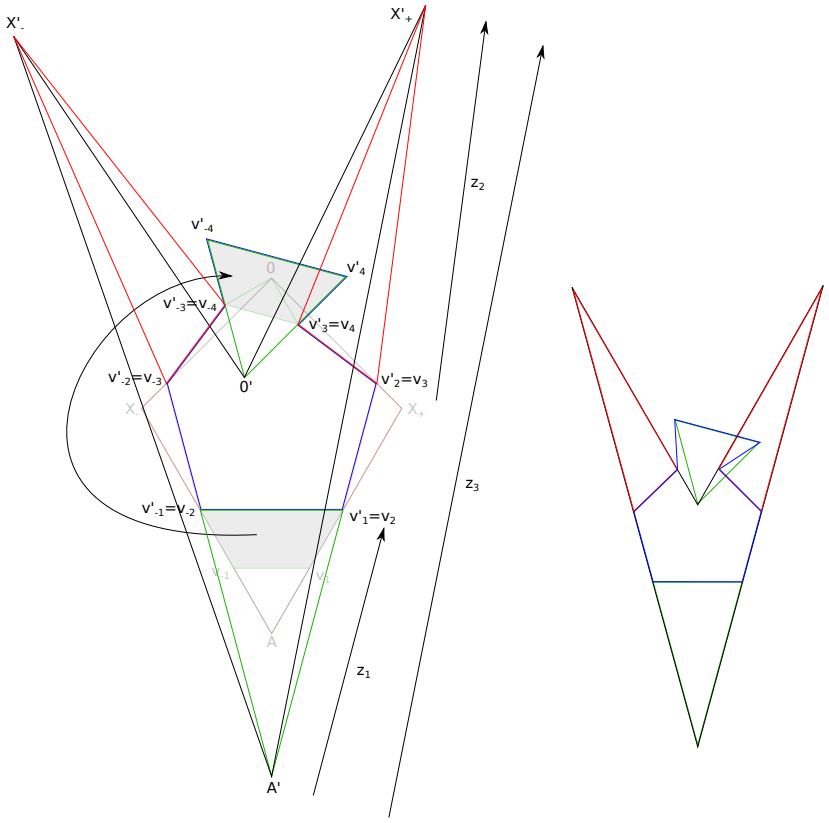

Figure 8.4: The change of coordinates that shifts the angles upwards.

Note that the new coordinates z_i' describe the configuration in terms of the new axis, which has O' as the origin. Moreover, the negative imaginary axis is along the line from O' pointing towards A'. Let γ be the angle between the line from O' to A' and the vertical and

$$\overrightarrow{v} = \frac{\sin(\varphi + \psi)}{\sin(\alpha + \psi)} e^{-2i\beta} z_1,$$

then the coordinates of the v_i with respect to the new axis $[v_i]_2$ are given by

$$[v_i]_2 = e^{-i\gamma} \left([v_i]_1 - \overrightarrow{v} \right).$$

Taking the coordinates of the v_i' as expressed in the above equations, but with

the angles primed, we need to solve

$$
\begin{aligned}
v_1' &= e^{-i\alpha} z_1' - \frac{\sin(\varphi)}{\sin(\varphi-\alpha)} z_3' \\
&\| \\
v_2 &= e^{-i\gamma}\left(e^{i(\varphi-\alpha)} z_2 + \frac{\sin(\varphi-\alpha)}{\sin(\alpha+\psi)} e^{i(\varphi-\alpha)} z_3 - \frac{\sin(\varphi+\psi)}{\sin(\alpha+\psi)} e^{-2i\beta} z_1 \right), \\
v_2' &= -e^{-i\alpha} z_2' - \frac{\sin(\alpha)}{\sin(\varphi-\alpha)} e^{i(\varphi-\alpha)} z_3' \\
&\| \\
v_3 &= e^{-i\gamma}\left(-\frac{\sin(\varphi)}{\sin(\psi)} e^{-i(\alpha+\psi)} z_2 + \frac{\sin(\varphi-\alpha)}{\sin(\alpha+\psi)} e^{-i(\alpha+\psi)} z_3 - \frac{\sin(\varphi+\psi)}{\sin(\alpha+\psi)} e^{-2i\beta} z_1 \right), \\
v_3' &= -\frac{\sin(\psi)}{\sin(\varphi+\psi)} e^{i(\varphi-\alpha)} z_2' - \frac{\sin(\alpha)}{\sin(\varphi-\alpha)} e^{i(\varphi-\alpha)} z_3' \\
&\| \\
v_4 &= e^{-i\gamma}\left(-e^{i(\varphi-\alpha-2\beta)} z_1 \right),
\end{aligned}
$$

which gives

$$
\begin{aligned}
e^{i\gamma} z_1' &= -\frac{\sin(\varphi-\alpha)}{\sin(\alpha)} z_2 + \frac{\sin(\varphi-\alpha)}{\sin(\alpha)} z_3, \\
e^{i\gamma} z_2' &= \frac{\sin(\varphi-\alpha)\sin(\varphi+\psi)}{\sin(\alpha+\psi)\sin(\varphi)} e^{-2i\beta} z_1 + \frac{\sin(\varphi+\psi)}{\sin(\psi)} z_2 - \frac{\sin(\varphi-\alpha)\sin(\varphi+\psi)}{\sin(\alpha+\psi)\sin(\varphi)} z_3, \\
e^{i\gamma} z_3' &= \frac{\sin(\varphi-\alpha)\sin(\varphi+\psi)}{\sin(\alpha+\psi)\sin(\varphi)} e^{-2i\beta} z_1 - \frac{\sin(\psi-\alpha)}{\sin(\alpha)} z_2 + \frac{\sin(\psi)\sin^2(\varphi-\alpha)}{\sin(\alpha+\psi)\sin(\varphi)\sin(\alpha)} z_3.
\end{aligned}
$$

Alternatively, one can geometrically recover the vectors $\overrightarrow{A'v_1'}$, $\overrightarrow{v_2'v_3'}$ and $\overrightarrow{A'x_+'}$ in terms of $\overrightarrow{Av_1}$, $\overrightarrow{v_2v_3}$ and $\overrightarrow{Ax_+}$ and use (8.2.1) to obtain the same equations as above, remembering that since the axis is rotated by $e^{i\gamma}$, the coordinates need to be changed accordingly.

Therefore the shift is given by the matrix

$$
T(\alpha,\beta,\varphi,\psi) = e^{-i\gamma} \begin{pmatrix}
0 & -\frac{\sin(\varphi-\alpha)}{\sin(\alpha)} & \frac{\sin(\varphi-\alpha)}{\sin(\alpha)} \\
\frac{\sin(\varphi+\psi)\sin(\varphi-\alpha)}{\sin(\varphi)\sin(\alpha+\psi)} e^{-2i\beta} & \frac{\sin(\varphi+\psi)}{\sin(\psi)} & -\frac{\sin(\varphi+\psi)\sin(\varphi-\alpha)}{\sin(\varphi)\sin(\alpha+\psi)} \\
\frac{\sin(\varphi+\psi)\sin(\varphi-\alpha)}{\sin(\varphi)\sin(\alpha+\psi)} e^{-2i\beta} & -\frac{\sin(\varphi-\alpha)}{\sin(\alpha)} & \frac{\sin(\psi)\sin^2(\varphi-\alpha)}{\sin(\varphi)\sin(\alpha)\sin(\alpha+\psi)}
\end{pmatrix}.
$$

Moreover,

$$
T^{-1}(\alpha,\beta,\varphi,\psi) = e^{i\gamma} \begin{pmatrix}
0 & \frac{\sin(\varphi)}{\sin(\psi)} e^{2i\beta} & -\frac{\sin(\varphi-\alpha)}{\sin(\alpha+\psi)} e^{2i\beta} \\
\frac{\sin(\varphi)}{\sin(\psi)} & \frac{\sin(\varphi)}{\sin(\psi)} & -\frac{\sin(\varphi)}{\sin(\psi)} \\
\frac{\sin(\alpha)\sin(\varphi+\psi)}{\sin(\psi)\sin(\alpha+\psi)} & \frac{\sin(\varphi)}{\sin(\psi)} & -\frac{\sin(\varphi)}{\sin(\psi)}
\end{pmatrix}.
$$

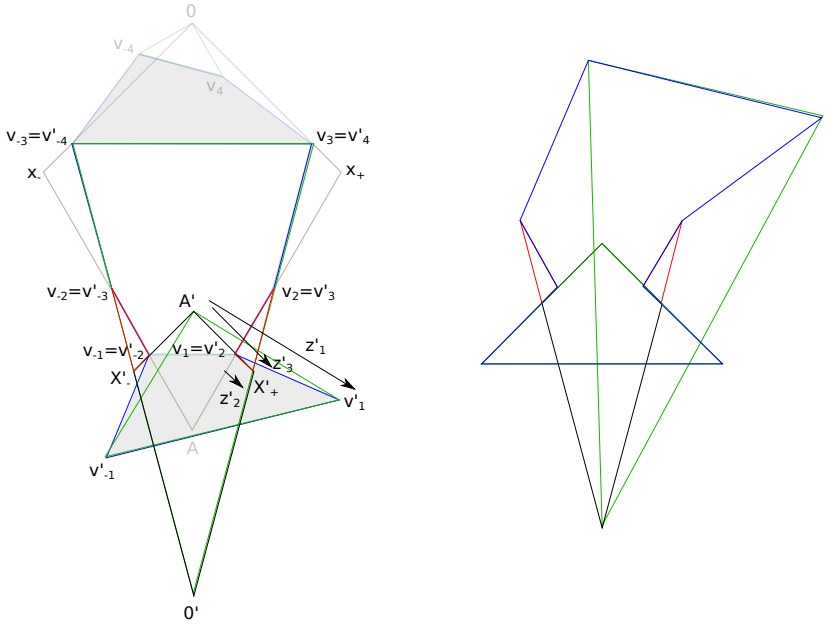

Figure 8.5: The inverse shift.

Remark 8.2.3. These matrices seem not to be the inverse of each other. This is because all the matrices we gave so far are applied to the configuration $(\alpha, \beta, \varphi, \psi)$. The matrix T^{-1} is, in fact, the inverse shift on φ, ψ and θ rather than the inverse matrix of T. In fact, T and T^{-1} satisfy $T^{-1}(\alpha', \varphi', \psi') = T^{-1}(\alpha+\psi-\pi, \beta, \psi, 3\pi-\varphi-\psi) = (T(\alpha, \varphi, \psi))^{-1}$, where $(\alpha, \varphi, \psi) \overset{T}{\mapsto} (\alpha', \varphi', \psi')$ and

$$T^{-1}(\alpha+\psi-\pi, \beta, \psi, 3\pi-\varphi-\psi) =$$
$$e^{i\gamma} \begin{pmatrix} 0 & \frac{\sin(\psi)}{\sin(\varphi+\psi)} e^{2i\beta} & \frac{\sin(\alpha)}{\sin(\varphi-\alpha)} e^{2i\beta} \\ \frac{\sin(\psi)}{\sin(\varphi+\psi)} & \frac{\sin(\psi)}{\sin(\varphi+\psi)} & -\frac{\sin(\psi)}{\sin(\varphi+\psi)} \\ \frac{\sin(\varphi)\sin(\alpha+\psi)}{\sin(\varphi+\psi)\sin(\varphi-\alpha)} & \frac{\sin(\psi)}{\sin(\varphi+\psi)} & -\frac{\sin(\psi)}{\sin(\varphi+\psi)} \end{pmatrix}.$$

This is the same idea as in the 2-fold symmetry case (see Chapter 6).

Then the move swapping v_3 and v_4 is $A_{34} = T^{-1}A_{23}T$, with the matrices applied to the correct configuration according to

$$\begin{aligned} (\alpha, \beta, \varphi, \psi) &\overset{T}{\mapsto} (\alpha+\psi-\pi, \beta, \psi, 3\pi-\varphi-\psi) \\ &\overset{R_{23}}{\longmapsto} (2\pi+\alpha-\varphi-\psi, \beta, 3\pi-\varphi-\psi, \psi) \\ &\overset{R_{23}}{\longmapsto} (\alpha+\psi-\pi, \beta, \psi, 3\pi-\varphi-\psi) \overset{T^{-1}}{\longmapsto} (\alpha, \beta, \varphi, \psi). \end{aligned}$$

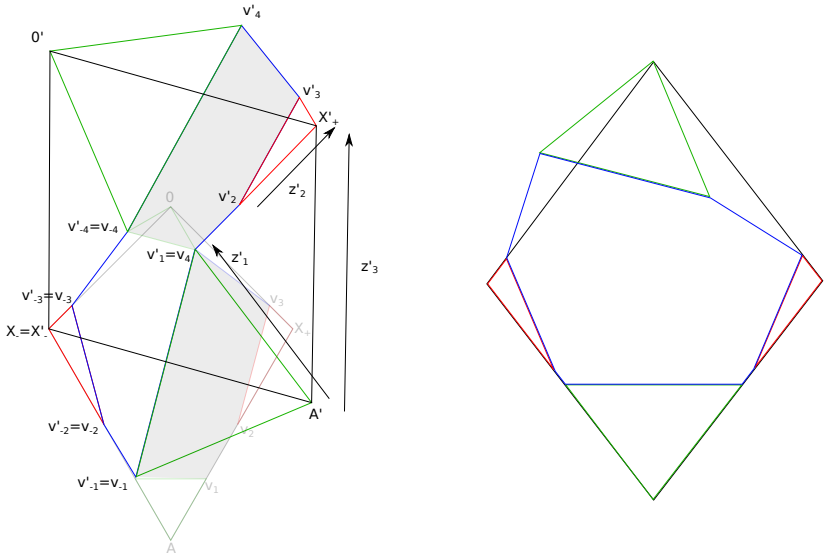

Figure 8.6: The first Dehn twist.

Similarly, we can find the move swapping v_1 and v_2 by shifting in the other direction. Remembering that the shift in the other direction is T^{-1}, the move will be $A_{12} = TA_{23}T^{-1}$, where the matrices are applied to the correct configuration according to:

$$\begin{aligned}(\alpha,\beta,\varphi,\psi) &\xmapsto{T^{-1}} (\pi+\alpha-\varphi,\beta,3\pi-\varphi-\psi,\varphi)\\ &\xmapsto{R_{23}} (\varphi+\psi+\alpha-2\pi,\beta,\varphi,3\pi-\varphi-\psi)\\ &\xmapsto{R_{23}} (\pi+\alpha-\varphi,\beta,3\pi-\varphi-\psi,\varphi) \xmapsto{T} (\alpha,\beta,\varphi,\psi).\end{aligned}$$

The geometric meaning of the inverse shift is shown in Figure 8.5.

The moves given by Dehn twists around the genus The next move we want to consider is a Dehn twist D_1 along a closed curve starting from the side $\overline{v_1v_{-1}}$ and closing up on the corresponding point of $\overline{v_4v_{-4}}$, without intersecting other sides of the octagon. This is shown in Figure 8.6.

Again, one can express the vectors $\overrightarrow{A'v_1'}$, $\overrightarrow{v_2'v_3'}$ and $\overrightarrow{A'x_+'}$ in terms of $\overrightarrow{Av_1}$, $\overrightarrow{v_2v_3}$ and $\overrightarrow{Ax_+}$ and use (8.2.1) to find the matrix of the move. Let η be the angle between the new negative imaginary axis (along the line through O' and A') and

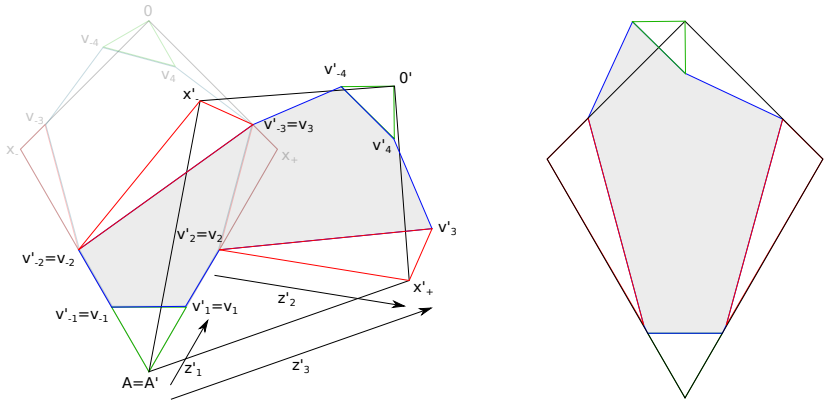

Figure 8.7: The second Dehn twist.

the vertical axis in our original coordinates. Then, defining

$$A = 2\sin(\alpha+\beta-\varphi)\sin(\alpha+\psi),$$

one can see that the Dehn twist is

$$D_1 = \frac{ie^{-i\eta}}{A}\cdot$$
$$\cdot\begin{pmatrix} -\sin(\varphi-\alpha)e^{-i(\alpha+\psi+2\beta)} - \sin(\alpha+\psi)e^{-i(\varphi-\alpha)} & 0 & \sin(\varphi+\psi) \\ 0 & Ae^{i(\alpha-\beta-\varphi)} & 0 \\ -\sin(\varphi+\psi)e^{-2i\beta} & 0 & -iAe^{-i\beta}+\sin(\varphi+\psi) \end{pmatrix}.$$

Note that

$$(\alpha,\beta,\varphi,\psi) \overset{D_1}{\longmapsto} (\alpha+\beta,\beta,\varphi,\psi).$$

Finally, we want to consider a Dehn twist D_2 along the closed curve starting from the side $\overline{v_{-2}v_{-3}}$ and closing up on the corresponding point of $\overline{v_2v_3}$, without intersecting other sides of the octagon. This is shown in Figure 8.7. Let ξ be the angle between the old and new axis and define

$$A = \sin(\varphi+\psi),$$

then the Dehn twist is

$$D_2 = \frac{ie^{-i\xi}e^{-i\alpha}}{A} \cdot$$
$$\cdot \begin{pmatrix} Ae^{-i(\varphi-2\alpha)} & 0 & 0 \\ 0 & -i\left(\sin(\varphi)e^{-i(\alpha+\psi)} + \sin(\psi)e^{-i(\varphi-\alpha)}\right) & 2\sin(\psi)\sin(\varphi-\alpha) \\ 0 & -2\sin(\varphi)\sin(\alpha+\psi) & 2\sin(\psi)\sin(\varphi-\alpha) - iAe^{i\alpha} \end{pmatrix}.$$

We remark that

$$(\alpha, \beta, \varphi, \psi) \xmapsto{D_2} (\alpha, \alpha+\beta, \varphi, \psi).$$

The next step would be to start studying what happens when pairs of cone points coalesce, as well as what happens when we pinch a curve around the genus, in order to study the lower dimensional strata of the cone manifold.

Our idea is to keep track of the main coordinates, as well as the two coordinates obtained after applying the two shifts, so that all the moves are reasonable to study.

My plans for my future research are to keep developing the ideas presented in this chapter to get a better understanding of complex hyperbolic lattices.

Bibliography

[BHC62] Armand Borel and Harish-Chandra, *Arithmetic subgroups of algebraic groups*, Ann. of Math. (2) **75** (1962), 485–535.

[BP15] Richard K. Boadi and John R. Parker, *Mostow's lattices and cone metrics on the sphere*, Adv. Geom. **15** (2015), no. 1, 27–53.

[Cor92] Kevin Corlette, *Archimedean superrigidity and hyperbolic geometry*, Ann. of Math. (2) **135** (1992), no. 1, 165–182.

[Der17] Martin Deraux, *Arithmeticity of the Couwenberg-Heckman-Looijenga lattices*, ArXiv preprint arXiv:1710.04463 (2017).

[DFP05] Martin Deraux, Elisha Falbel, and Julien Paupert, *New constructions of fundamental polyhedra in complex hyperbolic space*, Acta Math. **194** (2005), no. 2, 155–201.

[DM86] Pierre Deligne and George D. Mostow, *Monodromy of hypergeometric functions and nonlattice integral monodromy*, Inst. Hautes Études Sci. Publ. Math. (1986), no. 63, 5–89.

[DM93] ———, *Commensurabilities among lattices in PU(1,n)*, Princeton University Press, 1993.

[DPP] Martin Deraux, John R. Parker, and Julien Paupert, *On commensurability classes of non-arithmetic complex hyperbolic lattices*, ArXiv e-prints, https://arxiv.org/abs/1611.00330.

[DPP16] ———, *New non-arithmetic complex hyperbolic lattices*, Invent. Math. **203** (2016), no. 3, 681–771.

[FP06] Elisha Falbel and John R. Parker, *The geometry of the Eisenstein-Picard modular group*, Duke Math. J. **131** (2006), no. 2, 249–289.

[Gir21] Georges Giraud, *Sur certaines fonctions automorphes de deux variables*, Ann. Sci. École Norm. Sup. (3) **38** (1921), 43–164.

[Gol99] William M. Goldman, *Complex hyperbolic geometry*, Oxford Mathematical Monographs, The Clarendon Press, Oxford University Press, New York, 1999, Oxford Science Publications.

[GP17] Selim Ghazouani and Luc Pirio, *Moduli spaces of flat tori with prescribed holonomy*, Geom. Funct. Anal. **27** (2017), no. 6, 1289–1366.

[GPS88] M. Gromov and I. Piatetski-Shapiro, *Nonarithmetic groups in Lobachevsky spaces*, Inst. Hautes Études Sci. Publ. Math. (1988), no. 66, 93–103.

[GS92] Mikhail Gromov and Richard Schoen, *Harmonic maps into singular spaces and p-adic superrigidity for lattices in groups of rank one*, Inst. Hautes Études Sci. Publ. Math. (1992), no. 76, 165–246.

[Koj01] Sadayoshi Kojima, *Complex hyperbolic cone structures on the configuration spaces*, Rend. Istit. Mat. Univ. Trieste **32** (2001), no. suppl. 1, 149–163 (2002), Dedicated to the memory of Marco Reni.

[Mar84] G. A. Margulis, *Arithmeticity of the irreducible lattices in the semisimple groups of rank greater than 1*, Invent. Math. **76** (1984), no. 1, 93–120.

[McM17] Curtis T. McMullen, *The Gauss-Bonnet theorem for cone manifolds and volumes of moduli spaces*, Amer. J. Math. **139** (2017), no. 1, 261–291.

[Mos80] George D. Mostow, *On a remarkable class of polyhedra in complex hyperbolic space*, Pacific J. Math. **86** (1980), no. 1, 171–276.

[Mos86] ———, *Generalized Picard lattices arising from half-integral conditions*, Inst. Hautes Études Sci. Publ. Math. (1986), no. 63, 91–106.

[Mos88] ———, *On discontinuous action of monodromy groups on the complex n-ball*, J. Amer. Math. Soc. **1** (1988), no. 3, 555–586.

[Par06] John R. Parker, *Cone metrics on the sphere and Livné's lattices*, Acta Math. **196** (2006), no. 1, 1–64.

[Par09] ———, *Complex hyperbolic lattices*, Discrete groups and geometric structures, Contemp. Math., vol. 501, Amer. Math. Soc., Providence, RI, 2009, pp. 1–42.

[Pas16] Irene Pasquinelli, *Deligne-Mostow lattices with three fold symmetry and cone metrics on the sphere*, Conform. Geom. Dyn. **20** (2016), 235–281.

[Pas17] ———, *Fundamental polyhedra for all Deligne-Mostow lattices in PU(2,1)*, ArXiv preprint arXiv:1708.05267 (2017).

[Sau90] John Kurt Sauter, Jr., *Isomorphisms among monodromy groups and applications to lattices in PU(1,2)*, Pacific J. Math. **146** (1990), no. 2, 331–384.

[Thu98] William P. Thurston, *Shapes of polyhedra and triangulations of the sphere*, The Epstein birthday schrift, Geom. Topol. Monogr., vol. 1, Geom. Topol. Publ., Coventry, 1998, pp. 511–549.

[Vee93] William A. Veech, *Flat surfaces*, Amer. J. Math. **115** (1993), no. 3, 589–689.